Author:
Brodrick, Emelie A

Title:
Light and dark adaptation in the eye of the fiddler crab

mechanisms to cope with extreme fluctuations in brightness

Light and dark adaptation in the eye of the fiddler crab

Mechanisms to cope with extreme fluctuations in brightness

By

EMELIE ANN BRODRICK

School of Biological Sciences
UNIVERSITY OF BRISTOL

A dissertation submitted to the University of Bristol
in accordance with the requirements of the degree of
DOCTOR OF PHILOSOPHY in the Faculty of Life Sciences.

SEPTEMBER 2020

Word count: 57,625

Abstract

Light, in abundance or absence, can provoke a great variety of photomechanical changes in the compound eyes of crustaceans. The fiddler crab visual system is widely used as a model to study aspects of crustacean vision and neural pathways. Their apposition eyes are adapted for vision on sunny tropical and semi-tropical mudflats, but intermittent and temporary use of underground burrows to evade predators means their eyes are additionally exposed to short but frequent periods of darkness. Their light-adaptation mechanisms have not yet been examined, so my project uses a variety of complimentary approaches to investigate important gaps in our understanding of how their eyes cope with extreme fluctuations in brightness. The West African fiddler crab, *Afruca tangeri*, is also nocturnally-active, suggesting that their eyes undergo effective dark-adaptation at sunset. Transmission electron microscopy (TEM), light microscopy, and synchrotron X-ray tomography were used to describe ultrastructural changes in the eye of this species between day and night. In living crabs, widening of the deep pseudopupil was measured using an ophthalmoscopic camera. The impacts that adaptation state and time of day have on contrast sensitivity of the eye, were assessed using analysis of behavioural thresholds to visual stimuli. Electroretinogram (ERG) recordings from another fiddler crab, *Gelasimus dampieri*, provided additional evidence for circadian controls on changes in absolute sensitivity of light- and dark-adapted eyes.

Crystalline cones and rhabdoms undergo significant physiological change to effectively adapt the eye to dim light at dusk, however, screening pigment migrations remain immobile across the eye and are not part of the response to changes in light intensity. The eye returns to a light-adapted state at dawn and with bright light exposure. Thereafter, during daylight hours, minimal change occurs in response to dim light and the eye remains anatomically light-adapted, even after several hours in the dark. ERGs revealed that *G. dampieri* uses temporal summations as an alternative dark-adaptation strategy. This provides an explanation for sensitivity increases measured in both species in periods of dim light during daylight hours, which occurred without apparent anatomical change.

Effective dark-adaptation occurs at sunset to allow safe foraging and visual communication after dusk in diminishing light. However, during daylight hours, circadian controls prevent the eye making unnecessary adjustments to the fluctuating light levels frequently experienced as the crab moves between the bright mudflat surface and the dark burrow. This benefits the fiddler crab by ensuring that the visual system remains primed for predator detection in very bright light, immediately after spending time underground, where vision is not required.

Dedication and acknowledgements

This thesis is dedicated to my supportive parents, James Brodrick and Kristin Brodrick, who have always encouraged my enthusiasm to study sea creatures.

I would like to thank my advisers Martin How and Nicholas Roberts for giving me this chance to research a fascinating topic and for their continued supervision of my project. Their passion and enthusiasm was an inspiration. Thanks also to the rest of the Ecology of Vision group (Sam Smithers, Rochelle Meah, Ilse Daly, Alex Tibbs, David Wilby, Mike Bok and Ally Irwin) for invaluable help along the way and four very enjoyable years. Muchas gracias to Tato (José Ignacio Navas Triano) at IFAPA for supporting my fieldwork in Spain, allowing me to use labs and microscopes and always going out of his way to help and keep us safe on the mudflats. I was lucky to have some incredible research assistants in Spain, including Ally, Sam and Rochelle. A special mention goes to Seb Lloyd for his tireless work on the optomotor experiments and "crabmin", as well as his great humour and company, despite some dodgy Spotify playlists!

Thanks to Lauren Sumner-Rooney for including me in her synchrotron project and for thoroughly proof-reading my paper. The Technicians at the Wolfson Bio-imaging Facility were hugely helpful in assistance with my electron microscopy work. Thanks go to Jan Hemmi, Zahra Bagheri and the rest of the group at UWA for making me welcome in Perth and teaching me some electrophysiology, which became an invaluable part of my PhD.

I am very grateful to my partner John, who kept me sane and well-fed during the coronavirus lock-down when writing took over my life and patiently supported me throughout the tougher moments. Finally, the biggest thanks should go to the charming little crabs who participated in this research, some of whom made the ultimate sacrifice to Science.

AUTHOR'S DECLARATION

I declare that the work in this dissertation was carried out in accordance with the requirements of the University's Regulations and Code of Practice for Research Degree Programmes and that it has not been submitted for any other academic award. Except where indicated by specific reference in the text, the work is the candidate's own work. Work done in collaboration with, or with the assistance of, others, is indicated as such. Any views expressed in the dissertation are those of the author.

SIGNED: ..... DATE: .....

TABLE OF CONTENTS

List of Tables

List of Figures

CHAPTER 1

INTRODUCTION

Arthropods with compound eyes appeared in the fossil record ~541 million years ago [1] and after huge divergence during the Cambrian Explosion, they have become the most successful animal phylum on the planet [2]. Their eyes have evolved to cope with life in every ecological niche inhabited by life on Earth, and show a diverse range of strategies to handle large fluctuations in brightness. The fiddler crab makes a fantastic study animal, used globally as a model organism by researchers studying a variety of topics in crustaceans. In this thesis, I explore how the compound eye of the fiddler crab adapts to extreme changes in brightness. I use a range of complimentary approaches, from micro-anatomical study of eyes in two and three dimensions, to electrophysiology and behavioural tests to explore thresholds of their vision. I begin with introducing the apposition compound eye, my study animals, and some common strategies for light- and dark-adaptation in arthropods.

1.1 The crab visual system

1.1.1 Properties of light

Light is part of the electromagnetic radiation spectrum, a form of high-speed energy travelling through space and time. Visible light is defined by its wavelength within the range detectable by the human eye, which falls somewhere between 400 to 700 nm [3, 4]. Many vertebrate and invertebrate animals are able to detect radiation beyond this range, particularly in the ultraviolet spectrum [4]. Light can be explained by both wave theory with electromagnetic properties, and by quantum theory in which light can also be shown to behave as discrete particles called photons [5]. Light has several properties of interest to an animal, including its intensity (brightness), direction of wave propagation, its polarization and spectrum of wavelengths (frequencies). Researchers

over the years have come up with a multitude of photometric units by which to measure radiance and irradiance [6]. Light measurements in this thesis are of absolute irradiance measured by a spectrometer in W/cm^2/nm. The measurement by the spectrometer is calibrated to a lamp of known spectral power output at each pixel and accurately measures the amount of energy emitted at each wavelength from a radiant source such as the sun/sky, or an artificial light source such as an LED, creating a spectrum of light intensities across the visible wavelength range.

1.1.2 Optic apparatus

Compound eyes are composed of repeated eye units called **ommatidia**. Among the crustaceans, there are two main eye designs. Superposition eyes (Fig. 1.1a) are well-suited for very dim light vision (e.g. midwater shrimp) and contain refractive or reflective optical structures that direct light through from many facets through a "clear zone", in order to pool light and produce a single image onto the retina [7]. The parabolic superposition eyes of hermit crabs use complex optics such as internal parabolic mirrors to perform this task [8]. However, these eye designs are not relevant to the present study. Brachyuran crabs possess **apposition compound eyes** (Fig. 1.1b) in which each eye unit is optically isolated from its neighbours, often by sleeves of screening pigment separating the ommatidia. These eyes lack a "clear zone" pooling mechanism so this design can maximise spatial acuity, at the expense of sensitivity. Therefore, they are common among insects and crustaceans that are primarily diurnally active [7].

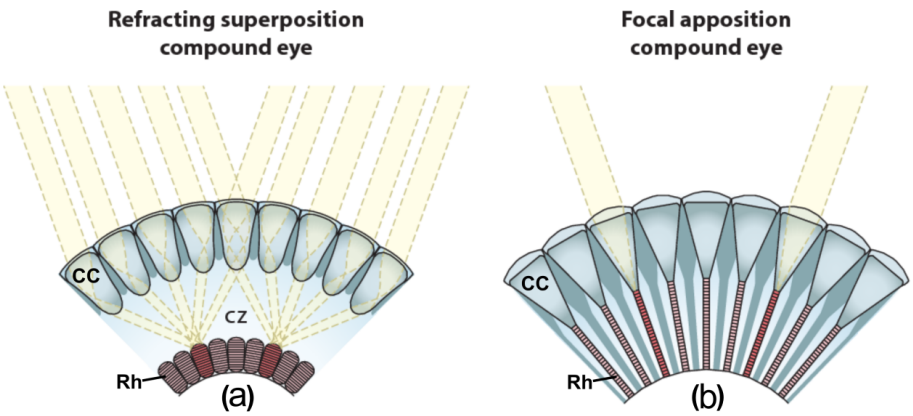

FIGURE 1.1. **(a)** A superposition compound eye design. Light is collected by multiple facet lenses and refracted by crystalline cones (CC) across a clear zone (CZ) toward rhabdoms of single photoreceptors (Rh). This works to pool light and boost optical sensitivity in nocturnal or deep water animals. Compare this to **(b)**, an apposition compound eye found in diurnal arthropods including brachyuran crabs. Light entering a facet lens is directed by the crystalline cone straight to its adjoined rhabdom. Ommatidia are optically isolated from one another by sleeves of screening pigment, which also reduce the overall photon capture in the eye. Diagram from ref: [9].

The corneal surface of an apposition eye is made up of hexagonal facet lenses (measuring roughly 30-50 μm across), which each sample light from a small area of space [7]. Behind each facet lens, a **crystalline cone** made of four semper cells directs light through a layer of screening pigment cells directly on to the light-sensitive region of photoreceptor cells. Photoreceptors are highly specialised neurons with an axon, cell body and brush-like light-sensitive receptor, made up of thousands of microvilli (measuring 40-55 nm in diameter). In the brachyuran crab, the elongated photoreceptor cells are arranged in a ring and together, the microvilli of several cells form a fused **rhabdom** (meaning "rod" in Greek). This is distinct from the separated / open rhabdoms of some insects. It is here in the rhabdom that phototransduction occurs across the large surface area of microvillar membranes. The intensity of light measured by each cell type in the rhabdom is pooled, forming one "pixel" of it's visual scene and therefore, the inter-ommatidial angle between facets determines the spatial acuity of the animal [10]. Due to physical constraints on an eye's size and limits of light diffraction through the tiny lenses, animals with compound eyes are rarely able to resolve objects subtending a visual angle of much less than 1 degree [11].

1.1.3 Phototransduction

The visual pigment **rhodopsin** is responsible for phototransduction in the rhabdom, the conversion of photons of light energy into electrical signals [12, 13]. Visual pigments are embedded in the microvillus lipid bi-layer membrane, which forms the rhabdomere of each photoreceptor [14]. Phototransduction occurs via an **opsin**, a G protein-coupled receptor formed of a ring of seven trans-membrane domains. The opsin is bonded to a central light-sensitive vitamin A-based retinaldehyde called a **chromophore retinal** [15]. Over a thousand opsins from seven subfamilies have been described in animals [12, 14] and in the crab, the opsin is coupled with invertebrate G_q protein [15, 16]. The amino acid sequences of both opsin and the chromophore attune the visual pigment to absorb light in a specific range of wavelengths, with a particular peak absorption wavelength (λ_{max}) [15, 17]. Crabs possess the most common chromophore retinal type, A1 (11-cis retinal) [18].

When a photon is absorbed by invertebrate rhodopsin, it triggers a phototransduction cascade beginning with an isomerization shift of the light-sensitive chromophore molecule. This causes a conformational change into **meta-rhodopsin**, which acts as a catalyst for a chemical pathway within the photoreceptor, ultimately causing its cell membrane to **depolarise** [13, 15]. This transient electrical signal (known as a **quantum bump** for single photon responses) travels along the photoreceptor axon toward the synapse in the first optic neuropil, the lamina (or medulla for some crustacean R8 axons [19–21]). Where there are many photons, the voltage amplitude of the signal produced is proportional to the logarithm of light intensity [22, 23]. In invertebrates meta-rhodopsin is thermostable and the chromophore can go on to absorb a second photon, which converts it back to ground state rhodopsin. Thus, in the presence of light, the visual pigments continually shift between rhodopsin and meta-rhodopsin [24].

1.1.4 Sensitivity of the visual system

There are several ways by which we can characterise the sensitivity of an eye. **Absolute sensitivity** thresholds refer to the minimum amount of light that can be detected by the eye and this is limited by signal-to-noise ratios created by the photons themselves and the pathways of phototransduction [25–27]. **Contrast sensitivity** measures the threshold to which an eye can discriminate two parts of a visual scene with different luminosity [28, 29]. The specific eye design and how densely packed photoreceptor channels are in the retina determines the **spatial sensitivity** of an eye [7, 10, 30], which is the ability of the eye to discriminate two adjacent objects of different brightness in space [31]. How quickly the visual system can respond to changes in luminosity over time determines the **temporal sensitivity** [30, 31]. Visual pigments in the membrane of the photoreceptor cells determine **spectral sensitivity** as they are tuned to absorb light within a certain range of wavelengths [7]. Finally, **polarization sensitivity** is an animal's ability to discriminate the angle at which the electric field vectors of light have travelled through space [32, 33].

Across the animal kingdom, different evolutionary directions, demands and limitations have created a huge diversity of eye designs [7]. Often, as sensitivity in one area is improved, physical constraints mean that another must be sacrificed. For example, photoreceptors adapted for vision in dark conditions often pool the small amount of available light in space or time. While this boosts absolute sensitivity for detecting slight contrasts in very dim light, it will result in poorer spatial or temporal resolution [30, 34–36]. Therefore, visual systems tend to specialise in order to maximise sensitivity for one or two of these tasks, with penalties in others. In an individual animal operating in a changing visual environment, priorities can change on short timescales (e.g. from day to night) or long timescales (e.g. habitat change from juvenile and adult), so their visual systems must adapt accordingly. Some animals experience extremely frequent changes in light levels due to movement through a habitat (e.g. flight in and out of shaded areas under tree canopies). Reversible and reactive changes in the eye help cope with these fluctuations in brightness [7].

1.1.5 Spectral sensitivity and colour vision in crabs

The amino acid sequences of the opsin and chromophore determine the precise shape of the rhodopsin protein, making it maximally absorbent at a particular wavelength of light ($\lambda_{\max}$) [15, 17]. Many animals have more than one type of rhodopsin, allowing light detection over a broader range of wavelengths and thus, a broader spectral sensitivity. Cronin and Forward [18] examined 27 species of crab from a various habitats with microspectrophotometry (MSP) and reported that all crabs possessed two classes of photoreceptor cells, R1-7 and R8, which contain different visual pigments. Photoreceptors R1-7 contribute to the majority of the rhabdom's length and contain one visual pigment with broad spectral sensitivity, maximally absorbent between 470 and 515 nm (cyan), depending on species. Their measurements from Ocypodid crabs were

abandoned. However, Jordão *et al.* [37] did later manage a successful MSP study of the R1-7 pigments of four species of fiddler crab, for which they identified λ_{max} of between 508 nm and 530 nm (Fig. 1.2). One of their study species was *Afruca tangeri*, with peak sensitivity at the longer end of the range for known crab species, at 530 nm.

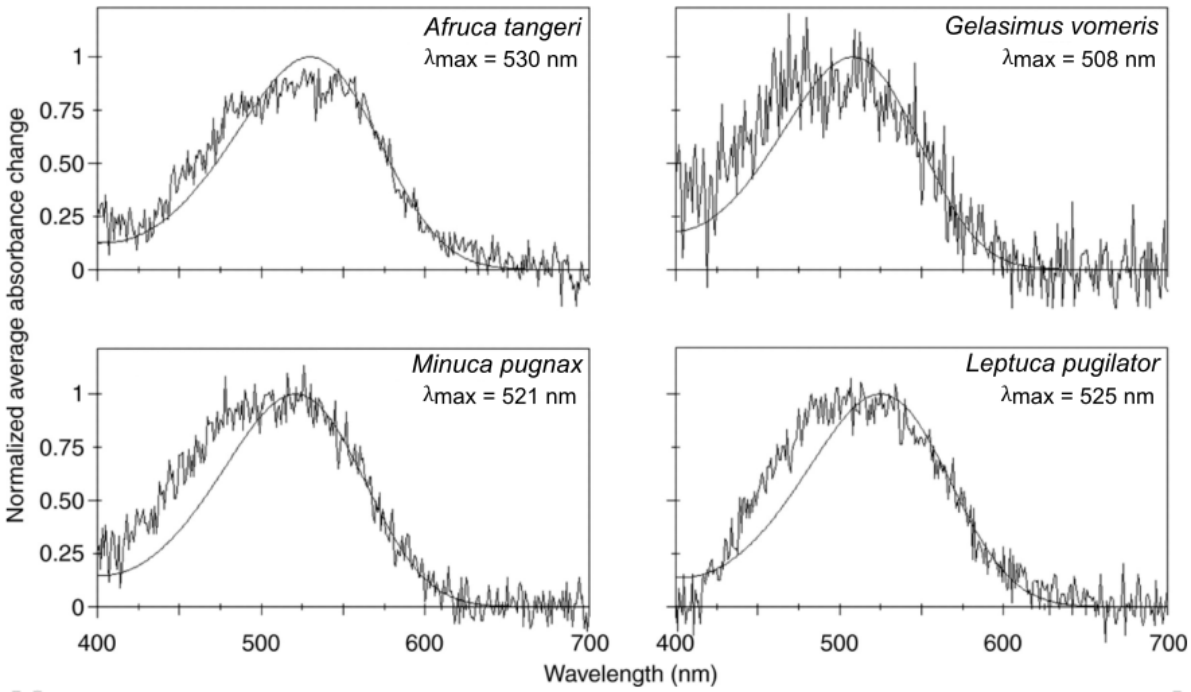

FIGURE 1.2. The normalised average absorbance change measured with *in situ* microspectrophotometry of R1-7 cell rhabdoms from four fiddler crab species. The smooth curve in each panel is the template from ref: [38] fitted to the data. Figure from ref: [37].

Neither MSP study managed to measure visual pigment in the little R8 cell, due to its close proximity to screening pigments and and its small size [18, 37]. Light passes through this cell's short disordered rhabdom first and it is known in other crustaceans to have a visual pigment sensitive tO short wavelengths, with peak sensitivity in the UV-blue part of the spectrum [19, 37, 39, 40]. Evidence of this visual pigment with short wavelength sensitivity (SWS) was provided via electrophysiology in the crabs *Carcinus* and *Callinectes* [41], along with suggestions for functional colour vision. It is thought that fiddler crab R8 cells also possess a SWS visual pigment [37] and electrophysiology provided conclusive evidence for UV detectors in *Leptuca* and *Gelasimus* fiddler crabs [42–45].

Intracellular recordings in *Gelasimus vomeris* and *Gelasimus dampieri* indicated not just one, but two additional medium wavelength sensitivity (MWS) visual pigments, which appear to be co-expressed within R1-7 cells [43, 45]. Molecular opsin analysis of *L. pugilator* photoreceptors

revealed differential expression of two MWS opsins in photoreceptors, with one per ommatidium co-expressing both [46]. This suggests that trichromatic colour vision may even be possible in that species, although this has not been confirmed behaviourally. In *G. vomeris*, Alkaladi [47] describes differential expression patterns across the eye whereby dorsal, ventral and posterior regions express all three opsins (one SWS and two MWS), but unusually, in the equatorial acute zone region, there are alternating rows of ommatidia that express just one of the two MWS opsins.

While all visual systems have spectral sensitivity, this is not to be confused with colour vision, which not all animals possess [48]. Colour vision is the ability to discriminate between two parts of a visual scene which only differ in their spectral composition, but are equally matched in overall irradiance and texture etc. [49]. To achieve this, you need to have an opponent system which compares excitation levels from at least two photoreceptor types containing visual pigments with different spectral sensitivity [48]. It can be tricky to demonstrate an animal's colour discrimination ability, as intensity matching requires excellent knowledge of its spectral sensitivity, which is not always available to provide accurate quantum catch data. The experiments also rely on a motivated behavioural response, such as a choice experiment [49]. Training a fiddler crab to select a shade of yellow from a range of grey stimuli for example, would be an onerous task and their detritivorous diet means food-searching behaviours cannot be exploited. Therefore, there is limited evidence pointing to colour vision in fiddler crabs, so far.

Fiddler crabs are often themselves very colourful, especially the Indo-West Pacfic species [50–52]. Furthermore, temporal changes in body colouration are commonly associated with age, moulting, temperament and reproductive status of an individual, which suggests a conspecific signalling function [51, 53]. From above, the carapace of *A. tangeri* is relatively dull for a fiddler crab, perhaps to provide camouflage from avian predators. However, they tend to have more colourful markings on mouthparts, claws and legs; parts of the body visible to conspecifics and involved in signalling [54]. This suggests that *A. tangeri* may possess colour vision abilities.

Some studies have provided behavioural evidence for a colour vision system. Hyatt [55] demonstrated a change in *L. pugilator* phototaxis behaviour from negative to positive when blue and orange lights were presented instead of white, although reasons for this are mystifying. Detto [39] showed that female *Austruca mjoebergi* prefer real and dummy males with yellow claws over intensity-matched grey claws. They have been shown recently to use hue, chroma and intensity to inform their decisions [56]. No electrophysiology or behavioural study exists yet on *A. tangeri*, so colour vision abilities in this species remain inconclusive, but plausible.

1.1.6 Polarization sensitivity in crabs

A beam of light consists of many electromagnetic waves passing through space, each with an electric field and magnetic field that oscillate perpendicular to one another (Fig. 1.3a). The polarization of a beam of light can be described in two ways with reference to the electric field

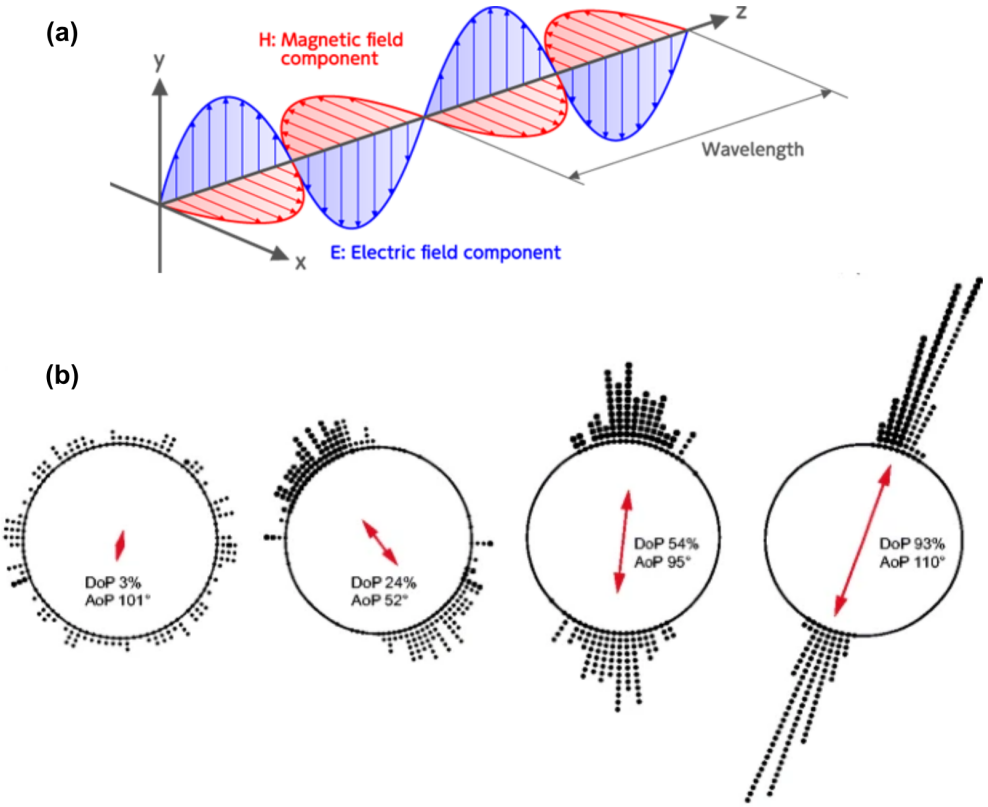

FIGURE 1.3. **(a)** Diagram of a single light wave with its magnetic and electric field vector components, which oscillate in perpendicular orientations to one another and the propagation direction. **(b)** The electric field vectors of waves within a beam of light are used to describe its polarization, in terms of angle and degree (AoP and DoP). Four examples are given from an unpolarized beam on the left, to highly polarized on the right. Points bordering the circle represent all angle distributions from waves in a beam and the direction of the central red arrow gives the resultant AoP. The spread of points around this angle determines the DoP and is represented by the length of the red arrow. Figure from ref: [33].

vectors of its constituent light waves. The **angle of polarization (AoP)**, measured between 0º and 180º, is the predominant electric field vector axis in the distribution of waves in the beam (i.e. the angle in which most of the waves are oscillating). The **degree of polarization (DoP)** is measured from 0 to 100% (or 0 to 1), and is a measure of the percentage (or proportion) of light waves that are oscillating along this particular predominant axis in the beam [33] (Fig. 1.3b).

There are many sources of polarized light in nature, for instance water bodies that strongly reflect horizontally polarized light. A mudflat beginning to dry in the sun at low tide may have the same AoP but a lower DoP due to more scattering from the coarser surface. The sky also has a conspicuous and distinctive polarization pattern caused by celestial Rayleigh scattering [57, 58]. This pattern is a circular DoP gradient, from unpolarized light in the sky immediately

surrounding the sun, to most strongly polarized scattering in the sky perpendicular from it [59]. As the sun moves across the sky during the day and changes its azimuth, this circular gradient with its stripe of highly polarized light at 90°, moves correspondingly.

While polarization properties of light are barely noticeable to the human eye [60], they are detected by other camera-eyed animals including some fish, spiders, birds and cephalopods [61–65]. Polarization vision is extremely common among arthropod animals with compound eyes [19, 66] and among the many insects and crustaceans, fiddler crabs are known to detect and utilise polarized light cues in their visual scene [67–69]. Polarization vision is useful for a range of tasks including polarotaxis, the location of habitats such as water body surfaces [70, 71], or enhancement of visual contrasts for object detection, e.g. [67, 72, 73]. The polarization pattern of the daytime and night sky can be used as a fixed and reliable reference, with which to navigate (as a compass) or spatially orientate the body during flight [74–77]. Some animals even use complex displays of polarized light reflections on their body surfaces to signal to conspecifics [78]. Notable examples include cephalopods [79, 80], which lack colour vision [81, 82], mantis shrimp, the only known animal able to detect circularly-polarized light (using quarter wave plate optics int he R8 cell) [83–85], and butterflies [86]. In the interesting case of circularly polarized light detection in mantis shrimp, it is thought that the distally positioned R8 cells of ommatidia within the specialised "midband" eye region, have microvilli aligned in a single direction to convert circularly polarized UV/visible light into linearly polarized light using quarter-wave plate optics [83, 87].

An easy way to look for evidence of polarization vision in a compound eye is to identify microvilli with ordered orientations in the rhabdom. Figure 1.4 shows an example of this architecture in the rhabdom of the fiddler crab *A. tangeri*. The highly ordered rows of microvilli are orientated horizontally and vertically. As the chromophores of the visual pigment molecules are approximately aligned within the microvillar membrane, they will be maximally absorbent to incoming light with electric field vectors orientated in the same plane [32, 88]. Photoreceptors R1, R2, R5 & R6 with vertically-orientated microvilli can compare excitation levels with photoreceptors R3, R4 & R7 with horizontal microvilli, providing an opponent system with which to compare angle and degree of polarization contrasts across their visual scene [19, 89].

By modifying a liquid crystal display (LCD) screen, it is possible to produce images that vary only in AoP and/or DoP [33, 69, 90], so to a human visual system the contrast is invisible, while to a polarization-sensitive eye, the image is detectable. Smithers *et al.* [68] recently demonstrated functional polarization vision in *A. tangeri* with behavioural experiments using looming stimuli on a modified LCD screen (Fig. 1.5). They found that this species of fiddler crab can detect visual stimuli with polarization-only contrasts, which is processed independently in parallel channels to intensity contrast information.

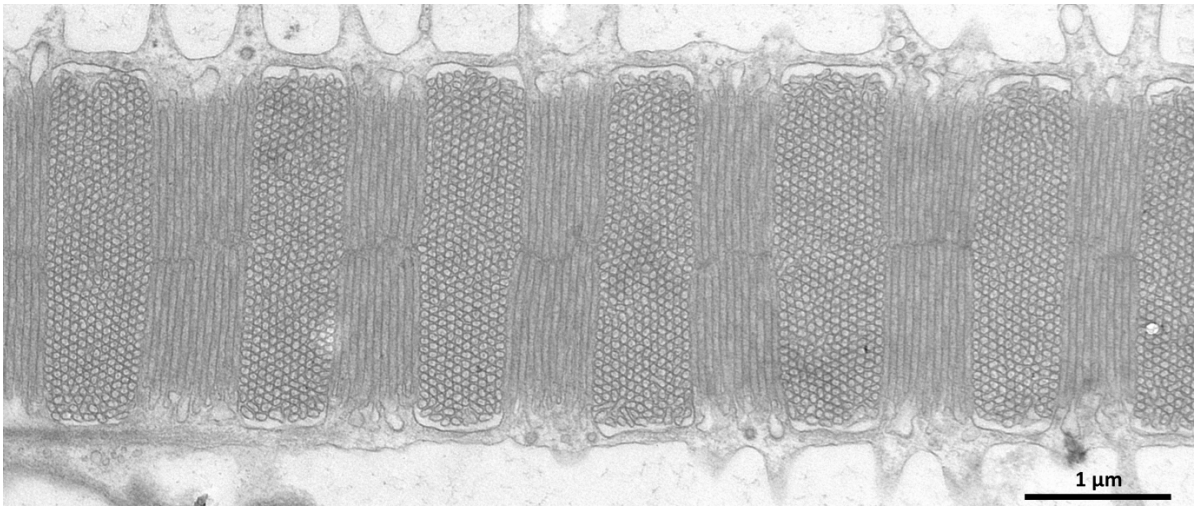

FIGURE 1.4. TEM of a fiddler crab rhabdom (*A. tangeri*) sectioned along its long axis to reveal microvilli arranged in neat bands with two perpendicular orientations, horizontal and vertical. The photoreceptors to which they belong can thereby compare excitation levels from incoming light and receive information on its polarization properties.

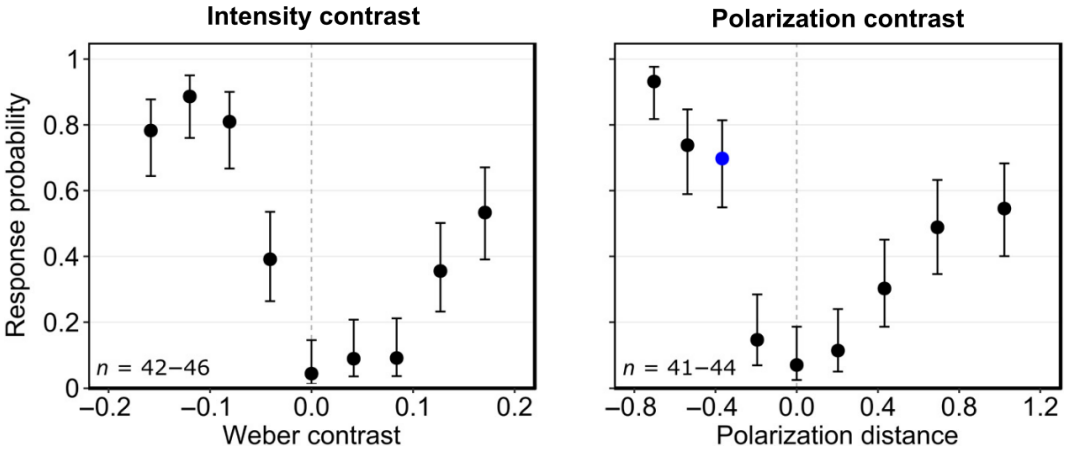

FIGURE 1.5. The results of a behavioural experiment showing that *A. tangeri* respond reliably to looming stimuli with high intensity contrasts (left), and high polarization contrasts (right). Note the similar response probabilities to the two types of visual information; Figure from ref: [68].

1.2 Fiddler crabs

1.2.1 Taxonomy and morphology

Fiddler crabs are highly active intertidal crustaceans, known for the extreme asymmetry of the male major claw and their charismatic waving behaviour associated with courtship. They are small burrowing crabs distributed widely across tropical and subtropical regions of the globe along intertidal flats, beaches, estuaries, mangroves and saltmarshes [50].

All fiddler crabs belong to the family **Ocypodidae** Rafinesque 1815 (Crustacea, Brachyura), which has recently undergone a major reclassification due to new molecular phylogenetic evidence [91]. Previously, Crane [50] had divided the family Ocypodidae into two subfamilies separating the ghost crabs (Ocypodinae) from the fiddler crabs (Ucinae). She grouped all 62 known extant species of fiddler crab from around the globe into one genus *Uca* Leach 1814, based on her extensive anatomical studies and geographic distributions of the animals, published in 1975. Fiddler crabs have recently undergone a major taxonomic revision. In 2016, Shih *et al.* [91] used molecular phylogenetics to radically reclassify the group, reorganising and renaming the species, raising many groups from subgenera to genera and expanding the number of recognised species to 105. They have now divided Ocypodidae into three subfamilies, containing 13 genera (Fig. 1.6).

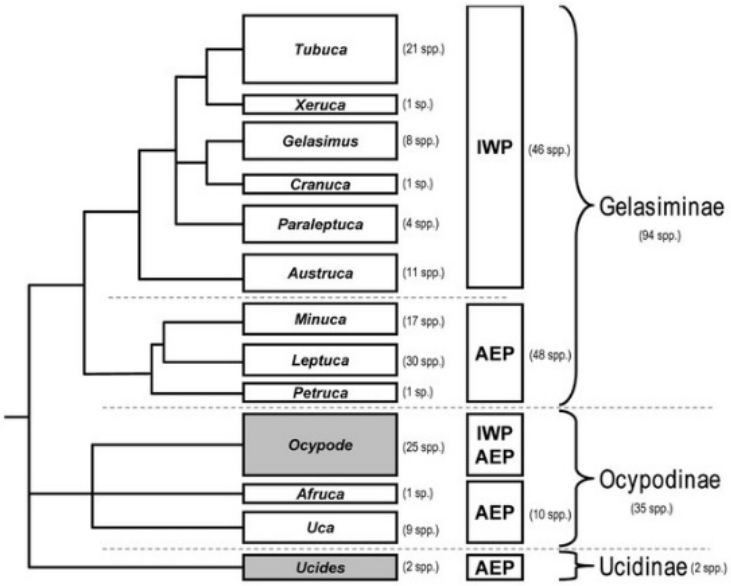

FIGURE 1.6. A simplified phylogenetic tree of the family Ocypodidae, showing the three subfamilies and their genera after reclassification with molecular data, source: [91]. Relationships between genera of fiddler crabs (white boxes) and non-fiddler crabs (grey boxes) are displayed with number of species beside/below the name. Geographic distribution is also shown as Indo-West Pacific (IWP) and/or Atlantic-East Pacific (AEP).

Fiddler crabs come from two of the subfamilies, the first is **Ocypodinae** Rafinesque, 1815, which contains the ghost crab genus *Ocypode* and two fiddler crab genera (*Uca* and *Afruca*). The second is **Gelasiminae** Miers 1886, which contains nine fiddler crab genera.

Fiddler crabs are small, adults typically measuring 10 to 35 mm across the carapace [50], although occasionally large individuals from *Uca* (*senso stricto*) reach nearly 50 mm [50, 92]. They are often colourful, especially during breeding periods and exhibit extreme sexual dimorphism (Fig. 1.7). Females have a wider abdomen than the males for carrying eggs and two small feeding claws. In males, one claw is hugely enlarged and can span the whole width of the body, weighing up to 40% its body weight [93]. These dominant chelipeds are used in combat with other males and in most species, including *A. tangeri*, left- and right-clawed crabs are found with equal frequency within a population with no female discrimination for "chelipededness" [94, 95]. Adult males from the species *Uca stylifera* have a long terminal ocular style of unknown function extending from the eye stalk on the same side as their dominant cheliped [50, 96]. Males of a closely related species, *Uca heteropleura*, have a longer eye stalk on the dominant side, meaning that one eye is higher than the other. Usually though, the eyes of most fiddler crab species are not sexually dimorphic, although males of some species may have slightly larger eyes than females in relation to body size [89, 97].

FIGURE 1.7. Sexual dimorphism in *A. tangeri*. The male fiddler crab (left) has one hugely enlarged cheliped, whereas the female (right) has two small feeding claws

1.2.2 Life history and ecology

Fiddler crabs live in dense colonies on tidal flats, often dominating the megafaunal communities. They spend high tides, cold weather periods and often nights sheltering inside individual burrows, which they plug themselves inside as a refuge from adverse weather, tidal currents and predators [50]. They leave their burrows during low tides to graze on the drained sediment until around an hour before the rising tide floods again. The crabs use their small feeding claws to scrape material from the sediment surface into their buccal cavity, where nutritious microalgae is separated from the inorganic material and ingested [98]. They are also known to feed on macroalgae and

occasional fish carcasses, but usually stay close to their own burrow for safety and to access water. During some low tides however, larger adult *A. tangeri* flock together in large numbers to venture some distance away and explore new feeding grounds [99].

Fiddler crabs have a typical brachyuran crab life cycle. Depending on species, males and/or females exhibit mate searching behaviours where they will leave the safety of their own burrow to tour neighbouring ones [100, 101]. In female searching species, such as *A. tangeri* [95, 101], successful mating is usually dependent on assessment of size and waving display of the male dominant claw, so males of these species tend to have more elaborate and vigorous displays [100]. Female *A. tangeri* will also assess male burrow characteristics [102, 103] before entering his burrow where she will spend two weeks gravid with eggs held under the abdomen [101, 104]. Male searching species (these including some *Gelasimus* species [100]) tend to have less complex waving displays and mating occurs at the entrance of the female burrow, where she will remain with her fertilised eggs [101]. Hatching is usually timed with nocturnal spring high tides to maximise dispersal [105], when the larval crabs (zoea) are released into the water and flushed offshore with the ebbing tide. In this pelagic environment they undergo metamorphosis and grow, passing through the planktonic megalopa stages until they moult into tiny juvenile crabs on returning to a suitable sheltered intertidal habitat [106]. They moult many times before reaching their adult size and individuals are thought to live for up to 7 years or more [107].

1.2.3 Habitat characteristics and adaptations to visual scenes

Fiddler crabs and ghost crabs from the family Ocypodidae are semi-terrestrial, occupying sheltered intertidal zones of soft sediment in tropical or semi-tropical estuaries, mudflats, swamps, mangroves and seashores [50]. They are found in high densities and construct burrows in the sediment [108], making them important for local bioturbation and sediment dynamics [109]. Each crab forages over a small territory of space close to its burrow, which males will defend with combat if challenged [110–112].

Brachyuran crabs have eyes on mobile stalks and are described as being either "narrow-fronted" (Fig. 1.8a) or "broad-fronted" (Fig. 1.8b), depending on the distance between basal joints of the eye stalks. Narrow-fronted species such as fiddler crabs are closely correlated with flat, open habitats [50, 113, 114] where the primary visual feature is the horizon between ground and sky. These crabs have regionally specialised eyes, elongated vertically with one or two acute zones across the horizon, near the eye equator [113, 115–117]. The compound eye wraps around the end of long eye stalks held almost vertically upwards, providing a panoramic visual scene (Fig. 1.8c).

While the eyes can be lowered into deep orbital grooves for protection and cleaning, they are usually held high above the body in a close-to vertical alignment with respect to the horizon [113]. This allows partitioning of the visual scene as conspecifics will always be viewed in the ventral hemisphere of the eye against a background of relatively dark, uniform substrate [113, 114, 118].

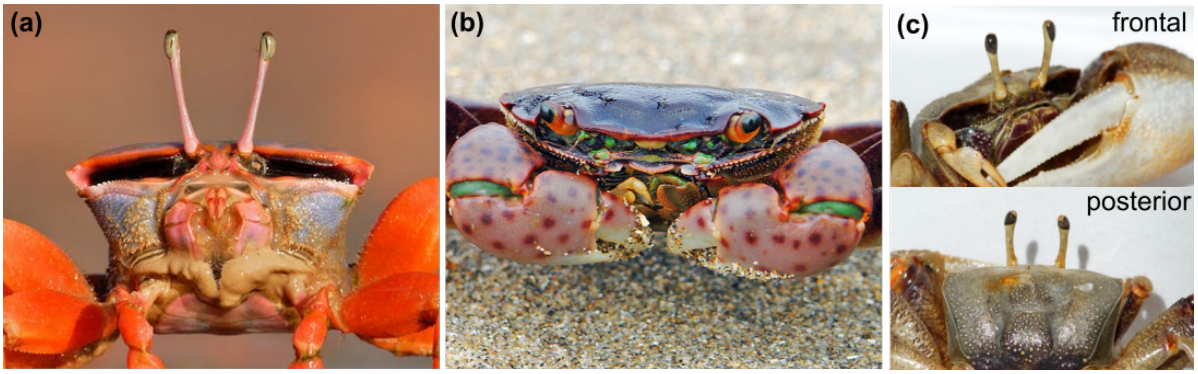

FIGURE 1.8. **(a)** Example of a narrow-fronted species, the flame-backed fiddler crab, *Tubuca flammula*, with small space between its long eyestalks, held high above the body. Photo credit: O. Levy (2012), retrieved with permission. **(b)** Example of a broad-fronted species, the purple shore crab *Hemigrapsus nudus*, with a wide gap between short eye stalks. Photo credit: D. Hogan (2007), retrieved with permission. **(c)** Male fiddler crab *A. tangeri* photographed in frontal and posterior view, to show the panoramic field of view that is provided by the compound eye that wraps almost fully around the eyestalks.

Objects that do not reach above the horizon will be smaller than the crab, so therefore, vision in this lower terrestrial zone of the visual scene can be dedicated to social interactions with nearby conspecifics, rather than predator detection (Fig. 1.9). Objects that are taller than the crab's own eye level, or that are in the sky (such as flying birds), appear above the horizon in their visual scene [113, 114]. Here, the upper hemisphere of the fiddler crab eye can reliably detect moving objects against a background of brighter, more polarized skylight [68, 114]. (Fig. 1.9). Thus, moving objects are perceived in the upper region of the eye as potential predators and behavioural experiments have demonstrated that moving objects above the horizon can reliably provoke an escape response in fiddler crabs [118].

Broad fronted crabs tend to have round eyes on short widely-spaced stalks (Fig. 1.8b). These crabs are mostly associated with complex intertidal or marine habitats and this lack of uniformity in the visual scene has not driven regional specialisations of the eyes to the same extent as in narrow-fronted species [50, 113].

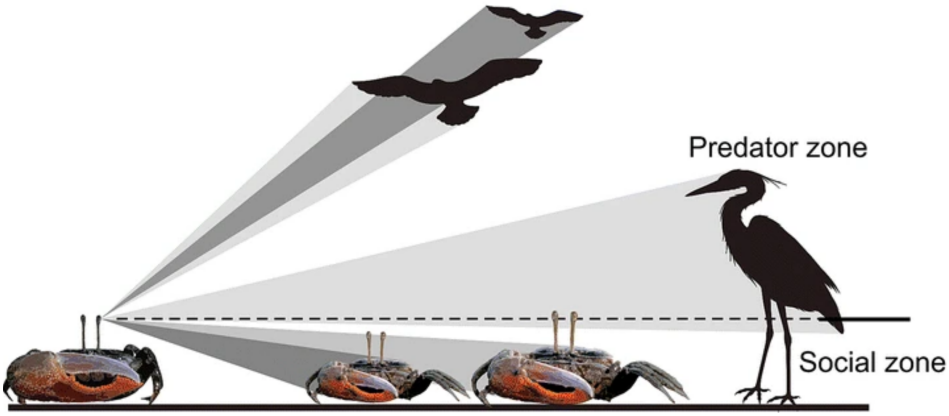

FIGURE 1.9. The visual scene of a fiddler crab is divided by the horizon, allowing discrimination of moving objects into a predator zone and a social zone. Eyes held high above the body mean that conspecifics usually appear below the horizon against a substrate background in the ventral hemisphere of the eye. Above the horizon, small dark objects against a brighter sky are usually perceived as a predator threat. Figure from ref: [114].

1.2.4 Intraspecific social interactions

Fiddler crabs are highly visual animals and live in close proximity with one another, regularly interacting and responding to conspecific behaviour. They monitor their scene constantly whilst foraging and respond instantaneously and almost synchronously to small sudden locomotive movements made by their neighbours, anticipating predator escape response. Males will compete for a good quality burrow that can attract high numbers of female visitors [103], meaning they may face frequent potential combat situations. Simply assessing the claw size of an opponent will often settle a dispute, however males with similar-sized chelipeds will sometimes use these giant claws to battle (Fig. 1.10a), occasionally resulting in serious injury or even fatality [110]. There have also been accounts of conspecific cannibalistic attacks by male fiddler crabs [119], although this is very rare in most species.

Males wave their large claws in a courtship display during the breeding season to attract a female mate [50, 95, 120] (Fig. 1.10b). To find a good quality burrow in which to spend her two weeks whilst gravid after mating, a female *A. tangeri* uses two main visual signals when choosing a mate. Large claw size and high rates of waving displays signal that a male is physically able to fight other males in order to defend his burrow [103]. Before making her choice, she may also inspect the mudballs surrounding her potential mate's burrow entrance, which are created during its excavation and then carefully arranged by the male to advertise its internal attributes, such as its depth [102].

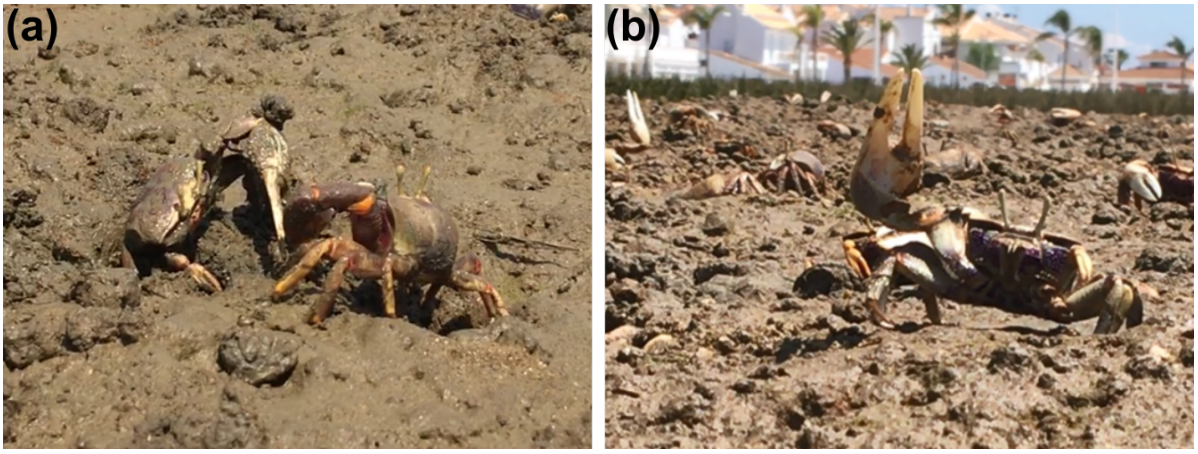

FIGURE 1.10. Intraspecific social interactions. **(a)** Two similar-sized *A. tangeri* males face off by locking dominant claws to test one another's strength. The crab on the right has approached the burrow of the defending crab. **(b)** A male fiddler crab photographed mid-wave during breeding season, in an ostentatious courtship display, performed on repeat whilst he feeds.

1.2.5 Predator escape responses

Predator avoidance is essential for survival and fiddler crabs are often regularly attacked by birds approaching from the air or across the ground [121]. Therefore, fiddler crabs use their visual system to constantly monitor the scene for danger. Tidal flats are home to many birds and other animals, but not all are interested in attacking the crabs, or close enough to be a danger. A bird flying at a distance causes a small change in light intensity or polarization contrast for very few ommatidia in the compound eye [114]. Fiddler crabs must constantly use a variety of visual cues to distinguish between threatening and non-threatening objects [122]. On detection of a potential predator above their horizon, the crabs use spatial information on its angular size and elevation [123, 124], as well as temporal properties of its velocity and flicker [125] to assess the threat level. This involves a calculation of the size and speed of the approaching object, which is used to determine the appropriate escape response [122, 126]. Typically, a sudden freeze is required to stabilise the visual scene, make a risk assessment and avoid detection by the predator [126, 127] and if necessary, the crab responds to a continued approach from the predator by running fast to the home burrow entrance. Here, it pauses again to make another decision based on continued surveillance on whether to retreat inside the safety of the burrow. Therefore, there is a multi-step decision-making process relying strongly on visual information [123, 124, 126, 127]. Bird attacks may happen frequently during diurnal low tide foraging periods [122] and there is new evidence to show that fiddlers are able to use selective attention to assess risk level of more than one simultaneous looming object, responding to the more dangerous (directly approaching) of the two [128].

1.2.6 Use as model organism

Fiddler crabs provide an excellent model system for arthropod behavioural studies and sensory biology and there is a wealth of literature covering many aspects of their biology and ecology. They display a suite of sophisticated behaviours associated with feeding, predator avoidance, burrow construction and maintenance. Fiddler crabs are known for their extreme sexual dimorphism and male claw asymmetry, which are used in various visual and auditory signalling behaviours as well as conspecific competition and predator defence [95]. These charismatic animals are very active at low tides and can be found in great numbers in suitable intertidal zones, interacting and feeding in dense social groups. Their burrow construction also has important effects on the physical, chemical and biological characteristics of their habitat systems [109].

The crabs will display clear predator avoidance behaviours, freezing still and then running to hide in their own burrow, a behaviour that can be replicated by dummy predators [122, 128], or even in laboratory conditions with a digital visual stimulus [129]. In their natural habitat they will behave as usual in front of a still camera or even a very still researcher, making it possible to perform observational studies with ease. Sex and even individual identity of fiddler crabs can be determined from their appearance (claws, body colouration, etc) or by the location of their burrow entrance, to which they tend to remain close to and visit frequently, especially on detection of a potential threat. They make a robust laboratory animal and can be transported, handled and housed for several months or years in an aquarium. This is due to a tough exoskeleton and intertidal euryhaline lifestyle, which provides tolerance to physical and chemical environmental changes [130].

As a result, fiddler crab behavioural ecology, evolution and ecological importance is well understood, due to an abundance of research. Their visual ecology is of particular interest and fiddler crabs, including *A. tangeri* continue to be widely used as a model by researchers investigating aspects of crustacean polarization vision [68, 69], colour vision [37, 39, 42, 45] and visually-guided behaviour [54, 95, 103, 111, 116, 128, 131].

1.2.7 Taxonomy and distribution of *Afruca tangeri*

The West African fiddler crab, *Afruca tangeri* Edyoux 1835, was the study species for much of the work in this thesis. It is distributed on shorelines reaching from the Algarve, Portugal in the north, along the northwest African coast, reaching Angola in the south [50] (Fig. 1.11, purple area). It is the only species of Ocypodid crab that can be found along Eastern Atlantic shorelines [132].

The West African fiddler crab was classified into subfamily Ocypodinae, which also contains the ghost crabs, *Ocypode* Weber 1795 and *Uca sensu stricto* (nine heavy-clawed fiddler crab species from American coastlines) [91]. The new taxonomic status means that despite fewer physical similarities, my study species *A. tangeri* is actually a closer relative of the ghost crabs than the majority of other fiddler crabs (see Fig. 1.6). They are one of the largest fiddler crab

species, reported to reach up to 50 mm across the carapace [50], although I personally have never seen one that exceeded 35 mm. Viewed via human colour space, they tend to be coloured brown to yellow on the dorsal carapace and legs, often with purple areas over the mouthparts, claws and legs. Males usually have a white front to their major cheliped.

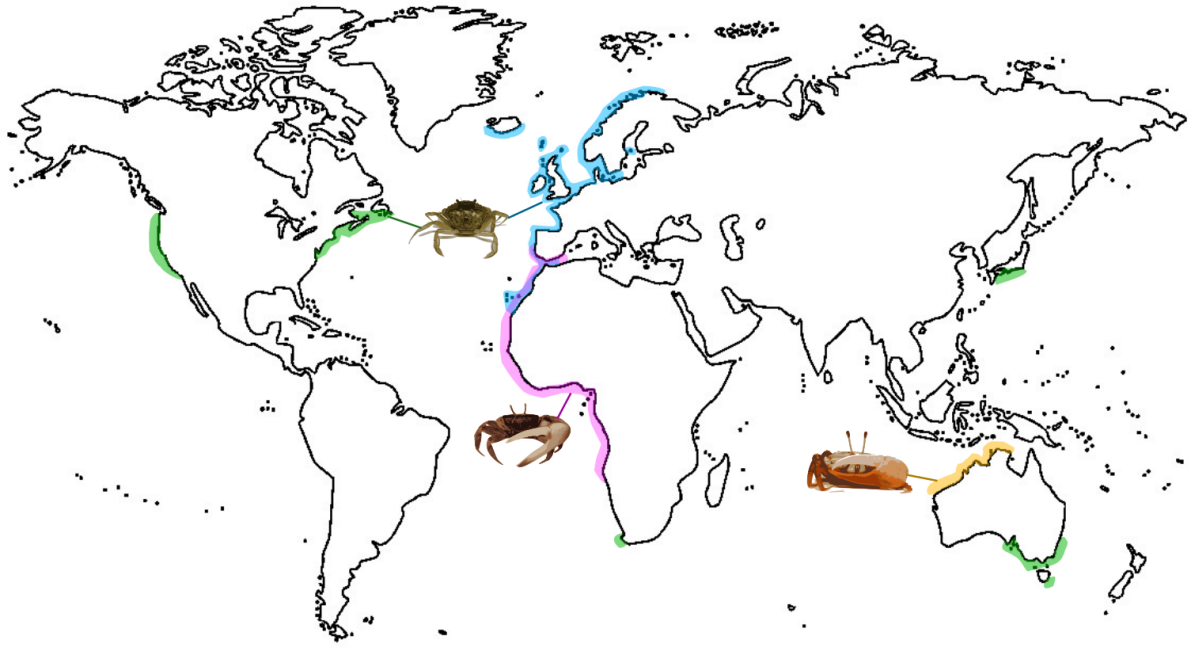

FIGURE 1.11. Global distributions of study species of crab. The native (blue) and invaded (green) ranges of *Carcinus maenas* [133] are mapped alongside the fiddler crabs *Afruca tangeri* (purple) [50] and *Gelasimus dampieri* (yellow)[134].

1.2.8 Taxonomy and distribution of *Gelasimus dampieri*

The fiddler crab *Gelasimus dampieri* (Fig. 1.12) was the study species used in my ERG experiments. It shares its tidal mudflat habitat with other fiddler crab species and is distributed along the northwest coast of Australia [134] from Isle Woodah in the Northern Territory, to Exmouth, Western Australia (Fig. 1.11, yellow area).

The species, named after the explorer William Dampier, was first described by Crane in 1975 [50]. Although she originally classified it within the genus *Uca*, along with *A. tangeri* and all other fiddler crabs, now with recent molecular evidence [91] we know that fiddler crabs are a widely divergent group containing two subfamilies. Dampier's fiddler crab is now classified in subfamily Gelasiminae and genus *Gelasimus* Latreille 1817. It is one of eight species from this genus, all from the Indo-West Pacific.

Despite the evolutionary and physical distances between them [91], the appearance and ecology of *G. dampieri* crabs is similar to that of *A. tangeri*. They are slightly smaller in overall

size, not known to exceed 22.5 mm in carapace width [50]. Although there is some individual variation in appearance, a human eye sees dark blue/black carapaces with white markings which brighten in breeding periods [50]. The dominant cheliped has an orange or yellow propodus with a white, sometimes pink dactylus. In comparison to *A. tangeri*, the eye stalks are slightly longer with respect to body size and the natural upright position is slightly more vertical. There are fewer studies on this species and it is not documented whether they are active after sunset. No nocturnal activity has been documented to date, or observed in the laboratory by researchers at University of Western Australia (personal observations and communications).

FIGURE 1.12. Photograph of a male *Gelasimus dampieri*.

1.3 The green shore crab *Carcinus maenas*

The fiddler crabs at El Rompido share their mudflat habitat with several other crab species, including a mud crab (species unknown, possibly *Scylla serrata*), the marbled rock crab *Pachygrapsus marmoratus* and the green shore crab, *Carcinus maenas*. The latter can also be found on UK shores and is often used for vision and neuroethology experiments by researchers at the University of Bristol. The eye anatomy and visual adaptation mechanisms of *C. maenas* were also unknown, so some histology using light and electron microscopy was carried out using a small number of individuals.

1.3.1 Taxonomy and biology

The green shore crab *Carcinus maenas* Linnaeus 1758 (Fig. 1.13) belongs to the portunid crab family Carcinidae MacLeay 1838 (Crustacea: Brachyura). The carapaces of adults, sometimes reaching 90 mm across [135], are coloured with cryptic colouration patterns to match their benthic backgrounds, becoming more uniform as the crab grows [136]. The phenotypic variation in colour and pattern correlates strongly with the visual features of its habitat [137]. The majority are coloured green (with dull brown/grey) to match the substrate and algae under which they hide in littoral zones. Red morphs with tougher carapaces (appearing dark brown underwater) are also

common, often associated with sexually-mature crabs who remain in deeper water, rather than intertidal zones [138, 139]. They are broad-fronted crabs, with round eyes on shorter eye stalks.

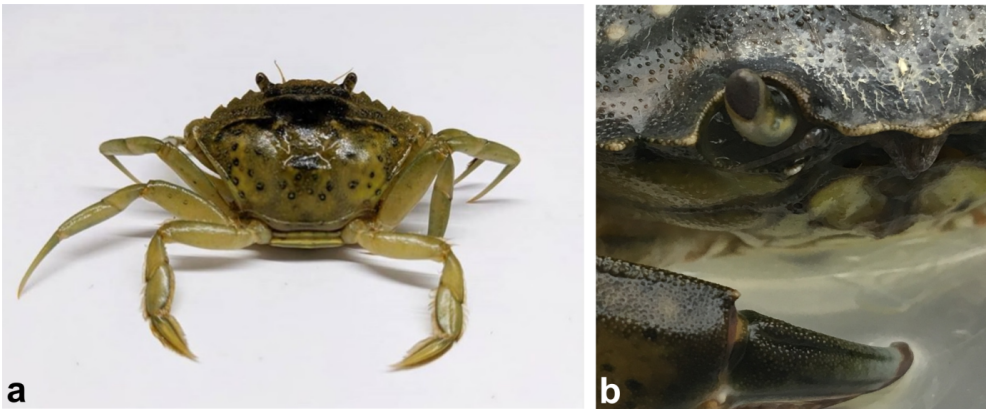

FIGURE 1.13. **(a)** Photograph of a *Carcinus maenas* individual collected from the mudflats in El Rompido, dorsal view. **(b)** Closer photograph of an individual of the same species collected from Clevedon UK, showing the eye, frontal view.

1.3.2 Habitat, distribution and ecology

In offshore waters, estuaries and along rocky shores [140], *C. maenas* is associated with a wide range of habitats and substrates [135]. It is a temperate water species, found in abundance around the British Isles and Ireland. Its native distribution extends from northern Norway to Mauritiana, northwest Africa [141] (Fig. 1.11, blue areas). Due to modern shipping it has been highly invasive and has now been introduced to other temperate shores (green areas, Fig. 1.11) in southern Australia, both Atlantic and Pacific coasts of North America, South Africa and southern Japan [142].

Broad-fronted crabs, like *C. maenas* are typically associated with visually complex habitats [113]. Although they can be found in the same mudflats as *A. tangeri*, they have a very different ecology. These crabs are mostly active at night and actively predate a wide range of available benthic invertebrate taxa, teleosts and algae [140, 143, 144].

1.4 Light / dark adaptation strategies in apposition eyes

Arthropod compound eyes first appeared ~541 million years ago and their evolution, bringing animals "into the light", is thought to be the predominant driver for the Cambrian Explosion [1]. In this relatively short period, there was a huge biodiversification in invertebrate taxa as eyes enabled visually-guided lifestyles that put strong evolutionary drivers on predator-prey relationships [145]. As well as complexification of brains and body plans to enable rapid locomotion, protection and cognition, eye designs also diverged widely to enable sophisticated

vision for arthropods, which began to occupy an enormous diversity of visual niches in land, air and water [2, 146].

Many terrestrial and shallow water animals must cope with light levels that vary from bright sunny skies to moonless nights a billion times dimmer [34]. Several different light- and dark-adaptation strategies have been described among members of the arthropods and they are as diverse as the optical architectures themselves, each highly specialised to suit the ecological needs and habitat of that animal. To cope with extreme fluctuations in brightness, an eye must alter its sensitivity to gather more photons in dim light, then prevent oxidative stress and photodamage to the photoreceptors in bright light [147]. Sigmund Exner [148] published the first detailed and comprehensive monograph on insect and crustacean eyes in 1891. It was in this work that pigment migrations were first described as a mechanism for adapting the compound eye of some animals to varying levels of brightness. Since Exner's research in the late 19^{th} century to the present day, scientists have continued to combine studies of optical physiology with neurophysiology, cell biology, molecular biology and animal behaviour, to gather insight into how the world might appear to animals with a very different visual system from our own. Here, I introduce the main mechanisms described in apposition compound eyes to temporarily adapt to changes in brightness in the visual scene.

1.4.1 Screening pigment migrations

Nearly all arthropod apposition compound eyes contain populations of screening pigment granules, either distributed within the photoreceptor cells themselves, or in adjacent accessory pigment cells, (sometimes referred to as glia) [7, 147, 149]. These granules are usually highly light-absorbent or reflective and may be fixed or mobile, travelling along microtubules in response to changes in light or circadian clock drivers [150, 151]. Often, an eye will contain various different pigment populations and even closely related species can present considerable differences in the distributions, size, chemical composition, spectral properties and mobility of these screening pigments [149, 152]. They function to intercept light paths with their absorbent or reflective properties and therefore, they are useful in reducing the amount of bright and potentially damaging light that reaches the photoreceptors [153]. Like the visual pigments of the rhabdom, they can be effectively tuned to light within a range of wavelengths, acting as spectral filters [154–156]. Sleeves of pigment surrounding the ommatidia can help to screen off-axis light from leaking between neighbouring eye units, to preserve fine spatial acuity [7].

1.4.1.1 Within photoreceptors

Migrations of mobile screening pigment granules provide an effective method for regulating light flux to the photoreceptor cells. Within photoreceptors, they may move either longitudinally in a distal-proximal direction, or radially in toward the light path to absorb photons as they

travel down the rhabdom, protecting the cells from over-exposure and light damage [157]. During radial pigment migrations, the granules contract inwards a short distance through the palisade bridges to tightly encircle the rhabdom in bright light (Fig. 1.14a,b). Here they interact with the wave-guide modes (transverse interference patterns) which propagate down the narrow rhabdom, ultimately reducing them in number [158, 159]. The pigment granules scatter and absorb modal light that travels outside the rhabdom, functioning as a elongated pupil. In dim light, the pigment granules recede outwards again, clearing the palisade and altering the refractive index of the medium surrounding the rhabdom. The watery electron-light palisade, made from modified endoplasmic reticulum cisternae, has a lower refractive index than to the rhabdom [160] and as a result, internal reflections maintain the rhabdom's function as an optical waveguide [161]. The outward migration of pigment granules in the dark supports the propagation of another mode (or two) through the rhabdom and surrounding palisade and therefore, this increases the sensitivity of the dark-adapted eye [7, 158, 160–162].

Longitudinal pigment migrations within photoreceptors are more common in superposition eyes [163], but there are examples of distal-proximal movements of pigment granules along microtubules in the cell somas of apposition eyes too. In the open rhabdom-type apposition eyes of the haematophagous insect *Triatoma infestans*, pigment granules within photoreceptors migrate longitudinally to facilitate their nocturnal lifestyles. During daytime, pigments surround the two central rhabdomeres to prevent light reaching the outer ones. At night the granules retract away from the rhabdoms, to concentrate in the proximal region of the cells, allowing light to reach the peripheral rhabdomeres, boosting sensitivity [151].

The crab *Libinia* has two populations of bi-directional screening pigment granules within photoreceptors. When the eye is light-adapted, they form a sleeve of continuous pigment that surrounds the length of the fused rhabdom. When dark-adapted, the pigments separate and half the granules migrate distally to concentrate in distal nuclear region, while the other group move proximally toward the basement membrane [164]. This was considered unusual at the time, but longitudinal migrations have also since been observed in *Hemigrapsus sanguineus* and *Leptograpsus variegatus* crabs [156, 165]. In the latter species, this is extreme. Under bright light exposure in daytime, the pigment granules surround the rhabdom along its length, most densely aggregated in the distal part of the photoreceptor cells. When dark-adapted at night, the screening pigment granules migrate proximally below the basement membrane, clearing away from the rhabdom almost entirely (Fig. 1.14c). The granules are very mobile and respond to changes in brightness differently in night and day. The distributions of these pigment granules not only affect light flux to the rhabdom, but also alter the crab's spectral sensitivity [156].

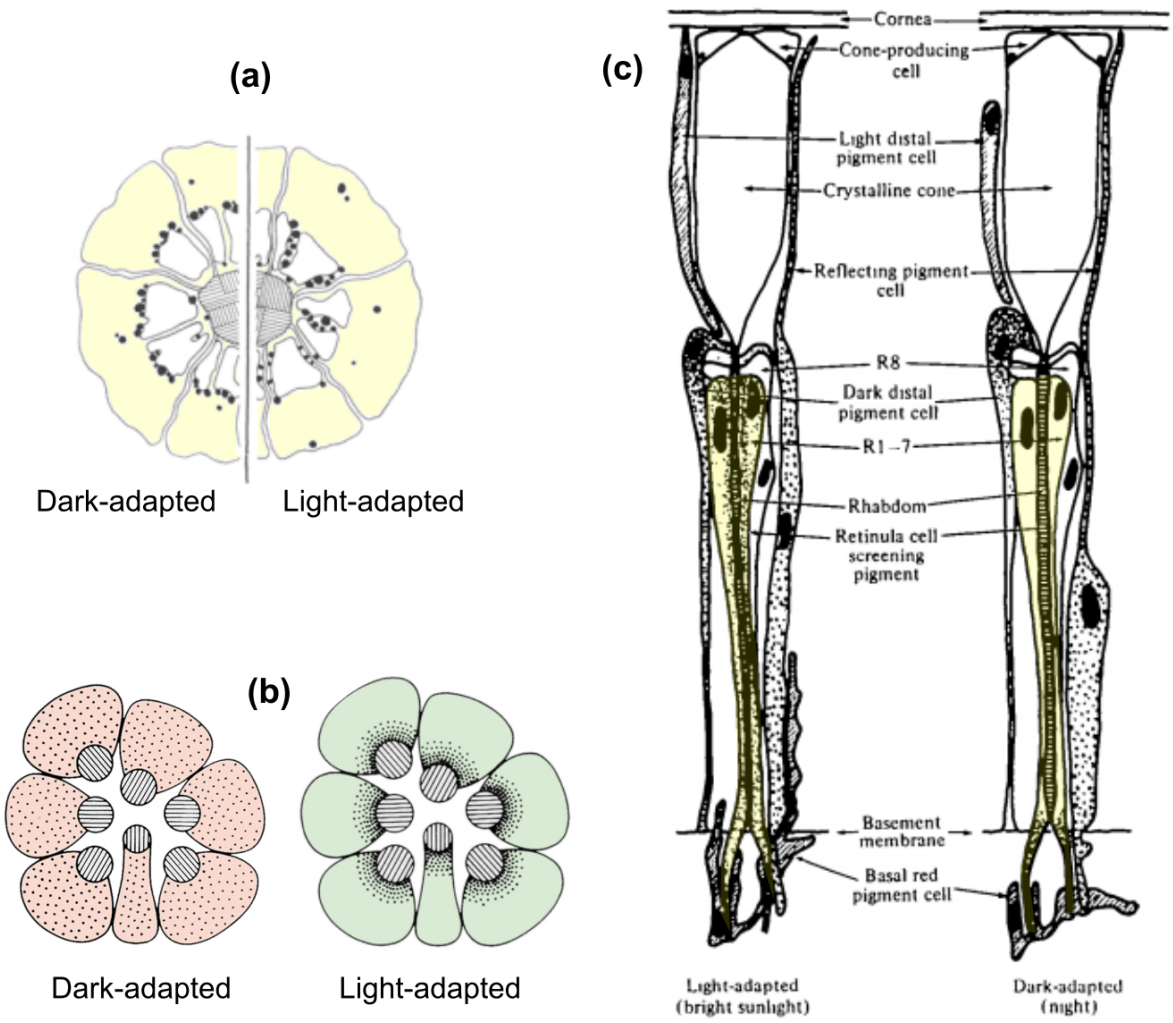

FIGURE 1.14. **(a)** Diagram of transverse sections through ommatidia of the stomatopod *Gonodactylus oerstedii*, showing radial migrations of screening pigment granules (black dots) in response to light, figure adapted from ref: [157]. **(b)** Radial pigment migrations also occur in the open rhabdom photoreceptors of the *Drosophila* apposition eye in response to light, figure adapted from ref: [166]. **(c)** Longitudinal pigment migrations in the photoreceptor cells (shaded yellow) of the crab *Leptograpsus variegatus*, note there are other conspicuous cell shape changes and pigment migration in other cell types. Figure from ref: [156].

1.4.1.2 Iris-like aperture mechanisms

Many apposition eyes possess accessory pigment cells associated with ommatidia to provide additional screening for the photoreceptors. There are often multiple types of these cells within a compound eye and they are commonly found associated with the basement membranes, stretched between photoreceptor cells or crystalline cones along their length, forming a sleeve to screen

from neighbouring ommatidia. Many arthropods have one or more sets of pigment cells located distally to the photoreceptors, which surround the proximal part of the crystalline cone tract, making a screening layer to prevent stray off-axis light from reaching the photoreceptors. There is great variety of absorbent and reflective pigment cell types and associated dynamic functions among the arthropods; in some pigment cells the granules remain immobile, while in others they migrate [149, 152].

In some animals, pigment cells form a collar above the rhabdom, around the proximal tip of crystalline cones, which stays wide for dim light vision at night to maximise light entering the eye. It can constrict the cone tract in response to bright light during daytime, like an iris. An excellent example of this variable aperture can be found in nocturnally-active *Camponotus*, *Myrmecia* and *Polyrhachis* ants [162, 167, 168], as well as the crane fly *Ptilogyna speetabilis* [169]. The pigment cells move apart to open an iris-type aperture in dim light at night, which increases acceptance angles considerably, as well as making the eye more sensitive. When insects with open rhabdom-type apposition eyes use equivalent pigment cell collars to constrict the crystalline cone tract, it can have the effect of cutting off the light flux to the peripheral rhabdomeres, only letting light into the central ones. This is true for the European earwig *Forficula auricularia* (Fig. 1.15), tenebrionid beetle *Zophobas morio*, the crane fly *Tipula pruinosa*, the backswimmer *Notonecta glauca* [170] and the parasitic insect *Triatoma infestans* [151]. Again, ommatidial acceptance angles are widened at night, so collecting light from a larger visual field means there is some sacrifice in spatial acuity [7].

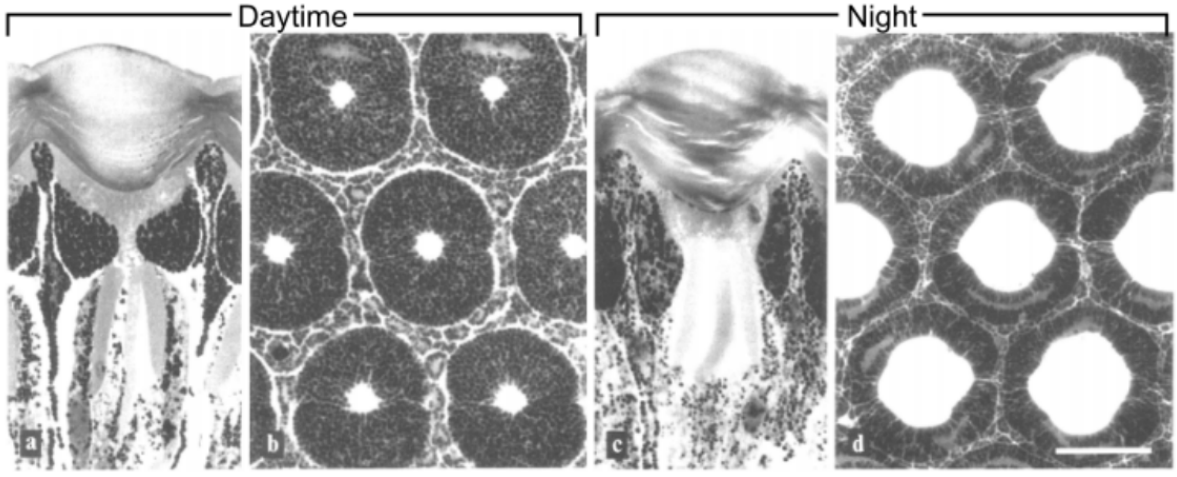

FIGURE 1.15. Semithin sections through the dark-adapted eye of *Forficula auricularia* during the day **(a,b)** and at night **(c,d)**. The longitudinal sections **(a,c)** show how the open rhabdom moves up and down as the primary pigment cells change their aperture. The screening pigment is aggregated around the rhabdomeres during the day, but not at night. The cross-sections **(b,d)** are at the level of the primary pigment cells, distal to the rhabdom. Scale bar 20 μm. Figure from ref: [170].

As a light- dark-adaptation strategy, several crab species are also known to undergo longitudinal and/or radial migrations of screening pigment granules within distally- and/or proximally-located pigment cells, e.g. [164, 165, 171–175], but there are major differences between even relatively closely related taxa.

1.4.2 Photomechanical changes in the lens

Theoretically, absolute sensitivity and acceptance angle of a single ommatidium in an apposition compound eye can be increased by shortening the focal length of the lens [176]. There are a few animals in which nocturnal crystalline cone shortening provides this function, for instance the brine shrimp, *Artemia* [177], which lacks any retinal pigment migrations. Its crystalline cone contains a central glycogen lens, solely responsible for focussing light onto the rhabdom tip (Fig. 1.16a). When light-adapted, the lens is rounded and the surrounding crystalline cone cells are long, creating a long focal length and small acceptance angle. When dark-adapted, the cone becomes shorter while the rhabdom elongates to come closer to the glycogen lens, which itself becomes less rounded [177]. This shortens the focal length, widening acceptance angle to improve photon catch, at the expense of poorer spatial acuity [7]. *Squilla* mantis shrimp and *Camponotus* ants have typical "eucone" type crystalline cones (as in crabs), in which glycogen particles are dispersed throughout its four constituent cells. The crystalline cones in these animals also shorten during dark-adaptation. As the proximal tip of the cone widens and contracts, there is a compensatory distal elongation of the rhabdom [167, 178]. This is then reversed during daytime so that focal length is shortened, creating smaller acceptance angles and a less sensitive eye.

1.4.3 Rhabdom changes

The microvillus-filled rhabdom is designed to maximise the amount of membrane surface area available for photon capture. Assuming the concentration of photopigment stays constant per square-micron of membrane material [179], increasing the volume of rhabdom is an effective method of increasing phototransduction rates, making the eye more sensitive during periods of dim light. This can be achieved by elongating the microvilli to widen the rhabdom, by or increasing the length of each rhabdom by adding more rows of microvilli. Lengthening the rhabdom as a dark-adaption strategy has been observed only in few cases, the previously mentioned *Camponotus* ants [167], *Artemia* brine shrimp [177] (Fig. 1.16a) and *Squilla* mantis [178], that compensate by shortening the crystalline cone lens. The only crab reported to increase the length of its rhabdom at night is *Grapsus* [180]. The crane fly *P. speetabilis* has a nice example of an eye that undergoes a combination of all the major adaptive changes described from day to night [169] (Fig. 1.16b). As well as pigment migrations inside photoreceptor cells and accessory pigment cells, it has a strong iris-type primary pigment cell constriction on the crystalline cone tip during bright light exposure in daytime. This causes the cone cells to lengthen and narrow, increasing focal length

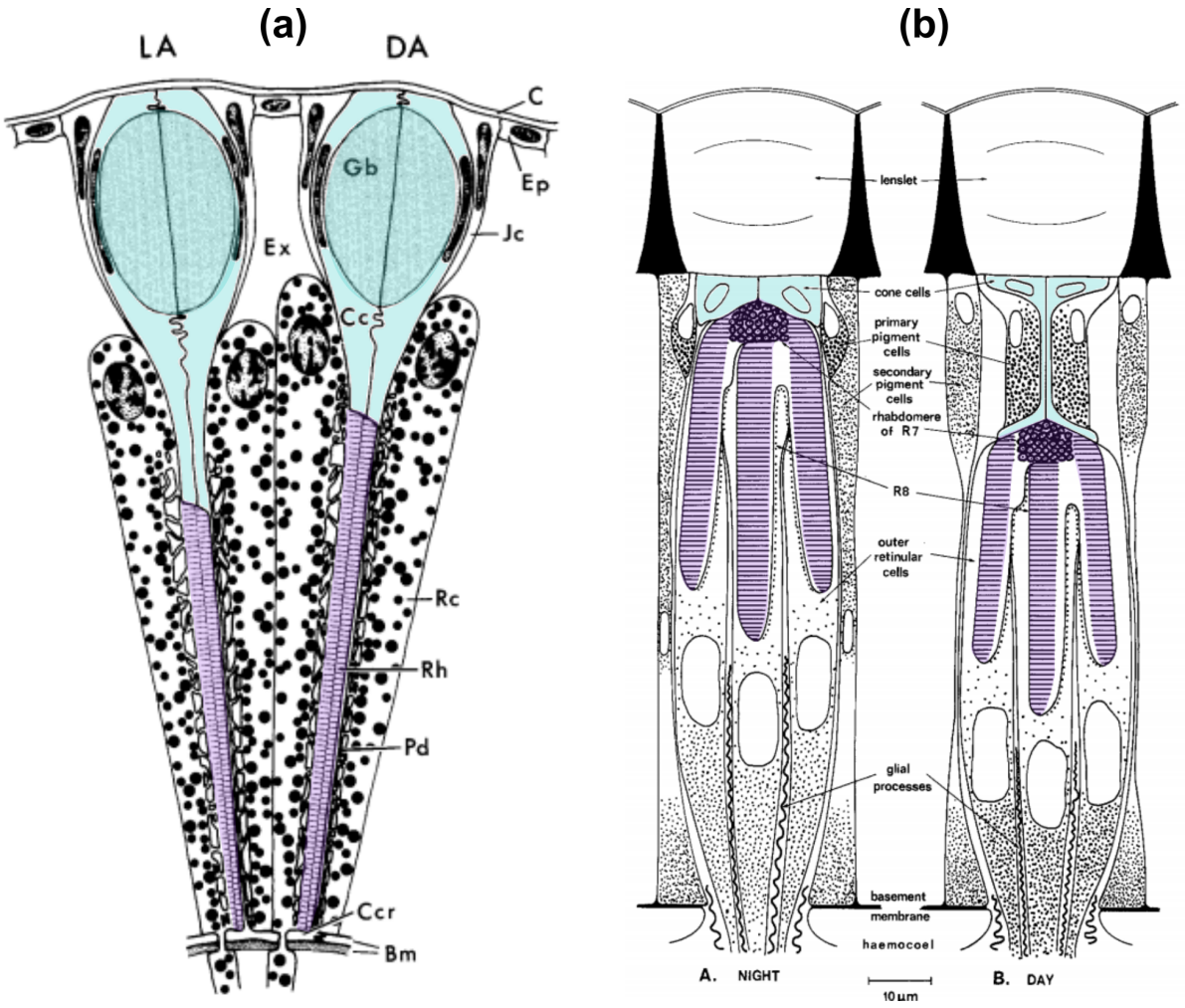

FIGURE 1.16. **(a)** In the eye of the brine shrimp, *Artemia*, there are changes in dimensions of the crystalline cone (Cc, blue) with its glycogen lens (Gb) and the rhabdom (Rh, purple), between a light-adapted (LA) and dark-adapted (DA) state. Figure from ref: [177]. **(b)** In the eye of the crane fly *Ptilogyna speetabilis* there are several changes from night to day. Primary pigment cells constrict and lengthen the crystalline cone tip (blue) in response to bright light, which shifts the photoreceptors in a proximal direction. Their rhabdomeres (purple) also become shorter and narrower in daytime. Note pigment migrations inside photoreceptors and surrounding accessory pigment cells. Figure from ref: [169].

and the position of the open rhabdom is shifted in a proximal direction. At night, the rhabdomeres themselves become ~10 μm longer, in addition to widening by 87% from midday to midnight.

Widening of the rhabdom diameter seems to be a common strategy among crabs [165, 180–184] and Orthopteran insects (e.g. a locust [185], cricket [186], praying mantid [187]). Increases in rhabdom volume boosts sensitivity in dim light for these animals after sunset. Changes of this

kind are also known in various other arthropod taxa, including a tipulid crane fly [169], crayfish [188] and spiders [181, 189]. There may be others, however there is little literature on this topic from the past two or three decades.

1.4.4 Summations in space and time

Vision in dim light may also be improved in visual processing by summation of channels over time or space to collect more photons, resulting in a strategic trade-off in spatial or temporal acuity, depending on the specific visual demands of the animal [34]. **Temporal summation** works by neural pooling of photoreceptor signals over time via an exponential low-pass filter in the photoreceptor cell membranes, to increase integration time [30, 176, 190, 191]. From a given portion of space, more photons can be collected by the photoreceptors and the scene will appear brighter. This works the same way as lengthening the shutter speed of a camera to photograph a dim scene. Fast moving objects will appear blurred as temporal resolution is lost in this process [34, 191, 192]. A tool widely used in evaluating the temporal resolution of an animal's visual system is **critical flicker fusion frequency (cFFF)**. Above a particular frequency, a flickering light stimulus will be perceived by the viewer to be continuous [31]. Human cFFF can be as high as 70 Hz in bright light [193], but this is reduced when the eye is dark-adapted, due to temporal summations [31]. Fast flying animals such as birds or insects tend to have a very fast temporal acuity, for example the tsetse fly *Glossina morsitans*, with cFFF that can exceed 200 Hz [194]. Longer integration times are correlated with slow moving, nocturnal lifestyles, or increasing water depth in deep sea crustaceans. Some mesopelagic shrimp (Pasiphaeidae and Sergestidae) have a maximum cFFF of just 17 Hz [195].

The flight activities in some nocturnal or crepuscular insects, such as the sweat bee, demand fast temporal acuity that cannot be sacrificed to improve photon catch in dim light [191, 196, 197]. **Spatial summation** provides an alternative neural mechanism with which to boost sensitivity. Long laterally-branching dendrites from the lamina monopolar cells reach over to collect and pool visual signals from neighbouring ommatidia, at the expense of spatial resolution in the cockroach, nocturnal bee and hawkmoth [30, 34, 191, 198]. Stöckl *et al.* [199] showed that the hawkmoth *Deilephila elpenor* uses both temporal and spatial summation simultaneously to enable the demanding task of hovering in flight in very dim light.

1.5 Research questions

With growing knowledge among the scientific community on aspects of fiddler crab vision on the primary retinal basis (eye optics), to how visual information is processed in neural circuits and used to direct behaviours (neuroethology), this PhD project aimed to answer important questions on their light- and dark-adaptation mechanisms. There is no previous research on this subject in fiddler crabs so it was assumed to be similar to other crabs e.g. ghost crabs or more

distantly-related grapsid crabs, which have been historically examined, [156, 164, 173, 180, 182–184, 200–204]. However, adaptation strategies, particularly of pigment migrations, appear to vary considerably between the brachyuran crab species studied, so it is not possible to make confident predictions for these in fiddler crabs. As there has been no systematic study on adaptive changes in the fiddler crab visual system, my first two questions were, **1. How does the fiddler crab eye adapt from light to dark?** and, **2. How do these changes affect functional aspects of its visual sensitivity?**

Fiddler crabs are associated with very bright sunny habitats, but there are two regular occasions when they will experience very dark conditions. The first is of course, between sunset and sunrise, and based on previous studies of other crab taxa e.g. [164, 180, 200], it is reasonable to expect that the eye undergoes a dramatic transformation at night, which is effectively inhibited during day. So my next question was, **3. Are there endogenous circadian rhythms involved in dark-/light- adaptation mechanisms?** The other regular instance of darkness is when an individual enters its burrow to re-hydrate or escape a potential predator. This can be a brief but regular occurrence and adaptations must be quick and reversible to allow effective vision in bright light on exit, important for their survival. So I asked, **4. What happens to the eye inside the burrow?** which led to the next related question, **5. How fast can their eyes adapt?**

Fiddler crab activity is restricted to the rhythmic low water phases of tidal periods. They are known to possess persistent biological clocks to predict these, which have strong effects on activity [205–209]. So I asked, **6. How important is it to consider tidal phase when designing experiments that assess aspects of vision?**

Sunlight reflecting off the sheltered intertidal flats on which they live creates an environment rich in bright horizontally polarized light. We know that the visual systems of fiddler crabs are sensitive to polarization information [67–69] and two Australian fiddler crabs (from subfamily Gelasiminae) have been shown to possess regional anatomical specialisations in the eye that favourably detect vertical e-vectors of light [210]. This functions to filter out some of the horizontal glare from the environment, a strategy also employed by pond skaters, *Gerris lacustris* [211]. This would also provide a useful light-adaptation mechanism, so the next question was, **7. Does the eye anatomy of *A. tangeri* also help to screen out horizontally polarized light?**

Fiddler crab habitats are often close to built-up areas and are affected by anthropogenic light pollution at night. This is certainly the case at my study site in El Rompido, a small town and popular holiday destination with beach-side restaurants and marinas. Animals can be affected in various ways by light pollution, but to investigate whether there are any noticeable effects on eye physiology, I asked, **8. Is adaptation state of the eye affected by local light pollution at night?**

CHAPTER 2

PRINCIPAL METHODS

To avoid repetition, this chapter contains some principal methods used within the following data chapters. These include collection and care of crabs used in the experiments, in addition to the complete transmission electron microscopy (TEM) protocol, outlining each step from eye sample collection to imaging. The common methods used in the electroretinogram (ERG) experiments of chapters 4 and 5 are also described herein.

2.1 Collection and care of animals

The three crab species studied as part of this project are common and numerous in their habitats and can easily be collected from shorelines at low tide. Crabs are physically robust and therefore, transportation and husbandry of these animals in the laboratory is relatively easy. Where possible, every effort was made to hold crabs for the minimum time necessary for experiments, and later return them unharmed to the place they were collected. Release was of course not possible for crabs involved in histological experiments. All experiments were conducted in accordance with UK legislation and with the ethical approval of Animal Welfare and Ethics Review Body at the University of Bristol, under UIN agreement number UB/18/070. At the University of Western Australia (UWA), I was authorised with "Permission to Use Animals" and completed the Programme in Animal Welfare, Ethics and Science (PAWES) course. Experiments were carried out with full compliance with Australian animal welfare legislation, in addition to UWA policies on The Use of Animals in Research and Teaching.

2.1.1 *Afruca tangeri*

Adult male and female fiddler crabs of the species *Afruca tangeri* were collected from mudflats in El Rompido, Andalucía, Spain (37°13'02.3"N, 7°07'08.1"W). Depending on time of day or weather conditions, the crabs could be simply picked up from the mud surface by intercepting their route to their burrow, but often they had to be dug by hand from inside the burrow. If captured, gravid females were returned immediately. The crabs were washed in clean seawater and transported in buckets to a nearby temporary field laboratory in El Rompido. Here they were separated into individual clear plastic pots, containing 1-2 cm of seawater and some paper towel to hide under. Individuals were given an identification number and sex was determined from examining the chelipeds and abdomen. Size was measured using calipers across the widest part of the carapace. The crabs were housed outdoors in their labelled pots under indirect solar illumination (unless otherwise stipulated) for the minimum time possible, typically 1-4 days before release (or euthanasia for TEM samples). For stays of more than 24 hours, the crabs were given fresh seawater and fish flake food daily.

2.1.2 *Gelasimus dampieri*

Collections of male and female fiddler crabs of the species *G. dampieri* were made from tidal mudflats near Learmouth (22°18'01.0"S, 114°09'11.3"E), Western Australia, by members of the Hemmi Lab, University of Western Australia (UWA) in January 2019. The crabs were transported by car to Perth and released into an artificial mudflat (Fig. 2.1) in an animal facility at UWA. This 2-metre diameter circular tank was filled 1 metre deep with sediment collected from the crab's natural habitat. Overhead, heat lamps and bright broad spectrum UV/white lights, warmed and illuminated the mud surface, operated by a timer on 12:12-hour light:dark cycle. Alternating "tidal" periods of high and low water occurred, whereby the mudflat surface was flooded and drained with seawater every 6 hours. An associated water storage tank and pump on a timer controlled the water level. Water quality checks for salinity, pH, temperature and dissolved nitrogen compounds (nitrate, nitrite and ammonia), were carried out three times a week. In this environment, the fiddler crabs behaved as in their natural habitat, building burrows in the sediment and feeding on algae on the surface, enriched with fish flake.

When required for experimentation, individuals were captured from the mudflat system. The captor waited motionless until the crab had surfaced and travelled a few inches away from its burrow, then the burrow entrance was quickly covered with a small aluminium sheet on a long pole. The crab would run to the entrance and try (unsuccessfully) to dig down on the metal, from which they could be picked up by hand and transferred to a smaller facility designed for temporary accommodation during experiments. This aquarium consisted of a wide polyvinyl chloride (PVC) half-pipe with small amount of sediment and 1-2 cm seawater running through. Barriers along the pipe only allowing water through, divided it into compartments so that individuals could be

separated and identified for experiments. They were each provided with a PVC tube "burrow" in which they could hide and were given food pellets three times a week. The small facility was subject to the same light and “tidal” cycle as the mudflat, and as it was fed from its own water tank, quality checks on the water system were made separately.

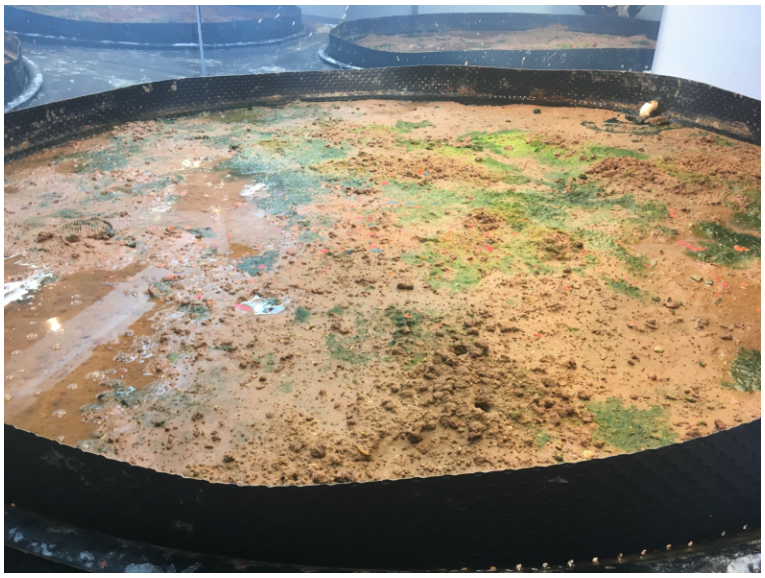

FIGURE 2.1. Artificial mudflat facility at UWA, in which fiddler crabs were accommodated for several months prior to experiments. Burrows built by the crabs themselves, extend down into the 1 metre deep sediment.

2.1.3 *Carcinus maenas*

Collections of green shore crabs (*C. maenas*) were made on the coast of Clevedon, UK (51°26’19.6"N, 2°51’54.3"W). Crabs were hand-collected by searching under rocks and seaweed at low tide and transported to an aquarium at laboratories in the University of Bristol. Here, individuals were separated into transparent plastic containers with holes to allow water circulation. The aquarium contained ~3 cm of filtered saltwater, circulating via a pump. Salinity was maintained around 35 ppt and crabs were fed a mixed diet of marine molluscs and crustaceans twice weekly.

2.2 Pre-adaptation of the crab visual system to light and dark

In many experiments within this thesis, the crabs are described as being light-adapted or dark-adapted. To clarify these terms, a dark-adapted state was achieved by placing a crab inside a lightproof box in a darkroom for several hours to prevent exposing its eyes to light. Any handling of crabs in this state e.g. preparing for experiments or dissection, was carried out in darkness with the aid of indirect illumination from a dim lamp covered with red filter (No.027, Lee Filters, Andover, UK). This filter removed all wavelengths shorter than 600 nm, with peak transmission

at 630 nm and was visible to the human eye as a dim red light (Fig. 2.2a). The spectral sensitivity of *A. tangeri* peaks at 530 nm and it is not sensitive to long wavelengths [37]. There is some overlap in the lamp emission and spectral sensitivity curves, but sensitivity declines steeply after 600 nm in this crab, so the light from the red lamp, if detectable, would appear very dim and is unlikely to evoke a light-adaptation response. Long wavelength sensitivity in *G. dampieri*, is even lower and according to ERG data [42], peak sensitivity is around 440 nm. The spectral sensitivity curve for this species [45] does not overlap with the red lamp emission at all (Fig. 2.2a), implying that this species cannot detect it at all.

A light-adapted state was achieved by placing the crab (in its seawater pot) under bright light to expose the visual system, either outside in the bright sunshine, or under intensity-controlled bright artificial lights. Figure 2.2b shows the normalised spectra of these lights as quantum catch values based on the spectral sensitivity of *A. tangeri*. There is some difference between the shapes of the absorbance curves. There is very little absorption of light from the red lamp by the visual pigments, as predicted.

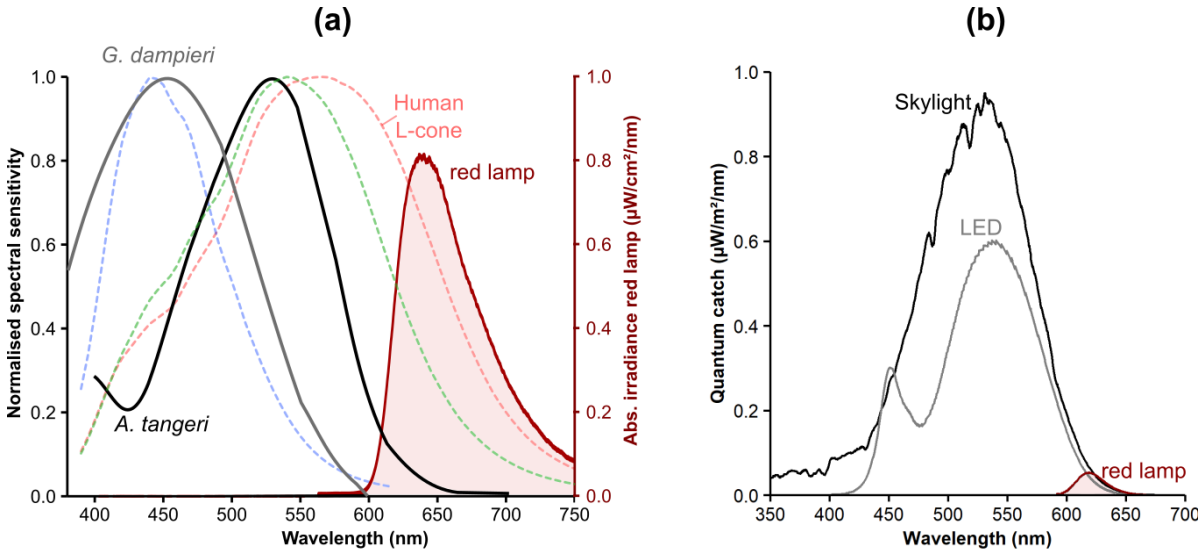

FIGURE 2.2. **(a)** Irradiance spectrum (right y-axis) of a dim red lamp used to illuminate dark-adapted crabs when handling (red shaded curve). Normalised spectral sensitivity (left x-axis) is represented by black solid line for *A. tangeri* (source: Fig. 3 in ref: [37]) and by grey solid line for *G. dampieri* (source: Fig. 3b in ref: [45]). The short, medium and long wavelength sensitivities of human cone cells are represented by blue, green and red dashed lines, respectively (source: transformed and normalised values from Table 2, ref: [212]). **(b)** Normalised spectra of the dim red lamp, natural skylight (midday, El Rompido) and LED lighting used to light-adapt crabs, plotted as quantum catch values based on a template of absorbance in invertebrate visual pigments [38], adjusted to *A. tangeri*'s λ_{max} of 530 nm [37].

2.3 Methods for anatomical study

2.3.1 Dissection and fixation of eyes

After pre-adaptation to the desired light level, both eyes were dissected by severing the connective tissue at the base of the eyestalk using a razor blade dipped in fixative, a method which best preserves the eye structures [89]. Crabs were euthanized immediately after by severing the thoracic and cerebral ganglia. Dissection took place under their adapting light level, using a dim red lamp to illuminate when necessary (emission spectrum in Fig. 2.2). Dissected eyes were placed directly into chilled fixative containing 2.5% glutaraldehyde and 4% paraformaldehyde in 2x PEMS buffer (adapted from [85]). Later (within 2-24 hrs), the soft eye parts were dissected away from the chitinous eye stalk in fixative using a dissection microscope under bright light for light-adapted eyes, or in a darkroom using only a dim red lamp for dark-adapted eyes. The eyes were left to fix in a refrigerator for at least three days.

2.3.2 Sample preparation and embedding protocol

After fixation, the eyes were transferred to small glass vials on a rotator in a fume hood. The fixative was washed away with 2x PEMS buffer, three times for 10 minutes. They were then stained with 2% osmium tetroxide (in distilled water and buffer solution) for 90 minutes. After cleaning away excess osmium with three 10-minute washes of distilled water, the samples were dehydrated with increasing concentrations of graded ethanol (in 25, 50, 70, 80, 90 and 96% concentrations, for 10 minutes each). Finally, they were dehydrated in three washes of 100% ethanol, then three washes of 100% propylene oxide. The samples were gradually infiltrated with EPON resin as follows: They were left overnight on a rotator in small vials containing 50% propylene oxide and 50% resin. The next day the resin concentration was increased to 100% and this was changed for fresh resin three times for 1-3 hours each time and left the final time overnight. Once infiltrated, the eye samples were transferred into individual wells in a rubber mould, oriented to facilitate the desired sectioning approach, and topped up with fresh EPON resin. The mould was then placed in a 60°C oven for 48 hours, to polymerise the EPON resin, embedding the eye samples in blocks.

2.3.3 Sectioning

The EPON blocks were mounted into a sample holder on an ultramicrotome (UC6, Leica, Wetzlar, Germany) and trimmed down with a razor blade to remove excess resin around the eye sample. The eye was rough-sectioned on the ultramicrotome on a glass knife edge until the region of interest was reached. Then using a diamond knife (DiATOME, Hatfield, UK), ultrathin 70 nm sections cut, which were individually collected on copper grids. These were placed onto grid trays with thin (silver interference colour) pioloform membrane. After air-drying overnight to the

pioloform, the sections were post-stained with 3% uranyl acetate for 3 minutes, and lead citrate for 1 minute and washed clean with distilled water before storage.

2.3.4 Transmission electron microscopy (TEM)

The thin sections mounted on copper grids were imaged with a transmission electron microscope (Tecnai 12, 120 kV BioTwin Spirit, FEI Company, Hillsborough, USA) at 120 kV (Fig. 2.3). Once the sample had been loaded, apertures were adjusted to optimise the beam intensity, image contrast and focus. Images were collected with an inbuilt FEI Ceta 4k x 4k CCD camera. Image analysis of the micrographs, including measurement of anatomical structures was carried out using Fiji-ImageJ software [213].

FIGURE 2.3. Photo of the Tecnai 12, 120 kV BioTwin Spirit transition electron microscope (TEM) used to image crab eye tissue in sub-micron detail.

2.3.5 Light microscopy

During sectioning of the EPON blocks for TEM, thick 1500 nm sections were also cut with the glass knife edge and mounted on glass slides. These were post-stained with methylene blue, a cationic stain that binds to cell components with negative charge, for instance nuclei and cell membranes. The sections were imaged using a camera mounted on a light microscope (DM750, Leica, Wetzlar, Germany) and the micrographs were analysed using Fiji-ImageJ software [213].

2.3.6 *Gelasimus dampieri*

Eyes of four *G. dampieri* crabs (that had already participated in ERG experiments) were collected for histological study. The eyes of each individual were fixed in a different state or time of day to allow changes involved with adaptation state and circadian cycles to be seen (refer to chapter 3).

Due to availability, phosphate buffer was used instead of PEMS buffer, but otherwise the dissection and fixation method in section 2.3.1 was followed. After 24 hours in fixative, the eye samples were placed into containers of phosphate buffer and stored in a refrigerator as much as possible. There were two long periods where, due to travel (within Australia and back to the UK), they were likely warmed to ambient temperatures. On reaching the UK, the samples were processed and embedded into EPON blocks using the usual method described above (using phosphate buffer in place of PEMS). Images were collected with light microscopy and TEM.

2.4 ERG methods

2.4.1 Animal preparation

Gelasimus dampieri crabs were pre-adapted to either bright light or darkness before experiments. To ensure a light-adapted state, they spent 2 hours inside an aluminium foil-lined container with 1-2 cm seawater, illuminated from above by a ring of bright white LEDs behind light-diffusing film (light spectrum of LEDs was equivalent to the ERG stimulus, section 2.4.3). Alternatively, they were placed in a lightproof box inside a darkroom at sunset to dark-adapt, where they remained until >2 hours after sunset, or until the following day. Whilst preparing the dark-adapted crabs for experiments, they were not exposed to any light other than a dim red lamp (emission >600 nm).

Crabs had a small insulated plastic disk adhered to their carapace with cyano-acrylate glue, which remained in place until its next moult, and was itself temporarily glued to a mounting post during experiments. Claws were restrained with electrical tape to avoid dislodging the electrode during the experiment. With a small dab of cyano-acrylate glue halfway up the back of an eyestalk, one eye was fixed still in its natural upright position (Fig. 2.4a). To prevent desiccation of the gills during experiments, the crab was suspended from the mounting post, half immersed in a tank of seawater. Ambient air temperatures fluctuated in the 20-25°C range.

2.4.2 ERG apparatus

The crabs and ERG recording equipment (Fig. 2.4a) were housed inside a lightproof grounded Faraday cage on a pressurised anti-vibration table during experiments to minimise movements or electrical noise in the signal and maintain darkness. A 2500 μm diameter platinum wire recording electrode, shaped into a small loop and coated with conductive gel (Livingstone International Pty Ltd, NSW, Australia),

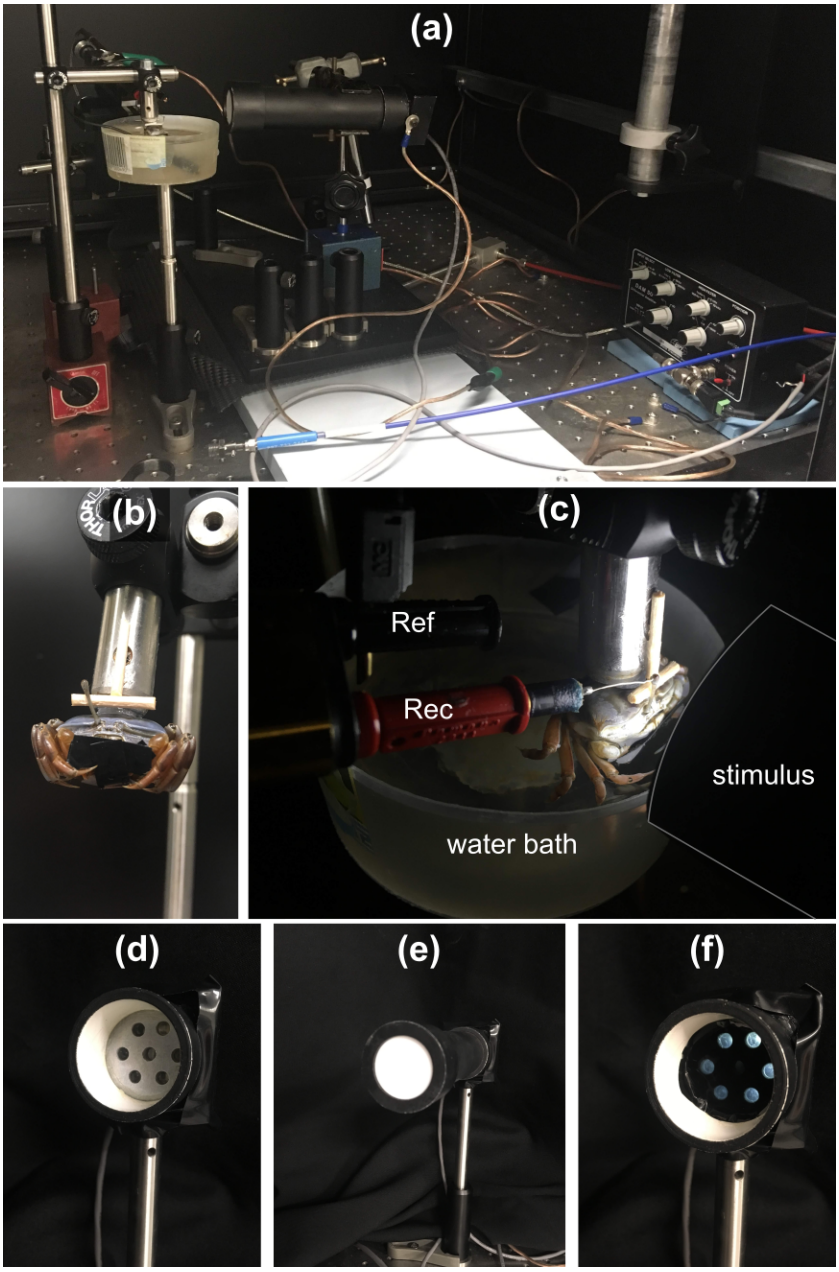

FIGURE 2.4. **(a)** Overall view of ERG apparatus in the Faraday cage. **(b)** Female crab adhered from the carapace to a mounting pole, with one eye fixed in position ready for an ERG experiment. Her claws are restrained with electrical tape. **(c)** Silver chloride wire recording electrode (Rec) shown in contact with the corneal surface of a crab eye. The reference electrode (Ref) terminus is immersed in the water bath. The crab is positioned in front of the stimulus, which is illuminating her whole frontal eye. **(d)** Back of ERG stimulus with the tube removed, so that the ring of six bare LED bulbs are visible. **(e)** The stimulus intact with internally reflective tube attached, covered with thick diffusing film, creating a large white illuminated disc. **(f)** Layers of neutral density filters covering the LED array to lower the light intensity for dark-adapted crabs.

was mounted on a micromanipulator. With help from a dissecting microscope on an articulated arm, the electrode loop was carefully positioned in contact with the corneal surface on the lateral region of the upright eye (Fig. 2.4c), allowing the frontal eye an unobstructed view of the stimulus. A pellet-shaped silver chloride indifferent (reference) electrode inside a lightproof rubber shield was placed by the crab within the seawater bath. The ERG signal was amplified 1000 times using an AC differential amplifier (DAM-50, World Precision Instruments, Florida, USA), with a bandpass filter for 1-100 Hz.

The signal was visualised on a digital storage oscilloscope (2211, Tektronix, Oregon, USA) and digitised by a multi-function data acquisition unit (USB-6353 X-series, National Instruments, Texas, USA), sampling at 5 kHz. Custom MATLAB programmes (R2015b, Mathworks, Massachusetts, USA) were used to acquire and analyse the signal and control the stimulus. All equipment inside the Faraday cage was grounded to eliminate electrical noise from the ERG signal.

2.4.3 Light stimulation

A ring of five white LEDs (Fig. 2.4d) provided light stimulation from the back of an internally reflective white tube of 3 cm diameter and 14 cm length. The tube opening was covered with a 3 cm diameter circle of thick diffusing film creating a diffuse light stimulus with 7.07 cm^2 area, positioned 4 cm in front of the crab (Fig. 2.4e). The eye to be recorded from was aligned with the centre of the stimulus, which illuminated the entire frontal side of the eye. No other light source was present within the Faraday cage.

The LED stimulus was controlled via a custom-built RGB LED controller and a multifunction data acquisition board, which moderated intensity and flicker frequency as per the experimental requirements, inputted through MATLAB. The LEDs could be dimmed through 49,000 steps via pulse-width-modulation from a maximum of 1 kHz. To lower the stimulus intensity further, layers of 0.9 ND neutral-density filter (No.211, Lee Filters, Andover, UK), were slotted into the tube in front of the LEDs when required (Fig. 2.4f). The absolute irradiance spectrum of each different stimulus intensity used in my experiments was measured with a calibrated spectrometer (USB-2000+, Ocean Optics, Largo, USA) and 600 nm diameter optical fibre. Figure 2.5 shows the spectrum of light produced by the stimulus on full brightness (without neutral density filter). Total irradiance ($\mu W/cm^2$) for each stimulus intensity was determined by calculating the area beneath the curve within the wavelength range 300 to 600 nm, for which the *G. dampieri* visual system is sensitive [42]. It is worth noting that the ERG stimulation lacked UV wavelengths (<400 nm).

To minimise disruption to their desired adaptation state, experimental stimulation and recording lasted 21 seconds only. Within intervals between each presentation, a light-adapted state was maintained (when required) by setting the stimulus LED to full intensity (no flicker). Alternatively, dark-adapted state was maintained with the stimulus off in between recording

periods, providing darkness. Intervals of 60 seconds were shown in preliminary trials to be sufficient in preventing meaningful changes in adaptation state, however this interval period was extended to 4 minutes in the experiment which investigated the rates of dark adaptation.

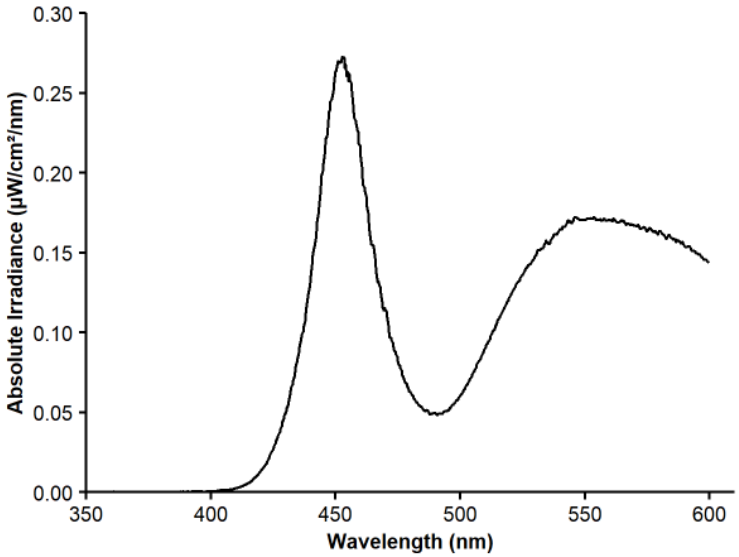

FIGURE 2.5. Absolute irradiance spectrum of white LED stimulus used in ERG experiments set to maximum brightness, without neutral density filter. This spectrum was measured via an optical fibre positioned 4 cm in front of the stimulus, equivalent to the position of the crab eye during experiments. A brighter LED array with the same spectrum was used to light-adapt crabs before experiments.

2.4.4 ERG data analysis

Fast-Fourier transformations were applied to the ERG signal recordings to separate their constituent frequencies. A median filter cleaned data of high frequency spikes in the signal (e.g. the crab heart beat) and anomalies of 5 standard deviations or more away from the mean signal amplitude were also removed; these occurred occasionally when the crab's legs or claws moved during the recording. From the remaining signal, mean response amplitude over the 21-second recording was calculated, along with mean, maximum and minimum noise values. Probability (alpha) values were also calculated for each signal recording to determine whether the response was statistically higher (at the 5% level) than the noise level. However, in my analyses I used more conservative thresholds of ERG responses to compare between treatment groups.

CHAPTER 3

FROM DAY TO NIGHT: CHANGES IN EYE ULTRASTRUCTURE

This chapter contains descriptions and measurements of the ultrastructural anatomy of the *Afruca tangeri* eye from light microscopy and transmission electron microscopy (TEM). The major physiological differences and similarities of light- and dark-adapted eyes are described between night and day. Synchrotron X-ray tomography was used to visualise these differences in intact eyes. Additionally, the effect of light pollution on the physiology of the *A. tangeri* rhabdom is explored. Some observations were made from limited eye samples of *Gelasimus dampieri*, another fiddler crab used in ERG experiments of chapters 4 and 5. Lastly, the previously unknown day-to-night changes in the eyes of a small sample of green shore crabs (*Carcinus maenas*) were examined, allowing comparisons to be made between well studied crab families with a very different visual ecology. Much of my research in this chapter regarding *A. tangeri* has been published in a peer reviewed journal, ref: [214].

3.1 Introduction

3.1.1 Background

Many terrestrial animals must cope with light levels that vary from bright sunny skies to moonless nights a billion times dimmer [34]. Several different light- and dark-adaptation strategies have been described among members of the arthropods, the most successful animal phylum, which occupy an enormous diversity of visual niches on land [2]. These strategies are as diverse as the optical architectures themselves, each highly specialised to suit the ecological needs and habitat of that animal. Fiddler crabs provide an excellent model for studying adaptations to light level fluctuations and many species have evolved to forage during both the day and night [50, 111, 215, 216]. They can be found in dense colonies on their mudflat habitats, and make a

robust laboratory animal. The fiddler crab has large compound eyes and is highly dependent on vision in its behavioural ecology [114]. The morphology of their typical decapod apposition eye has been thoroughly described for *Gelasimus vomeris* [89], and fiddler crabs are well-known for their distinctive scare-responses to a looming stimulus, making them ideal for behavioural experiments investigating crustacean vision [67, 123, 124]. The West African fiddler crab, *Afruca tangeri* is abundant and widespread on southwest European and northwest African coastlines [217].

Fiddler crabs, including *A. tangeri*, have been studied by those researching aspects of crustacean polarization vision [68, 69, 111, 218], colour vision [37, 39, 42] and visually-guided behaviour [54, 95, 103, 111, 131]. Experiments utilising thresholds of visual sensitivity as a response variable are commonplace in these studies. However, there is crucial information missing on how fiddler crabs adapt to large fluctuations in brightness and whether their adaptive mechanisms are regulated by a circadian clock. Considerations such as ambient light exposure before or during experiments, and the time of day crabs are tested, may have significant impacts on their ability to detect an experimental visual stimulus.

Fiddler crabs are mostly active on diurnal low tides when they emerge from burrows to forage in dense groups on the mudflat surface. They have highly visual lifestyles, frequently engaging in visually-dependent intraspecific social interactions whilst constantly monitoring their surroundings for potential predators [114]. The eyes wrap almost fully around the eyestalks and are held high above the head, providing a panoramic field of view [97, 117]. During daytime, they are exposed to bright tropical sunlight and strong reflected glare from the mudflat surface. In summer, when surface temperatures remain higher than 18°C after sunset, *A. tangeri* also remain active on the mudflat at night [111, 216, 217]. From my own observations during breeding periods, males continue to wave their major chelipeds for at least 2 hours after sunset, a behaviour used to visually signal to potential mates [95]. This suggests that effective vision is also possible in very dim light and led to my hypothesis that this species undergo considerable adaptation between day and night to cope with the large changes in available light levels, spanning 10 orders of magnitude.

A common mechanism for adaptation to light level fluctuations in compound eyes is migrations of mobile screening pigment granules within the photoreceptors or within adjacent pigment cells [7, 147]. Pigment cells are usually located distally where the crystalline cone and rhabdom meet, and/or proximally, near the basement membrane. Screening pigment granules within photoreceptors may move either longitudinally or radially toward the light path, to protect the microvilli, where phototransduction occurs, from over-exposure and excess light damage [157]. In dim light, the granules recede, boosting sensitivity by allowing more light to reach the photoreceptors. There is great diversity of screening pigment populations, distributions and their movements, among the crustaceans, even within closely related groups [152], including several crab species that are reported to use screening pigment migrations as a light- dark-adaptation

strategy [164, 165, 171–175].

Slower circadian changes may alter light sensitivity by changing the volume of the photoreceptor cells via a widening or lengthening of the rhabdom, increasing the surface area where phototransduction can occur. There are several intertidal crab species for which this has been identified as the primary dark-adaptation mechanism [165, 180–183], but although some species were well-researched in the late 1960s to late 1980s, there is no information on fiddler crabs.

Across the globe, levels of artificial light at night are increasing each year. In the four years between 2012 and 2016, satellite radiometers measured a 2.2% increase in artificially-lit outdoor area and 1.8% rise in total radiance at night [219]. Coastal areas are often lit artificially due to concentrated human populations and activities associated with tourism, shipping, leisure and transport industries. The extent to which light pollution affects intertidal invertebrates is relatively poorly understood [220], but it is likely to be very important. Many coastal marine animals have evolved to rely on celestial cues for navigation and timing of reproductive events at night [220, 221]. The fiddler crab *A. tangeri* is among many other crabs that tend to synchronise spawning events with new and full moons [111, 222]. Light pollution is known to disrupt the ability of animal visual systems to detect natural celestial cues for navigation such as the moon, solar system and sky polarisation pattern [223, 224]. In addition, increased light levels may increase an animal's foraging success at night, or its vulnerability to predators, which can have great consequences to compositions of coastal communities [220, 224–226]. The mudflats at El Rompido and many other locations where *A. tangeri* can be found, are areas closely inhabited by humans. The town's beach, lined with restaurants and houses, has bright lights that illuminate the habitat of the crabs from the north during the evening, most brightly until around midnight. There are also marinas and boats to the east and west of the mudflats that have lights.

In chapters 4 & 5, hypotheses tested in ERG experiments are based on the assumption that *G. dampieri* eye anatomy is similar to *A. tangeri* and undergoes similar effective adaptation at night to increase sensitivity of the visual system to darkness. However, these crabs are from different species, genera and subfamilies, so it cannot be assumed that eye morphology and adaptation strategies are the same. Knowledge on these aspects in *G. dampieri* was not available at the time of my experiments, so to check for consistencies and potential differences, four pairs of eyes were fixed, each in one of the same four adaptation states as *A. tangeri* (which are also equivalent to the ERG experimental treatments of chapter 4).

The green shore crab *Carcinus maenas* occupies a broad range of coastal habitats including rocky shores and colder water environments [135, 140], and is therefore widely distributed and invasive (refer to section 1.3). These crabs can be collected along UK shores and the species is currently used in crustacean vision research at the University of Bristol and elsewhere. Light- and dark-adaptation mechanisms have not yet been described for this species either, but like many crabs associated with complex habitats, *C. maenas* has widely spaced eye stalks (broad-fronted)

with little regional specialisation across the compound eye [113]. Although it has a very different ecology to the fiddler crab, *C. maenas* can be found in abundance on the same El Rompido mudflat habitat as *A. tangeri*, where it is primarily nocturnally active, emerging from its burrow /refuge to forage at dusk (and more rarely, active during daytime too). In this chapter, my observations of the main physiological changes in the eye between day and night are described from six eye samples to provide some comparative information on this species.

3.1.2 Aims and hypotheses

This work aimed to identify the eye anatomy of *A. tangeri* and compare it to that of another fiddler crab species, *Gelasimus vomeris* (subfamily Gelasiminae), for which there is a comprehensive description [89]. Next, the physiological differences between light- and dark-adapted eyes in *A. tangeri* are described between night and day to decipher the adaptation mechanisms in place. Using transmission electron micrographs (TEMs) and light micrographs, the screening pigment distributions in the eye are characterised by looking at both primary pigment cells (PPCs) and at pigment granule distributions within photoreceptor cells. Anatomical dimensions of the photoreceptors and crystalline cones are also compared between day and night in light- and dark-adapted eyes. Synchrotron X-ray tomography of eyes fixed at midday and midnight allowed visualisation and measurement of these changes across the whole eye in three dimensions.

A small sample of *G. dampieri* and *C. maenas* are also compared from TEM and light microscopy images after being fixed in light- and dark-adapted states during day and night. Anatomical similarities and differences to *A. tangeri* are noted in various regions of the eye in terms of general anatomy and light-adaption changes.

To study whether light pollution has an effect on the adaptation state of fiddler crabs, cross-sectional rhabdom area was compared between groups of six crabs held in sites of low and high light pollution, plus a third group kept in almost complete darkness. The hypothesised result was that the crabs held at a site with high light pollution would have a much reduced rhabdom cross-sectional area, due to anthropogenic light sources inhibiting the full dark-adaptation process in the eye. Crabs on a beach with low levels of light pollution were expected to have rhabdoms resembling the size of the control group held near total darkness.

3.2 Materials and Methods

3.2.1 Pre-adaptation and eye tissue sampling

In order to the identify physiological changes in eye structures that occur between night and day, *A. tangeri* crabs were collected and divided into four groups. They were pre-adapted in one of the four conditions described in Table 3.1 before their eyes were dissected, fixed and embedded for sectioning. See chapter 2 for detailed methods on fiddler crab collection (section 2.1.1), pre-adaptation (section 2.2), and dissecting and preparing eye samples for anatomical analysis (section 2.3).

Table 3.1: Pre-adaptation methods and dissection times used as experimental treatments to compare circadian changes in eye structures associated with light-adaptation.

Treatment	**Sample time**	**Pre-adaptation method**
Day light-adapted	12:00	Kept under natural skylight from sunrise until midday
Night light-adapted	00:00	Kept under natural skylight during daylight hours, then moved just before dusk under bright controlled LED lighting to prolong light-adaptation after sunset.
Day dark-adapted	12:00	Dark-adapted just before dusk by housing in a light-tight container within a darkroom, remaining there until midday the following day.
Night dark-adapted	00:00	Dark-adapted just before dusk by housing in a light-tight container within a darkroom, remaining there until midnight.

3.2.2 Crystalline cone tip aperture measurements

After pre-adaptation to light or dark at midday and midnight (Table 3.1), EPON-embedded eyes were cut into thin sections for TEM (full method in section 2.3). Sections were cut from the frontal part of the eye (Fig. 3.1a) after slicing through the corneal surface and crystalline cones, to expose the primary pigment cells (PPCs) (Fig. 3.1b). Due to the curvature of the eye there was a slight gradient in depths at which the ommatidia were sectioned, with those in the centre cut the deepest to expose their distal R8 cells. During TEM imaging, individual ommatidia were selected and an image collected if they were in cross-section exactly through the narrowest part of the light path. This point was the intersection of the four crystalline cone cell tips with the distal-most tip of the R8 rhabdom (Fig. 3.1c). From 10 TEM images of these apertures per eye, the combined cross-sectional area of the light transmissive crystalline cone tips and rhabdom were measured using in-built Fiji-ImageJ functions [213].

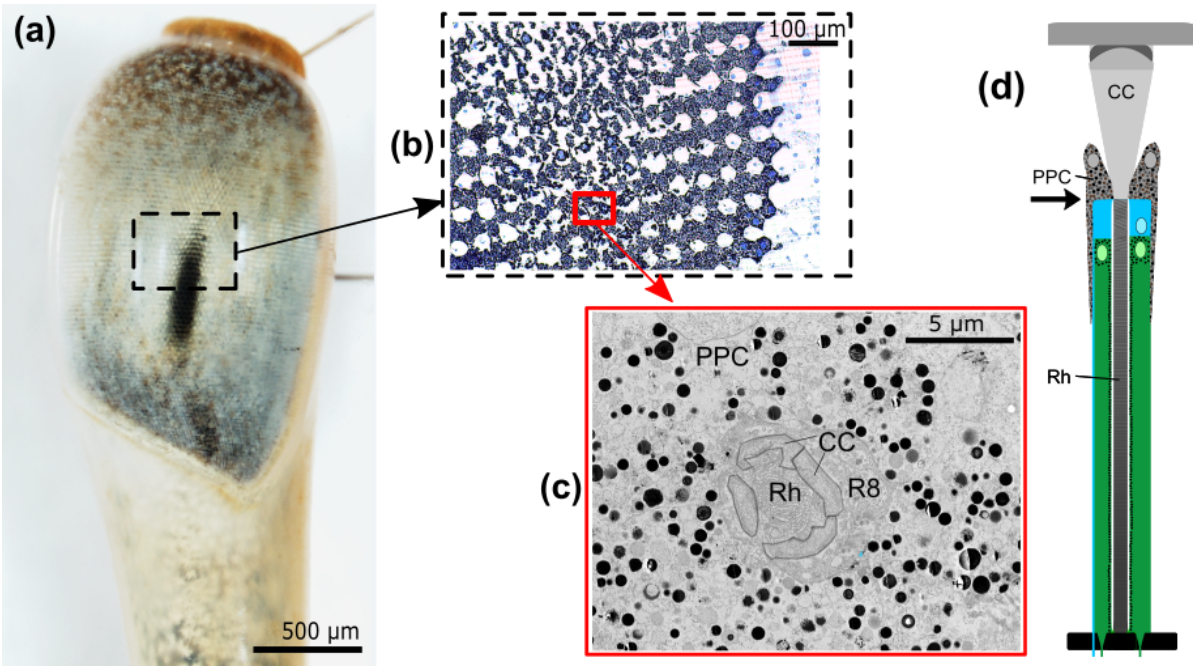

FIGURE 3.1. Sample location for cross-sectional area measurements of crystalline cone apertures. **(a)** Photograph of a whole eye with dashed outline showing the sample location for sections in the frontal eye, from which aperture areas were measured. **(b)** Light micrograph of semi-thin section showing the primary pigment cell layer of this eye region at the depth it was sampled. **(c)** TEM of one ommatidium in transverse section at the chosen depth for sampling. Surrounded by primary pigment cells (PPC), the aperture is formed by the four crystalline cone cell tips (CC) intersecting with the distal-most tip of the rhabdom (Rh) of the photoreceptor cell (R8). **(d)** Black arrow indicates aperture TEM sample level on a diagram of an ommatidium.

3.2.3 Primary pigment cells

Following sectioning at the PPC level, the blocks were sliced further through the frontal eye (Fig. 3.2a), past the R8 cells, into the R1-7 photoreceptor cells beneath. Semi-thin (1500 nm) sections were cut just proximal to the R1-7 nuclei (for ommatidia in the centre of the section) and imaged with a light microscope, see full method in section 2.3.5. Due to the curvature of the eye, crystalline cones are in cross-section around the edges of the section and pigment within the PPCs form a dark ring/strip around the crystalline cone tips (Fig. 3.2b). These pigment distributions were examined for six or more individuals and compared between the four treatments.

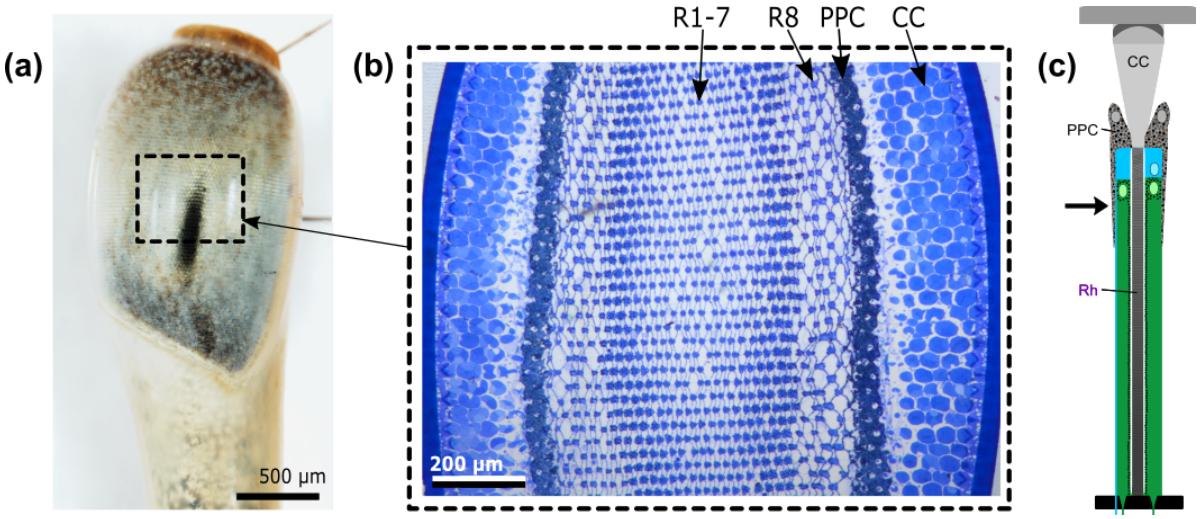

FIGURE 3.2. **(a)** Photograph of a whole eye with dashed outline showing the sample location for semi-thin sections in the frontal eye. **(b)** Example of semi-thin section cut at the sample depth and imaged with light microscopy. Across the section there is a gradient of depths at which the ommatidia were cut, with crystalline cones (CC) around the edge, a dark band of pigment within primary pigment cells (PPC), then R8 cells, and R1-7 in the centre. **(c)** Black arrow indicates rhabdom TEM sample level on a diagram of an ommatidium.

3.2.4 Rhabdom cross-sectional area measurements

At the same sample depth as the semi-thin sections were cut (Fig. 3.2b), thin (70 nm) sections were also cut on a diamond knife and imaged with TEM (full methods in section 2.3). Around the middle of the section, ommatidia were chosen for sampling and image collection if they were located just proximal to the nuclei of the R1-7 photoreceptor cells. Using in-built Fiji-ImageJ functions [213], the cross-sectional area of the rhabdoms at this level was measured from 16 TEMs per eye.

3.2.5 Pigment granule distribution analysis within photoreceptors

After measuring the rhabdom areas, the same set of TEM images were additionally analysed for pigment granule distributions to investigate whether radial migration occurs in response to light. After conversion to binary images using the 'Threshold' function in Fiji-ImageJ [213], they were processed with MorphoLibJ plugins 'Watershed' and 'Fill Holes' [227]. The inbuilt function 'Analyze Particles' quantified the number of pigment granules in close proximity to, and surrounding the palisade vacuole / rhabdom area. From these, the number of granules within the cytoplasmic bridges of the palisade were counted as a proportion of the total. Any pigment

granules distributed randomly in the cell cytoplasm and not associated with the palisade, were excluded from the count.

3.2.6 Effect of light pollution

Fiddler crabs were placed into individual transparent containers of 1-2 cm seawater and divided into three groups. After spending the daytime under natural solar illumination, they were placed at one of three site locations (see map in Fig. 3.3) just before sunset and left to dark-adapt for 4 hours until midnight. The experiment was carried out twice (using identical methods) with three animals per group each time making a total sample size of six per group; half the eyes were collected on the night of 3rd May and the other on 8th August 2018.

One group was taken to Site 1, a light-polluted beach at El Rompido with a large population of fiddler crabs, very close to where they were collected. Here, there are houses, restaurants, a marina, streetlights and floodlights nearby, illuminating the beach (Fig. 3.3, S1). The second group was taken to Site 2, around 3 km further east along the same coastline, halfway between the towns of El Rompido and El Portil. This site was more remote, away from houses and marinas, so nearby or direct sources of light pollution were few, although not completely absent (Fig. 3.3, S2). Due to unsuitable conditions on this more exposed beach, there were no crab burrows present naturally. Site 3, was a darkroom at a field lab in the town of El Rompido where crabs were placed inside a light-tight container to create near-total darkness as a control.

Around midnight, the eyes of the fiddler crabs were dissected at their experimental site location with no change to ambient lighting conditions other than indirect use of a dim red lamp. Their eyes were fixed, processed and embedding into EPON blocks as per the method in section 2.3. The rhabdom areas were measured with TEM, using the same protocol as for the previous data set (section 3.2.4). On 3rd May, close to the time of eye sample collections, light levels were measured at Sites 1 and 2 using a calibrated high sensitivity spectrometer (USB2000, Ocean Insight, Largo, USA) and optical fibre, which collected light from north, south, east and west directions in turn.

FIGURE 3.3. Site locations S1-3, where the effect of light pollution on the cross-sectional area of the rhabdom was tested, shown on a map overlaid with satellite photographs (Google.com/maps). Below, photographs show the beach facing east at Site 1 (S1), lit from the north by buildings and streetlamps after sunset; the beach at Site 2 (S2) facing west with the sun still setting above the horizon and no other nearby anthropogenic sources of light.

3.2.7 Synchrotron X-ray microtomography

Eyes from two male crabs of equal body size were dissected and fixed in 2.5% glutaraldehyde and 4% paraformaldehyde in 2x PEMS buffer, one naturally light-adapted at midday and the other dark-adapted at midnight. Using synchrotron X-ray microtomography, the samples were scanned at the TOMCAT beamline, Swiss Light Source (Paul Scherrer Institute, Switzerland; [228]), once under 40x combined magnification and again under 4x magnification, giving effective voxel sizes of 163 and 1625 nm respectively. The samples were scanned with a monochromatic 12 KeV beam, using a 20μm thick LuAG:Ce scintillator, exposure time of 380 ms and a propagation distance of 12 mm. 2000 projections were recorded as the sample rotated through 180 degrees.

The radiographic projections were reconstructed into aligned tiff image stacks and Paganin filtered (delta=1-7, beta=1-9 [229]) using custom in-house software [230]. These 3D reconstructed volumes were cropped and segmented using Avizo 8.0 (ThermoFisher Scientific, Waltham, USA). Features such as the cornea, crystalline cones, PPCs and rhabdoms were segmented and measured. Two whole-eye scans were used to count the approximate number of ommatidia by sampling 10 representative areas per eye and multiplying facet count by total eye surface. External and internal dimensions of the eye were measured, including area of eye tissue occupied by crystalline cones and photoreceptors, and the lengths of these cells across the eyes.

3.2.8 Lengths of photoreceptors and crystalline cones

EPON-emdedded eyes from six midday light-adapted crabs and six midnight dark-adapted crabs were trimmed down from the top of the dorsal eye to its equator to make sections of the whole eye horizontally across the equator (Fig. 3.4a). Semi-thin sections were made, precisely aligning the cutting angle to slice a row of ommatidia in half, so that their full length is in view along the section (Fig. 3.4b,c). Using a light microscope to image the sections, the crystalline cones and rhabdom lengths of the six lateral-facing ommatidia from each eye (located in the centre of the ommatidium sequence) were measured using inbuilt functions in Fiji-ImageJ [213].

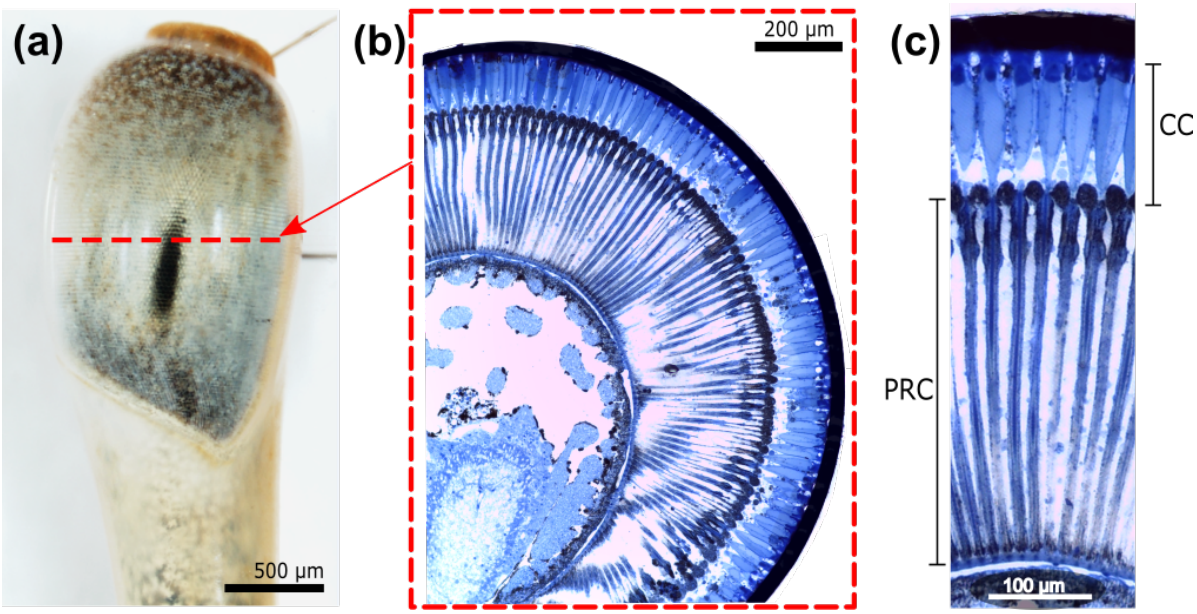

FIGURE 3.4. **(a)** Photograph of whole eye (frontal view) showing sectioning plane and sample location as a dashed red line across the eye equator. **(b)** Light micrograph of semi-thin section across the eye equator, showing the full lengths of a row of ommatidia. **(c)** Six ommatidia (with lateral view) were measured from the centre of the row where they are longest. Lengths of crystalline cones (CC) and photoreceptor cells (PRC) were measured and compared between treatments.

3.2.9 Anatomical study of the *Gelasimus dampieri* eye

Using the method outlined in section 2.3.6, the eyes of four individual crabs were compared using TEM and light microscopy. Sections were cut from the frontal eye equator region of the eye to view the PPC layer and crystalline cone apertures in cross-section, as well as further inside the eye to allow imaging of the photoreceptor column just below R1-7 nuclei. These locations are equivalent to eye regions studied in *A. tangeri* (Figs. 3.1 & 3.2) and the eyes of each individual were fixed in one of the four experimental treatments in Table 3.1, which are also equivalent to the treatments of the ERG experiments in chapter 4. Due to limited availability of animals, only one individual per treatment was sampled.

3.2.10 Anatomical study of the *Carcinus maeanas* eye

Six similarly sized *C. maenas* individuals were collected in Clevedon, UK (section 2.1.3). Three crabs were pre-adapted to bright sunlight in a laboratory window (Bristol, UK), from dawn until midday when the eyes were dissected into fixative. The remaining three were dark-adapted in a light-tight container from sunset (17:00 local time) until midnight, when their eyes were dissected in darkness using a dim red lamp. The usual full method for dissection, fixation, tissue processing and embedding was used (section 2.3). Semi-thin (1500 nm) sections were made from the frontal region of the eyes at various levels in order to observe crystalline cones, PPCs and the photoreceptors below using a light microscope. In particular, observations were made on the position of the PPC layer. Additional thin (70 nm) sections were made when central ommatidia were in cross-section just below their R1-7 photoreceptor cell nuclei. These sections were imaged with TEM and the cross-sectional areas of rhabdoms were measured using the same method as for *A. tangeri* (section 3.2.4).

3.2.11 Statistical analyses

Statistical tests were performed using R software (version 3.5.1; http://www.R-project.org/). Following Kolmogorov-Smirnoff tests for normality and Bartlett's test for homogeneity of variances, statistical analyses to compare physiological measurements between adaptation states were performed using the R package 'onewaytests' [231]. Where these assumptions were met, Student's t-tests were used for comparison between two groups, or Analysis of variance (ANOVA) was used to compare four treatments. Threshold probability (alpha) values were set to 5% throughout. For data with unequal variances, Welch's test was used instead. Following ANOVA, *post hoc* pairwise comparisons tests were performed using TukeyHSD (or Bonferroni corrections when using Welch's test).

3.3 Results

3.3.1 Anatomy of the *Afruca tangeri* eye

The apposition compound eye of an adult *A. tangeri* fiddler crab (Fig. 3.5a) is around 3-4 mm in size from top to bottom. Ommatidia are arranged in a regular hexagonal array (Fig. 3.5b,c) and number ~10,000 per eye (approximated from whole-eye synchrotron tomograms from two adult male crabs, carapace width 25 mm). The eye is of typical crustacean design and appears to be very similar to the eye of *Gelasimus vomeris*, a fiddler crab from a different subfamily (Gelasiminae), which was described thoroughly by Alkaladi and Zeil [89]. Each ommatidium consists of a corneal lens and crystalline cone that direct light to the long fused rhabdom of eight photoreceptor cells (Figs. 3.5d & 3.6a).

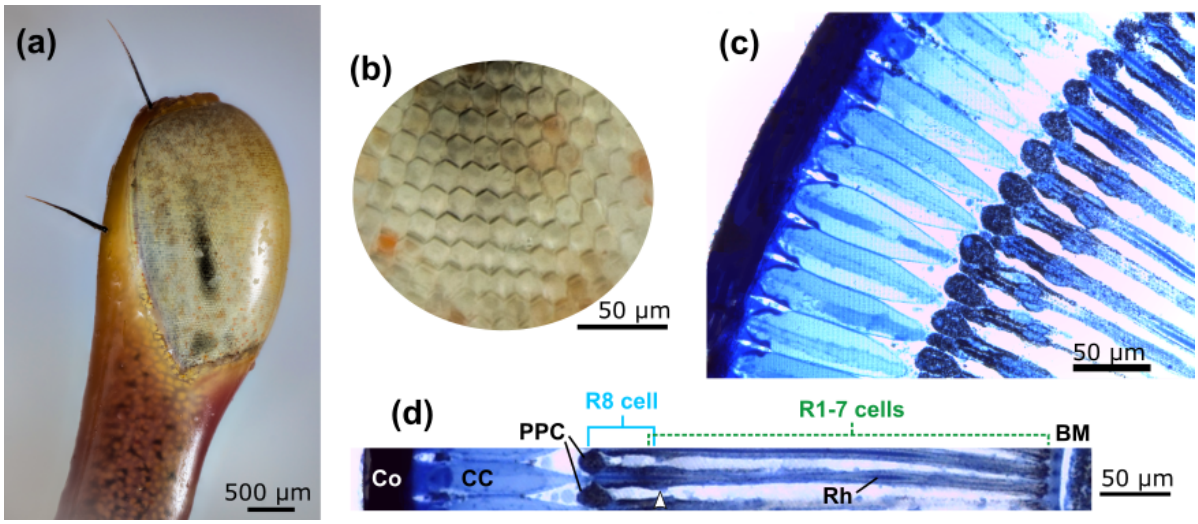

FIGURE 3.5. **(a)** Photograph of the whole eye of a living *A. tangeri* crab, frontal view. **(b)** Closer view of the flat corneal surface showing hexagonal lattice of facet lenses. **(c)** Light micrograph of a semi-thin horizontal section across the eye equator showing the distal region of rows of ommatidia under the corneal surface. **(d)** Labelled light micrograph of a whole ommatidium from cornea (Co) to basement membrane (BM) showing the arrangement of crystalline cone (CC), primary pigment cells (PPC), R8 and R1-7 photoreceptor cells, with central fused rhabdom (Rh) and nuclei marked by white arrow.

The corneal surface is flat, consisting of striated layers of varying density (Fig. 3.6c), perhaps creating a refractive index gradient to focus light through the facet lens. Attached below (via two cornaeageal cells) is the crystalline cone, formed of four soft and transparent cells that taper proximally to make a cone shape, directing light on to the rhabdom (Fig. 3.6d,e). The secondary pigment cells (SPC) match the detailed description given of *G. vomeris* [89], changing in morphology and pigment content across the eye.

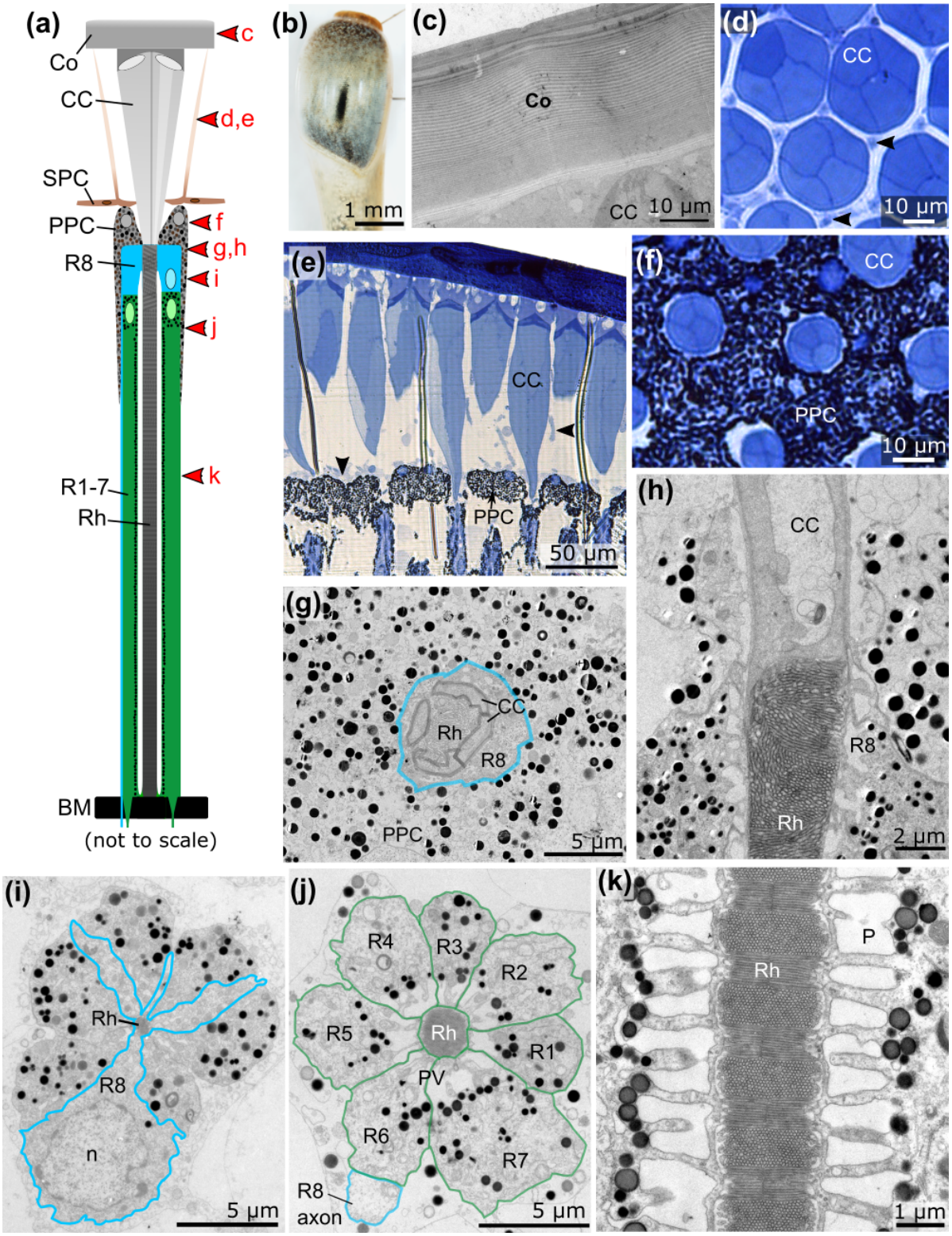
(a)
Co
CC
SPC
PPC
R8
R1-7
Rh
BM
(not to scale)
c
d,e
f
g,h
i
j
k
(b)
1 mm
(c)
Co
CC
10 µm
(d)
CC
10 µm
(e)
CC
PPC
50 µm
(f)
CC
PPC
10 µm
(g)
CC
Rh
R8
PPC
5 µm
(h)
CC
R8
Rh
2 µm
(i)
Rh
R8
n
5 µm
(j)
R4
R3
R2
R5
Rh
R1
PV
R6
R7
R8
axon
5 µm
(k)
P
Rh
1 µm

FIGURE 3.6.

⇐ FIGURE 3.6. Anatomy of the *A. tangeri* eye shown in TEMs and light micrographs (stained blue) of both longitudinal (LS) and cross sections (XS) of ommatidia from equatorial regions of light-adapted eyes, daytime. **(a)** Illustration of an ommatidium in LS with main structures labelled including the cornea (Co), crystalline cone (CC), primary (PPC) and secondary (SPC) pigment cells and basement membrane (BM). The photoreceptor cells R8 (blue), and R1-7 (green) contribute microvilli to a central rhabdom (Rh). Cell nuclei are shown in their relative positions. Red arrows indicate the corresponding locations of panels **d-k** along an ommatidium. **(b)** Photograph of a whole eye, frontal view. **(c)** The cornea in LS, showing striated layers of different densities. **(d)** Crystalline cones in XS showing their four component cells surrounded by six SPC extensions (arrows), empty of pigment. **(e)** The distal part of several ommatidia, LS, showing their crystalline cones stretching between the cornea and PPC layer; SPCs indicated by arrows. **(f)** Primary pigment cell layer in XS surrounding CC tips. **(g)** The distal R8 cell (outlined blue), where CC tips intersect with the start of the rhabdom in XS, forming a narrow aperture. **(h)** Same location as **g** showing CC and rhabdom intersection in LS. Note disordered rhabdom. **(i)** R8 cell (outlined blue) in XS showing its four-lobed design and nucleus (n) intersected with pigmented tips of R1-7 cells. **(j)** Photoreceptor cells R1-7 (outlined green) in XS just proximal to the nuclei (location sampled for comparative rhabdom measurements). **(k)** Rhabdom in LS from a dark-adapted eye, midday, showing the ordered bands of microvilli, ringed by palisade vacuoles (P) and screening pigment granules.

Anchored to the corner of each hexagonal corneal lens, long thin SPC processes stretch down the length of the crystalline cones to the primary pigment cells (PPC) below (Fig. 3.6d,e). In the dorsal eye these distal SPC processes contain the nucleus and brown screening pigment granules, presumably to screen excess skylight from above. In equatorial and ventral eye regions, the distal processes are empty of pigment granules (Fig. 3.6d, arrows) and the main proximal cell bodies contain the nucleus, plus an assortment of pale reflective pigment granules. This narrow T-shaped soma is stretched in a dorso-ventral (vertical) direction along the eye (Fig. 3.6a, left arrow in e), covering the dark PPCs below with a more reflective layer, giving the eye it's colour.

Below, the narrow proximal tip of each crystalline cone is surrounded by four highly pigmented PPCs forming a dense and highly absorbent screening layer (Fig. 3.6f). Very thin extensions of these cells reach down between the ommatidia toward the basement membrane. Within the PPC layer, the crystalline cone meets the distal-most rhabdom of R8 (Fig. 3.6g,h), a four-lobed photoreceptor cell with disordered microvilli (Fig. 3.6h,i). At the CC tip and R8 rhabdom interface, the light path is at its narrowest, forming an aperture. R8 lacks polarization sensitivity and is likely to be sensitive to short wavelengths (ultraviolet to blue) [232]. The cell cytoplasm contains no pigment granules itself but is screened by the PPCs above, in addition to the pigmented extensions of the R1-7 cells, which intersect between the four R8 lobes (Fig. 3.6i).

The remaining majority of the ommatidium's length is formed by seven long photoreceptor cells, R1-7, arranged in a ring around a central rhabdom (Fig. 3.6j), to which they contribute vertically (R1, R2, R5, R6) and horizontally (R3, R4, R7) orientated microvilli, facilitating sensitivity to the polarization of light (Fig. 3.6k) [67, 89]. Palisade vacuoles (appearing white in Fig. 3.6j,k) border the rhabdom, perforated with cytoplasmic bridges. There are at least two populations of "soma" pigment granules distributed throughout the distal part of the photoreceptor cells, most densely around the nuclei. Proximal to the nuclear region, extending to the basement membrane (the majority of the rhabdom's length), a third population of electron-dense pigment granules tightly encircles the palisade vacuole, forming a distinctive ring around the rhabdom. The proximal end of the photoreceptor cells terminate as axons, which pass through a basement membrane toward the lamina. There are no proximal pigment cells above the basement membrane in this species.

3.3.2 Screening pigment distributions

3.3.2.1 Within photoreceptors

Ignoring the "soma" pigment granules (largely associated with nuclei in the distal part of R1-7 cells), many of the screening pigment granules are distributed in a ring around the outside the palisade vacuoles surrounding the rhabdom in all adaptation states (Fig. 3.7). Very few granules are located inside the cytoplasmic bridges of the palisade vacuoles in light-adapted eyes, or any treatment (Table 3.2). There are slightly more pigment granules within bridges in light-adapted eyes than dark-adapted eyes, especially during daytime; however, this is still a small number (1.9 ± 1.8 granules per image); 4.3% of the total granules. When light-adapted, pigment distributions do not resemble that of a mantis shrimp, *Gonodactylus oerstedii*, in which radial pigment migrations are known [157]. On an observational note, in daytime the palisade of light-adapted eyes appears less "solid" with more numerous and wider bridges than other conditions.

Table 3.2: Mean number of pigment granules per ommatidium (± standard deviation) associated with rhabdom and palisade vacuole, counted in 15 ommatidia per individual eye in different adaptation states. Number of granules within cytoplasmic bridges is shown as a proportion of the total.

Treatment (*n*=8)	**Total granules**	**Within bridges**	**% within bridges**
Day light-adapted	47.3 ± 9.7	1.9 ± 1.8	4.3
Night light-adapted	51.9 ± 19.2	0.3 ± 0.4	0.7
Day dark-adapted	38.4 ± 10.9	0.0 ± 0.1	0.1
Night dark-adapted	51.5 ± 17.5	0.1 ± 0.1	0.1

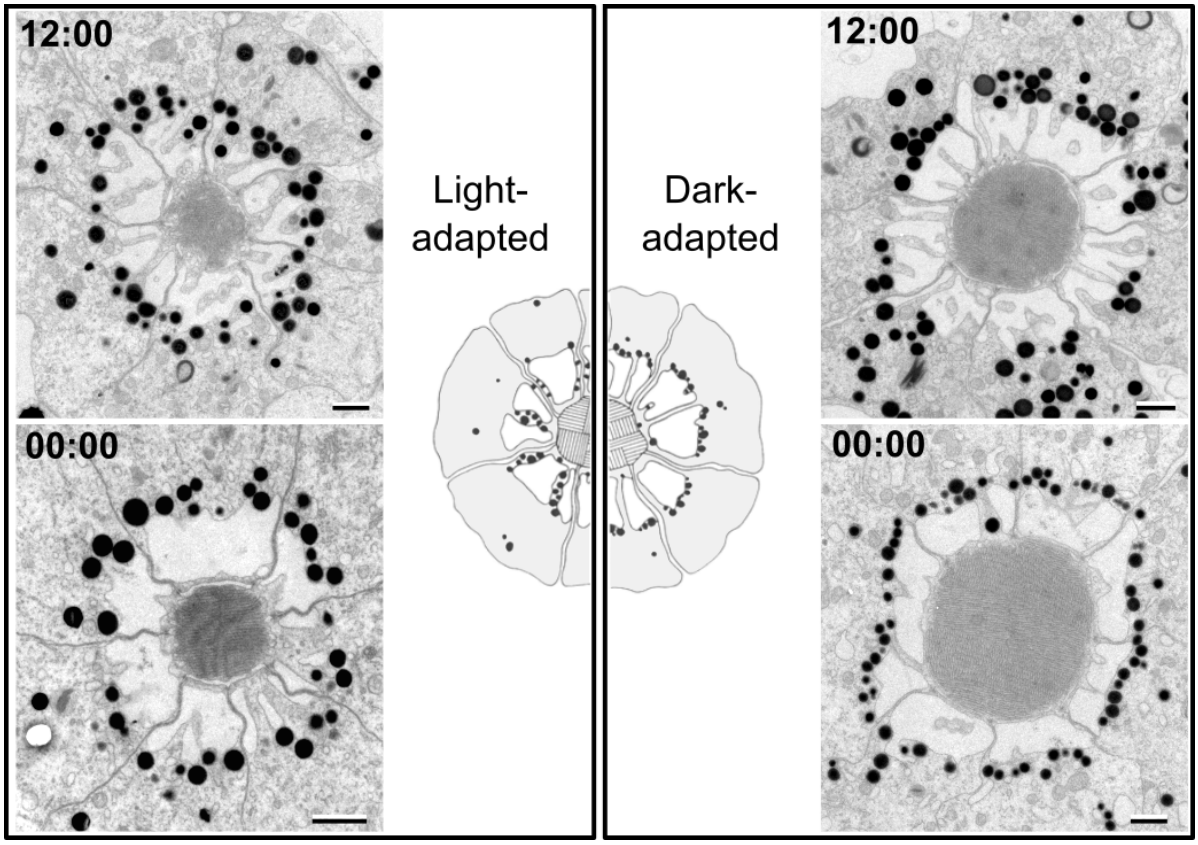

FIGURE 3.7. Typical arrangements of screening pigment granules observed with TEM in light- and dark-adapted *A. tangeri* eyes at midday and midnight (ommatidia in XS). The central rhabdoms are surrounded by palisade vacuoles (white) perforated with cytoplasmic bridges. Distributions of black pigment granules in light-adapted *A. tangeri* eyes do not match distributions in the central hypothetical diagram of *Gonodactylus oerstedii* (adapted from ref: [157]), which undergo radial migrations. Instead, all treatments resemble a dark-adapted state. One or two granules are occasionally located inside bridges nearer the rhabdom, but the majority border the palisade. Scale bars= 1 μm.

3.3.2.2 Within primary pigment cells

Light microscopy (Fig. 3.8a), TEM, and synchrotron X-ray tomography (Fig. 3.8b) revealed that pigment granules within PPCs do not appear to migrate as there is no difference in cell appearance or shape between light- and dark-adapted states, or day and night. The screening pigment appears consistently in a dense layer surrounding the region where the narrow crystalline cone tips meet the distal R8 cell in all eyes examined. Due to the low contrast pigment and thin string-like shapes of the secondary pigment cells, they appear irregularly on sections, if at all, and are invisible in synchrotron scans. Therefore, meaningful measurements of the cells were not possible

and their positions could not be reliably compared between treatments. However, there are no obvious conspicuous differences between treatments from general observations.

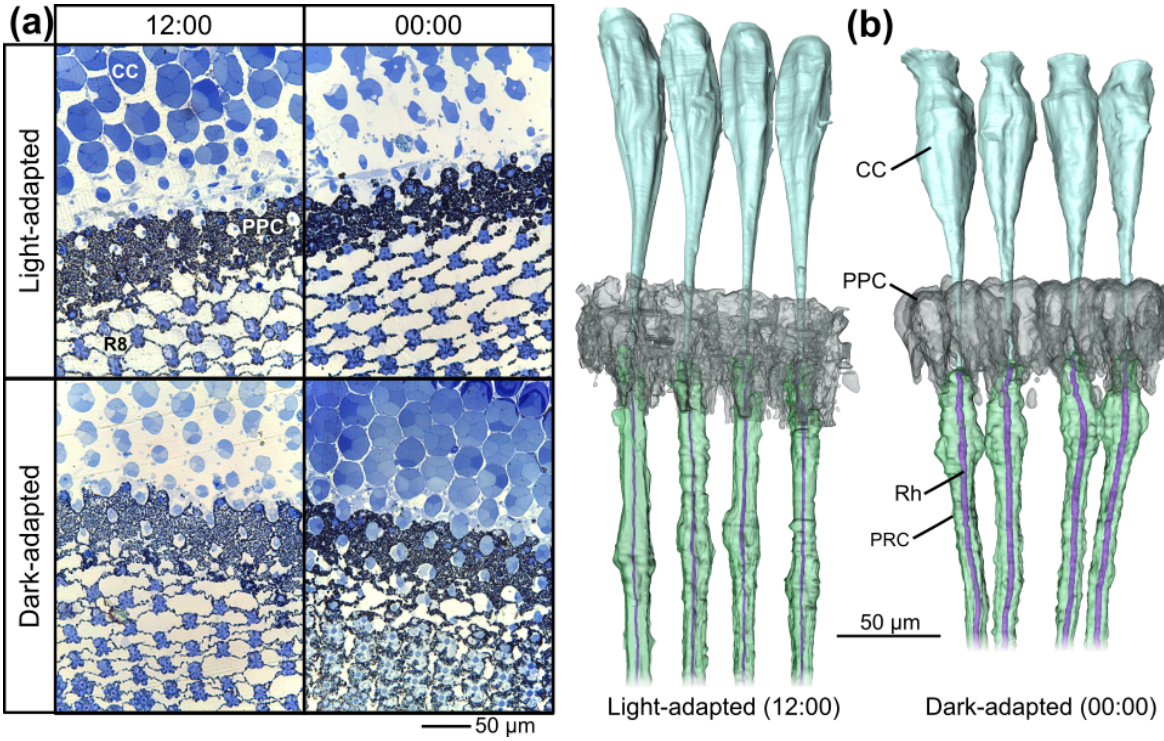

FIGURE 3.8. **(a)** Light micrographs of oblique sections through the primary pigment cell layer in light-adapted and dark-adapted *A. tangeri* eyes at midday and midnight. The primary pigment cell layer (PPC) appears as a dark band between crystalline cones (CC) and R8 cells (R8), remaining similar in appearance in all conditions. Secondary pigment cells appear as pale streaks / small dots above the PPCs. **(b)** Segmented X-ray tomograms of four ommatidia from a light-adapted eye at midday (left) and a dark-adapted eye at midnight (right). The PPCs surround the region where crystalline cones meet the photoreceptor cells (PRC) with central rhabdoms (Rh) in both eyes, with similar pigment distributions

3.3.3 Crystalline cone tips

From TEM images within the PPC layer, cross-sectional area of the light-transmissive aperture changed as a function of the adaptation state (Welch's ANOVA, $F_{(3,10.5)} = 18.4$, $p<0.001$, $n=6$; Fig. 3.9a-c). Pairwise comparisons (using Bonferroni corrections) revealed that apertures were narrower when light-adapted, significantly more so at midday (mean area 2.9 ± 1.1 μm^2) than at midnight (6.3 ± 1.6 μm^2) (p=0.01). Apertures in dark-adapted eyes at midday (5.3 ± 1.8 μm^2) were similar in area to the light-adapted eyes at that time (p=0.14). At midnight, however, dark-adapted crabs had aperture areas of 20.9 ± 6.2 μm^2, significantly larger (by almost 4 times)

than dark-adapted crabs at midday ($p<0.001$).

The diameter of the pupillary opening between PPCs (surrounding an aperture) was also measured (Fig. 3.9a, blue diamonds), example indicated by dashed line in Fig. 3.9b. There was a significant effect of adaptation state (ANOVA, $F_{(3,236)} = 7.27$, $p<0.001$), but differences between treatments were small. Pairwise comparisons (Tukey tests) between groups showed that mean pupil openings in dark-adapted eyes at midnight were slightly larger than the other three treatments ($p<0.011$), with mean value 7.0 ± 1.3 μm. However, this difference was due to wide diameters from just three individuals in this group; the other three crabs had similar diameters to other treatments. Pupillary openings between PPCs of the dark-adapted crabs at midday (6.2 ± 0.6 μm) and light-adapted eyes at midday (mean value 5.8 ± 0.5 μm) and midnight (6.0 ± 0.6 μm) did not differ from one another significantly (TukeyHSD, p=0.608-0.974).

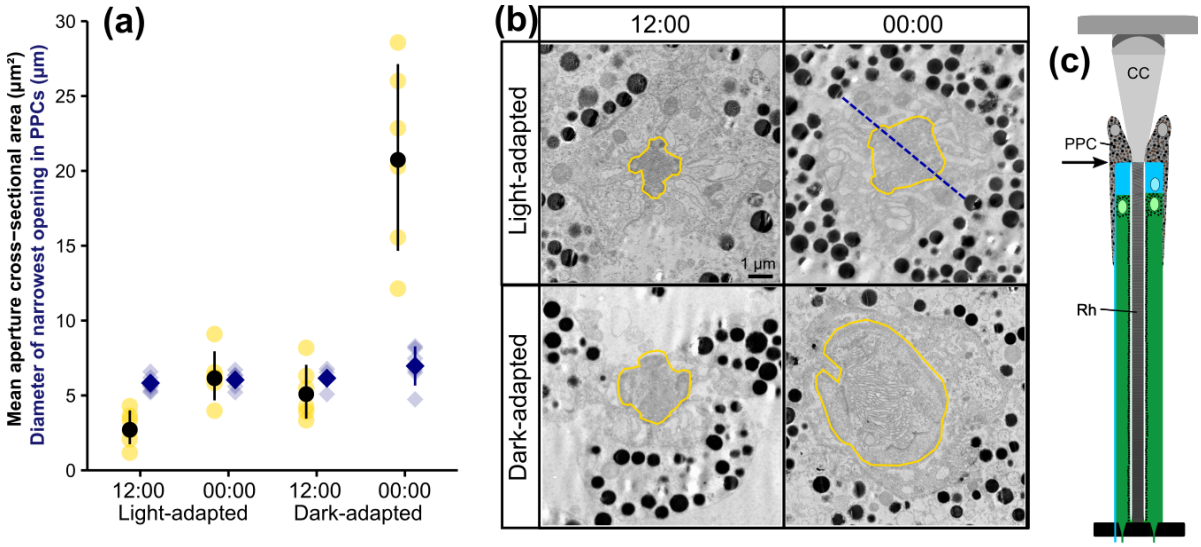

FIGURE 3.9. **(a)** Cross-sectional area of the crystalline cone tip aperture in light-adapted and dark-adapted eyes, at midday and midnight. Yellow circles represent individual means (n=6); black filled circles show global means with standard deviation bars. Blue diamonds plotted alongside show mean individual (pale) and mean group (dark) diameters of the pupillary opening between PPCs, surrounding the aperture, with standard deviation bars. **(b)** Representative TEMs of apertures (outlined in solid yellow) for each adaptation state, each measuring close to the mean for that treatment for visual comparison. Navy dashed line in the top right TEM exemplifies the pupillary opening (measured as the shortest diameter between pigment granules on opposite sides of the crystalline cone aperture). **(c)** TEM sample location indicated by black arrow on ommatidium diagram.

3.3.4 Rhabdom cross-sectional areas

In cross-section, the area of the rhabdom differed between adaptation states (Welch's ANOVA, $F_{(3,14.4)}$ = 56.91, p<0.001, n=8; Fig. 3.10) and pairwise comparisons showed that all treatment combinations differed significantly from one another (Bonferroni corrections, p<0.05). Dark-adapted crabs at midnight had significantly wider rhabdoms (mean area 18.4 ± 4.5 μm^2) than all other treatments, including by a factor of ~2.6, the daytime dark-adapted crabs (7.1 ± 1.0 μm^2). Light-adapted crabs at midday had the narrowest rhabdoms (3.3 ± 0.4 μm^2), exceeded slightly by midnight light-adapted crabs (4.3 ± 0.3 μm^2). Therefore, the rhabdom area in cross-section appears to fluctuate by an average factor of 5.6 during a typical 24-hour period in *A. tangeri*.

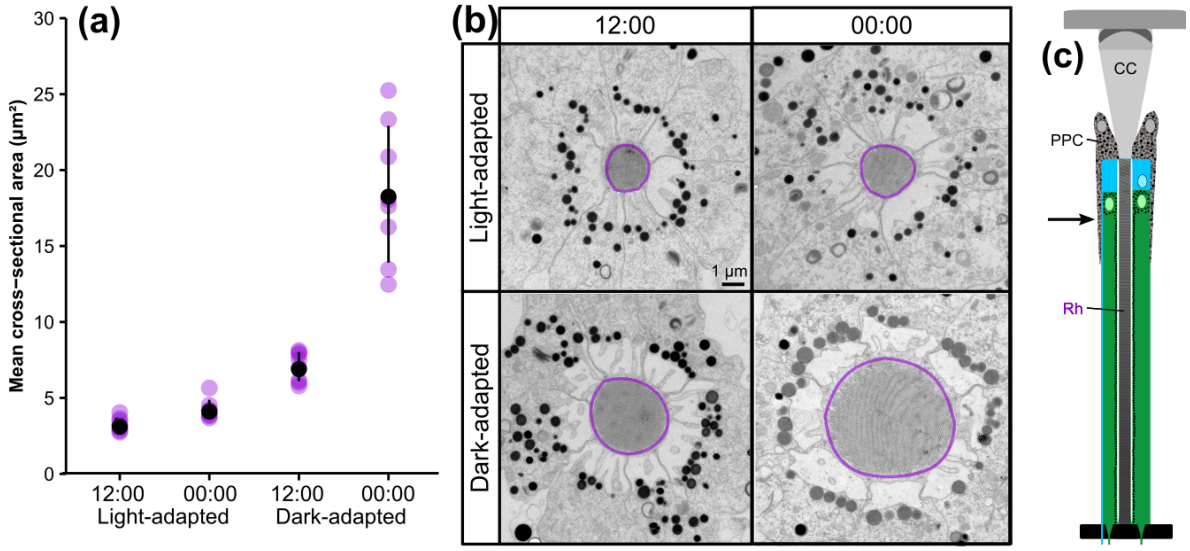

FIGURE 3.10. **(a)** Cross-sectional rhabdom areas of light-adapted and dark-adapted *A. tangeri* eyes, at midday and midnight. Purple points represent individual means (n=8) and global means are shown by black points ± standard deviation bars. **(b)** Representative TEMs of ommatidia when light-adapted and dark-adapted, at midday and midnight. Each rhabdom (outlined purple) approximates to the mean cross-sectional area for the crabs in that treatment, allowing visual comparison. **(c)** TEM sample location indicated by black arrow on ommatidium diagram.

3.3.4.1 Tidal phase comparison

The eyes sampled to collect data for rhabdom cross-sectional area comparisons were dissected from individual crabs at various stages during the tidal cycle, some at low tides and some during high tides. In order to investigate whether rhabdom cross-sectional area is affected by an autonomous tidal clock in the fiddler crab, a multiple linear regression model was fitted to the data. The model described rhabdom area as a function of the interaction between adaptation state

and time (midday/midnight), plus tidal phase, which was scored as the length of time since/until the nearest high water.

The results of the regression indicated that the model explained 84.1% of the variance in rhabdom cross-sectional area of the eyes (R^2=0.841), however tidal phase did not significantly contribute to this model (ANOVA, $F_{(1,29)}$=0.165, p=0.688). This left only the interaction between adaptation state and time as significant predictors of rhabdom cross-sectional area (R^2=0.846) (ANOVA, $F_{(3,30)}$=61.29, p<0.001). Figure 3.11 shows the extent to which individual rhabdom cross-sectional areas deviated from the global mean for each treatment, plotted against the number of hours away from the closest high water time that the eye was dissected. Regression lines indicate no relationship between rhabdom area and tidal phase in any of the four conditions. The measurements during high tides (0-2 hours) are no more anomalous or further from group means than those near low tides (4-6 hours).

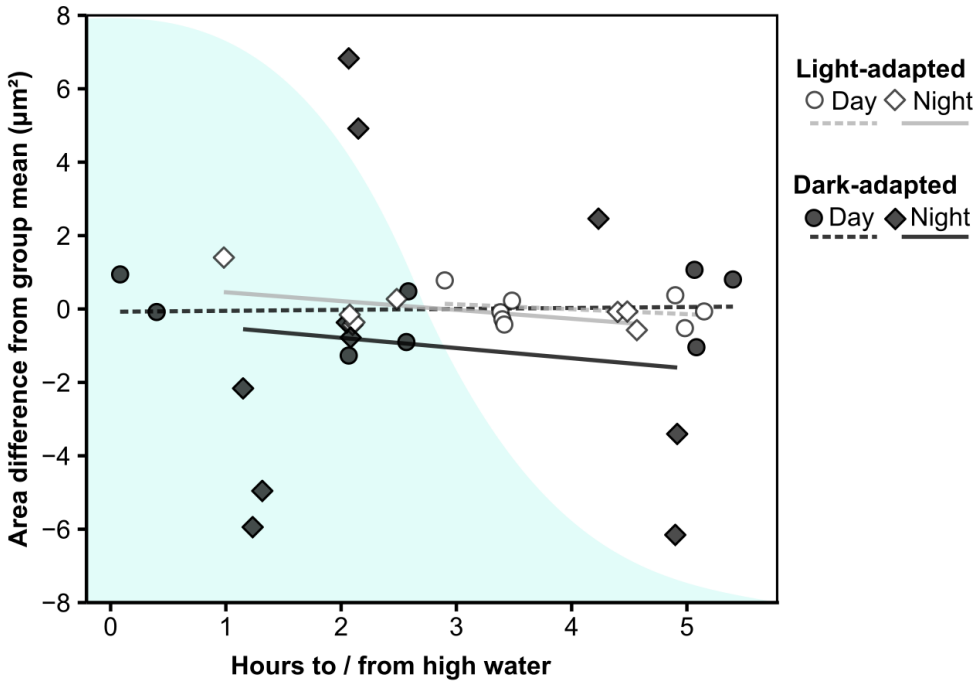

FIGURE 3.11. For each of the four treatments (light and dark-adapted, day and night), the positive or negative deviations in rhabdom cross-sectional area from from the global mean, are plotted for each individual crab (Difference = individual mean - global mean). These values are plotted against the number of hours to/from the closest high tide to which their eyes were sampled (water level represented by blue shaded area). Linear regression lines (dashed=day, solid=night, light grey=light-adapted, dark grey=dark-adapted.) display the relationships between the variables.

3.3.4.2 Photoreceptor ultrastructure

The photoreceptor cells of fully dark-adapted eyes at midnight and fully light-adapted eyes at midday were relatively empty of organelles. However, a close look with TEM of eyes in the process of undergoing light- or dark-adaptation revealed the presence of membrane-bound organelles involved with membrane turnover in the cytoplasm of photoreceptor cells. These include pinocytotic vesicles (Fig. 3.12a), which form multivesicular bodies (Fig. 3.12b) and ultimately, multilamellar bodies (Fig. 3.12c), as well as mitochondria and endoplasmic reticulum (Fig. 3.12d), involved in production of opsin-filled vesicles (Fig. 3.12e).

Rhabdoms become narrower during light-adaptation. The outer edges of the rhabdom in a light-adapting eye are surrounded by vesicles formed by pinocytosis (budding off) of the microvillar bases (Fig. 3.13a). The cell somas of these eyes also contained many organelles including multivesicular bodies and multilamellar bodies involved with protein and lipid recycling and storage. When imaged in longitudinal section, fully light-adapted eyes also had a characteristic scalloped edge to the rhabdom (Fig. 3.13b), whereas edges were straight in dark-adapted eyes (explored further in chapter 7).

At dusk, the cell soma fills with vesicles (Fig. 3.13d) likely to contain opsins [233], in addition to a large accumulation of rough endoplasmic reticulum (Fig. 3.13c) which provide membrane material for elongating microvilli. The palisade vacuoles of dark-adapted eyes tend to appear more solid with fewer gaps than in light-adapted eyes (compare Fig. 3.13 b with d). When sectioned along the long axis of the rhabdoms, some transitioning rhabdomeres were occasionally observed in a state of degradation and turnover of the microvillar membranes, appearing disordered and loosely packed (Fig. 3.13d).

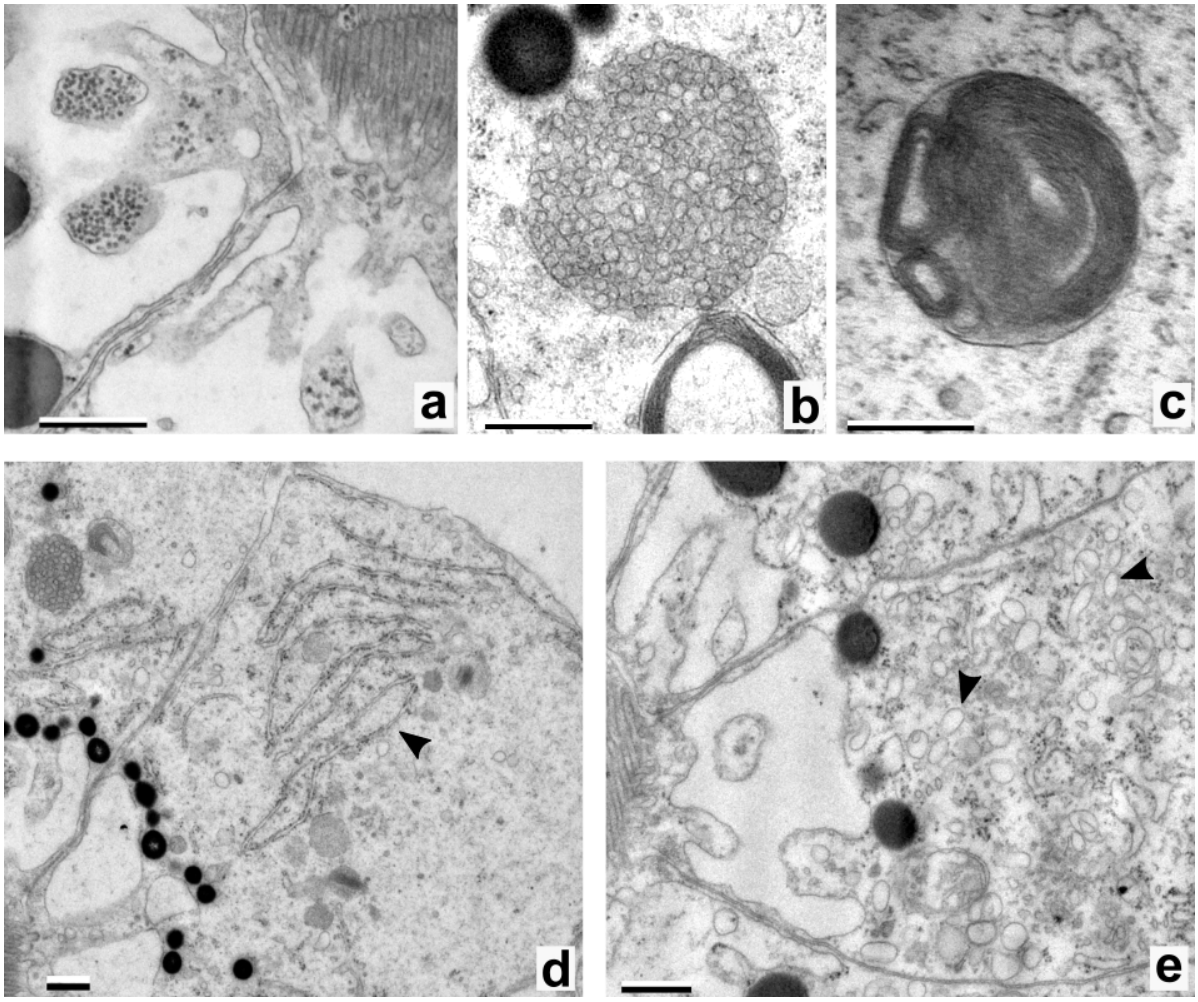

FIGURE 3.12. TEMs of photoreceptor organelles in eyes undergoing light-adaptation (**a-c**) and dark-adaptation (**d-e**). **(a)** Pinocytotic vesicles budding off from the edge of the rhabdom and travelling out to the soma through bridges (gaps) in the palisade vacuole. These vesicles assemble into a **(b)** multivesicular body in the cell cytoplasm, which eventually is condensed into a **(c)** multilamellar body. **(d)** A photoreceptor soma from an eye after 2 hours in darkness in the mid-afternoon. It is largely empty of organelles, except for some long strands of rough endoplasmic reticulum (arrow) involved in protein and lipid synthesis. **(e)** Later at dusk, the photoreceptor soma of a light-adapted eye is full of vesicles containing opsin (examples indicated by arrows), ready to travel through the palisade vacuole and be incorporated into the growing rhabdom with onset of darkness. Scale bars= 500 nm

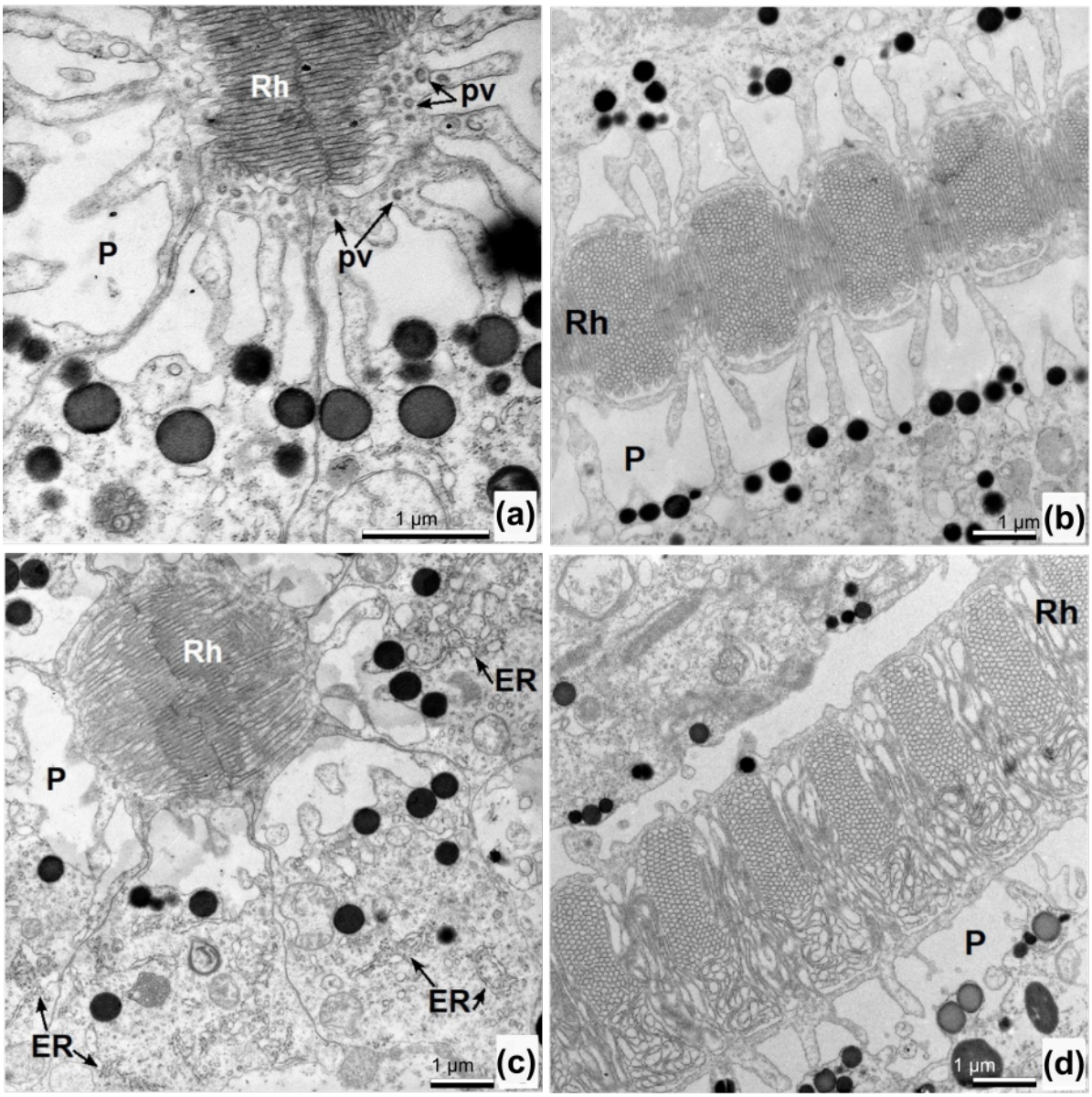

FIGURE 3.13. TEMs of **(a)** an ommatidium during light-adaptation, midday, showing pinocytotic vesicles (pv) budding off from the edge of the rhabdom (Rh) to be transported into the cell soma via bridges in the palisade vacuole (P). **(b)** Longitudinal section through the rhabdom of a light-adapted eye, midday, showing the distinctive scallop-shaped edge. **(c)** Ommatidium during dark-adaptation after sunset, where photoreceptor somas were full of rough endoplasmic reticulum (ER) and other organelles involved with protein synthesis for the extension of rhabdomere microvilli (Rh). **(d)** Longitudinal section through a dark-adapted eye, midday, where all but one rhabdomere are in the process of reassembly with disordered microvillar membranes.

3.3.5 Lengths of photoreceptors and crystalline cones

3.3.5.1 Synchrotron data

Comparisons were made between 3D synchrotron scan reconstructions of two eyes, one naturally light-adapted during daytime, the other dark-adapted from dusk until midnight. Seven horizontal tomogram slices were sampled at equivalent evenly-distributed positions along the vertical (dorso-ventral) axis of each eye (Fig. 3.14a,b). The eyes were of similar overall dimensions (measurements in Appendix Table A.3), but lengths of individual ommatidia varied substantially across each eye (78.2 to 510.4 μm), depending on the location in both vertical and horizontal planes, always shortening toward the edges of the eye.

At the top of the dorsal eye, crystalline cones (and photoreceptor cells to a lesser extent) were longer in the midnight dark-adapted eye (Fig. 3.14c,d). Below, in equatorial and ventral regions, this reversed and both cell types became longer in the midday light-adapted eye, meaning the ommatidia were longer overall. Crystalline cones contributed a similar proportion of the mean ommatidium length in both eyes (they were only 2% longer on average in the dark-adapted eye).

Proportional areas of crystalline cone and photoreceptor cell regions (Fig. 3.14e) were found to differ negligibly between the two eyes at all elevation angles. In the ventral region, the longer ommatidia of the light-adapted eye resulted in larger areas than the dark-adapted eye. However, the proportion of each cell type area remained equivalent to the dark-adapted eye, as shown by its similar percentage area of crystalline cones (Fig. 3.14f). Moving ventral to dorsal in both eyes, the percentage area of eye tissue containing crystalline cones increased slightly, ranging from 38.3% to 53.7%.

3.3.5.2 Light microscopy data

The synchrotron data suggest that crystalline cones and photoreceptor cells do not change in absolute or proportional length between day and night. However, comparing two individuals with an unknown population variability provides insufficient statistical power to dismiss an adaptive change in anatomy between day and night. Therefore, to allow statistical analysis, lateral-facing ommatidia at the eye equator (real world elevation of 0°) were measured from a further 12 individuals. Their eyes, light-adapted at midday, or dark-adapted at midnight (n=6), were compared using light microscopy (Fig. 3.4).

Photoreceptor lengths (Fig. 3.15a) differed considerably between individuals, ranging from 286 to 338 μm (both dark-adapted crabs). However, mean lengths were almost identical between the light-adapted and dark-adapted crabs (308 ± 14 and 307 ± 18 μm respectively) (Welch's t-test: $t_{(9)}$=0.109, p=0.916). Crystalline cones (Fig. 3.15b) were significantly longer in light-adapted crabs (156 ± 4 μm) than in dark-adapted crabs (136 ± 14 μm) (Student's t-test, $t_{(5)}$=3.39, p<0.007), conflicting with the result from the synchrotron data where no difference was measured between the two treatments (albeit n=1).

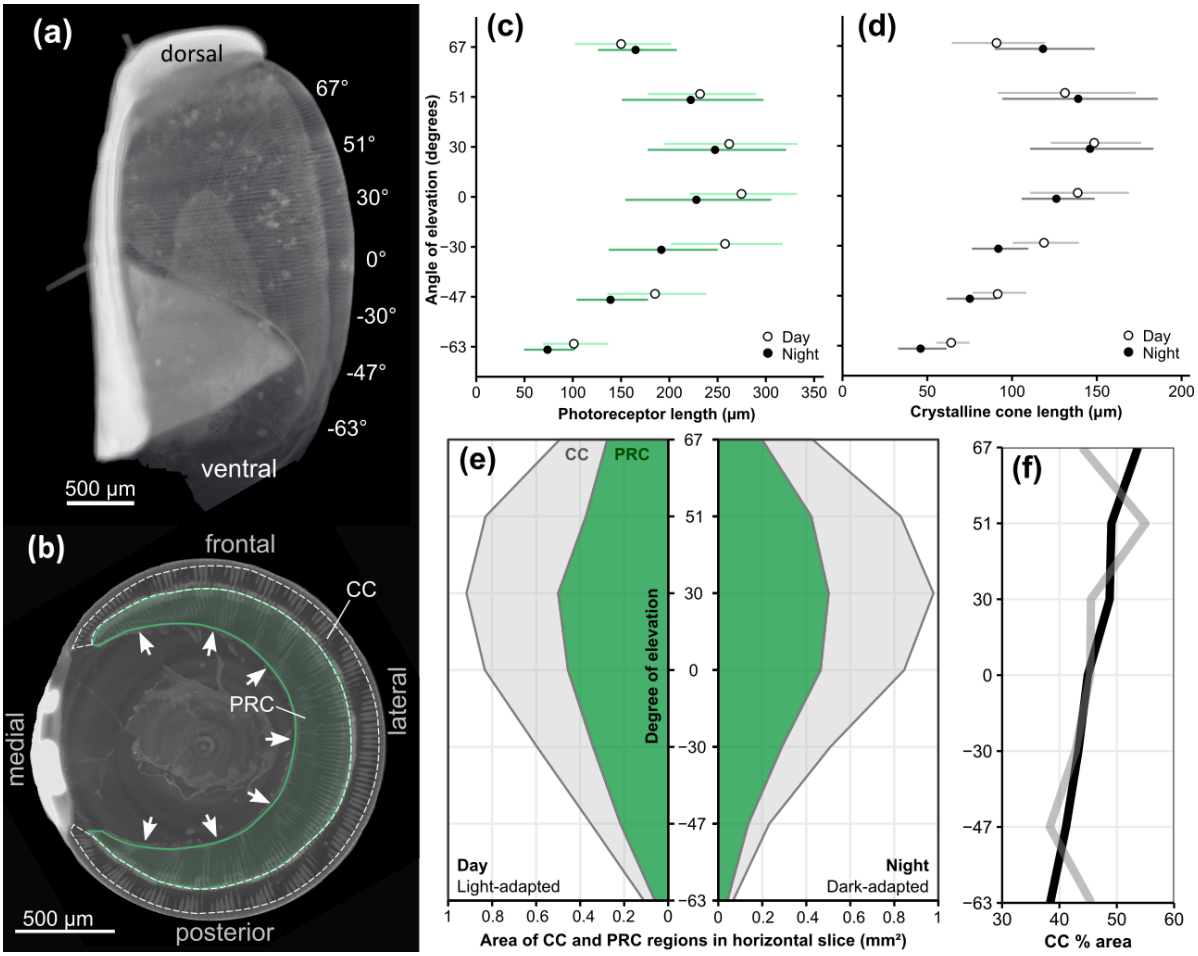

FIGURE 3.14. **(a)** Reconstructed synchrotron tomogram of a whole eye, frontal view. Horizontal slices were sampled at seven angles of elevation labelled along the eye's vertical (dorso-ventral) axis. **(b)** Annotated example slice from the eye equator (0°). Areas occupied by crystalline cones (CC) and photoreceptor cells (PRC) were measured, as well as their lengths in ommatidia marked by arrows. Mean length measurements of **(c)** PRCs and **(d)** CCs (from seven ommatidia per horizontal slice) shown at each angle of elevation along the dorsal-ventral (vertical) axis of a light-adapted eye at midday (open points), compared to a dark-adapted eye at midnight (filled points). **(e)** Areas (mm²) of regions containing CC (grey) and PRC (green) at each angle of elevation along the eye are displayed for a light-adapted eye, midday (left) and a dark-adapted eye, midnight (right). **(f)** CC area as a percentage of the total eye tissue area (PRC+CC) in the light-adapted (grey) and dark-adapted eye (black), at each angle of elevation.

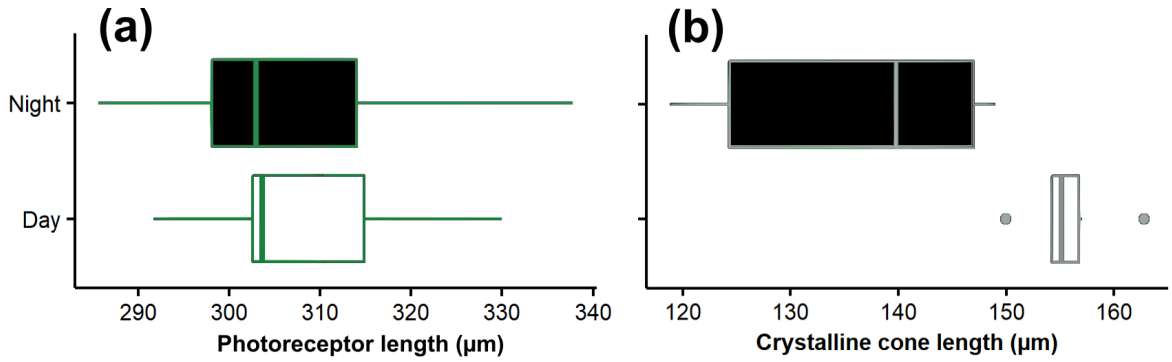

FIGURE 3.15. Lengths of **(a)** photoreceptor cells and **(b)** and crystalline cones measured from lateral-facing ommatidia at the eye equator from light micrographs. Six midday light-adapted eyes (white) and six midnight dark-adapted eyes (black) were compared. Box contains the first to third quartiles with median line. Whiskers extend over the full range of measurements, outliers shown by points.

3.3.6 Light pollution effects on rhabdom cross-sectional area

Ambient light levels were higher at Site 1, El Rompido beach, than at Site 2, an area away from built-up areas (Fig. 3.16a). Facing north (inland) at Site 1, light pollution from the town with its beach floodlights, houses, streetlamps, restaurants and traffic, meant that at its wavelength of highest irradiance (617 nm), Site 1 was 16.1 times brighter than the equivalent measurement from Site 2. There were also artificial lights from the east and west from small boats and marinas. Light levels were lower at Site 2 due to few nearby sources of light pollution. The irradiance level at Site 3 (the darkroom) was assumed to be undetectable by the spectrometer or visual systems of the crabs.

The differing levels of light pollution between sites did not have a significant effect on the mean cross-sectional area of rhabdoms of the fiddler crabs (ANOVA, $F_{(2,15)}$=3.322, p=0.064) (Fig. 3.16b). There was considerable overlap in rhabdom measurements between all three treatments, however, the mean values for rhabdom area for each site did weakly follow the hypothesised trend of being smaller with higher light level exposure. Cross-sectional rhabdom area of the crabs exposed to light pollution at Site 1 varied greatly between individuals from 10.1 and 21.7 μm^2, with mean value 17.2 ± 4.1 μm^2. Crabs exposed to very little light pollution at Site 2 did not have significantly wider rhabdoms than crabs at Site 1 (19.9 ± 2.4 μm^2; TukeyHSD, p=0.317). Crabs in the darkroom control group (Site 3) had the largest rhabdom area measurements (21.9 ± 2.7 μm^2), but they were not significantly larger than those at Site 2 (TukeyHSD, p=0.552), as hypothesised. They were not significantly different from Site 1 either (TukeyHSD, p=0.053). To summarise, the level of light pollution present on El Rompido beach was not sufficient to significantly prevent full rhabdom widening in the rhabdom of the crabs sampled in that location.

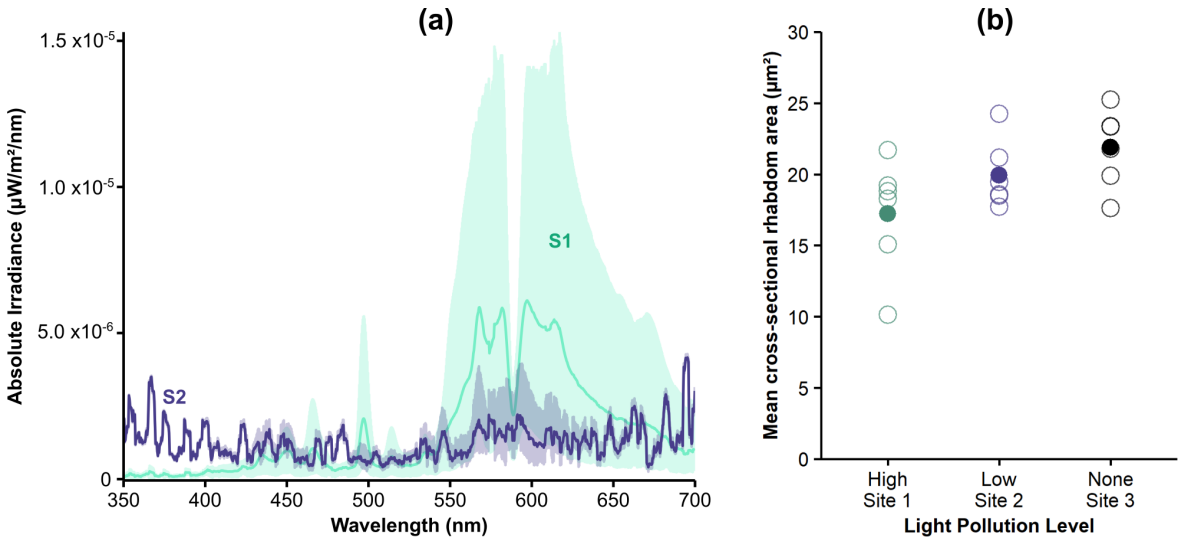

FIGURE 3.16. **(a)** Mean absolute irradiance from four measurements at each site is shown by a green line for Site 1 (S1) and dark purple for Site 2 (S2). The shaded areas of equivalent colour represent the full range of light levels measured at each site. **(b)** Mean cross-sectional area of rhabdoms for individual fiddler crabs (n=6) are represented by open circles, comparing eyes exposed to differing levels of light pollution at Site 1 and 2, and for eyes exposed to no light in a control darkroom (Site 3). Overlaid are group means for each site, shown by filled circles.

3.3.7 Physiological changes in the *G. dampieri* eye

Tissue quality in the *G. dampieri* eye samples was not optimum, probably due to limited time in fixative (24 hours) and a long journey in warm phosphate buffer. Therefore some lysed external photoreceptor membranes are visible in the TEMs. Organelle membranes were also poorly preserved, including around pigment granules inside the R1-7 cells, which resulted in some merging together within the cell. Therefore, data were not collected on pigment distributions inside photoreceptors. The microvillus membranes of the rhabdom remain mostly intact although some evidence of deterioration is visible as the membranes are not well defined.

Comparative observations of the four eyes revealed that eye anatomy is analogous to *A. tangeri*. The main cell somas of PPCs surround the region where the crystalline cone tips meet the distal R8 cells. There are subtle differences in the appearance of the PPCs between light- and dark-adapted eyes (Fig. 3.17a). In dark-adapted eyes (day and night), the PPCs have a defined upper edge because this distal part of the cell is densely packed with pigment granules surrounding the cell nuclei. There is a conspicuous gap around the lower crystalline cone tract, until they pinch in at the very proximal end where the rhabdom begins.

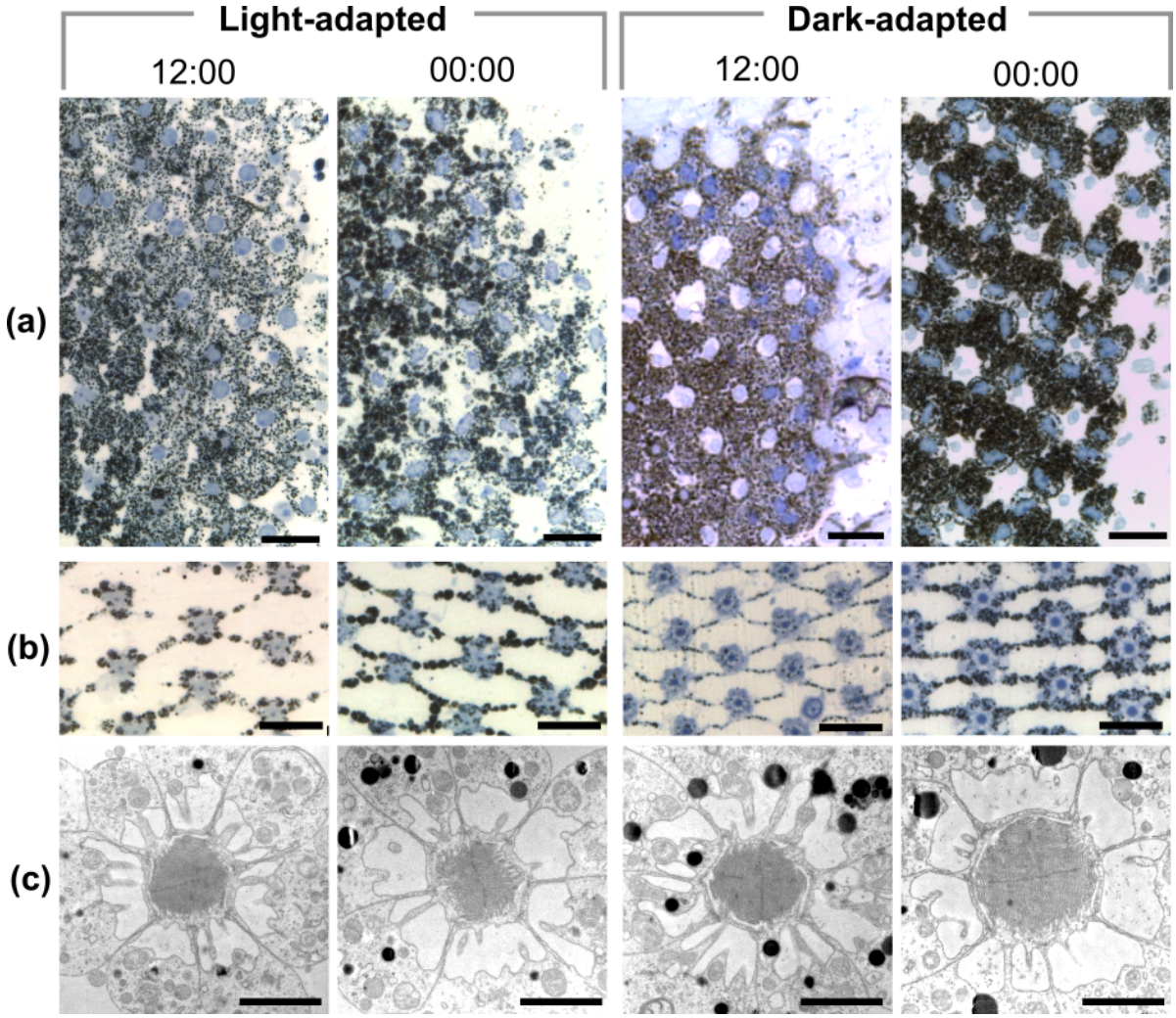

FIGURE 3.17. **(a)** Examples light micrographs of semi-thin oblique sections through the primary pigment cell layer of four *G. dampieri* eyes fixed in different adaptation states. Towards the right side of each panel are the distal ends of the PPC cell bodies containing their nucleus (stained bright blue). These parts of the cells are sparsely pigmented in light-adapted eyes but dense in dark-adapted eyes. Scale bars = 20 μm. **(b)** Several R8 cells in cross-section showing differing rhabdom diameters. The ommatidia are screened from one another by a network of thin primary pigment cell projections. Note the density of pigmentation in the cells between night and day. Scale bars = 20 μm. **(c)** Rhabdoms in cross section imaged with TEM. Scale bars = 2 μm.

Table 3.3: Mean rhabdom and crystalline cone (CC) tip areas (± standard deviation) for four *G. dampieri* eyes in different adaptation states.

Eye condition	**CC tip area (μm²)**	**Rhabdom area (μm²)**
Midday: Fully light-adapted	1.5 ± 0.2	3.3 ± 0.3
Midnight: Fully light-adapted	1.6 ± 0.3	3.0 ± 0.4
Midday: Fully dark-adapted	4.9 ± 1.2	4.0 ± 0.4
Midnight: Fully dark-adapted	7.8 ± 0.4	8.0 ± 0.5

The distal part of the PPCs in the two light-adapted crabs (both day and night) have a sparse distribution of pigment granules, with fewer surrounding the nuclei, meaning the cell edge is not as defined as in dark-adapted eyes. Pigment granules appear to be concentrated lower, more proximally in the cell around the distal-most tip of the R8 cell. The thin proximal projections of the PPCs surrounding photoreceptor cells further within the eye appear to contain fewer pigment granules during daytime (in both light- and dark-adapted eyes) than at night (Fig. 3.17b).

Similar to *A. tangeri*, the lower crystalline cone tract and the rhabdom appear to be wider in dark-adapted eyes, particularly at night (Fig. 3.17c). Measurements of the crystalline cone tips and rhabdoms in cross-section confirm this (Table 3.3). Rhabdoms measure 8.0 ± 0.5 μm² in the night dark-adapted eye, with crystalline cone tips of a similar size. This is not as wide as those of *A. tangeri*, but there could have been some shrinkage due to poor fixation. Both crystalline cone tracts and rhabdom areas are much narrower in the light-adapted eyes of both day and night, while the dark-adapted eye in daytime has intermediate measurements.

3.3.8 *Carcinus maenas*

The eye anatomy of *C. maenas* is similar to the fiddler crab, although ommatidia are generally shorter and wider. Each ommatidium is formed by a corneal lens and crystalline cone, distal R8 cell and longer R1-7 photoreceptor cells, which form a fused rhabdom. In addition to a PPC layer, this species have a population of screening pigment cells near the basement membrane.

Comparisons between light- and dark-adapted eyes from *C. maenas* revealed that the eyes undergo great changes between day and night (Table 3.4). When light-adapted at midday, the PPCs are distributed in a dense layer around the distal part of the R8 photoreceptor cells, with pigment not observed around the crystalline cones (Fig. 3.18a). In the midnight dark-adapted eyes, the pigment disperses distally, surrounding the lower regions of the crystalline cones, which are much wider than in light-adapted eyes. This indicates vertical pigment migration within the PPCs and widening of crystalline cone tips at night.

Rhabdoms of the midday light-adapted eyes measured 11.9 μm² in mean cross-sectional area (Fig. 3.18b). The midnight dark-adapted crabs had rhabdoms 7.7 times wider, with mean value 91.6 μm². While *C. maenas* R1-7 photoreceptor cells lack the distinctive ring of screening pigment

granules around the palisade observed in fiddler crabs, they do contain disordered granules within the distal cell soma near the nuclei. In daytime light-adapted eyes, this surrounds the nuclei, with some granules distributed in mid-proximal regions of the ommatidial column. At night the pigment granules in dark-adapted eyes appear to have emptied from the majority of the photoreceptor cell length leaving the nuclei exposed, and are located in a dense clump right at the very distal tips of the cells.

Although the sample size was small, there was strong consistency in these compelling differences between the three individuals per treatment. Therefore, it was not considered necessary to sacrifice more animals to collect more data.

Table 3.4: Observations of primary pigment cell (PPC) distributions in the eye tissue of *Carcinus maenas* described from light micrographs. Three were pre-adapted to bright light until midday and three were pre-adapted to darkness until midnight. Mean (± standard deviation) cross-sectional areas of their rhabdoms are also displayed for each individual, measured from TEMs.

Crab ID	**Condition**	**PPC distribution**	**Rhabdom (μm²)**
C1	Light-adapted, midday	Dense layer around R8 cells	10.5 ± 5.9
C2	Light-adapted, midday	Dense layer around R8 cells	12.0 ± 6.0
C3	Light-adapted, midday	Dense layer around R8 cells	13.2 ± 6.0
C4	Dark-adapted, midnight	Dispersed around crystalline cones	90.2 ± 5.3
C5	Dark-adapted, midnight	Dispersed around crystalline cones	93.6 ± 5.1
C6	Dark-adapted, midnight	Dispersed around crystalline cones	90.9 ± 5.1

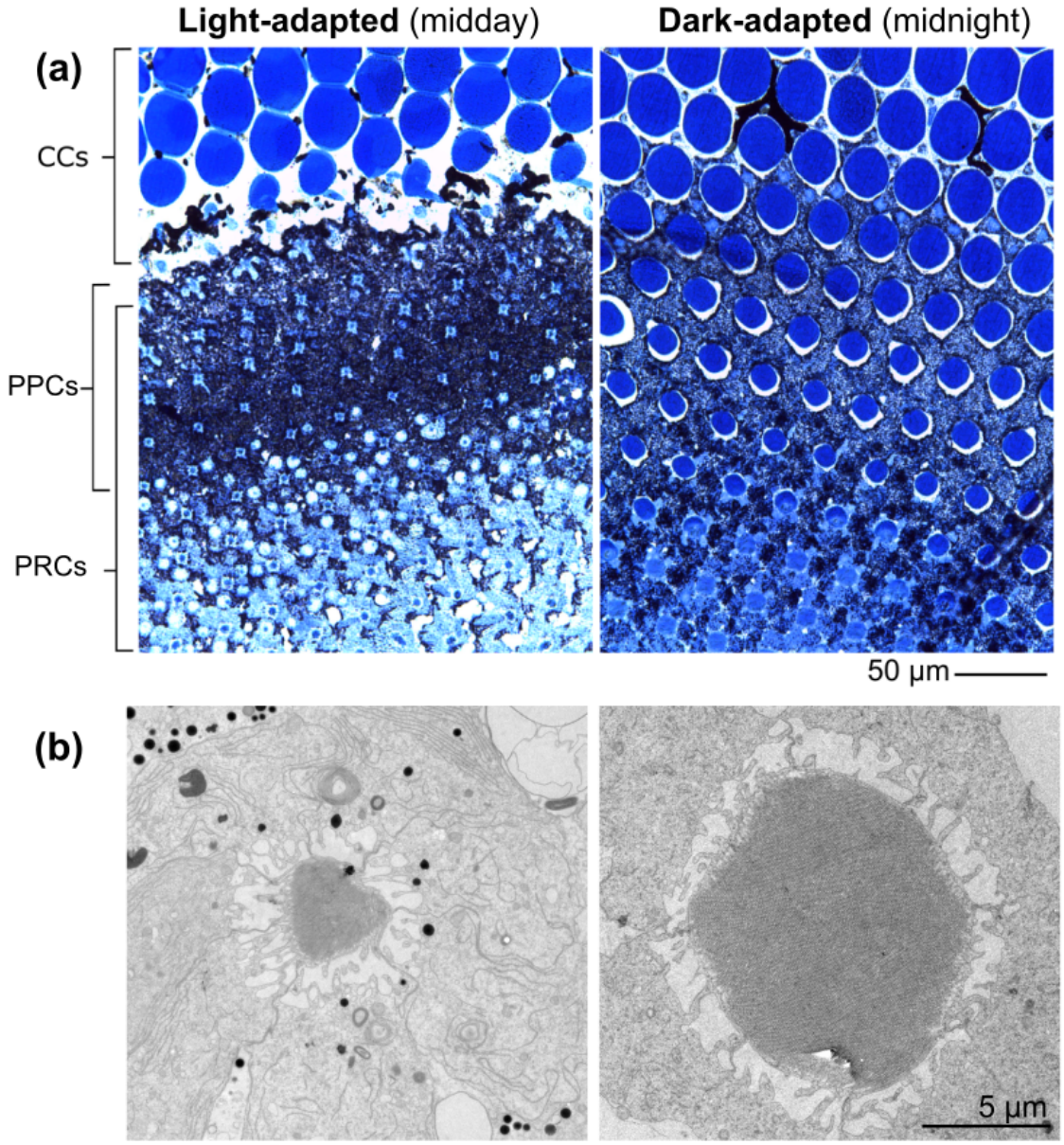

FIGURE 3.18. **(a)** Light micrographs of sections through the eye of *Carcinus maenas*. The primary pigment cells (PPCs) are densely concentrated around the distal photoreceptor cells (PRCs) when light-adapted at midday (left). However, they are dispersed distally around the lower crystalline cone cells (CC) and dark-adapted and midnight (right). **(b)** TEMs of ommatidia cut just proximal to their R1-7 cell nuclei. In the midday light-adapted state (left), the rhabdom is narrow and a few pigment granules are visible. in the midnight dark-adapted eye (right), the cross-sectional rhabdom area is much larger and the cells are empty of pigment granules.

3.4 Discussion

3.4.1 Rhabdom changes

Rhabdom widening apparently provides the main structural mechanism in *A. tangeri* for increasing visual sensitivity at night, with cross-sectional area expanding by a factor of 5.6 from day to night. This would effectively adapt the eye from the very bright conditions in their diurnal tropical mudflat habitats to the relatively slow and predictable decreases in light at dusk. This appears to be a common mechanism across many arthropod taxa [185] and it is also described as the primary adaptation strategy in *Ocypode* and *Grapsus* crabs, for which the ultrastructural processes involved in microvillar membrane recycling by pinocytosis and reassembly have been closely examined [165, 180–184, 200–204, 233].

Day-to-night rhabdom changes are reported for several other crab species suggesting that nocturnal rhabdom widening may be widespread among intertidal brachyuran crabs. In the literature to my knowledge, only one study of optical light-adaptations in crabs lacks mention of nocturnal rhabdom volume increases. The study in question, focussed on pigment migrations in the intertidal crab *Neohelice granulata* [174]. However, it is still likely that rhabdom diameter increases do occur (as in other crabs) but were outside the scope of their investigation and have not yet been measured. Known day-to-night rhabdom cross-sectional area increases in other intertidal crabs range from a factor of 2.4 in *Callinectes sapidus* [202] to 12.8 in *Ocypode ceratopthalmus* [200] (Fig. 3.19). My rhabdom measurements of *Carcinus maenas* eyes also indicated vast rhabdom area changes, with rhabdoms reaching 91.6 μm^2 at night, exceeding even the large ~63 μm^2 night-time rhabdoms of *Hemigrapsus sanguineus* [233]. In comparison to some other species, *A. tangeri* does not appear to be as extreme in its rhabdom diameter cycling, although it does have longer rhabdoms than *C. maenas*, so there may be a smaller difference in total rhabdom volume increase between the two crab species than the cross-section data suggest. All the crabs in Fig. 3.19 require vision in both day and night, but some are also found in deeper water, as well as intertidal zones, so depending on visual requirements and habitat, some crab species may have evolved larger cyclic changes in photoreceptor membrane surface area than others.

Rhabdom widening appears to be strongly linked to a circadian clock in *A. tangeri*. While mostly inhibited by bright light, the rhabdom only widens to its full extent when dark-adapted after sunset. Very similar findings have been reported for several other crabs [180, 182, 200, 234], and the process even takes place in eyes that have been isolated from the animal at dusk [235]. A conceivable evolutionary driver for this strong circadian control on rhabdom widening, may be the associated time and metabolic cost of synthesising membrane for its microvillar elongations. Widening the rhabdom frequently to cope with short temporary periods of darkness during daytime may be too expensive to use as a strategy. Instead, rhabdom diameter is strongly associated with the predictable decrease in light intensity at dusk and daily membrane turnover.

From observations of transitioning rhabdoms, this happens as described by Matsushita *et al.* [233] in *H. sanguineus*. Refer to chapter 5 for more detail on this, as well as timescales of rhabdom changes involved with light- and dark-adaptation. Further behavioural or electrophysiological work is now necessary to test how rhabdom volume changes affect the visual sensitivity of living crabs (see chapter 4).

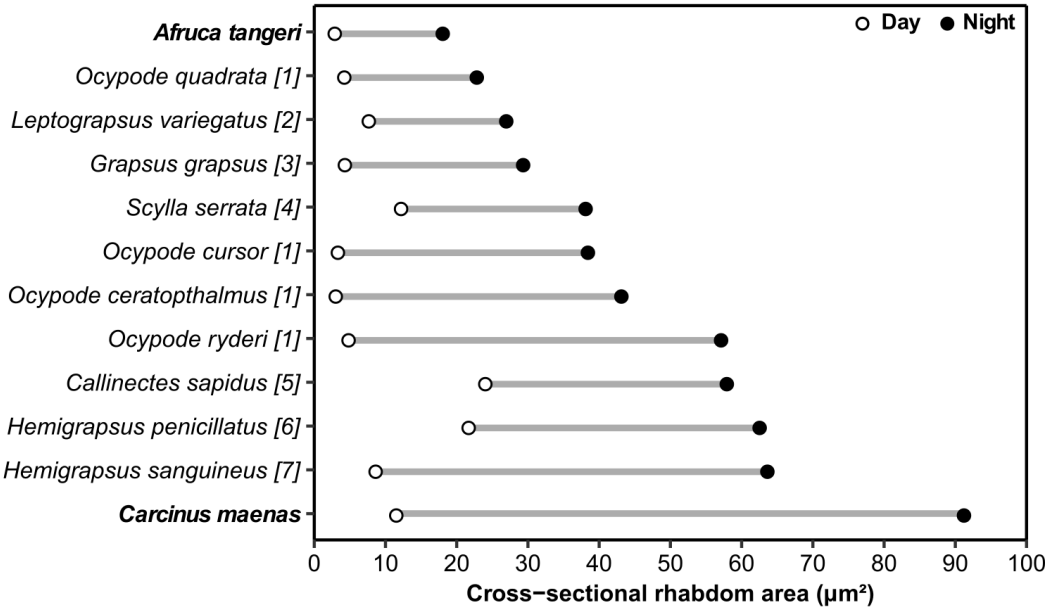

FIGURE 3.19. Mean cross-sectional area of rhabdoms of several intertidal brachyuran crab species between daytime light-adapted eyes (open circles) and night dark-adapted eyes (filled circles). Source indicated after species name: 1= Rosenburg and Langer [200], 2= Stowe [182], 3= Nässel and Waterman [180], 4= Leggett and Stavenga [173], 5= Toh and Waterman [202], 6= Toh [203], 7= Matsushita et al. [233]. Some of the published area measurements were calculated from diameters (d) using: Area = $\pi(d/2)^2$.

Increases in rhabdom length should also increase photopigment volume for light capture. As a dark-adaption strategy this has been observed only in few cases, including a tipulid fly [169], *Camponotus* ant [167] and *Grapsus* crab [180]. The 3D synchrotron datasets showed that rhabdom lengths vary substantially across the eye and differences of up to 18.2% existed between equivalent regions in equally-sized individuals of the same adaptation state. This may explain why Nässel and Waterman [180] reported a 16% increase in the length of *Grapsus* crab rhabdoms from day to night, from four individuals. My light micrograph measurements of equatorial eye regions indicate no rhabdom elongation from day to night in *A. tangeri*.

3.4.2 Crystalline cones

Rhabdom widening in *A. tangeri* was accompanied by equivalent increases in the diameter of the lower crystalline cone tract, which tapered to match the diameter of the distal rhabdom in each treatment. Like the rhabdom, widening of the crystalline cone tip aperture appears to be under strong circadian clock influence, remaining narrow during daytime in dark-adapted eyes. Perhaps the very narrow diameter (sometimes <800 nm) of this region of the light path in daytime functions as a short-pass filter. It might explain the evening 25 nm red shift in spectral sensitivity revealed in G. dampieri by Jessop *et al.* [45]. Differential interference of red light, with wavelengths approaching the size of the narrow aperture, could result in blue-shifted (shorter wavelength) spectral sensitivity in daytime. At night, when the acceptance angles widen to allow longer wavelengths to reach the rhabdom, a red shift in spectral sensitivity could occur. In light micrographs of the PPC layer of *C. maenas*, large increases in the thickness of the lower crystalline cone tract is also evident at night in comparison to daytime.

There were substantial variations in ommatidial lengths across the eye in *A. tangeri* (demonstrated by synchrotron data). Interestingly, with increasing elevation in the eye, the crystalline cones appear to gradually lengthen in proportion to the photoreceptors, dorsally. This may be associated with regional specialisation to facilitate a visual task, for example helping to optimise predator detection above the horizon, not required in the ventral eye, which is involved with detection of conspecifics [113, 114, 118]. Alternatively, photoreceptors may be shorter at higher elevations due to a relatively brighter scene (the sky) and associated increased rates of photon capture. There was negligible difference in the proportional length of crystalline cones between the two tomograms, suggesting no shortening from day to night. However, conflictingly in the length data from light-micrographs, the crystalline cones were slightly shorter on average (by ~20 μm) at night when dark-adapted. Nocturnal crystalline cone shortening also occurs in *Camponotus* ants [167] and brine shrimp, *Artemia* [177]. It is possible that that whilst maintaining constant cell volume, the crystalline cones in *A. tangeri* become shorter and wider at night, resulting in reduced focal length and wider proximal aperture, revealing a rhabdom that is also widening in diameter. These processes increase the acceptance angle and photon capture of each ommatidium, at the expense of spatial acuity [7].

3.4.3 Primary pigment cells

In crustaceans, migrations of screening pigment granules within accessory pigment cells are not uncommon as a light-adaptation strategy e.g. [164, 165, 171–175] and a prime example of this can be seen by comparing the light micrographs of *C. maenas* eyes fixed in day and night. Just like the mud crab *Scylla serrata*, pigment within the PPCs migrates distally away from the distal rhabdom tip to a more dispersed arrangement between crystalline cones. In *S. serrata* this was demonstrated both histologically and in the living eye using an ophthalmascope, showing

as a bright "iris" of pigment around the psuedopupil [173]. Only observed after several hours of dark-adaptation at night, it was absent in the daytime or when light-adapted.

Microscopy and X-ray synchrotron tomography of *A. tangeri* eyes indicate that pigment granules within the PPCs remained in fixed position from day to night and are thus unlikely to effectively moderate light flux to the photoreceptors below. This was surprising given that Fingerman [171] measured substantial migrations of screening pigment in the fiddler crab *Leptuca pugilator*. His method of measuring the width of the back-lit translucent area (crystalline cones and cornea) in comparison to the total eye width, using a light microscope, generated a rough ratio given the apparatus employed. Contrary to my own findings, his measurements strongly indicated a circadian distal movement of screening pigment into the crystalline cone region at night, showing that it retracts proximally again during daytime even in the absence of light. Fingerman's study did not identify the cells involved and it is possible that the pigment migration occurred in the finer, low contrast secondary pigment cells (not examined in this study); or that shortening crystalline cones at night could give an illusion of pigment migrations. Alternatively, the contradictory data on *A. tangeri*, may simply be due to species-specific differences in this strategy (the two crabs are from a different subfamilies) and it would be interesting to try and replicate his experiment with *A. tangeri.* Large differences in visual adaptations are not unusual between related species of arthropods [152].

In *G. dampieri*, limited observations on PPC arrangements suggest a subtle migration of pigment granules, from a slightly more dispersed arrangement when dark-adapted, to a concentrated dense layer around the crystalline cone tip apertures in bright light. The travel distances of the granules appear short (perhaps 20 μm maximum) and some granules were left behind, creating a sparse distribution in the distal part of the cell. Therefore, it is unlikely that these migrations would be measurable by Fingerman's method. It is interesting that this species appears to differ from *A. tangeri* in this way, however, and further study to confirm these findings would be useful.

In *A. tangeri*, TEMs revealed that the four PPCs encircling each crystalline cone make no contact in any adaptation state until the very proximal tip of the cones where they meet the rhabdom. They do not appear to actively constrict the proximal cone tract in bright light as they do in some nocturnal ants, for example [162, 167, 168] and possibly in *C. maenas* too (refer to Figs. 3.18a). Diameter increases at night in the pupillary opening between PPCs were found to be unconvincingly small, with just a 1.2 μm mean diameter increase (19.7%) from light-adapted eyes at midday to dark-adapted eyes at midnight. This further dismisses pigment migrations in PPCs as a likely adaptation strategy in *A. tangeri*.

3.4.4 Acceptance angles

Theoretical acceptance angles ($\Delta\rho$) for midday light-adapted eyes and midnight dark-adapted eyes, were calculated from measurements of ommatidial dimensions using the following equation proposed by Snyder [176],

$$\Delta_\rho = \sqrt{\left(\frac{\lambda}{D}\right)^2 + \left(\frac{d}{f}\right)^2}$$

Mean ommatidial measurements of lateral-facing facets at the eye equator were used in the calculations (Table 3.5), including values for rhabdom length (l) and diameter (d). Peak spectral sensitivity (λ_{max}) for *A. tangeri* is ~530 nm [37], therefore this was used as the wavelength (λ) in the calculations. In the equatorial acute zone of the eye, spatial resolution is highest and facets are largest [117]. Facet diameter (D), the distance between the centre point of adjacent facets at the cornea, was measured from light micrographs (n=12). Focal length (f), the distance from the distal rhabdom tip to the nodal point of the corneal lens, was approximated to the length of the crystalline cone (slight error likely as precise location of nodal point was unknown).

Table 3.5: Mean dimensions of *A. tangeri* eyes in a daytime light-adapted and midnight dark-adapted state (n=6-8), used to calculate theoretical acceptance angles and optical sensitivity.

	Light-adapted, midday	**Dark-adapted, midnight**
Facet diameter (D)	34 ± 3 μm	34 ± 3 μm
Rhabdom diameter (d)	2.0 ± 0.4 μm	4.8 ± 4.5 μm
Rhabdom length (l)	308 ± 14 μm	307 ± 18 μm
Focal length (f)	156 ± 4 μm	136 ± 14 μm
Acceptance angle ($\Delta\rho$)	1.2 ± 0.0°	2.2 ± 0.1 °

The calculations demonstrate that acceptance angle ($\Delta\rho$) doubles from 1.2 ± 0.0 ° in a midday light-adapted eye, to 2.2 ± 0.1 ° when dark-adapted at night. This is caused mainly by wider apertures and rhabdom tips, in addition to a slightly shorter focal length (crystalline cone) associated with dark-adapted eyes at night. A scaled diagrammatic summary of the anatomical findings (Fig. 3.20) displays the mean measurements for crystalline cone and rhabdom changes in dark- and light-adapted eyes of *A. tangeri* between night and day.

3.4.5 Photoreceptor screening pigments

The ommatidial changes described thus far are slow and circadian and allow sensitivity adjustments to cope effectively with the regular and predictable changes in light levels between day and night. So how does the fiddler crab react to fluctuations in brightness during the daytime, for example when entering the burrow for short periods? Many insects such as dipteran flies,

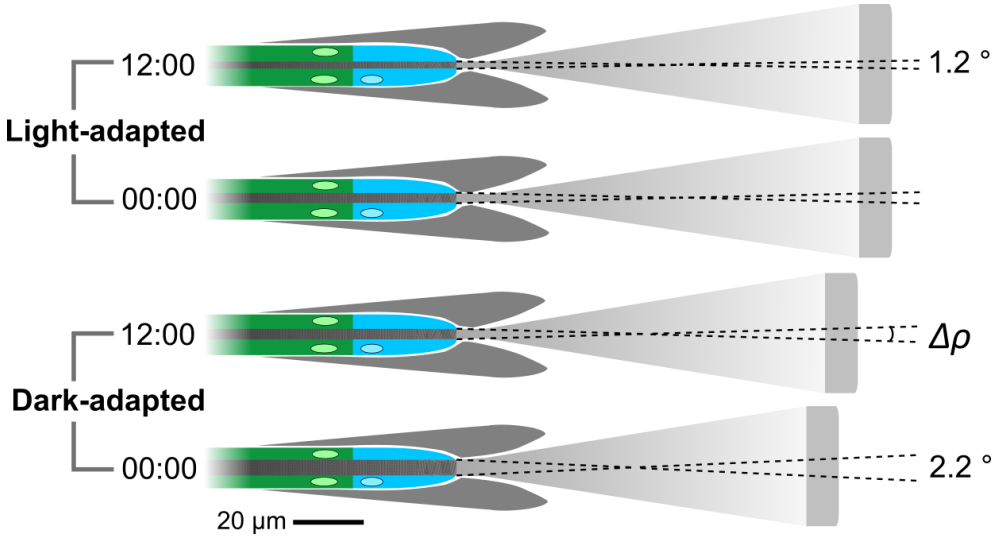

FIGURE 3.20. Summary of the ultrastructural differences observed in *A. tangeri* ommatidia in light- and dark-adapted eyes between midday and midnight. Dimensions of the crystalline cones and adjoining distal rhabdom tracts are to scale and PPCs (dark grey) are shown in their unchanging position. Relative acceptance angles ($\Delta\rho$) are indicated by dotted lines through the crystalline cones.

butterflies [7] and ants [162] use radial pigment migrations in the eye to react quickly to fluctuating light levels. Screening pigment granules contract inwards to tightly encircle the rhabdom in bright light, then move away from the light path in darkness, functioning as a pupil. Though not widely reported in marine arthropods, it has been observed in the mantis shrimp *Gonodactylus oerstedii* [157, 236], a horseshoe crab, *Limulus polyphemus* [237] and the amphipod *Paryhale hawaiensis* [238], a diverse mix of arthropod taxa.

In light-adapted *A. tangeri* eyes fixed at midday, TEMs revealed ≤4.3% of pigment granules to be within the cytoplasmic palisade bridges and they did not resemble the distributions of light-adapted *G. oerstedii* eyes, in which radial pigment migrations occur [157]. Therefore, despite the presence of one or two granules occasionally located in bridges (examples found in all treatments), I did not find convincing evidence of effective radial screening pigment migrations within photoreceptors in this species. The palisades in light-adapted eyes appeared less solid in shape with larger gaps so this may explain the slightly greater number of granules therein. This reduced volume of palisade material surrounding the rhabdom in daytime compared to night, has also been reported in closely-related *Ocypode* (ghost crabs) [200].

The travel distance through palisade bridges is very short (<3 μm) and there was concern about granules snapping back to dark-adapted positions during dissection and fixation. Eyes were dissected immediately into fixative using the method described by Alkaladi and Zeil [89] to best preserve the pigment distributions in fiddler crabs, although anaesthesia with ice was avoided as cold temperatures are known to disrupt radial pigment migrations in mantis shrimp [157, 236]. I

also tried dissecting light-adapted eyes straight into 70-80°C fixative, which has also been claimed historically to maintain true pigment distributions by instant protein denaturation, e.g. [239]. Still, evidence of radial pigment migrations was not observed with this prep and it produced substandard tissue quality. Further evidence for lack of pigment migrations was collected using an ophthalmoscope in chapter 5. This, plus the absence of any examples of light-induced radial screening pigment migration (as seen in other mentioned species) in any of my extensive library of *A. tangeri* eye TEMs, supports the conclusion that this is not a strategy used by this species.

The unchanging screening pigment distributions in the eye between light and dark, night and day, imply that the eye remains fully adapted to bright light even after periods in a dark burrow during daytime. While this may seem disadvantageous, a reason for this could be simply lack of necessity to dark-adapt during daytime. The habitats and lifestyles of some arthropods (e.g. flying insects) necessitate fast visual adaptation, however the mudflat or sandy habitat is mostly free from large shady patches, except passing clouds. Whilst entering the burrow to access water or shelter from predators can be a frequent activity, there is no requirement for vision inside the burrow. However, on exiting, it is extremely important that they can see well enough in the bright light to detect the presence of potential predators. Therefore, we believe effective daytime dark-adaptation is neither necessary nor beneficial to a fiddler crab. Similar ideas have been proposed by Leggett and Stavenga [173] for a mud crab, *Scylla serrata* which may spend much of the daytime moving between dark refuges. Similarly, pigment migrations in the superposition eye of nocturnal moths keep it light-adapted during inactive daytimes spent in a dark refuge. This prepares the eye for flight in bright daylight in case the moth is suddenly discovered by a predator [240].

3.4.6 Optical sensitivity

To estimate the effect of physiological changes on the light-absorbing potential of the eye as it adapts from bright daylight to darkness at night, I calculated theoretical optical sensitivities (S) to white light using the following equation proposed by Warrant and Nilsson [241]:

$$S = \left(\frac{\pi}{4}\right)^2 D^2 \left(\frac{d}{f}\right)^2 \left(\frac{kl}{2.3+kl}\right)$$

Again, mean measurements from lateral-facing facets at the eye equator were used (Table 3.5), including diameters (d) and lengths (l) of the rhabdoms, the size of the aperture through which light enters the eye, i.e. the facet diameter (D) and focal length (f). The absorption coefficient (k) of the photoreceptor was assumed to be 0.0265 μm^{-1}, a typical value for crabs [18].

Optical sensitivity (S) of a light-adapted eye at midday was 0.096 ± 0.017 μm^2 sr. At night, due to the wider rhabdom and slightly shorter focal length, the light-gathering power of a dark-adapted eye is boosted to 0.704 ± 0.086 μm^2 sr, an estimated 7.4-fold increase in photon capture.

3.4.7 Visual ecology

The flat habitat and ethology of fiddler crabs mean there is little need to adapt to darkness during daytime hours. At night, darkness can be used to the crab's advantage. A lack of aerial predators means a safe extended period of foraging or mating time on warm evenings. By my own observations during the breeding season, male crabs continued to signal visually for at least 2 hours after sunset on warm nights, although acoustic signals via tapping the substrate or body with the major cheliped became more frequent as the evening progressed (also observed by [217, 242]). Crabs were noted to be uncharacteristically bold at night and could be approached by torchlight, showing little concern about potential capture until the last few seconds (personal observation). This has also been noticed by Andalucían fishermen, to whom the males will occasionally lose their dominant claw. They are often collected after sunset when they are of more relaxed temperament (personal communications). Interestingly, Knopf [215] also mentions the same "complete absence of wariness" among *Leptuca pugilator* fiddler crabs at night. *Afruca tangeri* activity is also constrained by declining ambient temperatures in the evening and they retreat into burrows below 18 °C surface temperature [217], meaning nocturnal foraging is restricted to summer months. To the human eye at least, as the light fades, the brilliant white claws become highly conspicuous against the dark mud background [93] and courtship often occurs after sunset [216]. Perhaps signalling activity after dusk in this species has driven selection for a highly reflective cheliped with uniform white colouration, at a potential cost of increased visibility to predators. Meanwhile, the rest of the body shows much temporal and spatial polymorphic variation within and between individuals, but relative to other fiddler crabs, is generally dull [54].

3.4.8 Light pollution

In *Leptograpsus*, Stowe reported that prolonged bright light exposure after dusk produced narrower rhabdoms than crabs in normal dim light conditions. However, she noticed that the cell ultrastructure indicated that synthesis of new rhabdom microvilli *had* taken place despite the narrow rhabdom. The many pinocytotic vesicles around the microvillar bases suggested that the rhabdom was also being degraded at the same time in reaction to the bright light [182]. These two counterproductive processes may be significant energy cost to the animal. If bright lights extend late into the night and then are suddenly switched off (this happens shortly after midnight in El Rompido), it may be too late for circadian clock-driven dark adaptation processes to occur fully, meaning the animal's visual system would remain insensitive for the remainder of the night.

Prolonged exposure to very bright direct LED lighting has been demonstrated to maintain a narrowed rhabdom at night. However, the levels of light pollution experienced by crabs on the El Rompido beach (Site 1) did not significantly reduce the cross-sectional area of their rhabdoms, compared to those allowed to adapt in almost complete darkness. Fiddler crabs continue to forage

in abundance on light polluted areas of the beach in El Rompido after sunset (see chapter 6), however the numerous bright artificial light sources they are exposed to are usually many meters away or indirect. Therefore, despite potentially causing alterations to their behaviours, ability to detect visual cues and their own conspicuousness, the ambient light levels are not necessarily high enough to provoke a measurable anatomical change in the eye as a light-adaptation response.

The variance in rhabdom area for all sites was high, especially for Site 1 (with a range of 11.6 μm^2 in the measurements). This may have been partly due to differences in viewing direction between individuals. The main sources of light pollution were from the north and the crabs were allowed to move freely in containers during their evening exposure, creating a small possibility that an individual could face south for the majority of the evening and therefore avoid the brighter light exposure to the frontal region of the eye (which was sampled for measurements). However, generally when contained, fiddler crabs tend to be very active, moving all the time in attempt to climb out of their pots.

Even in fiddler crabs that were dark-adapted until midnight in controlled darkroom conditions (section 3.3.4), the variance in their rhabdom area measurements is very high compared to equivalent data for the daytime or bright-light exposed eyes. This indicates that there may be large naturally-occurring differences in rhabdom sizes between individuals at night; or that rhabdom expansion is determined by additional unknown factors, unrelated to light exposure (e.g. stress due to capture). Therefore, it may be difficult to pick out the subtle effects of something like light pollution from rhabdom area measurements alone where individual differences are large.

To conclude, *A. tangeri* appear not to be negatively impacted by the bright lights at El Rompido and are numerous in light-polluted areas. Perhaps the light even benefits the crabs by facilitating longer foraging and courtship periods into the evening when predatory birds are less active. The light levels present were not bright enough to provoke a significant reduction of the cross-sectional area of their rhabdoms, which appears to be the principal mechanism for adapting effectively for sensitive vision at night.

3.4.9 Tidal phase

As well as the large predictable changes in light and temperature experienced from day to night, *A. tangeri* are constrained by tidal cycles and activity levels are exclusively associated with low tides when the mud surface drains to allow foraging. Fiddler crabs are known to possess effective biological clocks for timing these regular events [205–209] (this is explored in detail in chapter 6).

The daily rhabdom changes for increasing visual sensitivity at night may be associated with high metabolic costs and for two long periods of a solar day, foraging is not possible due to high tides. If, for instance, there is an evening high tide, dark-adaptation may not be necessary at all that night, allowing significant potential metabolic gains to be made from remaining light-

adapted. Does a fiddler crab adapt to the lighting conditions outside the burrow, when it is likely not to leave it at all during that light phase? The data were analysed to look at effect of tidal phase on rhabdom cross-sectional area, but no relationship was found between them. Rhabdom sizes were not more anomalous during high tides, compared to low tides in light-adapted or dark-adapted crabs during night and day, so endogenous tidal clocks do not appear to have an effect on the retinal state. However, one must consider that the crabs had not been in their natural habitat for up to 48 hours at the time of eye collection. Perhaps an experiment could better test these ideas using fiddler crabs acclimatised to an artificial mudflat with regular changing water levels to simulate tides (e.g. Fig. 2.1). If the crabs could be quickly collected from burrows at "high tide" and mud surface at "low tide", the eyes could be compared in a more natural state.

3.4.10 *Gelasimus dampieri*

One cannot assume that two closely related species will have the same eye anatomy and light-adaption strategies. Eye design of *A. tangeri* closely resembled Alkaladi & Zeil's description of *G. vomeris* [89], which is from a different subfamily. In fact, I was not able to identify any differences, except in some of the fine microvillus arrangements of the rhabdom (see chapter 7). *Gelasimus dampieri* is from the same genus and geographic location as *G. vomeris* [50, 91], so it is likely that their eye physiologies are akin and from observations, they do appear similar. However, we do not know the light-adaptation strategies of any *Gelasimus* species (or any fiddler crab other than *A. tangeri*). Fingerman's evidence of distal pigment migrations in *L. pugilator* (an East Atlantic fiddler crab) suggest there may be some species specific differences within the family Ocypodidae.

The anatomical study of *G. dampieri* was limited by the small sample size (n=1) and tissue quality. However observations suggest that rhabdoms widen at night in this species also, doubling in size at least. It is not known whether this species is nocturnally active (not by researchers at UWA at least), but a strictly diurnal lifestyle may be why the rhabdoms in the dark-adapted crab's eye fixed at midnight, did not reach the large size of equivalent *A. tangeri* eyes. From experience however, I have observed some rhabdom shrinkage in poorly fixed eyes.

There may also be some change in the PPCs as there were subtle differences between dark- and light-adapted eyes. It appears that screening pigment granules concentrate in the proximal portion of the main cell soma of PPCs in response to bright light, and disperse slightly in the dark to create the more defined edge to the PPC layer when viewed with microscopy. The granules do not appear to move to a light-adapted position in the dark during daytime as Fingerman observed in *L. pugilator* [171]. It is unlikely that the subtle changes observed in the *G. dampieri* eyes would be measurable using his methods as the pigment granules only appear to move over distances of a few microns. The differences in distribution were not as prominent as those observed in *Carcinus maenas*.

3.4.11 Conclusions and future research

The most conspicuous adaptation method in the eye of the fiddler crab from day to night, is the large changes in rhabdom and crystalline cone tip diameter, serving to increase acceptance angle of each ommatidium, as well as creating a larger surface area for photon capture by the photoreceptors. We now know that while fiddler crabs will experience large increases in visual sensitivity around sunset, they will not fully dark-adapt during daytime and might struggle effectively to adjust to fluctuating light levels due to static distributions of pigment populations throughout the eye.

When measuring responses to visual stimuli in these animals during future behavioural or electrophysiological experiments, it is very important to consider time of day and prior ambient lighting conditions. Next is to investigate the extent to which rhabdom increases affect the relative sensitivity of the visual system of this species in these different adaptation states (refer to chapter 4). There are also questions remaining about whether the metabolic cost of membrane production involved with rhabdom increases is offset by a slower temporal resolution. Although fast ultrastructural changes are visibly absent in the optics of the *A. tangeri* eye, there are likely to be alternative strategies to alter optical sensitivity over short timescales, for example neural summation to increase sensitivity further at night and during temporary periods in darkness during daytime [34].

CHAPTER 4

SENSITIVITY OF THE FIDDLER CRAB VISUAL SYSTEM

We now know that the eye of the fiddler crab *Afruca tangeri* experiences some dramatic physiological changes from light to dark; but how do these affect its functional sensitivity? Three complimentary experiments using behavioural response and electroretinogram (ERG) response thresholds to visual stimuli were performed to test differences between light- and dark-adapted fiddler crabs during night and day (the same four treatments compared anatomically). The experiments were designed to assess differences in (**1**) ability to detect contrasts in dim light, (**2**) relative thresholds of absolute sensitivity, and (**3**) whether temporal summation is a strategy used by fiddler crabs when dark-adapted. Tests were performed during both day and night to assess the role of the circadian clock.

4.1 Introduction

4.1.1 Background

During daytime, the eye of a fiddler crab is prepared for exposure to the extremely bright light typically experienced on the surface of their semitropical or tropical mudflat habitats [50, 114]. Although no evidence was found of pigment migration to help moderate light flux to the retina in the *A. tangeri* eye, a narrow lower crystalline cone tract during daytime reduces acceptance angles and restricts the amount of light reaching the photoreceptors [214]. Theoretical calculations using Snyder's equation [176] in chapter 3 suggested that from a light-adapted state at noon, acceptance angles ($\Delta\rho$) double at night in a dark-adapted eye. In addition, the volume of photopigment-packed microvillus membrane in the rhabdom increases by over 5 times at night to boost the surface area and volume for photon capture in dim light. A larger diameter of the combined rhabdom and surrounding palisade also supports a larger number of wave-guide modes

to propagate through [158, 159]. According to a formula proposed by Warrant and Nilsson [241], these physiological changes should increase optical sensitivity to white light (S) by 7.4 times. Histological examinations of a few *G. dampieri* eye samples suggest that similar phenomena exist in this species, potentially in addition to subtle migrations of screening pigment within primary pigment to help moderate light flux.

4.1.2 Contrast sensitivity

To assess how circadian physiological changes affect the visual abilities of fiddler crabs from day to night, two experiments were carried out to compare contrast sensitivity in dim light. If the relative luminosity (difference in brightness) is very small between an object and its background, it creates a low contrast which becomes difficult for a visual system to detect. This is due to **extrinsic noise**, the inherently random dynamics with which photons (discrete units of light) arrive at a detector, also known as photon shot noise; in addition to **intrinsic noise** within photoreceptor pathways of a visual system (photoreceptor noise) [25, 26, 29]. Without the presence of sufficient photons (in very dim light), a pattern that is usually highly contrasting in bright light may not be detected [29, 243]. In brighter settings, to resolve a low contrast pattern made from two areas of very similar brightness, photoreceptors need to collect many photons to discern each region's edges [243]. Therefore, eyes capable of collecting more light (with greater absolute sensitivity) will be better at discerning small contrasts in dim light. Thus, contrast sensitivity can be tested as a proxy for light-collecting performance of a visual system between different adaptation states [29].

To assess differences in contrast sensitivity between light- and dark-adapted fiddler crabs, my first experiment tested behavioural responses to low-contrast visual stimuli in *A. tangeri*. Behavioural response thresholds provide a conservative and reliable channel by which to measure sensory abilities, including visual contrast discrimination in an animal. A strong and reliable behavioural response can often be produced from a stimulus designed to startle the animal, provoking an innate predator avoidance behaviour such as recoiling, "freezing" still, or moving away from a perceived threat [122]. A computer-generated expanding object on a screen, a **looming stimulus**, can effectively simulate an approaching object [129]. Prey animals from across invertebrate and vertebrate phyla show strong defensive responses to this type of stimulus, due to its association with predator threat [244]. Fiddler crabs are no exception and exhibit a strong, conspicuous startle response to a looming stimulus, whereby they will usually stop suddenly and freeze still on detection, or attempt escape by sprinting away [67, 69, 123, 124, 126, 127, 129, 245]. Additional reactions that are sometimes associated with a freeze response include defensively tucking in claws and legs, or sometimes large males will raise the dominant claw towards the stimulus in a defensive display [246].

Hemmi demonstrated that the fiddler crab *Gelasimus vomeris* will use visual information to make a calculation on the size and speed of the approaching object in order to assess the

threat level and decide on how to behave [123, 124, 126, 127]. This is a complex process with several stages but typically, on first detection a crab will stop suddenly and freeze . This works to minimise its chances of detection by the predator and observe its surroundings without motion blur [126, 127]. Sudden changes in gait or other reactionary movements can therefore be used as a proxy for a detected visual stimulus, and like several other studies [68, 69, 245], behavioural response probabilities were used in this experiment to assess contrast sensitivity. The rate of expansion, angular size and elevation of the black disk stimuli used in experiments, was designed so that it appeared sufficiently alarming to a fiddler crab, in order to provoke an predator response under adapted light conditions [124].

Preliminary trial experiments revealed that *A. tangeri* were less likely to respond to a looming stimulus if both background and object were presented on screen in high intensity greyscale values (i.e. pale grey object against white background), perhaps as the object appears bright and transparent, like a shadow. A more effective stimulus design was to always present a dark solid-looking object (black disk) and increase the brightness of the background behind it (using shades of dark grey) to create a low contrast. A range of looming stimuli from zero contrast to fairly strong (Weber contrast -0.94) were presented to the crabs and the proportion of crabs to respond was compared between light- and dark-adapted treatments during daytime and after sunset.

4.1.3 Relative thresholds of absolute sensitivity

My second experiment measured ERG responses from *G. dampieri* eyes to a series of 10 Hz flickering LED stimuli of different intensities. The brightness range for the stimuli presented to the crabs was selected to cross over the absolute detection thresholds of the fiddler crabs in each treatment. With decreasing stimulus intensity, the ERG response pattern matching the frequency of its flicker will diminish in amplitude until it is no longer above the noise level in the signal. I chose to compare the stimulus intensities required to provoke a low but significant threshold level response amplitude, allowing comparisons of relative visual sensitivity under four different treatments in the same eight crabs. Again, responses were compared between light- and dark-adapted eyes during daytime and after sunset.

Unlike intracellular recordings, ERGs are non-invasive and measure extracellular electrical activity from the corneal surface of the eye. The relatively large electrode is in contact with multiple ommatidial facets and a variety of underlying retinal cell types contribute to the signal, including slow responses of pigment cells and neurons of the lamina [247]. However, the combined synchronised depolarisation of many photoreceptor cell membranes in response to a flash of light is what primarily makes up an ERG signal [23, 247]. A small significant response amplitude may be recorded from an eye, which would not necessarily elicit a noticeable behavioural response. The amplitude of a photoreceptor response is proportional to the logarithm of the stimulus intensity [23] and ERG output is measured on a continuous scale rather than a binary one.

An additional major advantage is that ERG measurements do not rely on gaining motivation or attention of the animal and ERG stimuli need not frighten the animal; simple flashes of light work well. ERG recordings tend to be robust and repeatable [23, 247], meaning smaller sample sizes can be used. Crabs are restrained but left unharmed during ERG experiments, so experimental designs can incorporate repeated measures (the same animals are tested in all treatments). As stimulus habituation need not be considered (as in behavioural experiments [114, 248]), many stimuli can be presented to an individual during a test, permitting smaller intervals between presentations.

4.1.4 Temporal resolution

In addition to the physiological changes observed with TEM and light microscopy, photon capture can be increased by neural temporal summation in dim light [34, 199]. Many animals boost their visual sensitivity when dark-adapted by increasing integration time over which the eye collects light [34, 118, 190, 199, 249]. Visual signals from photons arriving over a longer time period can be combined from a given region of space, but this tactic comes at the expense of their temporal resolution, which is the fastest frequency at which an eye can discriminate changes in luminosity [34]. To test whether temporal summation is a strategy used in dark-adapted *G. dampieri* eyes to enhance dim light vision, **critical Flicker Fusion Frequency (cFFF)** was compared after light- and dark-adaptation during daytime and night (immediately after the previous experiment). The same eight crabs were presented with a series of stimuli flickering at different frequencies, whilst recording ERGs. The response amplitudes provide a direct measure of the crab's ability to resolve the flicker in time.

The temporal resolution of an animal's visual system tends to be linked strongly to requirements of their visual ecology [34, 36, 192, 194, 195, 250]. Fast moving animals, notably flying insects [34, 36, 192, 194, 196] and birds [251, 252], require rapid cFFF of between 100 - 200 Hz to update their visual scene as they zoom through it. In contrast, animals with sedentary or slow-moving lifestyles tend to have very slow temporal resolution, sacrificing fast vision in order to maximise absolute visual sensitivity [34]. A good example is the slow vision of the nocturnal spider *Cupiennius salei*, with its sit-and-wait predatory lifestyle [253] and the incredibly slow integration times (up to 3 seconds) in the nocturnal toad, *Bufo bufo* [254]. Both animals sit still in the dark and wait for prey to crawl past them. Fiddler crabs are active above the waterline on intertidal habitats and are capable of rapid movement [93]. They respond quickly to visual stimuli [114], so it is likely that their temporal resolution would reflect these fast behaviours. Falkowski [42] used ERG and intracellular recordings to demonstrate that in bright conditions, the maximum cFFF in light-adapted *G. dampieri* was around 70 Hz. However, it is not known whether they use temporal summation as a strategy in dim light and/or at night.

It is worth noting that spatial summation is another potential strategy for increasing sensitivity of the visual system, however this was not investigated in this study and has not been

previously described as a mechanism in Brachyura (to my knowledge). Spatial resolving power could be compared in light- and dark-adapted crabs using the pattern electroretinography (PERG) technique [255, 256]. Assessing dendrite branching in the lamina monopolar cells would also provide some information on whether spatial summation is a strategy used by fiddler crabs [30, 34, 191, 198].

4.1.5 Aims and hypotheses

Experiments in this chapter aimed to examine the effect that light- and dark-adaptation have on the functional visual performance of light- and dark-adapted fiddler crabs from day to night. Two complementary experiments using ERG and behavioural responses were designed to compare relative thresholds of "absolute" and contrast sensitivity in fiddler crabs. Due to local animal availability, two different fiddler crab species were used in experiments.

Circadian control on physiological changes was apparent from examining the eye anatomy (outlined in chapter 3 and ref: [214]). Therefore, dark-adapted eyes at night were hypothesised to have the highest contrast sensitivity and detect dimmer stimuli than other conditions. During daytime, dark-adapted crabs have narrower rhabdoms and crystalline cones than at night and therefore, visual performance in dim light was expected to be poorer. Light-adapted crabs during daytime were predicted to be least responsive to low contrast and dim stimuli. A circadian clock may also allow light-adapted eyes to be slightly more sensitive after sunset, as the visual system anticipates and prepares the eye for darkness.

To explain differences in visual sensitivity between adaptation states that were not apparent as conspicuous anatomical differences, a third experiment was designed to assess whether neural temporal summation is activated in dim light. Comparisons of cFFF in light- and dark-adapted eyes were made with ERG recordings. Layne *et al.* [118] showed that cFFF in the fiddler crab *Leptuca pugilator* decreased by ~18 Hz after dark-adapting the eye, so a similar result was hypothesised for this experiment. It is not known whether cFFF falls further at night in the fiddler crab, so individuals were tested both during daytime and after sunset to to assess whether temporal summation is under circadian clock influence.

4.2 Materials and Methods

4.2.1 Behavioural tests for contrast sensitivity

Experiments were carried out on several days between 10th and 19th September 2017 in El Rompido, Spain. Male and female *A. tangeri* were collected from the mudflats during low tide and were separated into four treatments to be pre-adapted and tested according to Table 4.1. The crabs in all four treatments were similarly sized with similar mean carapace width of 26 ± 2-3 mm. Each crab had a small piece of steel wire with a loop at each end temporarily attached to its carapace with cyano-acrylate glue, through which a wire harness could be threaded during experiments.

Table 4.1: Pre-adaptation methods and experimental time-frames for the four treatments used to test behavioural thresholds of contrast sensitivity in dim light.

Treatment	**Pre-adaptation**	**Experiment time**
Day light-adapted	Crabs kept under natural sky conditions from sunrise until turn in experiment	13:00 to 17:00
Night light-adapted	Crabs kept under natural sky conditions during daylight hours, then moved just before dusk under bright controlled LED lighting to prolong light-adaptation after sunset until experimentation	21:00 to 00:00
Day dark-adapted	Crabs kept in a light-tight container within a darkroom from dusk the previous day until testing on the day of experimentation	13:00 to 17:00
Night dark-adapted	Crabs kept in a light-tight container within a dark room from just before dusk until experimentation	21:00 to 00:00

The light- or dark-adapted crabs were tested during daytime or after sunset using a custom-built treadmill (Fig. 4.1a). One crab at a time was tethered to a flexible harness above a free-moving polystyrene ball (15 cm diameter) upon which it could walk, keeping its position on the top with freely moving legs and claws whilst the ball rotated on an air cushion below (provided by the non-heated setting on a hairdryer and flexible air duct). The experiments were carried out in a darkroom and the treadmill area was screened from all sides so that the experimental arena was as dark as possible. For the light-adapted crabs, the bright room light was kept on until the crab was in place to maintain its adaptation state. The crab was positioned to face a LCD screen controlled by Matlab software (M.J. How) (2016a, Mathworks, Massachusetts, USA). A dim red lamp and video camera were placed above the crab to view and record the experimental trials.

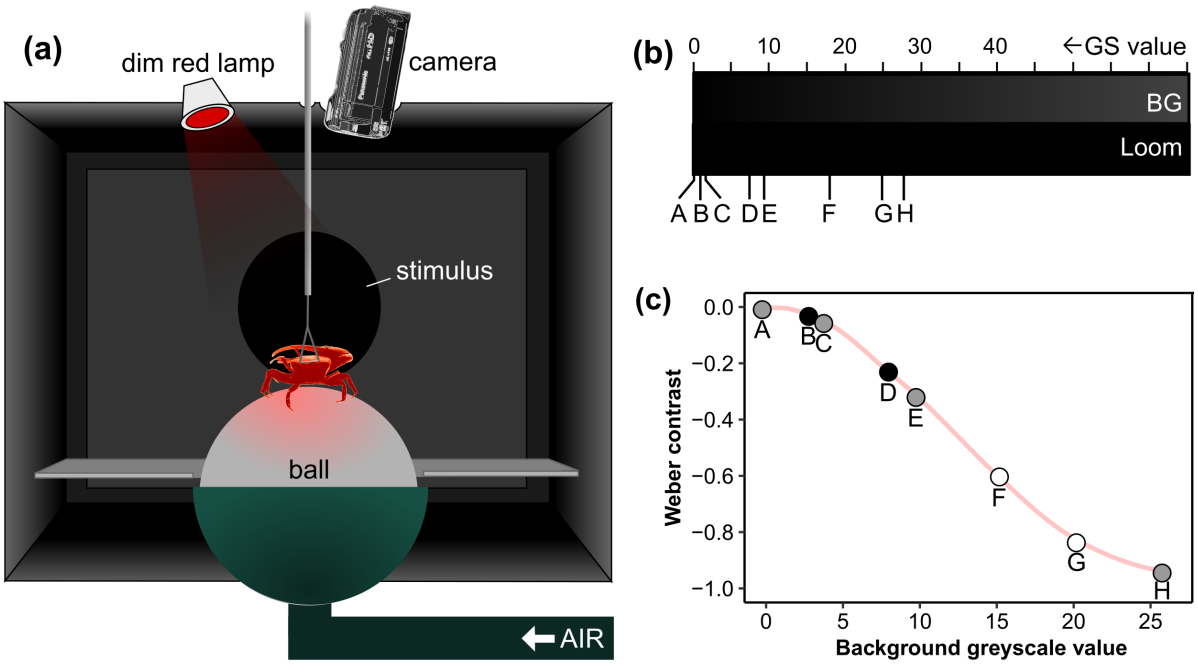

FIGURE 4.1. **(a)** Treadmill apparatus for testing contrast sensitivity. In a darkroom, the crab was tethered within a screened experimental arena using a wire harness. It was positioned above a polystyrene ball, which rotated below on an air cushion as the crab walked. An LCD screen in front of the crab displayed black looming stimuli against a dark background, while a video camera recorded behavioural responses using dim red illumination. **(b)** Background (BG) greyscale values (GS) are displayed for stimuli A-H next to a black bar, which represents the zero greyscale value of the looming stimulus. This provides an idea of the low contrasts presented to the crabs. Note: the intensity/contrast will vary depending on the screen or paper they are viewed on. **(c)** Weber contrast for each stimulus A-H is shown against its background greyscale value. Dark-adapted crabs at night were shown stimulus contrasts represented by black and grey points and the other three treatments were shown contrasts represented by white and grey points.

After tethering the crab on the ball, a 2-minute acclimatisation period was given for the crab to begin walking and adjust to the given background intensity on the screen. After 2 minutes, the first 5-second looming stimulus was presented and the response was recorded using a binary scoring system. After a presentation, the screen background changed immediately to the next experimental greyscale value for 2 minutes allowing undisturbed acclimatisation to this intensity, before the next stimulus presentation. Each individual was shown six stimuli, taking 12.5 minutes in total, to prevent habituation and keep tests short, minimising the chance for dark-adaptation processes beginning in the eyes of light-adapted crabs as much as possible.

4.2.1.1 Visual stimulus

The stimulus was presented on a LCD screen positioned in 25 cm front of the crab (Fig. 4.1a). It was formed by a simple black disk of 8-bit value 0, in the centre of the screen, that increased exponentially in diameter from 0 to 400 pixels, causing its visual angle (from the crab's perspective) to grow from 0° to 24°, over 5 seconds. It appeared just above the visual horizon of the crab and was designed to resemble a looming object. After a series of preliminary tests, experimental stimuli A-H were selected for use and were created by adjusting the greyscale value of the background behind the looming disk (Fig. 4.1b).

All four treatments were shown stimuli within the same overall range of contrasts, however the dark-adapted crabs at night were presented with two fewer stimuli (F, G) at the high contrast end of the range, but were replaced by two extra stimuli (B, D) towards the lower contrast range than other treatments (Fig. 4.1c). The highest contrast (stimulus H) was always shown last and due to its reliability in eliciting a response in all treatments, it was used as a positive control. The order of the five other stimuli was randomised using the function "randperm(5)" in Matlab to generate a sequence of five random numbers that corresponded to the stimuli. These included a negative control (stimulus A) with background greyscale value of 0 (the same as the stimulus), making it zero contrast and thus, invisible to the crabs.

4.2.1.2 Visual contrast calculations

Radiance spectra of the screen backgrounds for each experimental greyscale value were measured with a calibrated spectrometer (Flame-S, Ocean Optics, Largo, USA), via a cosine corrector-coupled optical fibre with 3900 μm² aperture. Using a template function for absorbance of invertebrate visual pigments [38] and the assumption that visual pigment in *A. tangeri* R1-7 photoreceptors has peak sensitivity (λ_{max}) at 530 nm [37], quantum catch values were calculated by multiplying the area under the absorbance curve, with the area under the radiance spectrum for each background intensity. Weber contrasts (C_W) were determined using the following equation,

$$C_W = \frac{Q_{\text{loom}} - Q_{\text{bg}}}{Q_{\text{bg}}},$$

where Q_{bg} is the quantum catch of the background and Q_{loom} is the quantum catch of the black looming stimulus disk. As the loom was always darker than or equal to the background intensity, the Weber contrast values were negative.

4.2.1.3 Data analysis and statistics

Although responses were noted during the experiment to initially monitor the results, the videos were scored again "blind" afterwards by disguising the treatment and stimulus contrasts during analysis to prevent researcher bias. Successful visual detection by the crab caused a response, whereas continuing to walk as usual signalled that they could not detect it. A gradient of

responses was observed when assessing the video sequences. The crabs showed the following responses (in order of strength): attempt to sprint away, sudden freeze for a few seconds, sudden slowing of walking pace, lowering body, tucking legs and/or claws closer to the body, or attentive shift in orientation of body or eyes toward the loom. For the purpose of this experiment, all these behavioural responses were allocated the same binary score of 1. When a crab continued to walk without altering behaviour in any way, it was assumed the crab did not detect the stimulus and was scored as 0. To be conservative, if the behaviour was ambiguous e.g. a very subtle response, or the crab had ceased walking just before the stimulus presentation, a score of 0 was given.

Collective response probability for a stimulus contrast was determined in each treatment from the mean of the binary responses. Wilson score confidence intervals were calculated using sample size (n) and number of successes with R package "Hmsic" (F. Harrell Jr; version 3.5.1; http://www.R-project.org).

Using the R package “lme4” [257], a generalised linear mixed-effects model (GLMER) for binomial responses was fitted to the data and included all the possible parameters which may have affected the response probability. Stimulus contrast was given as the continuous fixed effect, and other fixed effects included the interaction between adaptation state and whether it was day or night, size and sex of the animal, tidal phase (high, low or between tides) and the number of minutes into the experimental time that the stimulus was presented (ranging from 2 to 12 minutes). Crab identity was given as a random effect. This model was then simplified via deletion of terms that caused insignificant increases in deviance when tested against the original with a Chi-square test, until a minimal adequate model was reached.

4.2.2 ERG experiments

Two experiments using light-adapted and dark-adapted *G. dampieri* fiddler crabs during both day and night were conducted to investigate and compare, **(1)** thresholds of visual sensitivity and, **(2)** temporal resolution of the eye. A detailed account of the methods common to all ERG experiments can be found in chapter 2, section 2.4.

4.2.2.1 Intensity thresholds

Fiddler crabs (*G. dampieri*) were presented with a series of 15 stimuli every 60 seconds, consisting of a 10 Hz on-off square wave flicker. Starting from the dimmest intensity (to minimise changes in dark-adapted eyes), the intensity of consecutive stimuli was increased step-wise by a third of a log unit each time (Fig. 4.2). Due to large response variation between treatments detected in preliminary trials, neutral density filter was placed in front of the LED array to lower the intensity for dark-adapted treatments only. Two layers were added during daytime and four at night. Each individual crab was tested in four different conditions: light-adapted during the day and at night; and dark-adapted in the day and at night.

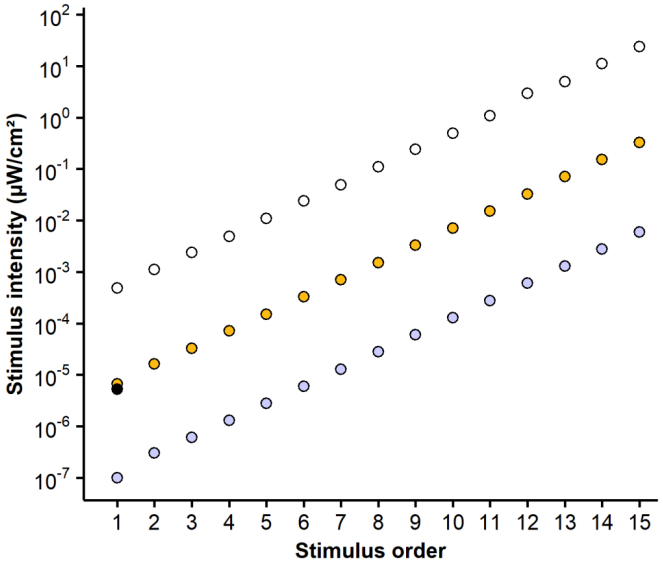

FIGURE 4.2. Intensity of the experimental stimuli used in ERG experiments on a $\log_{10}$ scale. White points show stimuli used for light-adapted treatments during both day and night. Dark adapted treatments where shown dimmer stimuli resulting from use of neutral density filter, two layers during daytime (yellow points) and four at night (lilac points). Stimuli were shown in stepwise order of dimmest to brightest. The black filled point (at x=1) indicates the stimulus intensity used in the ERG experiment in chapter 5, section 5.2.3.

ERG response amplitudes were acquired and measured using a custom Matlab programme (J.M. Hemmi). After fitting a best-fit line to the resulting data points, the intensity required to evoke a threshold mean response amplitude of 0.001 mV was determined for each individual crab. Although significant responses above the signal noise level were often recorded below this threshold for intensities the individual could probably detect, the small amplitudes produced meant that they were unreliable when it came to replication. As these experiments aimed to make relative comparisons between adaptation states, rather than determine absolute sensitivities, the 0.001 mV threshold was used to compare the dimmest reliably detected light intensity between treatments.

4.2.2.2 Critical Flicker Fusion Frequency (FFF)

A flicker fusion test was performed shortly after the previous experiment and in the couple of minutes between the two tests, the LED stimulus was left either on full brightness for light-adapted crabs, or off completely for dark-adapted crabs to maintain their adaptation state, while preparations for the second test were swiftly made. The Faraday cage did not need to be opened and all apparatus were already in place.

The stimulus intensity used in the cFFF test was altered between treatments and between

individual crabs and was chosen based on results of the previous experiment. From plotted mean response amplitudes (measured to increasing intensities) just recorded, the stimulus intensity required to evoke a response of 0.0032 mV was read from the best-fit line plotted to that individual's data. This response threshold was chosen as it was reliably above noise but did not tend to require bright light stimulation, which could provoke light-adaptation processes in dark-adapted eyes.

Using this individually-determined stimulus intensity, a series of 11 stimuli lasting 20 seconds were presented to the crab. The square wave flicker frequency was increased from 10 Hz to 120 Hz in step-wise increments of 10 Hz. Data for 50 Hz was excluded from the results due to mains frequency contamination of the signal. To maintain adaptation state, in a 60-second gap between stimulus presentations, the eye remained in darkness (for dark-adapted treatments) or was exposed to the stimulus on highest intensity (light-adapted treatments). The cFFF was deemed the lowest frequency at which the crab produced a significant response above a threshold of 0.0006 mV.

4.2.2.3 Statistical analyses

Using the R software package "lme4" [257] (v3.5.1; http://www.R-project.org), a linear mixed effects model (LMER) was fitted to data for both ERG experiments, using response amplitude as the continuous fixed effect each time. Crab identity was given as a random effect. Using the R package "predictmeans" (v1.0.1; https://CRAN.R-project.org/package=predictmeans), several other potential explanatory fixed effect terms (listed in Results 4.3.2) were tested for statistical significance by running 10,000 random permutation recalculation tests [258] on the data. *Post hoc* pairwise comparisons between each of the four conditions were performed with Tukey contrasts using the glht function in R package "multcomp" [259].

4.3 Results

4.3.1 Behavioural thresholds of sensitivity

During daytime, the contrast sensitivity of the light-adapted visual system appeared to be poorer than in other treatments when presented with stimuli of lower contrasts, yielding fewer responses (Fig. 4.3 & 4.4a). The majority of crabs (60%) did not respond to stimulus E (Weber contrast -0.31), which provoked reliable startle responses (≥95%) in all other treatments. In dark-adapted crabs at night, response probability to low contrast stimuli was highest and 58% of the crabs responded to stimulus C, with a very low Weber contrast of -0.05.

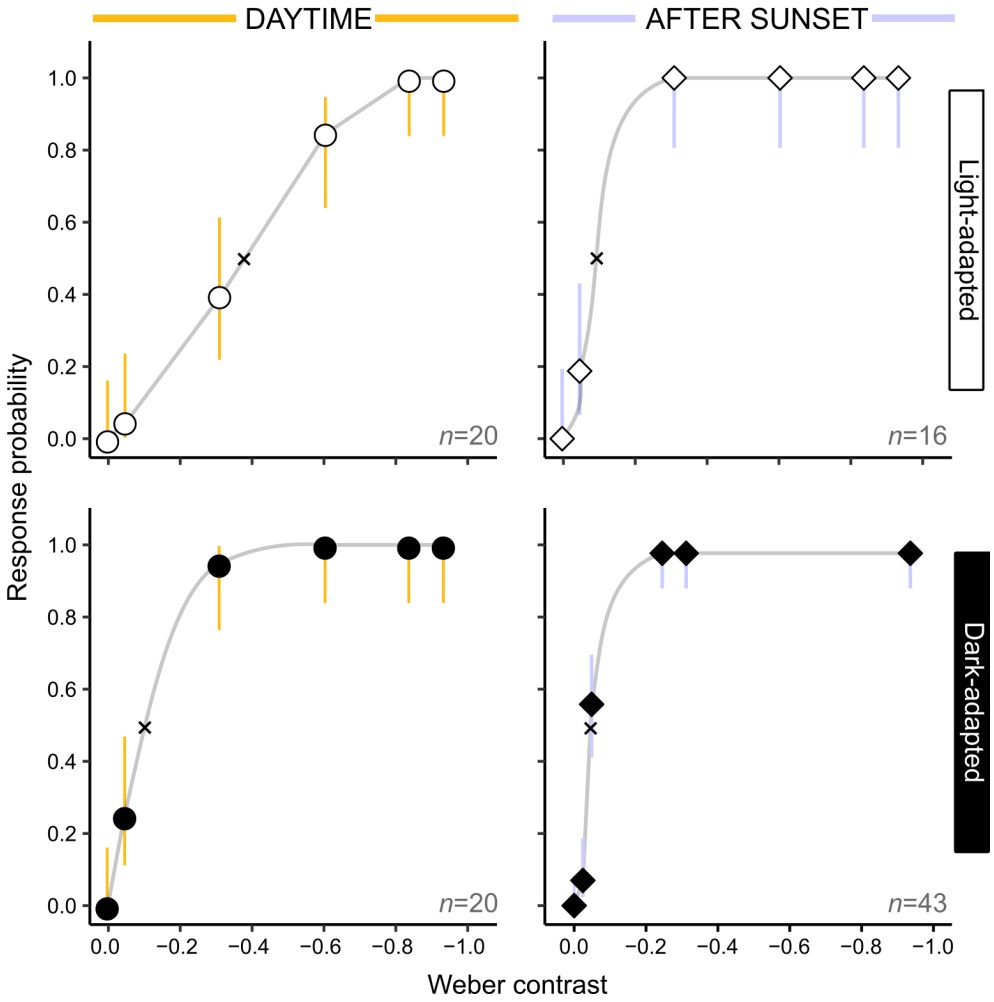

FIGURE 4.3. The probability of a response to a visual "looming" stimulus with increasing Weber contrast in *A. tangeri*. Crabs were tested when fully light-adapted (white points) or fully dark-adapted (black points), during both daytime (circles) and after sunset (diamonds). The number of individuals, *n*, contributing to the data for each treatment is indicated in the bottom left of each panel. Bars display Wilson score confidence intervals. An 'X' marks the 50% value on each sigmoidal best-fit curve.

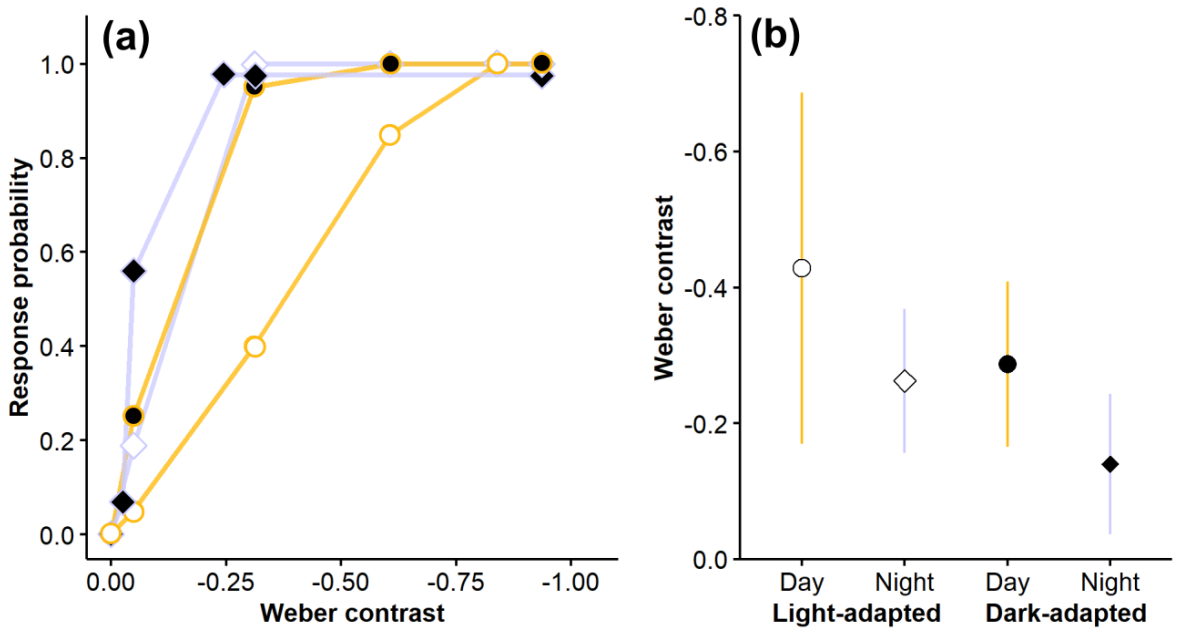

FIGURE 4.4. **(a)** Data from Fig. 4.3 are plotted again, together in one graph with coloured lines joining points (lacking error bars) so that responses between treatments can be compared directly. Mean response probabilities to looming stimuli of increasing Weber contrast are shown for light-adapted (white points) and dark-adapted (black points) fiddler crabs, during both daytime (circles/yellow) and after sunset (diamonds/lilac). **(b)** The minimum Weber contrast value to provoke a response (minimum detectable stimulus) in each fiddler crab is shown as a mean for each treatment with standard deviation bars.

Prolonged light-adaptation after sunset and prolonged dark-adaptation into the day, produced intermediate response curves, which were very similar to one another in shape (Fig. 4.4a). No crabs responded to the (invisible) zero-contrast stimulus A in any treatment (used as a control), indicating that false positive responses are unlikely. In addition, all crabs across treatments responded to the strongest contrast (stimulus H), suggesting that all individuals possessed functional visual systems and neural circuits for behavioural responses. It also demonstrated that the repetitions were not sufficient to cause full habituation.

Mean values for lowest stimulus contrast to cause a response in the fiddler crabs were compared across treatments (Fig. 4.4b). In daytime, the mean minimum Weber contrast required to produce a response in light-adapted crab was -0.43 ± 0.26. This was considerably higher than the other three treatments. Nighttime light-adapted and daytime dark-adapted crabs had very similar mean minimum detectable stimulus contrasts (-0.26 ± 0.11 and -0.28 ± 0.12 respectively). Dark-adapted crabs at night responded to the lowest mean contrast of -0.14 ± 0.10.

A GLMER was fitted to the data, but tidal phase ($X^2_{(1)}$=0.68, p=0.710), carapace width

($X^2_{(1)}$=1.95, p=0.163), sex of the crab ($X^2_{(1)}$=2.72, p=0.099), as well as the number of minutes into the experiment time that each contrast was shown ($X^2_{(1)}$=2.37, p=0.124), did not significantly affect the likelihood of a response, so these were all excluded from the model. However, the interaction between adaptation state and whether it was day or night did affect the responses significantly ($X^2_{(1)}$=10.72, p=0.001), as did the stimulus contrast ($X^2_{(1)}$=494.82, p<0.001). This suggests that there is a strong circadian control over the ability of a fiddler crab to increase contrast sensitivity to see well in the dark, which cannot just be explained by its adaptation state.

4.3.2 ERG intensity thresholds

Increasing the stimulus intensity caused a corresponding significant increase in the ERG response of the eye ($X^2_{(1)}$=730.3, p<0.001, Perm-p<0.001, n=8) and there were large differences between all treatments (Fig. 4.5a,b). So much so, that to extract threshold responses in each treatment, a lowered range of stimulus intensities had to be presented to the crabs when dark-adapted, especially at night. This was achieved by slotting layers of neutral density filter in front of the LED array.

The interaction between adaptation state and time (day or night) had a significant effect on the ERG response amplitudes ($X^2_{(1)}$= 51.7, p<0.001, Perm-p<0.001). When light-adaptation was prolonged at night, the mean stimulus intensity required to provoke a threshold response of 0.001 mV was significantly higher (3.05 x10^{-2} μW/cm^2), than during daytime (1.77 x10^{-1} μW/cm^2) (p<0.001). When the fiddler crabs were dark-adapted, their eyes were significantly more sensitive (p<0.001) and the mean intensity required for this threshold response was 2.01 x10^{-3} μW/cm^2 during daytime, and three orders of magnitude lower again during night 3.91 x10^{-6} μW/cm^2 (p<0.001).

After excluding carapace width for having no significant effect on the results ($X^2_{(1)}$=0.06, p=0.805, Perm-p=1), the minimal model to explain the ERG responses included the stimulus intensity, plus the interaction between adaptation state and time (day or night). Sex of the crab also significantly explained the results as the four females produced slightly higher responses than the four males overall ($X^2_{(1)}$= 8.6, p=0.003, Perm-p=0.013).

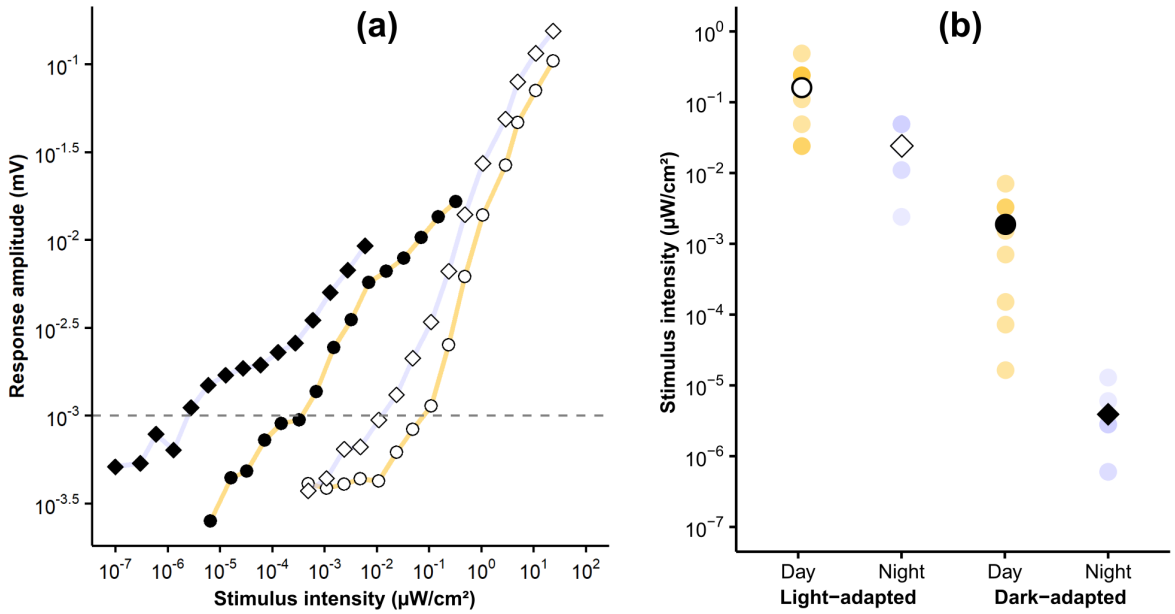

FIGURE 4.5. **(a)** Mean ERG response amplitudes on $\log_{10}$ scale from eight fiddler crabs (G. *dampieri*) to increasing stimulus intensities ($\log_{10}$ scale), recorded in a light-adapted state (open points) and a dark-adapted state (filled points), during daytime (circles) and night (diamonds). A response threshold of 0.001 mV is marked by a dashed line, at which ERG amplitudes were reliably above noise in the signal, allowing comparison between groups. **(b)** The stimulus intensity on $\log_{10}$ scale required to elicit a response amplitude of 0.001 mV is plotted for each crab (blue and yellow points), along with the mean value, when light-adapted (open points) and dark-adapted (closed points) during daytime (circles) and night (diamonds).

4.3.3 ERG temporal resolution

The ERG response amplitudes in the fiddler crabs in all four treatments all showed the typical negative association with increasing stimulus flicker frequency ($X^2_{(1)}$= 463.3, p<0.001, Perm-p=1, n=8) (Fig. 4.6a). There was a significant effect of the interaction between adaptation state and time (day/night) on the responses ($X^2_{(1)}$= 14.8, p<0.001, Perm-p=1) and light-adapted crabs produced larger responses than dark-adapted crabs for frequencies up to 90 Hz, particularly during daytime.

Figure 4.6b shows the critical flicker fusion frequency (cFFF) required to produce 0.0006 mV response from the eye in each treatment. When light-adapted, the cFFF required was significantly higher during daytime (mean ±standard error = 73.6 ± 6.1 Hz) than at night (58.8 ± 2.3 Hz) (p<0.001). When the crabs were dark-adapted, temporal resolution was lower still, but cFFF was not significantly different between day (34.5 ± 5.9 Hz) and night (39.8 ± 3.4 Hz) (p=0.142). Carapace width ($X^2_{(1)}$= 0.2, p=0.695, Perm-p=1) and sex of the crabs ($X^2_{(1)}$= 3.3, p=0.071, Perm-

p=1) were not included in the final model as neither had a significant explanatory effect on the responses.

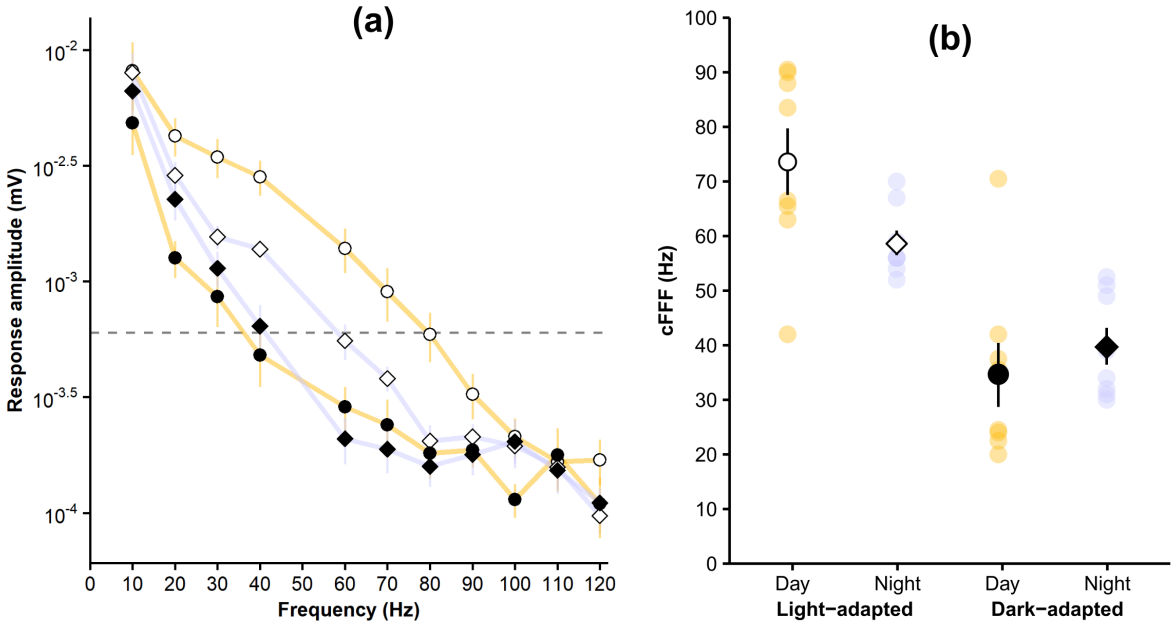

FIGURE 4.6. **(a)** Mean ERG response amplitude on $\log_{10}$ scale with increasing stimulus flicker frequency for eight *G. dampieri* fiddler crabs tested when light adapted (open points) and dark-adapted (filled points) in daytime (circles) and night (diamonds). A horizontal dashed line marks the 0.0006 mV critical threshold at which the signal to noise ratio was sufficiently high for comparison. **(b)** The cFFF for individual crabs (yellow/lilac points) required to provoke a threshold response of 0.0006 mV. Global mean cFFF are overlaid for each of the four conditions by the black or white points, with standard error bars.

4.4 Discussion

4.4.1 Contrast sensitivity improves in the dark-adapted eye

Behavioural responses revealed that dark-adaptation significantly improves contrast sensitivity in *A. tangeri* allowing detection of objects in very dim light. This is particularly apparent after sunset and crabs were able to detect very small Weber contrasts of -0.14 at night, presumably due to increased modal light propagation and greater volume of phototransduction machinery in the rhabdom, in addition to crystalline cone changes that result in wider acceptance angles [214]. This indicates that the adaptive changes are very effective in terms of functional performance of the crab's visual system. The boost in visual sensitivity would allow them to forage safely at night when the lack of available light would vastly reduce the contrast of potential predators against the dark sky [29]. Circadian controls on dark-adaptation processes mean that rhabdom and crystalline cone tips do not reach their full size during daytime [214] and as a result, photoreceptors do not collect the amount of light necessary for the high contrast sensitivity that was measured at night. This may be beneficial in protecting the eye from damaging radiation or photo-pigment bleaching, which may temporarily blind a crab when it emerges onto the bright mudflat surface after a long period inside its burrow during daytime [173].

An abundance of bright natural light during daylight hours means fiddler crabs are unlikely to require keen contrast sensitivity for dim light vision at this time and consequently, crabs with light-adapted eyes during daytime performed the poorest. Stimulus E (Weber contrast -0.311) was detected reliably by all other treatments, but only provoked responses in 40% of light-adapted crabs during daytime. To the human eye, it was easily detectable (if reading this on a computer screen, see Appendix Fig. A.1), which was noted with some surprise during data collection. This indicates that (relative to humans) the *A. tangeri* eye remains very insensitive to dim light during daylight hours.

Despite only subtle anatomical differences in light-adapted eyes between midday and midnight [214] a considerable boost in contrast sensitivity was apparent from the behavioural responses at night. As the crabs were not exposed to bright light between stimulus presentations, the increased contrast sensitivity after sunset may be partly due to the eye's metabolic readiness to begin cellular processes involved with dark-adaptation, which then began to occur in the dim light during the 12 minute experiment [233]. Acceptance angles partially widen via crystalline cone tip diameter increases at dusk, even under bright light exposure [173, 214]. However, microvillus elongations in the rhabdom are (mostly) inhibited by the bright pre-adapting light conditions [180, 200, 214]. Therefore, the microvilli are very unlikely to elongate fully during the experiment on such short timescales [180, 184] (see chapter 5). Furthermore, stimuli shown towards the end of the experiment did not have significantly higher probabilities of response, as one would expect if effective dark-adaptation processes were occurring during the 12.5 minute tests. A more likely reason for the discrepancies between day vs. night anatomical difference and

the disproportional increase in functional sensitivity, is neural temporal summation [260].

4.4.1.1 Methodology critique

Behaviour in *A. tangeri* indicates that the daytime light-adapted crabs have a much reduced perception of contrast in dim light compared to the other three treatments, which were more similar to one another in their results. Perhaps the experimental design was not sensitive enough to pick out potential differences between contrast sensitivities of the daytime dark-adapted and the night light-adapted crabs. Ideally, inclusion of additional stimuli with smaller contrast increments around the lower range of the scale (Weber contrasts 0.0 to -0.3) would better identify the finer differences in their thresholds. Tests were kept as short as possible (12.5 minutes) to avoid dark-adaptation processes occurring in the light-adapted animals. As crabs are known to habituate to looming stimuli when presented in series [114, 248], presentations were separated with 2-min intervals, meaning just six stimuli could be included per test. Contrasts were chosen due to their linear steps in background greyscale values, however, if I were to repeat this experiment, I would choose contrasts with more evenly spaced intervals in Weber contrast.

Gradients of behavioural responses were noted during video analysis, higher contrast stimuli provoked stronger responses. Contrasts near the crab's sensory detection threshold often elicited subtle or "uncertain" responses, such as inward movements of claws / legs, or vertical alignment of eye stalks as attention was caught by a barely detectable change on the screen. Processing and filtering of visual information as it passes through the optic neuropils [261], plus decision-making processes using visual information in the brain [262], introduce the possibility that although a stimulus is detected and noticed (perhaps partially so), it may fail to elicit a behavioural response in an animal [263, 264]. Thus, behavioural thresholds provide a conservative but meaningful proxy for visual abilities. Perhaps a discrete scoring system grading responses based on strength, e.g. 5 = sprint, 4 = freeze.... 1 = eye movement, would have provided a more sensitive analysis.

4.4.2 ERG responses to dim flashes of light

ERG responses revealed vast differences in optical sensitivity between treatments, whereby the stimulus intensities needed to provoke the same threshold response in the crabs varied over 6 orders of magnitude. The results followed a similar general trend to the behavioural experiments and dark-adapted eyes at night were most sensitive to low light levels. Dark-adapted eyes during daytime were much less sensitive than at night, which is likely due to the narrower rhabdom and crystalline cone aperture (assuming they are under the same circadian controls as *A. tangeri* and other crabs [173, 180, 200, 214]). I could not establish whether *G. dampieri* are nocturnally active in their natural habitat, having no access to those remote collection sites during this project. It was assumed that they are strictly diurnal by members of the Hemmi Lab (UWA), as they tend to disappear into burrows at dusk and have not been seen to emerge at night on their artificial laboratory mudflat (personal communication, J. Hemmi). The ERG responses indicate that they

should be very capable of adapting their visual system to enhance vision in dim light and do so to a great extent. Therefore, I would be very interested to learn of any future assessment of evening or nocturnal activity in their natural habitat. Crane, who spent many years studying fiddler crabs across the globe, reported nocturnal activity for many species [50], which is often associated with courtship behaviours using acoustic signalling, exclusive to this time [242].

As expected, light-adapted crabs during daytime required the brightest stimulation for a threshold response and were therefore least sensitive. Again, it was surprising how bright the stimulus had to be before it produced significant responses when they were tested in this treatment. In dark-adapted crabs at night, light stimulation of 0.000004 μW/cm^2 was required to produce a threshold response. When light-adapted during daytime, the stimulus required to produce the same response was over 45,000 times brighter (0.18 μW/cm^2) on average. Presumably their narrow acceptance angles and fine rhabdoms would be very effective at only letting small amounts of light reach the photoreceptors, screening out the excess bright light typical in their habitat at this time [18, 114, 214]. Their apposition eyes have certainly evolved to cope well with the extremely sunny conditions on the exposed tropical marine flats of northwest Australia [50, 114]. Like the behavioural results, light-adapted eyes after sunset produced greater ERG responses than during daylight hours, despite the same exposure to bright light before the test as well as between recordings during the experiment to prevent dark-adaptation. This could be (at least partially) explained by temporal summation, as cFFF was reduced by an average of 15 Hz after sunset.

Interestingly, ERG response amplitudes in the females were overall slightly larger than the males when presented with the same range of stimulus intensities. The four animals of each sex were of similar size (mean carapace in males was 1 mm wider than females). Male *G. vomeris* tend to have slightly larger eyes than equivalent sized females [97]. As larger animals and compound eyes are often correlated with larger facet lenses [265–267], this would suggest that, if anything, the ommatidia in males would have slightly greater light-gathering power [176, 241] leading to better absolute sensitivity; however the results suggest the opposite. Differences between male and female visual abilities were not found in any of the other experiments (throughout this thesis); therefore, this particular result is, most likely, coincidental.

4.4.2.1 ERG vs. Behaviour

The experiments provide two complimentary examinations of relative visual thresholds in light- and dark-adapted eyes during daytime and after sunset. If the eye adapts to collect more light and performance for absolute sensitivity is improved, this is likely to also improve its contrast sensitivity in dim light [29]. The results of the two experiments show similar trends, but cannot be be directly compared to one another. The two experiments tested different fiddler crab species, which are likely to possess very similar eye designs. However, there will undoubtedly be small differences in their absolute optical sensitivities due to divergent evolution over time

and geographical habitat differences, and possibly some ecological differences such as tendency for nocturnal activity [50, 91, 92, 132]. Experimental designs varied in terms of stimulus type and ambient lighting conditions. The LCD screen used in behavioural tests was back-lit so even when fully "black", the screen was dimly radiant and the eye was exposed to this throughout the experiment. Between the stimulus presentations and ERG recordings, light- and dark-adapted eyes were exposed to bright light or near-darkness respectively to maintain desired adaptation states. There were also, of course, large differences in the response criteria, which make them incomparable.

Comparing previous behavioural and electrophysiologcial studies which test visual detection thresholds in the same animals, it is often the case that electrophysiology reveals greater acuity than behavioural techniques, suggesting a more refined and sensitive approach [42, 268, 269]. One must be very careful when comparing across studies however, as age and body size [265, 270], time of day [271] and temperature [269, 272], among many other variables can all have enormous effects on responses. Some of the individual variance within treatments in my results may be explained by small differences in electrode placement on the eye between individuals, but otherwise, ERG recordings are considered to be reliable and repeatable [23, 247]. More numerous and smaller increments between stimulus intensities could be produced with the LED apparatus and neuronal responses are measured on a continuous scale rather than a binary one, making the ERG test more sensitive than the behavioural experiment.

4.4.3 Dim light vision is enhanced by temporal summation

It is reasonable to expect that anatomical changes are largely responsible for the differences in relative sensitivity and contrast sensitivity measured in *G. dampieri*. However, the cFFF experiment provided a convincing demonstration that temporal summation is also a strategy used by this species to improve signal-to-noise ratios in dim light. Dark-adaptation resulted in significantly reduced temporal resolution and this was just as effective in daytime (cFFF = 35 Hz) as at night (40 Hz). Temporal summation by increasing integration time for dim light vision is a strategy used by many species that must operate over extremely differing brightness levels (e.g. day to night, or shallow to deep water), therefore, cFFF can vary greatly between light- and dark-adapted states. This has been demonstrated in flies [192], butterflies [190], the bumblebee [273], a spider (*C. salei*) [274] and cleaner shrimp [275], to name a few. Doujak [260] was first to propose that temporal summation strategies are likely to utilised in the crab, *Leptograpsus variegatus*. Since then, although the subject is fairly well understood in compound eyes [30, 34, 190, 195, 199, 276], there have been few other studies concerning crabs. The only previous study (presently known to me) comparing dark- and light-adapted crabs showed that cFFF dropped from 50 Hz in a light-adapted fiddler crab (*Leptuca pugilator*) to 32 Hz when dark-adapted [118]. This reflects well the differences found in my experimental animals during daytime.

Slower vision presents an additional benefit. An energy saving opportunity is created due to the reduced metabolic cost of producing much slower signal responses [192, 277]. These savings could be large and important given the significant energetic investment required for production of large volumes of photoreceptor membrane every dusk to widen the rhabdom. To my knowledge, there have been no studies examining these specific cost:benefit offsets in compound eyes, so this would be a useful topic to investigate in future.

During daytime, mean cFFF in light-adapted eyes was particularly fast, at 74 Hz. This was close to Falkowski's results [42] for light-adapted *G. dampieri* of ~70 Hz, despite his slightly different methodology and levels of light stimulation. In my experiment, two of the crabs in this treatment produced threshold responses close to 90 Hz, suggesting very fast vision is possible in this species; brighter light stimulation may facilitate even faster temporal resolution by providing a higher signal-to-noise ratio [192]. Temporal resolution of >70 Hz is very fast for a crustacean [147, 195, 260, 275, 278, 279] and may be linked to its ecology and lifestyle out of the water in a primarily terrestrial environment. Fiddler crabs are not usually exposed to the wave induced flicker noise that many shallow water crustaceans experience [280]. Furthermore, fast vision is often correlated with fast locomotion [29, 192] and air provides a less dense and resistant medium for the relatively un-streamlined crab body plan, allowing more rapid movement than in water [281]. The strongest driver on fast vision though, is likely to be the birds that attack them. These avian predators are often distant, fast flying and in regular pursuit [121, 122], which necessitates rapid vision to track flight trajectories and assess the threat level. Birds may be numerous in their habitat, but not all birds are predatory or flying low enough to be a danger [122]. Fiddler crabs (*G. vomeris*) show a much earlier escape response to an approaching dummy "predator" if it has visual flicker, than if it is solid black, presumably as it emulates the flapping wings of a bird [122, 125]. To best identify distant bird predators from other objects using these rapid flickering movements (with fairly poor spatial acuity [97, 117]), fiddler crabs must rely on relatively fast vision. It is thought that they use information on the strength of the flicker to assess the flight speed of animals above them [122, 262].

Despite the continued bright light exposure and identical experimental conditions to daytime, cFFF in light-adapted *G. dampieri* eyes was reduced to 59 Hz after sunset. Temporal summation appeared to be in effect to a partial extent at night and is likely linked to a circadian clock that regulates ion channels in the photoreceptor membrane, possibly with serotonin as in the locust [282]. In the horseshoe crab *Limulus* (actually a primitive chelicerate, rather than a crab), efferent optic nerve impulses are sent to the photoreceptors at night to increase the signal gain (response per photon) to improve dim light vision [283–286]. This works by filtering away fast "noisy" quantum bumps by altering the ionic conductance of the photoreceptor cell membranes, amplifying slower signals and improving photon absorption [191, 284]. Assuming this phenomenon occurs in fiddler crabs, this gain increase appears to be only partially inhibited by the continued exposure to bright light before and during the experiment. Perhaps it is

activated immediately after the bright light is switched to the dimmer stimulus intensity. Unlike the horseshoe crab and locust, temporal summation does not only occur at night in *G. dampieri*, as cFFF was equally slow after dark-adaptation in daylight hours.

4.4.4 Conclusions

The results of the three experiments of this chapter complement the anatomical findings of chapter 3. They provide convincing evidence that circadian physiological changes in the fiddler crab eye, in addition to neural temporal summations, are very effective at adjusting sensitivity of the visual system. At night, these mechanisms boost sensitivity in the dark-adapted eye to allow it to effectively detect small contrasts and objects of low irradiance. Fiddler crabs can then remain active on the mudflat surface after sunset and continue to visually monitor their surroundings in very dim light. In the unlikely event that a crab needs to see well in dim light during daylight hours (perhaps a thick passing cloud), temporal summation can be employed to increase sensitivity of the eye in dim light, without having to make physiological alterations. Questions still remain about how quickly temporal summations, which require changes in membrane potential, take to activate in dim light.

Faced with very bright conditions on the mudflat during daytime, the tiny apertures and rhabdoms allow a relatively small amount of light to enter the light-adapted ommatidia. This, coupled with short integration times and very fast temporal resolution, greatly reduces their sensitivity and ability to detect low contrasts in dim light. The reduced sensitivity at this time is beneficial when scenes are typically very bright [114] as it allows the eye to effectively screen out excess damaging radiation. The fast temporal resolution in bright light assists in the detection of fast-flying distant birds and quick escape behaviours. When bright light exposure continued after dusk, the light-adapted eye appeared to partially dark-adapt regardless, becoming slightly more sensitive. Circadian clocks appear to encourage temporal summation after sunset, causing slower integration times, which may account for this increase in sensitivity, in addition to a slightly wider acceptance angles (apertures).

CHAPTER 5

INVESTIGATING THE DYNAMICS OF LIGHT- DARK-ADAPTATION PROCESSES

So far, pre-adapting the fiddler crab to bright light and near-darkness has revealed dramatic effects on eye physiology and functional sensitivity of vision from day to night. This chapter uses five different experimental methods in continuing to explore the adaptation processes as they happen. This was achieved by measuring changes in rhabdom size and acceptance angles over time, in addition to testing aspects of absolute and contrast sensitivity throughout the stages of dark-adaptation. The extent and rate of these adaptation processes is compared between daylight hours and after sunset. Some of the content in this chapter (ophthlamoscopy and anatomical data) is replicated from my research paper, ref: [214].

5.1 Introduction

5.1.1 Background

During a typical 24-hour period, fiddler crabs will experience extreme fluctuations in light intensity every time they move between the mudflat surface and their dark burrow. These underground hide-outs can be frequent and brief, depending on the threat of pursuing predators above ground. A fiddler crab will pass several hours inside the burrow during rhythmic high tide periods [50] and will often spend the night underground, particularly when temperatures decline [217]. However, *Afruca tangeri* are a species known to remain active on the mudflat on certain nights, even under moonless conditions [111, 214, 216, 217]. This chapter aims to develop an understanding of the rate of changes in eye physiology and functional visual abilities as the crab moves abruptly between the very dark (burrow) and bright (surface) conditions experienced daily.

Although the burrow is a place of safety and visual tasks are not required inside, experiments in chapter 4 showed that during daytime, sensitivity of a dark-adapted fiddler crab visual system is significantly increased compared to a light-adapted one. This is at least partly due to temporal summations at the visual processing stage, but in addition, anatomical work has shown that the rhabdom and crystalline cone aperture would have been of an intermediate cross-sectional area, between that of fully day- and night-adapted states (see chapter 3). However, this physiological state is not necessarily a reaction to entering dark conditions and could be a vestige from the widened nighttime state. There is a possibility that the rhabdom only partially degrades at dawn due to circadian clock systems, and that bright light exposure is essential to fully reduce the rhabdom to its daytime narrow state.

5.1.2 Physiological changes

5.1.2.1 During dark-adaptation

In *A. tangeri*, the dramatic rhabdom widening process at dusk involves elongations of many thousands of microvilli in each ommatidium. The crystalline cone aperture also widens during this time to allow more light to enter each ommatidium, almost doubling acceptance angles [214]. This process must require a significant energetic investment and is unlikely to happen very quickly. Sunset comes at a predictable time each day and in other crabs, biological circadian clocks play a role in readying the crab eye for dark adaptation. Endoplasmic reticulum and golgi apparatus in *Leptograpsus variegatus* prepare the photoreceptor cells in the late afternoon by filling the cytoplasm of the soma with saccules [184]. Equivalent vesicles in *Hemigrapsus sanguineus* were shown to contain opsin, required for phototransduction in the rhabdom [233]. With onset of darkness, these vesicles are already in place to cross the palisade bridges and attach to microvillar bases to extend the projections, widening the rhabdom. In this chapter, I first aimed to discover whether similar processes are in place in *A. tangeri* and asked, **how fast does the rhabdom widen at dusk?**

Once fully light-adapted after exposure to morning sunlight, **what happens during an extended period in the dark burrow during daytime?** Retinal screening pigment distributions in *A. tangeri* do not change between light- and dark-adapted eyes (chapter 3), so these were not targeted in these investigations. I aimed to determine whether the rhabdom and crystalline cone aperture partially widen again in the dark, and whether this occurs to the extent measured in crabs that have not had any light exposure that morning (i.e. refer to the daytime dark-adapted treatment in chapter 3 sections 3.3.3 and 3.3.4). Alternatively, these regions may remain narrow during daylight hours until sunset, regardless of time spent in darkness.

Experiments to measure anatomical changes over time were carried out during daytime and after sunset to obtain an idea of, **(1)** how long the main physiological changes of dark-adaptation take to occur at dusk (widening of rhabdom and crystalline cone aperture) and, **(2)** whether there

is any change at all in the dimensions of these structures during periods of dim light exposure in daylight hours. Fully light-adapted crabs were suddenly placed in a darkroom at midday or at sunset, and their eyes were dissected at different stages during dark-adaptation (over 3 hours), so that rhabdoms could be measured and compared with TEM.

The rate of aperture expansion was also assessed over the same 3-hour timescale. However for this, histology was not necessary and measurements could be made using an ophthalmoscope from unharmed, living fiddler crabs. Ophthalmoscopy provides a useful tool for visualising changes in the living eye associated with light-adaptation [287]. When illuminating a compound eye, a black spot or pseudopupil can often be seen where the optical axes of the ommatidia are in line with the observer [288]. Focussing a camera deeper within the eye on the distal tip of the fused rhabdom of an apposition eye produces a superimposed image of the combined apertures of several neighbouring ommatidia [289]. This is known as the **deep pseudopupil**, the centre of which is dark due to the light-absorbing central rhabdoms, surrounded by a ring of more reflective pigment cells. Changes in the appearance and shape of the deep pseudopupil can be measured to visualise the associated pigment migrations or increases in acceptance angles and photoreceptive area, in response to light level changes. Aperture diameter correlates directly with the size of the deep pseudopupil and resulting acceptance angles. To compliment the TEM data on rhabdom sizes, the deep pseudopupil was measured at equivalent time intervals over a 3-hour dark-adaptation period during daytime and after sunset, allowing measurement of the extent and rate of aperture widening in the same six living fiddler crabs.

5.1.2.2 During light-adaptation

The apposition eyes of the fiddler crab are suited for optimising vision in bright light [37, 114]. Screening out much of the light in this very sunny habitat, with exposed and often reflective substrate, is important for preventing over-excitation, oxidative stress or even physiological damage to the photoreceptors [153, 290]. Therefore, to cope with the bright scenes typically experienced in their habitats, the fiddler crab eye becomes less sensitive by narrowing the aperture (acceptance angles) of each ommatidium and reducing the volume of receptive membrane across which phototransduction can occur [89, 214].

Do fiddler crabs have to wait for their eyes to adjust to bright light when they first emerge from dark burrows in the morning? Field observations showed that *A. tangeri* tend to very suddenly unplug and exit their burrows (in a second or two) after the morning tide had gone out, and typically travel some distance away from the safety of the entrance within 20-60 seconds of first light exposure (e.g. Fig. 5.1). Results from chapter 3 indicate that the rhabdoms and crystalline cone apertures of fiddler crabs that remain in extended darkness during the morning, would be partially widened, compared to the daytime state. Therefore, it led to the question, when exposed to first light during daytime, **how long does it take for the rhabdom to narrow to the daytime light-adapted size?**

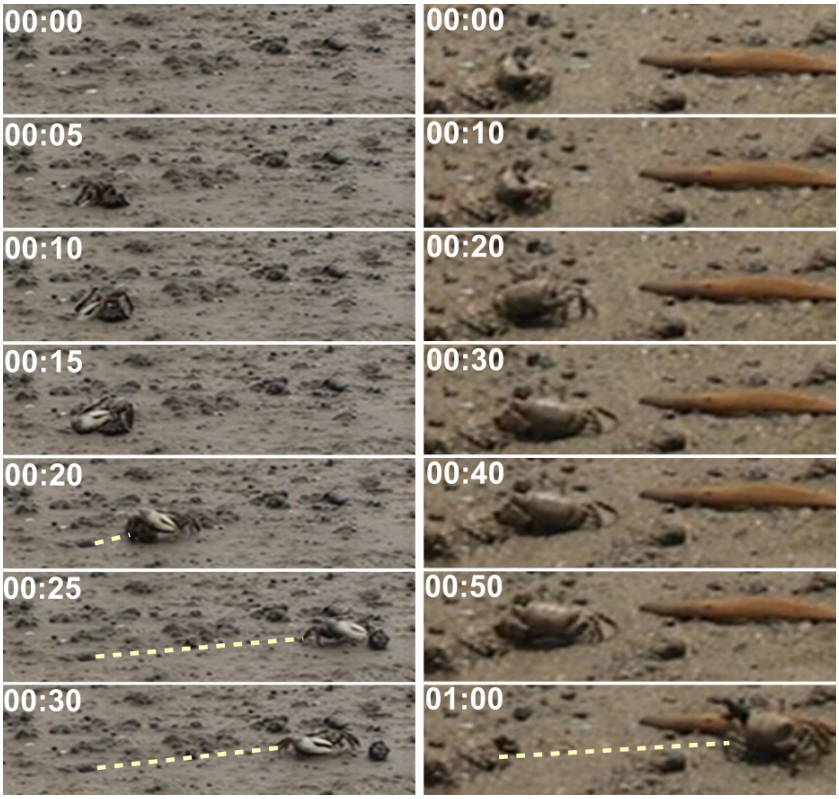

FIGURE 5.1. Two examples of typical *A. tangeri* behaviour when unplugging and exiting the burrow for the first time that day shortly (30 mins) after the tide had gone out. Time (mm:ss) since first sight of the crab is shown in the top left of the images, demonstrating the relatively quick exits followed by travel some distance away (marked by dashed lines). Both male crabs moved away from the safety of the burrow entrance between 20 and 60 seconds after breaking the surface, suggesting vision is functionally pre-adapted to the bright daylight.

To reduce the volume of the rhabdom for bright light-adapted vision during daytime, the microvilli must shorten again. Membrane is shed from the bases of the microvilli, which buds off forming small vesicles in a process called pinocytosis. The pinocytotic vesicles travel out into the cell soma via palisade bridges and are incorporated into multivesicular bodies, which are eventually transformed into multilamellar bodies [156, 164, 165, 181–183, 291, 292]. In this way, the shed material of the microvillar membranes is recycled within the photoreceptors. Rhabdom shedding is not a trivial process, requiring extensive membrane modifications. Therefore, it is unlikely to happen instantaneously during the minute or two they typically wait to first venture away from the burrow. An aim of this chapter was to investigate how long the complete light-adaptation process takes. Dark-adapted *A. tangeri* crabs that had not been exposed to light all morning (as if in the burrow), were suddenly exposed to bright light (as if surfacing) and eyes were fixed at various stages of light-adaptation over a 2-hour period. Cross-sectional rhabdom areas were measured from each individual to provide an idea of how quickly the rhabdom reduces.

The process was expected to take several minutes. Eyes were also fixed at regular intervals over a 4-hour period at dawn on the mudflat, to investigate the process at this time under natural illumination (sunrise).

The opthalmoscope was used in a further test to find evidence of fast light-adaptation changes. After the eye had been dark-adapted for various lengths of time (for the previously described aperture measurements), another image was analysed after 10 seconds of bright light exposure to see if there was any change in colour of the surrounding pigments, or shape of the pseudopupil, as a fast reaction to the bright light. I expected to see no change in this timeframe based on the histology work, which identified a lack of pigment migrations in both photoreceptor cells and primary pigment cells.

5.1.3 Rates of sensitivity change during dark-adaptation

In addition to examining rates of change in the anatomical aspects of the eye, experiments testing functional sensitivity of the *A. tangeri* eye during dark-adaptation were performed. In the behavioural experiment of chapter 4 (see results in section 4.3.1), the majority of light-adapted crabs failed to respond to a looming stimulus with Weber contrast -0.32 (Stimulus E) during daytime, while in other treatments it provoked a reliable response (in ≥95% of the crabs). On further inspection, the 40% of light-adapted crabs that *did* respond were shown this particular stimulus toward the end of their 12-minute test, whereas the crabs that did *not* respond, were shown this loom near the beginning. Therefore, in this chapter, another behavioural experiment tested the hypothesis that a dark-adaptation mechanism occurs during daytime, which can improve contrast sensitivity in this short timescale. Using the same treadmill apparatus, stimulus E was presented in 2-minute intervals, while responses were monitored over a 16-minute period.

From *G. dampieri*, ERGs were recorded during identical stimulus presentations as the eye adapted from a fully light-adapted state to the dark conditions in the Faraday cage. The experiments lasted an hour and stimuli were shown every 4 minutes throughout. They were conducted during both daytime and after sunset (using the same eight crabs), to compare the rate and extent of sensitivity increases as the eye adapts. The hypothesised result, based on previous experiments is shown in Fig. 5.2. Temporal summations increase sensitivity in the dark during both night and day (refer to chapter 4), but so far, the timescales and extents to which the changes occur at these times are unknown.

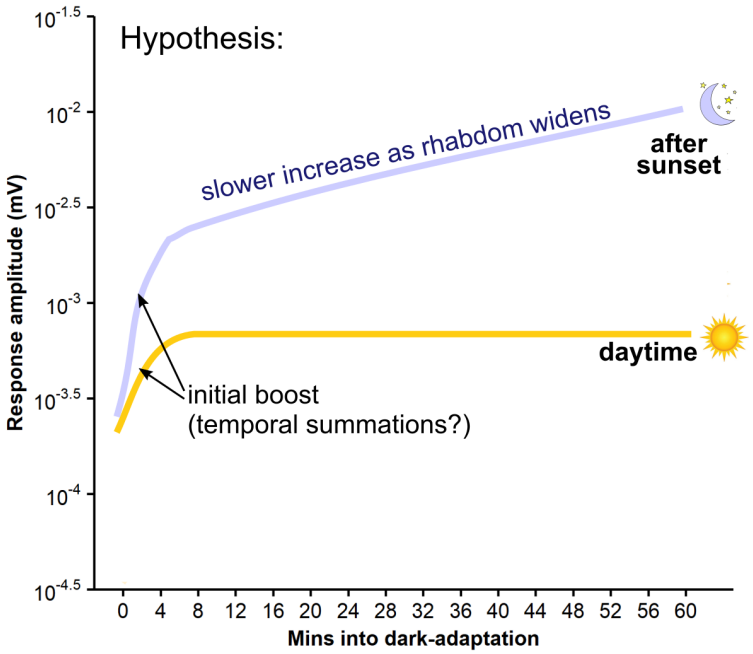

FIGURE 5.2. Hypothesised results of ERG experiment. When shown identical stimuli every 4 minutes as the eye adapts to dim light, it was expected that after sunset, there would be a steep initial increase in sensitivity, due to aperture widening and/or temporal summations. After this, sensitivity continues to increase more steadily over the hour, as the rhabdom widens. During daytime, after a smaller initial increase in sensitivity (aperture opening and/or temporal summations), the eye would cease to undergo further adaptation, reaching a final sensitivity level much lower than after sunset.

5.1.4 Is vision in bright light compromised after long periods in the burrow?

Control by a circadian clock appears to result in inhibition of full-scale dark adaptation processes during daytime. This presumably maintains the eye in a light-adapted state so that periods in the burrow do not negatively affect photopic visual sensitivity, which is primed for predator detection in a very bright visual scene [214]. Dark-adapting to the dim conditions inside the burrow would be unnecessary, and increasing absolute sensitivity could result in retinal overexposure to damaging radiation on surfacing, causing oxidative stress, photoreceptor cell damage and temporary blindness [153, 290].

Observations suggest that the crabs do not wait more than a few seconds in the burrow entrance while their eyes light-adapt after several minutes inside, and this was true even on first emergence in the morning after a high tide. During a low tide period when the crabs were actively feeding and displaying courtship behaviours on the mudflat, I filmed burrow exits after disturbing them a few minutes earlier. Typically, they came straight out and continued feeding, moving away from the burrow entrance immediately, even when they had been underground

for up to 15 minutes. Males began waving their claws in ostentatious courtship displays as soon as they surfaced and one engaged in a conflict within a minute of surfacing (Fig. 5.3). This bold behaviour very soon after hiding in the dark to escape danger implies that their ability to detect objects in a bright visual scene (with active predators) is not impaired by short periods in the burrow. Light diminishes rapidly inside the narrow burrow entrance but they may possibly wait in the short region of partial sunlight just inside the entrance (out of sight).

FIGURE 5.3. A timelapse photo series of a male *A. tangeri* crab quickly exiting his burrow after being inside for 4 minutes. He begins his waving display within 10 seconds and then engages in combat with another similar-sized male within a minute of surfacing. Time (mm:ss) since first sighting shown in bottom left corners.

Optokinetic nystagmus responses are involuntary eye movements made by animals to compensate for locomotor turns. The eyes move in the opposite direction to the body in order to fixate on and stabilise the visual scene, reducing motion blur [293]. Optokinesis is a reflex displayed by all sorts of invertebrate and vertebrate animals alike and has been exploited by many researchers as a measure of visual ability, e.g. [48, 294–298]. Crabs have long mobile eye stalks and thus exhibit overt and easily quantifiable movements [299]. If a crab is tethered still in the centre of a clockwise rotating drum with vertical stripe pattern, it will exhibit a characteristic nystagmus response. This is made up of a slow clockwise tracking phase with gain matched to the velocity of the rotation, followed by a fast anticlockwise re-adjustment phase whereby the eyes flick back to the start position [299, 300] (Fig. 5.4a). Nalbach *et al.* conducted several studies on eye movement control and optokinesis in crabs, particularly *Carcinus maenas* [301–306]. Reducing the contrast or angular size of the stripe pattern of the visual stimulus for example, can allow researchers to determine limits of contrast sensitivity or spatial resolution. Below their

detection threshold, the stripes cannot be resolved and the stimulus would appear uniform and plain, lacking motion cues. Thus, it would fail to evoke an optokinetic nystagmus response in the animal. In bright light conditions, the optokinetic response in *C. maenas* is strong, whereas eye coupling is weak, as each eye has sufficient visual information to be stimulated independently by its panorama. Decreasing the illumination, the eye coupling becomes stronger with one eye's movements the driving the other in opposite directions [301]. Strength and control of optokinetic response [304, 305] and sensitivity across the eye are linked to ecology and habitat in crabs [302], with semi-terrestrial flat-world species relying more on vision for stabilisation, relative to swimming crabs, which predominantly use statocysts, or rocky shore crabs that rely heavily on leg proprioception [304]. Nalbach *et al.* [302] demonstrated that flat-world crabs (although Ocypodidae were not tested) respond to optokinetic stimulation only along and above the equator, which views distant objects, thereby avoiding the more complex visual flow caused by locomotive activity in the ventral view of the substrate.

Contrast sensitivity in bright light (i.e. the mudflat surface) was assessed after varying periods in dim light (i.e. the burrow). Fiddler crabs were held for different lengths of time (up to 3 hours) in a darkroom before sudden exposure to a rotating low contrast (pale) stripe grating in a bright outdoor setting. Optokinetic responses to the stimulus on initial bright light exposure were recorded as a measure of how effectively the crab could resolve the contrast. Trial experiments carried out the previous year using this stripe contrast revealed that fully light-adapted crabs responded reliably, while fully dark-adapted crabs (not exposed to any light that day) often failed to respond at all during the first 30 seconds. Two hypothesised results for the present experiment were conceived (Fig. 5.4b). Either the *A. tangeri* visual system would remain functionally light-adapted across all periods in darkness, so that it stays primed for surfacing after any length of time **($\mathbf{H_0}$)**. Alternatively, the eye would become progressively dark-adapted and more sensitive to dim light, perhaps via physiological changes, during time spent in the "burrow". This would mean poorer contrast sensitivity after sudden return to bright light as the sensitive photoreceptors experience over-excitation **($\mathbf{H_1}$)**.

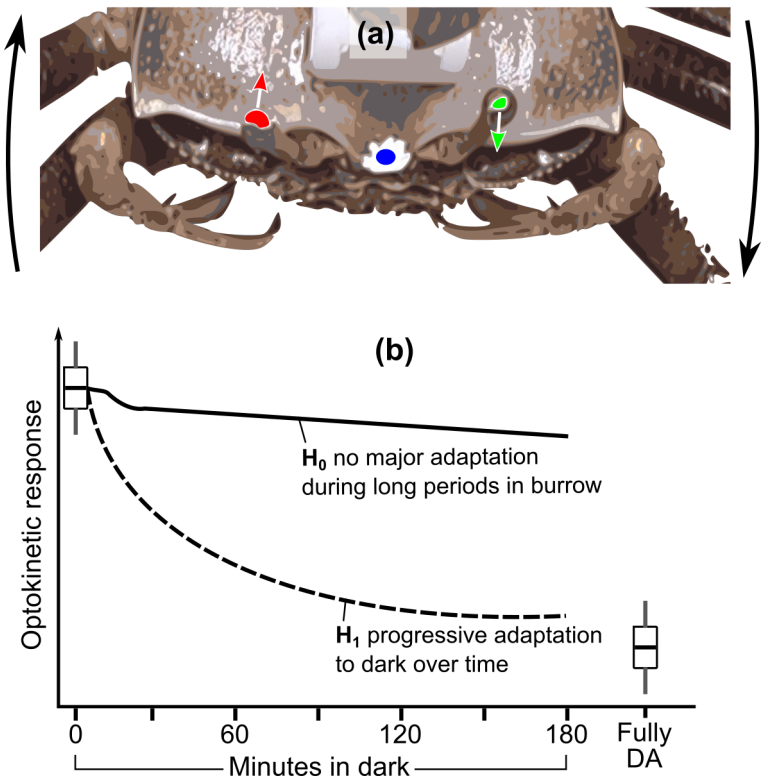

FIGURE 5.4. **(a)** Optokinetic nystagmus response in the fiddler crab to a clockwise rotating stimulus (direction shown by black arrows). Both eyes, marked by red and green spots, follow the grating in alternating slow clockwise (arrows) and fast anticlockwise movements. The blue spot marks a fixed point painted on the carapace, against which the eye positions can be tracked. **(b)** Two hypothetical results for optokinesis experiment. Either there is little adaptive response to long periods in dim light and contrast sensitivity stays prepared for photopic visual tasks immediately after (H_0, solid line), or adaptation processes occur during time spent in dim light, causing progressively poor contrast sensitivity in bright light afterwards (H_1, dashed line). The hypothesised results from fully light-adapted (0 mins) and fully dark-adapted crabs (represented by boxplots) are based on the results of a previous trial experiment.

5.2 Materials and Methods

5.2.1 TEM study of rhabdom changes

To investigate how rapidly the rhabdom volume can grow or shrink with changing light conditions, *A. tangeri* were collected from El Rompido mudflats on 8th August 2018 and divided into experimental groups (Table 5.1). Individuals were pre-adapted to either controlled bright LED light or near-darkness and then the lighting conditions were suddenly reversed at a certain time (midday or dusk) to provoke an adaptation response. The eyes of each individual were dissected at various stages during the adaptation processes using the methods described in section 2.3.

Table 5.1: Experimental treatments used to investigate rates of cross-sectional rhabdom area changes during light and dark-adaptation processes.

Treatment	**Sample times**	**Pre-adaptation method**	**Sampling method**
Daytime: dark to light	12:00 to 14:00	Six crabs dark-adapted just before dusk in a light-tight box within a darkroom, remaining there overnight.	From 12:00 the following day, eyes were collected from one dark-adapted individual, and then from the other five individuals 10, 20, 30, 60 and 120 minutes after sudden exposure to LED light.
Daytime: light to dark	12:00 to 15:00	Seven crabs were light-adapted under bright controlled LED light from dawn onward.	At 12:00, five individuals were placed inside a light-tight box in a darkroom. Eyes were sampled after 15, 30, 60, 120 and 180 minutes of darkness. The other two crabs remained light-adapted and were sampled at 12:00 and 15:00.
After sunset: light to dark	21:00 to 00:00	Seven crabs were light-adapted under bright controlled LED light from dawn onward.	At 21:00 five individuals were placed inside a light-tight box in a darkroom. Eyes were sampled after 15, 30, 60, 120 and 180 minutes of darkness. The other two crabs remained light-adapted and were sampled at 21:00 and 00:00.

In a separate experiment investigating light-adaptation at dawn, five crabs were kept outdoors under natural illumination overnight. Between 05:30 and 09:30 am, the eyes of one crab were dissected and fixed every hour. The eye samples were prepared for TEM-imaging, targeting 16 ommatidia in the frontal eye and sectioning them just proximal to the R1-7 nuclei (see method

3.2.4). Cross-sectional rhabdom areas were measured to allow comparisons between individuals.

5.2.2 Ophthalmoscopy of deep pseudopupil changes

An ophthalmoscope (Fig. 5.5) was constructed to visualise changes associated with dark adaptation in the deep pseudopupil of living fiddler crabs. The apparatus incorporated a UI-3590CP-C-HQ-R2 camera with CMOS colour sensor (Imaging Development Systems, Obersulm, Germany), 10x objective lens (Plan N, Olympus, Tokyo, Japan), beam-splitter (Thorlabs, Newton, USA) and a light source with halogen and deuterium bulbs (Mikropack DH-2000), that provided both a coaxial adapting light and imaging light.

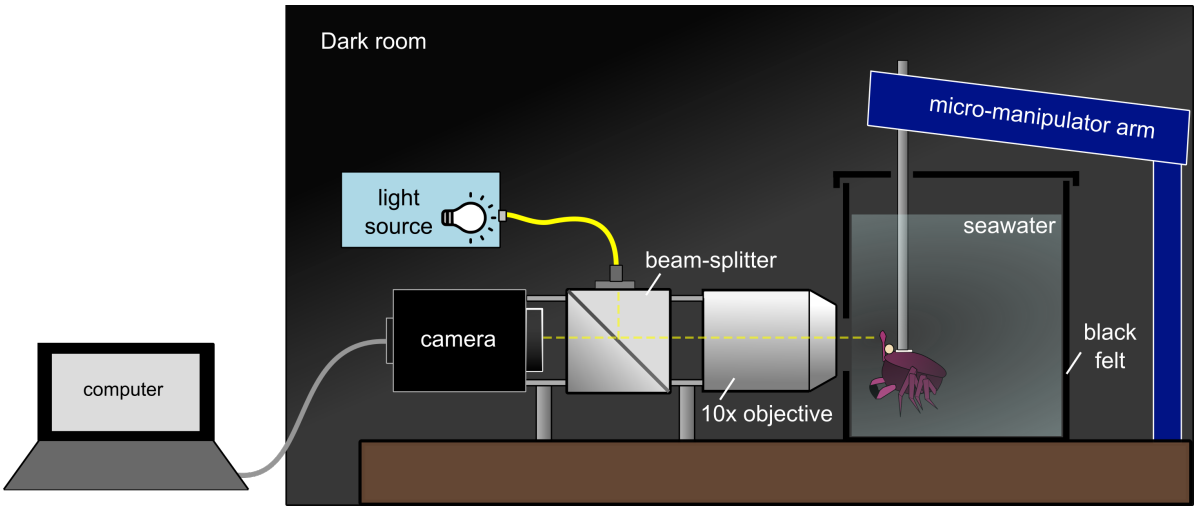

FIGURE 5.5. Ophthalmoscope apparatus used to image the eye of live crabs during dark-adaptation. A halogen/deuterium light source produced a coaxial light, directed via a beam splitter and 10x objective lens, onto the eye of a tethered fiddler crab. The crab was attached to a micro-manipulator and submerged in a tank of seawater lined with black felt, except for a small quartz glass viewing window between the crab and the lens. A camera focussed on the deep pseudo-pupil, recorded images when the light source was on at the start (when fully light-adapted) and finish of the experiment dark-adaptation period, during which all lights were off.

Six adult crabs (three females, three males) with carapace width of 16-19 mm were used in this experiment. Crabs were temporarily tethered, one at a time, to a post held by a micro-manipulator via a small polypropylene disk fixed to their carapace with cyano-acrylate glue. Claws were carefully wrapped and held close to the body with electrical tape to help immobilise the crab and prevent it pushing against the glass. One eye was held in its usual upright position using a small dab of cyano-acrylate glue on the back of the eye stalk, attached to a small wooden stick. The crab was submerged in a small glass tank of seawater lined externally with black felt

to remove external illumination, except for a small window of quartz glass. Through this, the ophthalmoscope was positioned to image the front of the eye.

The camera was focused on the equatorial eye deep pseudopupil while illuminated with coaxial and broad-field light. Then with just coaxial illumination, an image was taken of the light-adapted eye. This light was subsequently switched off and the crab was left to dark-adapt. After a period of either 15, 30, 60, or 180 minutes in darkness, the coaxial illumination was switched on and an image collected within 75 ms of light exposure. Another image was collected after a further 10 seconds, to look for evidence of fast pigment reactions to sudden bright light exposure. All six crabs were tested at these four different time points during adaptation to darkness during both daytime (11:25–18:50) and after sunset (20:28–00:54). Only one test per crab was conducted during the evening to avoid excessive unnatural disruption of the circadian light-dark cycles.

The edges of the deep pseudopupil were determined in Fiji-ImageJ by drawing a horizontal line across the middle at its widest point, and using the inbuilt 'Plot Profile' function to produce a histogram profile of greyscale values against distance along the line. The intensity profiles were characterised by two maximum peaks in intensity (the pigment cells) either side of a central minimal trough (the dark rhabdom). The distance across this trough (along the x-axis) was considered the deep pseudopupil and its width was compared to the equivalent image taken just before dark-adaptation.

5.2.3 ERG responses during dark-adaptation

Much of the procedure used in this experiment is common to all ERG experiments in this thesis and is detailed in chapter 2 section 2.4. The same eight individuals of species *G. dampieri* were used in this experiment, as in chapter 4. Before the ERG tests, their eyes were pre-adapted to bright light by keeping the crabs in a container lit with bright LEDs. While the crabs were prepared for the ERG test and set up on the apparatus, a bright LED array illuminated frontal region of the crab to keep the eyes fully light-adapted. This light was switched off the moment the first stimulus was presented (at 0 mins), beginning the experiment. Subsequently, the crab remained in darkness in the Faraday cage for the rest of the experiment (except for the stimulus), to encourage the eye to dark-adapt.

A stimulus intensity of 0.00384 μW/cm^2, with 10 Hz flicker was used in all presentations (to visualise this intensity in context with treatments used in chapter 4's ERG experiment, see black point in Fig. 4.2). This intensity was chosen as it was relatively dim and usually failed to provoke a significant response when crabs were fully light-adapted, while provoking reliable significant responses when dark-adapted. The same stimulus, lasting 21 seconds was repeatedly presented every 4 minutes for 1 hour while ERGs were recorded. All eight crabs were tested both during daytime (>2 hours before sunset) and after sunset (2-5 hours after sunset).

On a different day, each individual was tested again during both day and night, but this time the stimulus was shown just twice, once at 0 minutes when fully light-adapted, then again after 60 minutes adapting to full darkness (no stimulus displays in between). This test was performed as a control to assess the potential disruption that the stimulus itself had on sensitivity increases over time as the eye dark-adapts.

5.2.3.1 ERG Statistical analysis

Using R software (v3.5.1; http://www.R-project.org) and package "lme4" [257], a linear mixed effects model was fitted to the data, with response amplitude as the continuous fixed effect. Crab identity was given as a random effect and time of test (daytime or night) and sex, size of the crab were added as other fixed effects. Using the R package "predictmeans" (v1.0.1; https://CRAN.R-project.org/package=predictmeans), these potential explanatory fixed effect terms were tested for statistical significance by running 10,000 random permutation recalculation tests [258] on the data. Non-significant variables were excluded to produce a minimal working model.

The ERG responses at 60 minutes for the control test (uninterrupted dark-adaptation) were compared to the ERG responses at 60 minutes in the main test (when stimuli were presented every 4 min). The data were pre-checked for normality (Kolmogorov–Smirnov test) and homogeneity of variances (Bartlett's test) and found not to satisfy the assumptions of a parametric test, so Welch's T-test was used.

5.2.4 Behavioural assay of changes in contrast sensitivity

Fiddler crabs (*A. tangeri*) were collected from the mudflats at El Rompido and 26 individuals were light-adapted under bright natural sunlight outdoors from dawn after having wire harnesses attached. This behavioural experiment utilised the same crab treadmill apparatus and general methods as the previous contrast sensitivity tests in chapter 4, so please refer to section 4.2.1 for detail on the methods and an illustration of the apparatus (Fig. 4.1).

The looming stimulus presented to the crabs was identical each time; an expanding black disk against a dark grey background, "Stimulus E" with Weber contrast -0.32 (see Appendix Fig. A.1). Crabs were tethered one at a time through their wire harness, atop the treadmill ball upon which they walked. For the light-adapted crabs, the bright room light was kept on until the crab was in place to maintain its adaptation state. When the experiment began, a looming stimulus was presented every 4 minutes and responses were recorded with a video camera. Experimental conditions were dark, the only luminous source was the stimulus screen, which was only very dimly radiant. This was sufficient light to illuminate the crab for the camera however, so no dim red light was used in the set-up this time.

Crabs eventually habituate behaviourally to a stimulus when presented multiple times, failing to respond after it is learnt that the visual threat will not result in harm [248]. Therefore,

on Day 1, half of the crabs were shown the looming stimulus at 2, 6, 10 & 14 minutes into the experiment, while to the other half were shown it at 4, 8, 12 & 16 minutes. On Day 2, the same crabs were tested again but at the opposite times. This ensured that over the two days, all crabs were shown eight stimuli in 2-minute intervals, without risk of habituation.

An additional 10 crabs were dark-adapted from sunset the previous day in a darkroom until the time of the experiment the next day. They were tested the same way as the light-adapted crabs (over two days), but care was taken not to expose their eyes to any light before the experiment or during positioning on the treadmill. This second group of crabs was used as an already dark-adapted control treatment.

Videos were scored "blind" after data collection by disguising the treatment in file names to prevent researcher bias. The same binary scoring system as the previous chapter 4 behavioural experiment was used to analyse responses (see 4.2.1.3 for details). Collective response probability for each time interval from 2 to 16 minutes was calculated for light- and dark-adapted crabs from the mean of the binary responses. Wilson score confidence intervals were calculated using sample size (n) and number of successes with R package "Hmsic" (F. Harrell Jr; version 3.5.1; http://www.R-project.org).

5.2.5 Optokinetic nystagmus in bright light

Between 23rd September and 8th October 2019 fiddler crabs (*A. tangeri*) were collected regularly from the mudflats of El Rompido, Spain and kept at a nearby field laboratory for 1-3 days. A small dot of white acrylic was carefully painted on the dorsal eye stalk cap of both left and right eyes, avoiding the eye tissue itself (Fig. 5.6a). A third dot was painted between the eyes on the carapace, to serve as a fixed point for which to track eye movements against. Each crab had a small plastic mount (made from the square end of a cut cable tie) temporarily glued to their carapace with cyano-acrylate adhesive. Crabs were housed in individual plastic containers containing 1-2 cm seawater under natural illumination outdoors.

Around 12:30 pm on an experiment day, a timer was started the moment that all crabs in their containers were placed inside a light-tight box in a darkroom. Here, they spent varying periods of time, from 3 to 180 minutes, adapting to darkness until their turn in the experiment. When this time came, before leaving the darkroom, the crab was tethered by slotting the plastic mount glued to the carapace inside a hollow stick using only indirect illumination from a dim red lamp. The crab was transferred to a black felt-covered container with drawstring opening (Fig. 5.6b), so that it could be transported outdoors to the experimental apparatus without exposing the visual system to light until the last moment. The crab was quickly removed from the bag and the stick attached to its carapace was clamped into position in the centre of the rotating drum as the test began.

The apparatus (Fig. 5.6c) consisted of a motorised rotating drum of 17 cm diameter, which turned clockwise at a constant speed of 14.4 degree/s, meaning a full rotation took 25 sec. A

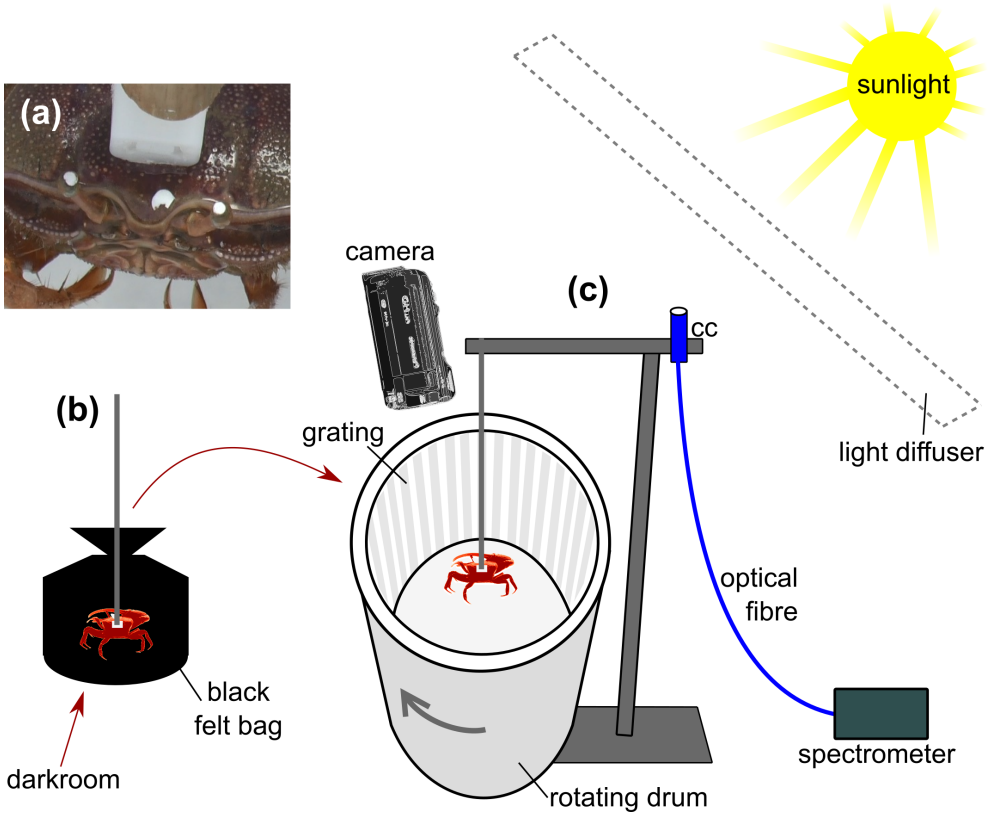

FIGURE 5.6. **(a)** White eye markers painted on both eye stalk caps allowed computer eye movement tracking, relative to a fixed point painted on carapace between the eyes. **(b)** A glass container surrounded by a lightproof black felt bag was used for transporting crabs from a darkroom to the experimental apparatus outdoors. A drawstring top opening closed tightly around the stick attached to the crab's harness, meaning the crab could be kept in darkness until the moment it began its turn in the experiment. **(c)** Illustration of apparatus used in the optokinetic response experiment. A motorised clockwise-rotating drum was lined with paper printed with a low contrast grating. The crab was suspended in the middle of the drum and filmed from above with a video camera. A spectrometer measured the spectrum of natural illumination from sunlight via a cosine corrector-coupled (CC) optical fibre, and strong shadows were minimised with light diffusing plastic.

grating stimulus, very pale grey bars printed on white paper, lined the inside. This stimulus was chosen following trial experiments, which showed that this particular contrast reliably evoked a response in fully light-adapted crabs, who tracked the drum with an **optokinetic nystagmus response**, whereas fully dark-adapted crabs often failed to respond at all, particularly in the first 30 seconds of the test, keeping eyes mostly still. The apparatus was situated outdoors at a field laboratory in El Rompido and experiments were exclusively conducted under clear skies and bright sunshine between 12:30 and 16:10 local time. Direct solar illumination passed through a sheet of light-diffusing plastic held over the apparatus to diffuse strong shadows on the stimulus

without darkening the area.

A crab took 5-10 seconds to be positioned in the centre of the rotating drum once it had been removed from the lightproof bag. The time the individual had spent dark-adapting (rounded to nearest minute) was recorded from the timer when the crab was in position and the experiment began. While the drum rotated around the stationary crab, a video camera recorded eye movements of the crab from above. An ambient light measurement was made during each test from near the top of the apparatus by a calibrated spectrometer (Flame-S, Ocean Optics, Largo, USA), via a cosine corrector-coupled optical fibre with 3900 μm² aperture. After 2 minutes, the test was finished for that individual and the plastic mount on the crab's carapace was carefully removed. Crabs were later returned to their mudflat home unharmed at the beginning of the following diurnal low tide.

The experimental treatments were as follows:

- **Main group:** previously light-adapted fiddler crabs were placed in a darkroom for varying periods of time between 3 and 180 minutes, before being tested, n=166
- **Fully light-adapted:** crabs were tested after being kept outdoors under the same bright natural illumination as the experimental apparatus (0 minutes in darkroom), n=32
- **Fully dark-adapted:** crabs were tested after being held in the darkroom since dusk the previous day, so had not been exposed to any light at all that morning, n=30

5.2.5.1 Contrast of stimulus grating

The grating stimulus consisted of alternating 0.88 cm bars of 255-white and 230-greyscale (8-bit pixel values), printed onto white paper to form a low contrast stripe pattern, 6 degrees in angular size when viewed from the centre of the drum. Irradiance spectra for the grey and white stripe were measured from within the experimental drum arena under the same bright natural lighting conditions that the crabs were tested in during the experiment (Fig. 5.7a). As the bars were fairly narrow, measurements were made from plain white paper and a 5 cm² printed area of 230 greyscale using a calibrated spectrometer (Flame-S, Ocean Optics, Largo, USA).

A template function for absorbance of invertebrate visual pigments [38] was adjusted to spectral sensitivity data for *A. tangeri* R1-7 photoreceptors ($\lambda_{\max}$ = 530 nm) [37]. At each wavelength, the values from each irradiance curve was multiplied by the equivalent value from the visual pigment absorbance curve (Fig. 5.7b). Then, the area under the resulting curves were calculated to determine quantum catch values for the grey and white stripes (Fig. 5.7c). Michelson's contrast (C_M) was calculated using the following formula,

$$C_M = \frac{Q_{max} - Q_{min}}{Q_{max} + Q_{min}}$$

where Q_{max} and Q_{min} represent the quantum catch values for the white and grey stripes, respectively. The stimulus had a Michelson's contrast (C_M) of 0.34.

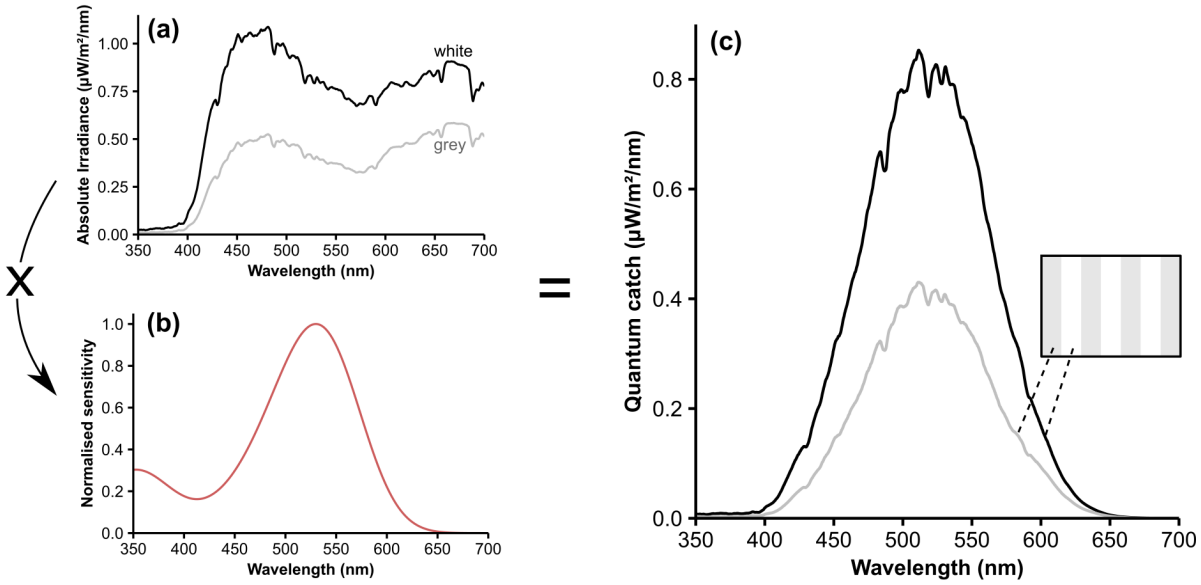

FIGURE 5.7. **(a)** Irradiance spectra for the grey and white alternating bars that made up the grating pattern used as a visual stimulus in the optokinetic response experiment. The areas under these curves were multiplied by **(b)** the template for normalised spectral sensitivity based on absorbance by invertebrate visual pigments [38], adjusted to *A. tangeri*'s λ_{max} of 530 nm [37]. This produces **(c)** approximations of photon quantum catch spectra by the R1-7 photoreceptors of the fiddler crab, plotted for the white and printed grey bars of the grating.

5.2.5.2 Data analysis and statistics

For each individual, 30 seconds of video was analysed, beginning the moment the crab was in position in the rotating drum. First, the total number of **optokinetic responses (OKRs)** was recorded, by counting completed nystagmus eye movements. Second, yaw movements of the eyes were measured with a custom MATLAB programme (M.J. How), which extracted spatial x,y coordinates from the eye markers, relative to the fixed point marker on the carapace every 20 ms (examples in Fig. 5.8). Using trigonometric calculations, the angular velocities of the left and right eyes were computed from these coordinates. At the end of an optokinetic movement after following the grating around clockwise to the extreme of the eye stalk's limit, the eyes conduct a fast anticlockwise saccade back into place. The data were filtered to remove these fast movements of >30 deg/s, which also effectively removed the fast eye-lowering movements associated with eye cleaning.

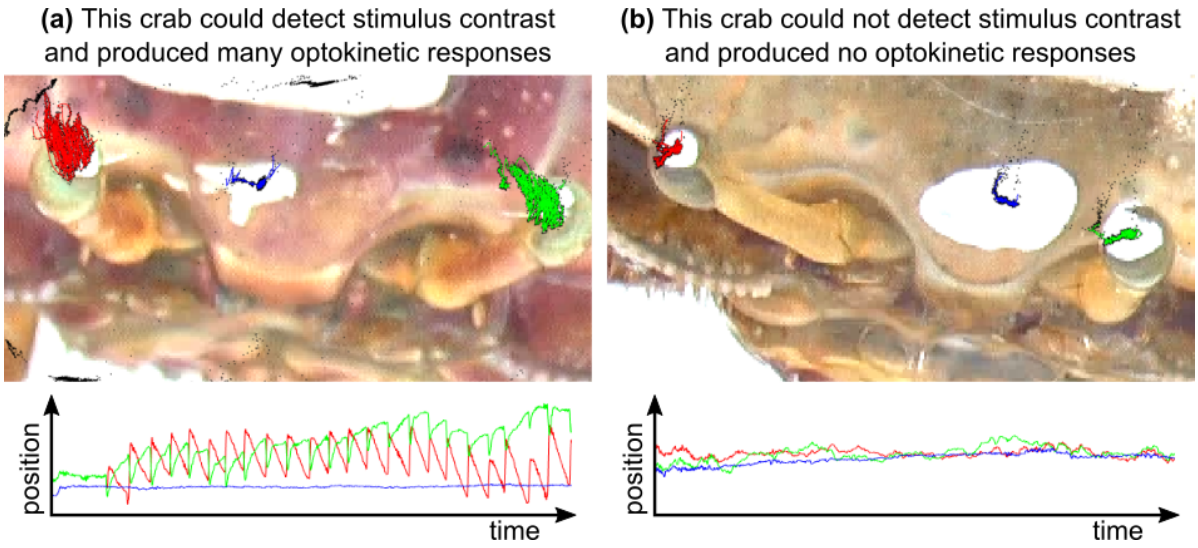

FIGURE 5.8. Examples of eye movements in two crabs. Above, a screenshot of the video is overlaid with x,y coordinates of eye positions, shown by red and green points, with blue points marking the fixed carapace marker. Below, they are plotted against time to allow better visualisation of movements. After a few seconds, Crab **(a)** began to follow the grating well with saccadic eye movements, displaying the characteristic fast and slow phases of optokinetic response and indicating her ability to detect the stimulus contrast effectively. Crab **(b)** made no nystagmus eye movements at all, indicating that he could not detect it.

The remaining angular velocities for each eye were averaged and divided by the speed of the rotating stimulus (14.4 deg/s) to produce a **Relative Velocity Ratio (RVR)**. If both eyes were in view all the time, they would each contribute 50% of the total RVR for that individual. However, often the crabs lowered an eye at a time for cleaning (especially frequent after longer periods in darkness), and sometimes a crab managed to remove a paint marker, making one eye undetectable. Therefore, the relative number of velocity observations for each eye determined the weight to which it contributed to the total RVR, i.e. if the left eye was out of view for half the time, while the right was always in view, left would only contribute a third of the RVR score.

Using R software (v3.5.1; http://www.R-project.org) with package "lme4" [257], a linear regression model was fitted to the data (excluding fully dark-adapted crabs) to test for a correlation for optokinetic responses with number of minutes spent in the darkroom previously. Additional fixed effect terms such as sex and size of the crab, and whether male dominant claw was on the right or left, were included in the model. As there was some natural variation in ambient lighting between crabs, which would affect the contrast of the grating, light intensity was also included in the model. The explanatory probability of each fixed effect term was tested using ANOVA tests and if they failed to significantly contribute to the model, they were excluded, producing a final minimal working model.

The data were also pooled into groups according to their treatment and state of adaptation to allow further analysis. The main treatment (of varying lengths of time spent in the darkroom) was divided into 15 minute intervals to assess the rates of adaptation. Second, it was divided more generally into three groups, corresponding to up to 1, 2 or 3 hours spent in the darkroom. Optokinetic responses for each group were compared to one another statistically with ANOVA and subsequent pairwise TukeyHSD tests.

5.3 Results

5.3.1 Rhabdom area changes

Eyes of individual crabs were sampled at various time points during dark- and light-adaptation to assess the approximate timescales over which the cross-sectional areas of their rhabdoms can grow or narrow (Table 5.1). The results are displayed in Fig. 5.9, but as just one individual was sampled per time point, statistical analyses were not performed.

Light to dark: After sunset, from the narrow rhabdom of the light-adapted crab (mean area 3.0 μm^2), individuals undergoing dark-adaptation had progressively wider rhabdoms, with cross-sectional area of 8.2 μm^2 after just 15 minutes in the dark and a maximum size of 19.7 μm^2 after 1 hour. Rhabdoms sampled at 2 and 3 hours into dark adaptation were not widened beyond this. During daytime, rhabdom widening also appeared to reach completion within 1 hour of darkness; however, growth was minimal and the largest rhabdom area was just 4.5 μm^2. Fully light-adapted crabs (n=1) were additionally sampled at the same time (15:00 and 00:00) as the 3-hour dark-adapted crabs, showing that rhabdoms did not widen very much over this circadian period in the absence of darkness.

Dark to light: From the dark-adapted crab's mean rhabdom measurement of 6.2 μm^2 at midday, crabs sampled after 10, 20, and 30 minutes bright light exposure had progressively narrowed rhabdoms, down to a minimum of 3.4 μm^2 at 30 min. Longer light exposure periods (1 and 2 hours) did not result in narrower rhabdoms than this, suggesting the rhabdom takes <30 minutes to narrow during light-adaptation.

At dawn, rhabdom areas of eyes fixed between 05:30 and 09:30 am varied between 6.4 and 4.7 μm^2. The crab fixed at 05:30 had rhabdoms measuring 5.3 μm^2, indicating light-adaptation processes were already well underway by this stage. Crabs fixed after this point had rhabdoms of similar size, although there was perhaps a slight narrowing over the 4 hours. Sunrise was at 07:23 am, but the morning was unexpectedly overcast with clouds (Fig. 5.9f). The largest change in light intensity occurred between 06:30 and 07:30 when the sun rose, however there was not a great change in rhabdom area between the two individuals fixed at these times. The data for an individual fixed at 08:30 am was not included due to poor tissue fixation, meaning rhabdom measurements were unreliable.

5.3.2 The deep pseudopupil

The deep pseudopupil appeared as an elongated dark centre (light-absorbing rhabdoms) surrounded by a brighter ring (reflective pigment cells). The deep pseudopupil of six individuals expanded in size during dark adaptation in both daytime and after sunset (example in Fig. 5.10a). However, the rate and extent to which this occurred was much greater after sunset, both in proportionate and absolute measures. In a fully light-adapted state, it was significantly wider

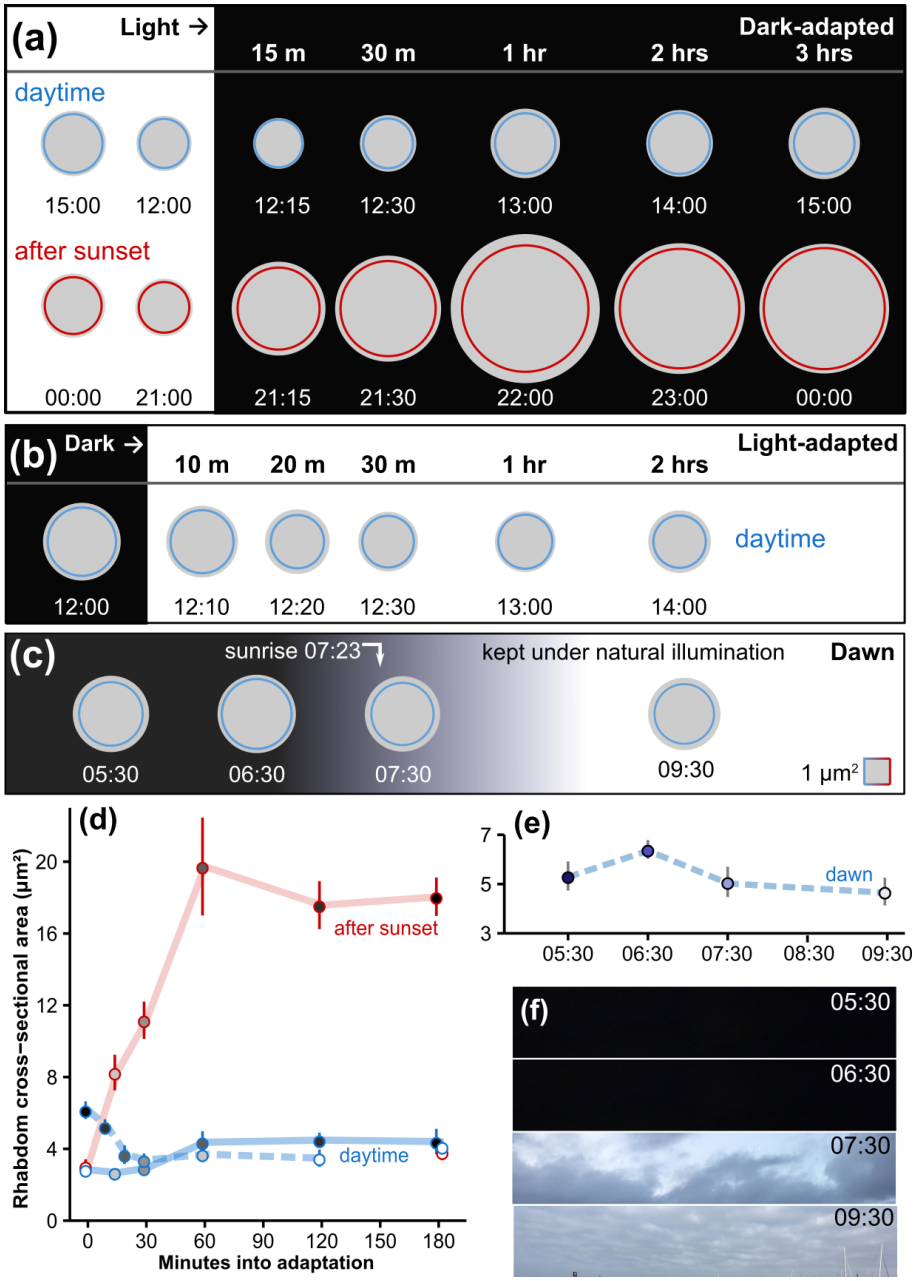

FIGURE 5.9. Scaled circles show relative cross-sectional areas of rhabdoms from individual crabs (n=1), sampled at progressive times as they **(a)** widen during dark-adaptation in daytime and after sunset, **(b)** or narrow during light-adaptation at midday and **(c)** under natural illumination at dawn. Red/blue outlines indicate mean area (μm²) for each individual +standard deviation (grey outer edge). **(d)** These data (individual means ± SD bars) are plotted together to show various stages of adaptation between light (white filled points) and dark (grey to black filled points), during daytime (blue) and after sunset (red), and from dark to light during daytime (blue dashed line). White points at 180 minutes represent individuals that remained fully light-adapted until 15:00 (blue outline) and 00:00 (red outline). **(e)** Rhabdom areas from crab eyes fixed over dawn and **(f)** photos of the sky at these sample times, showing overcast conditions.

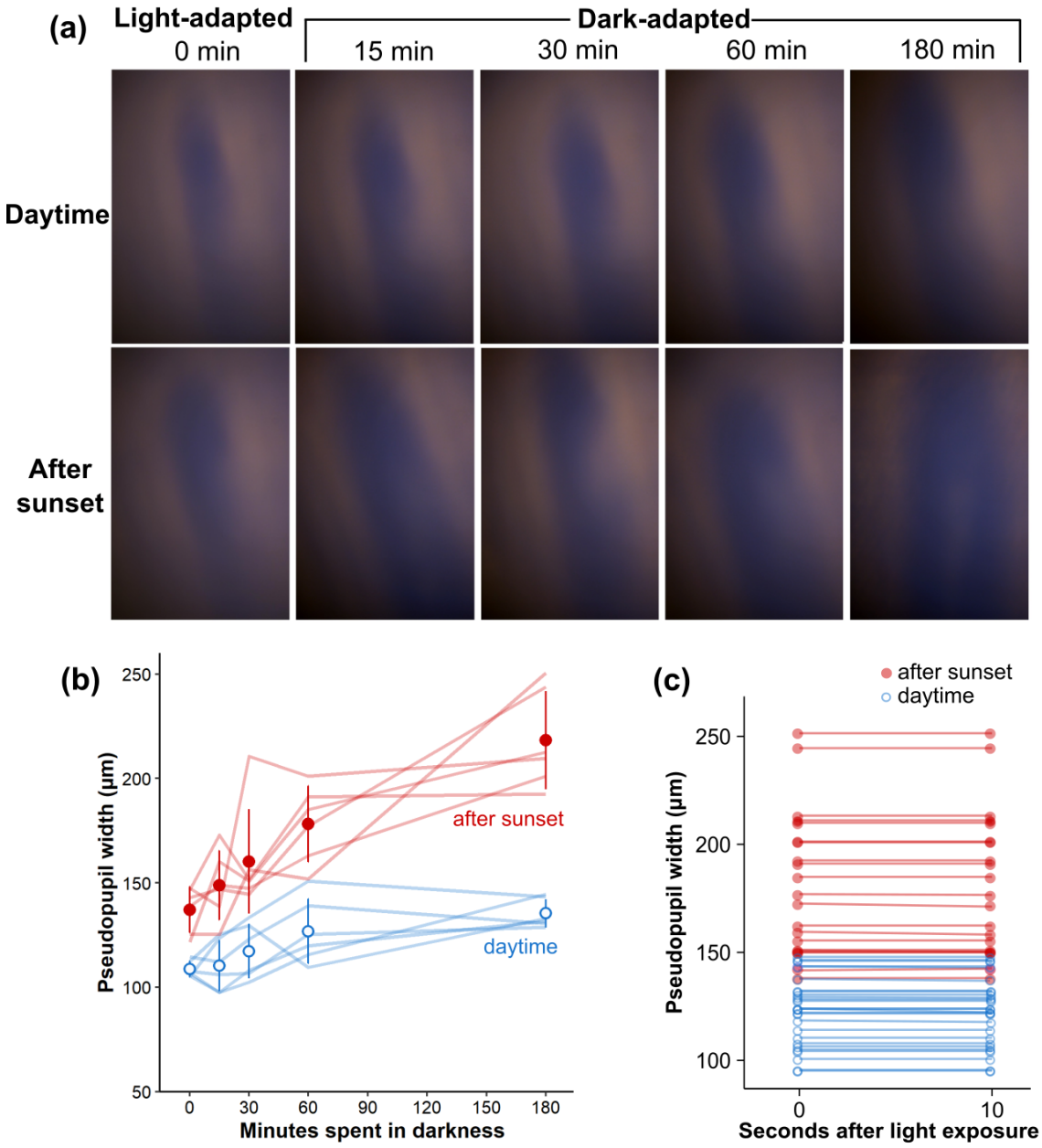

FIGURE 5.10. **(a)** Ophthalmoscope images of the deep pseudopupil of a single male crab (*A. tangeri*) after varying periods adapting to darkness during daytime and after sunset. **(b)** Width measurements of the deep pseudopupil, as fully light-adapted eyes (0 mins) spend varying periods (15 – 180 mins) adapting to darkness. Lines show data for each individual crab (n=6) during daytime (blue) and after sunset (red) and mean widths are represented by open/filled points ± standard deviation bars. **(c)** Deep pseudopupil width at the moment the dark-adapted eye is first exposed to bright light (0 sec), and again after 10 seconds of light exposure, during daytime (blue open points) and after sunset (red filled points). Lines link pairwise individual measurements.

after sunset (137.1 ± 11.0 μm) than during the day (108.7 ± 4.0 μm) (Student's t-test, $t_{(5)}$=-6.0, p<0.05) (Fig. 5.10b). In daytime, the pseudopupil width increased by 21.5% during the 3 hours. It had grown to its maximum size after 60 minutes of dark adaptation, as mean widths at 60 and 180 minutes were not significantly different to one another (Student's t-test, $t_{(5)}$=-1.2, p=0.12). At night, the pseudopupil grew much wider during dark-adaptation and continued to significantly increase between 60 and 180 minutes (Student's t-test, $t_{(5)}$=-3.3, p=0.004), resulting in a total width increase of 56.4% in the 3 hour period.

After 10 seconds of bright light exposure following these varying dark adaptation periods, there was no measurable reduction in deep pseudopupil width, or any change in general appearance in the eye during both daytime and evening (Fig. 5.10c). This suggests that no pigment migrations or any other visible change to alter the acceptance angle of the ommatidia occurred in reaction to bright light, within the timeframe of 10 seconds.

5.3.3 ERG sensitivity changes during dark-adaptation

ERG response amplitudes increased significantly with time during dark-adaptation ($X^2_{(1)}$= 41.8, p<0.001, Perm-p<0.001, n=8) as vision became more sensitive, much more so after sunset than during the day ($X^2_{(1)}$= 118.9, p<0.001, Perm-p<0.001) (Fig. 5.11). In both these periods, when shown the first stimulus (0 min) their fully light-adapted eyes gave similar responses. However, after sunset there was a steep initial increase in sensitivity during the first 12 minutes of dark adaptation, whereas during daytime, the responses increased more slowly and to a lesser extent.

Carapace width ($X^2_{(1)}$= 0.2, p=0.695, Perm-p=1) and sex of the crabs ($X^2_{(1)}$= 3.3, p=0.071, Perm-p=1) were not included in the final model as neither had a significant effect on the responses. Therefore, the final model to explain response amplitudes includes number of minutes spent in darkness, plus the time of day the crab was tested.

At night, a sudden decline in response amplitudes occurred (after the initial increase) at around 12-16 minutes. In some individuals this was extreme, sometimes almost reaching the initial response level of the light-adapted state (see faint lilac lines, Fig. 5.11). After 26-28 minutes individual response amplitudes started to climb again, before some peaked and declined again towards the end of the hour. The responses for the control test after sunset, where crabs were allowed to dark-adapt uninterrupted for an hour (without the stimulus every 4 minutes), were significantly higher (mean value 0.0156 mV) than the final values for when the stimulus was presented throughout the hour (mean response 0.0082 mV) (Welch t-test, $t_{(9.4)}$=2.9, p=0.018). This indicates a strong effect of the stimulus itself on the response amplitudes, despite its relatively dim intensity and brief intermittent presentation.

During daytime, a very shallow increase in sensitivity occurred to a much lesser extent, but some crabs also produced a (more subtle) peak and decline curve in response amplitude during the hour test period. By 60 minutes, a mean response amplitude of 0.0025 mV was recorded

from the crabs. This was slightly lower but not significantly different to the control treatment at 60 minutes, when dark adaptation was uninterrupted by stimulus presentations, with mean response 0.0038 mV (Welch t-test, $t_{(12.9)}$=-0.9, p=0.344).

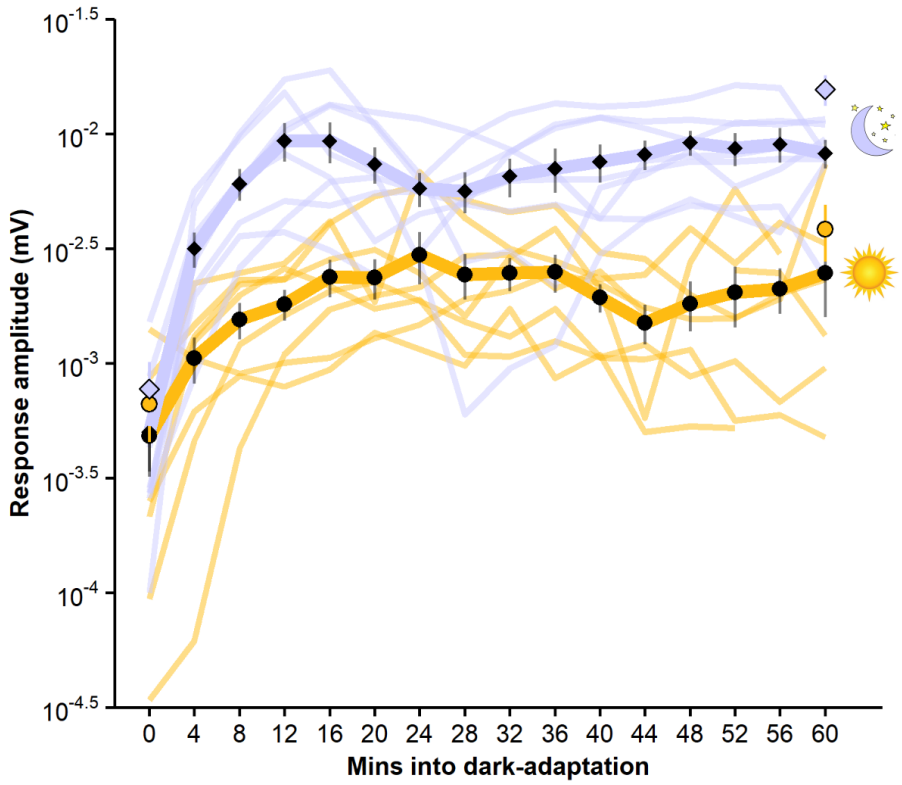

FIGURE 5.11. Response amplitude to a 10 Hz flickering stimulus of 0.0038 μW/cm^2 intensity, over the course of 1 hour, shown in 4-minute intervals as *G. dampieri* fiddler crabs (n=8) adapt from bright light to darkness. Data for each individual are represented by faint yellow or lilac lines for tests carried out during daytime and after sunset, respectively. Overlaid are black filled points ± standard error bars, to represent the mean values for day (circles) and night (diamonds). Points filled with yellow or lilac at 0 and 60 minutes show the mean response amplitudes (± standard error bars) for the same eight crabs when they were tested at just these two times, allowing an hour of uninterrupted dark adaptation in between.

5.3.4 Contrast sensitivity increases during dark-adaptation

Behavioural responses indicated that the fiddler crabs that were already dark-adapted were able to detect the looming stimulus immediately and all ten individuals responded to it on the very first presentation, 2 minutes into the experiment (Fig. 5.12). The mean (and unanimous) first response time of 2 minutes indicated that this contrast was reliably detectable by their visual systems in this condition. To all further looming stimuli (of unchanging contrast), 90-100% of the dark-adapted crabs responded.

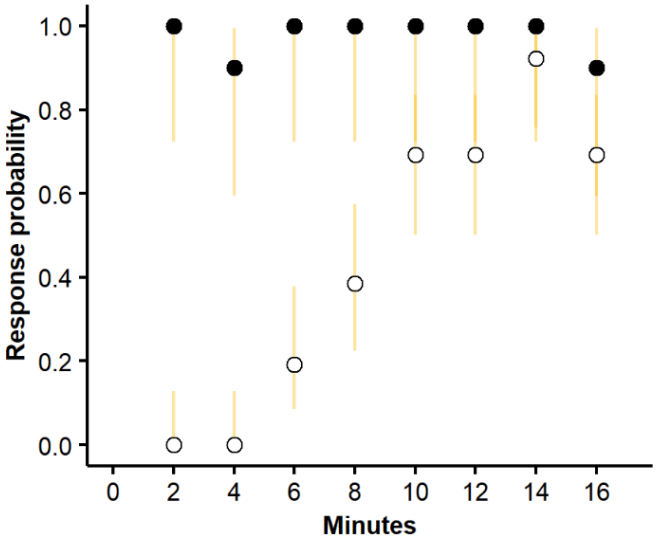

FIGURE 5.12. Open points represent response probabilities of light-adapted *A. tangeri* fiddler crabs (n=26) when shown the same low contrast looming stimulus in 2-minute intervals over a 16-minute period as they adapted to dim light. Filled points show results for crabs that were already dark-adapted prior to the experiment (n=10). Yellow bars represent Wilson score confidence intervals.

In comparison, none of the 26 light-adapted crabs responded to the looming stimulus when shown at 2 or 4 minutes into the experiment. By 6 and 8 minutes a minority responded, 19% and 39% of the crabs, respectively. However, it was not until they had spent 10 minutes in darkness that the majority of crabs (69%) detected this contrast, however not all, and some response behaviours were very subtle and only just noticeable. Nearly all (92%) responded to the stimulus in some way at 14 minutes (but this reduced again to 69% at 16 minutes). The mean "first response time" for the light-adapted fiddler crabs was 9 minutes.

5.3.5 Optokinetic nystagmus responses in bright light

5.3.5.1 Relative Velocity Ratio (RVR)

The rate of optokinetic responses (OKR) provides a reliable measure of the visual ability of an animal to see a given stimulus [48]. However, the RVR data from this experiment were noisy and there was a only a weak positive correlation (R^2=0.31) between total number of OKRs in the 30-second period and RVR (Fig. 5.13a). One would expect to see a stronger correlation if they were both reliable predictors of ability to detect a stimulus. Some crabs who failed to manage more than 2-3 OKRs, still produced some fairly high RVR values (>0.5) from other general eye movements they made. In contrast, some individuals who could clearly track the grating well with >25 nystagmus eye movements, had lower RVR values of <0.5. Most of the RVR values were

closely grouped between 0.4 and 0.7, and there was a weak correlation (R^2=0.14) with number of minutes spent in the dark (Fig. 5.13b).

Unfortunately, I was not able to tweak my RVR calculation formula in a way that worked well for all instances, while remaining automatic and objective. The RVR values did not provide a sensitive measure of the crabs' visual abilities. It was decided that the number of optokinetic nystagmus responses (OKR) was to be used as the response variable in comparisons instead. So, despite the time and effort spent analysing the video and calculating RVRs for each individual, these data were not used.

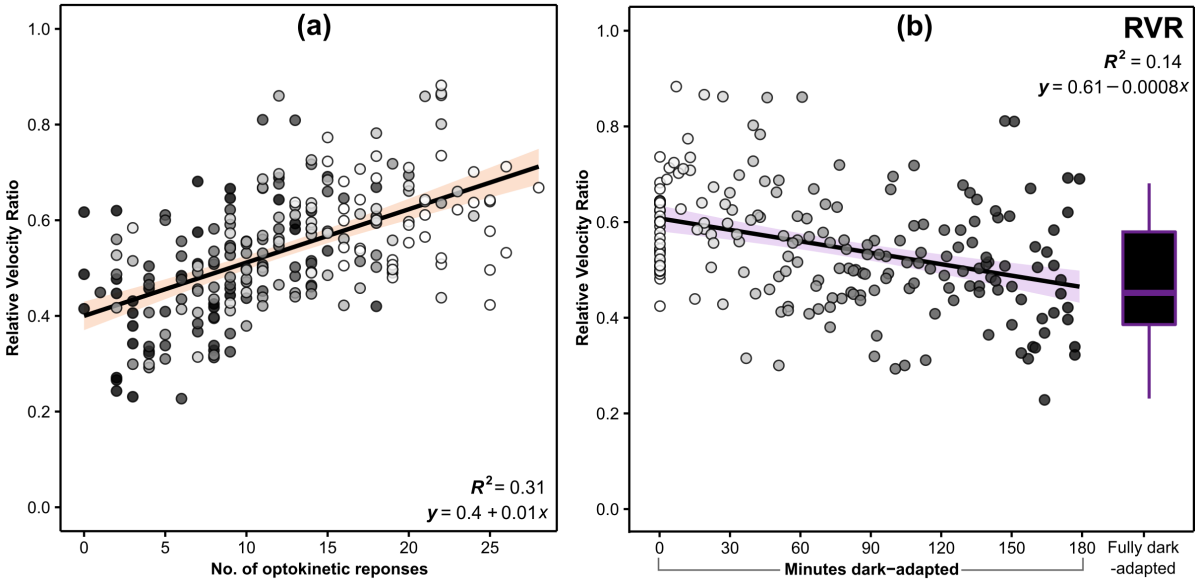

FIGURE 5.13. **(a)** The relative velocity ratios (RVR) are plotted against number of optokinetic responses (eye movements), known as a reliable proxy of contrast sensitivity. A regression line illustrates the weak positive correlation between them, the shaded area shows standard error. The points are shaded from light to dark according to how many minutes in the dark they had spent prior. **(b)** RVR is plotted against number of minutes spent in the dark with points shaded accordingly (as in **a**). The regression line and R^2 value illustrate the very weak negative correlation between them. Data for fully dark-adapted crabs are displayed in a boxplot that includes upper and lower quartiles with a central median line. Whiskers indicate the full range of data.

5.3.5.2 Optokinetic response (OKR)

The number of OKRs produced by the fiddler crabs in 30 seconds ranged from 0 to 28 (Fig. 5.14a). Although these data were fairly noisy, a linear regression model fitted to the data (excluding the fully dark-adapted group), revealed a significant decrease in number of OKRs with increasing

minutes spent in the darkroom prior (ANOVA, $F_{(1,196)}$=107.7, p <0.001). Male claw handedness (which side the dominant claw was on), did not significantly affect the responses (ANOVA, $F_{(1,164)}$=0.049, p=0.826); neither did carapace width (ANOVA, $F_{(1,165)}$=0.957, p=0.330) or sex (ANOVA, $F_{(1,166)}$=1.794, p=0.182) of the crabs.

The tests were carried out under natural illumination, which varied in intensity over time, although this was minimised by conducting tests within the same 4-hour period of the day, only under clear skies. Higher light intensity increases the visible contrast of a grating pattern. Irradiance spectra measured during each crab's test (see Appendix Fig. A.2a) were converted to total light intensity values by calculating area under the curve across the visible spectrum. Variations in light intensity were found not to have a significant effect on number of OKRs ($F_{(1,197)}$=3.133, p=0.078), so this term was also excluded from the model (see Appendix Fig. A.2b to visualise relationship). Therefore, the resulting minimal model describes a significant reduction in number of OKRs with increasing time spent in the darkroom prior ($F_{(1,196)}$=107.7, p<0.001). The negative correlation between them had an adjusted R^2 value of 0.35 (see regression illustrated in Fig. 5.14a).

Grouping data by how long crabs spent in the dark by intervals of 15 minutes (Fig. 5.14b) showed that compared to fully light-adapted crabs, those that spent 1-15 minutes in the darkroom before the test were still able to produce an almost equally high number of responses. After this, number of OKRs declined most steeply after 15-60 minutes of dark-adaptation, and then the response likelihood levelled, reducing only slightly thereafter. With this in mind, data were also grouped more generally by hour (Fig. 5.14c), to allow ANOVA comparison and pairwise Tukey tests between treatments. The test revealed that state of adaptation did have an overall significant effect on number of OKRs (ANOVA, $F_{(4,223)}$=48.88 , p=<0.001). Number of responses in fiddler crabs that had been dark-adapted for up to 61-120 minutes were not significantly different to crabs that had been dark-adapted for 121-180 minutes (TukeyHSD, p=0.552), indicating no further adaptation processes occurred after some time between 1 and 2 hours. Fully dark-adapted crabs who were not exposed to any light that morning, had significantly poorer contrast sensitivity in bright light (mean OKR = 5.3 ± 3.8) compared to the crabs adapted that were in the dark for 2-3 hours before (mean OKR = 9.7 ± 5.4) (TukeyHSD, p<0.001). All other pairwise combinations were also significantly different from one another (TukeyHSD, p<0.001).

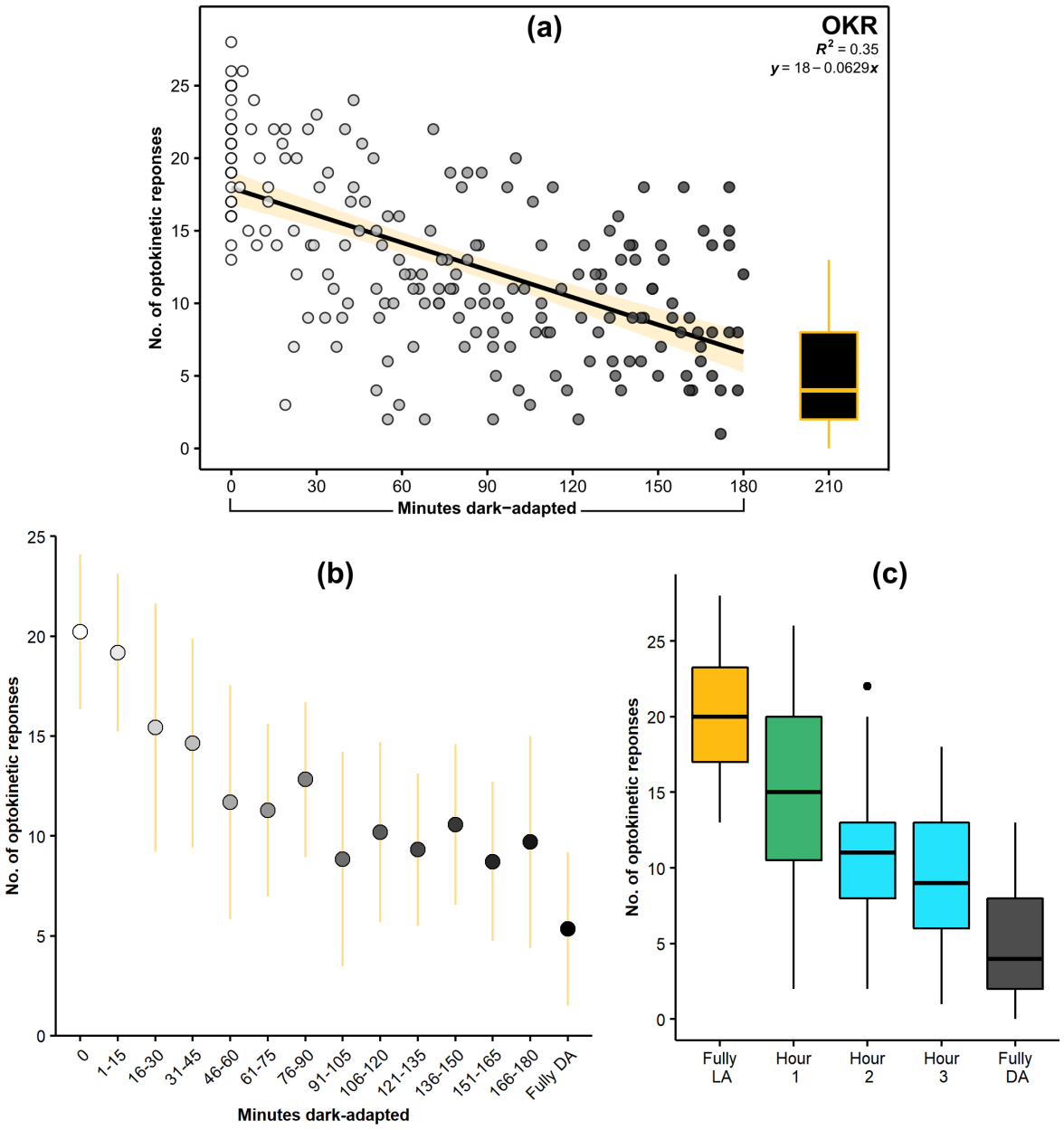

FIGURE 5.14. **(a)** Number of optokinetic responses (OKRs) during 30 seconds of bright light exposure plotted against time spent previously adapting to dark, points shaded according to this time. Negative correlation is indicated by the R^2 value and regression line (formula in top right) with yellow area showing standard error. Data for fully dark-adapted crabs are displayed in a boxplot with upper and lower quartiles and central median line. Whiskers indicate the full range of data. **(b)** The same results are grouped by time spent in the dark, in 15 minute intervals, with mean (points) and their standard deviation bars. **(c)** Data for the main treatment are pooled by number of incomplete hours spent in the dark as boxplots. Different colours indicate groups that were significantly different in their number of OKRs.

5.4 Discussion

5.4.1 Rapid dark-adaptation at dusk

After sunset, both rhabdom and aperture undergo dramatic transformations, whereby they widen by several times. In the rhabdom, this process involves the elongations of thousands of microvilli along rhabdomeres from many thousands of photoreceptors, many of which exceed 300 μm in length. Each microvillus is extended from its base by incorporating new membrane into it, within a multi-step process [165, 182, 184, 233, 234, 307]. This presumably requires a significant energy investment and is unlikely to be a quick operation.

The *A. tangeri* eye fixed after 15 minutes in the darkroom had a rhabdom 2.7 times the volume of the light-adapted individual, already. Synthesis appeared to be well-underway by this stage so the process is likely to begin immediately after lights off at dusk. The rate of rhabdom growth remains fast for up to 60 minutes, by which time it seems to have reached its maximum and final size for the night (a cross-sectional area increase of 6.5 times compared to the light-adapted crab). This is consistent with Stowe's observations of the purple rock crab, *L. variegatus* around sunset [184]. She found that rhabdomeres of this crab had usually completed synthesis within 1 hour after lights off, although occasionally animals would still be in the final stages of this 2-3 hours later. Rhabdom measurements in *H. sanguineus* showed that rhabdoms had almost reached full nocturnal size (8 times larger than daytime) after just 30 minutes in darkness [165].

The bulk of this process does not take long, considering the large volume of membranes synthesised. The experiment aimed to identify the fastest duration over which the rhabdom can widen, and thus the fiddler crabs were switched from bright light to near-darkness instantly. At dusk, solar illumination diminishes by many log units over 1-2 hours, depending on the geographic latitude and time of year. The presence of bright light appears to inhibit microvillar elongations, so it is likely that the rhabdom grows more gradually under normal circumstances, the duration matching the rate of celestial irradiance decreases during nightfall. The 60-minute timescale is perhaps well-matched to the fastest duration of declining light intensity that can occur over sunset (Fig. 5.15).

In other crabs, the photoreceptors begin cellular preparations for this rapid daily transformation up to 4-5 hours before sunset, allowing synthesis to begin immediately on onset of darkness [184, 233, 307]. The full rhabdom widening process is said to be dependent on the presence of opsin-filled vesicles in the photoreceptor soma, as precursors [233]. These only appear in the cells during late afternoon and are subject to intrinsic control by a biological clock [184, 234]. Although this work did not closely study the steps of the membrane turnover, organelle presence in the TEM images of photoreceptors (used for rhabdom measurements) were examined to allow comparison to descriptions of nocturnal rhabdomere growth processes in *L. variegatus* [184] and *H. sanguineus* [165, 233].

Stowe [184] describes a total breakdown of the *L. variegatus* rhabdomeres, one by one,

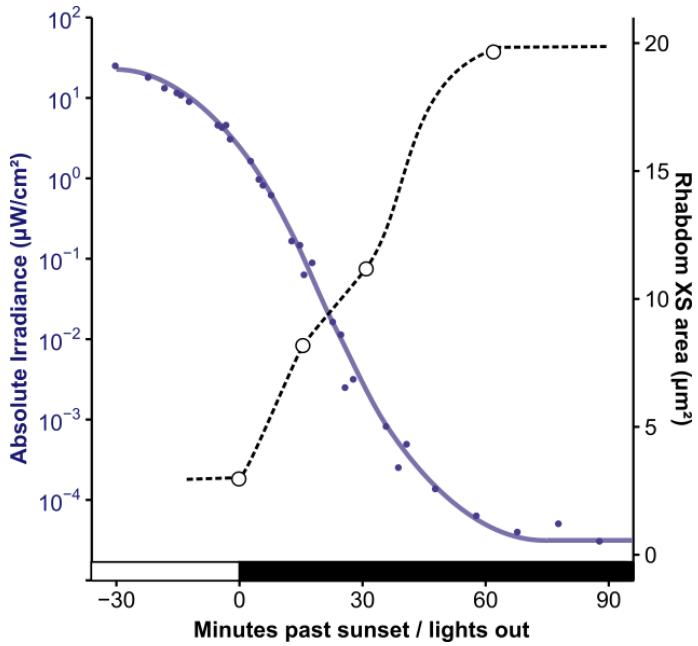

FIGURE 5.15. Declines in light intensity on El Rompido mudflats on several clear-skied late summer evenings from 30 minutes before sunset, to 90 minutes after (blue filled points and solid line). Irradiance spectrum data from Fig. 6.7 were reused after conversion to total irradiance values. Alongside, mean values for cross-sectional rhabdom areas are represented by open points and a dashed line, over the same period from lights out suddenly at sunset (same data as in Fig. 5.9). White and black bars represent light/dark phase exposure for the eyes.

before they are reassembled at dusk with new microvillus membrane material. Pre-dusk, the photoreceptors start preparations for this process with the presence of distinctive endoplasmic reticulum (ER) and golgi tubules seen in the cell somas, e.g. "crenate ER". She found that sometimes the early stages of rhabdom disassembly had partially begun before lights out. There were some parts of the process that were recognisable in *A. tangeri*, however, I did not see any examples of the characteristic crenate ER forms she depicts. Nor did I see any evidence of total rhabdomere dissolution in *A. tangeri* ommatidia TEMs from eye samples around dusk.

Matsushita *et al.*'s [233] account of this mechanism in *H. sanguineus* did not include full breakdown of rhabdomeres as part of this process, and they note this disparity between the two species. Opsin-filled vesicles fill the soma before sunset and then shortly after lights off, pinocytotic vesicles start to border the microvillar bases (without shortening them), before the vesicles move in to begin incorporating with and elongating the microvilli from their bases. This description and the TEM images presented, appear more consistent with my observations from *A. tangeri* (Fig. 5.16). However, it must be noted that there were only a few examples to go by. Further study is needed to fully understand this process in detail in the fiddler crab, especially in light of the differences reported in the mechanism between crab taxa.

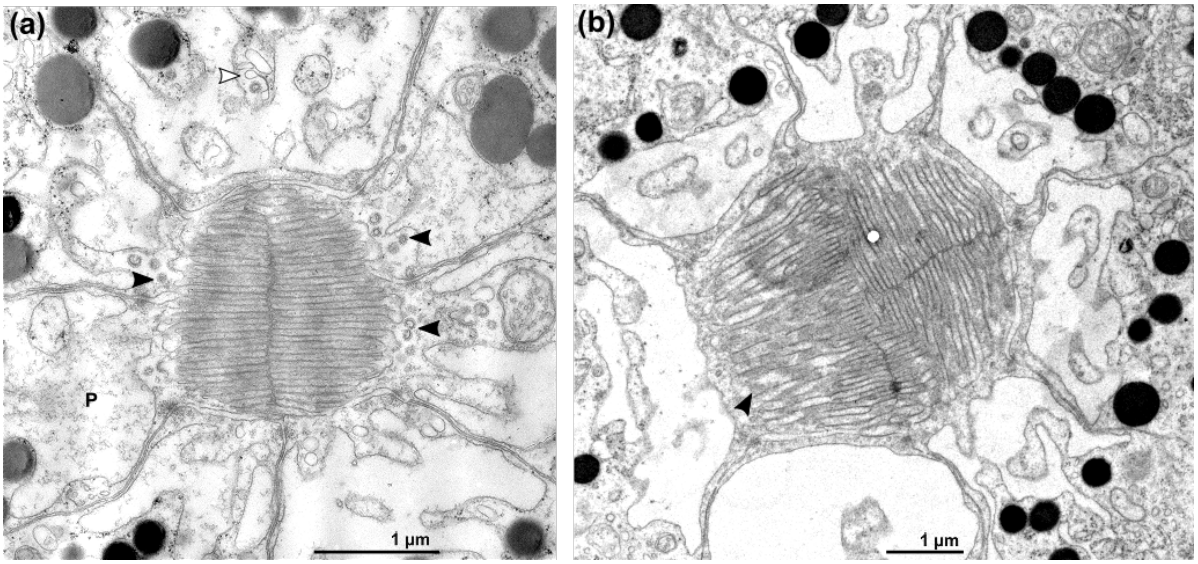

FIGURE 5.16. **(a)** TEM of ommatidium in a light-adapted *A. tangeri* eye at 21:00 (sunset), ready to begin widening. Pinocytotic vesicles are visible around the rhabdom's microvillar bases (black arrows) and structures resembling opsin-filled vesicles [233] and/or doublet ER [184] (white arrow) fill the cell soma and sometimes bridges of the palisade (P). **(b)** The rhabdom of an eye adapting to dim light at dusk, fixed after spending 30 minutes in near-darkness. Some microvilli appear loose (black arrow) as the they elongate from their bases.

Ophthalmoscopy revealed that crystalline cone apertures in light-adapted eyes after sunset were slightly wider than their daytime size (represented by the deep pseudopupil). They appeared to have already begun the dark-adaptation process before lights off after sunset, despite prolonged exposure to bright light. When suddenly exposed to near-darkness, the apertures continued to widen steadily within the first 60 minutes and beyond; they were significantly wider again after 180 minutes. Therefore, acceptance angles increased by 1.6 times after 3 hours in the dark. This is consistent with the theoretical acceptance angle calculations made using histological measurements (section 3.4.4), which increased by 1.9 times. That it took this long (more than an hour) was surprising, although the exact mechanism for this width increase is unknown.

It is worth noting that the equatorial region of the eye (chosen to match the eye regions sampled via microscopy), was in hindsight, not the optimal region to measure and observe colour changes in the deep pseudopupil. Alkaladi & Zeil [89] illustrate a striking difference of pseudopupil appearance between eye regions in *G. vomeris* (see Appendix Fig. A.3). Bands of differing cell types (i.e. photoreceptor rhabdoms, primary and secondary pigment cells) in the dorsal and ventral eye regions form a clearly defined cylindrical "bulls-eye", pattern, which would have been better to sample and measure chromatic changes (or lack of) associated with screening pigment distributions, than the elongated and blurry-looking pseudopupil of the equatorial eye.

Pigment cells do not appear to be responsible for acceptance angle increases as they are in many other animals [162, 167, 168, 173]. For example, Leggett & Stavenga [173] used an ophthalmoscope to measure acceptance angle changes in the crab *Scylla serrata* and found similar nighttime-only dramatic increases in dark-adapted eyes. These were accompanied by a change in appearance, with pigments showing as a bright "iris" of pigment around the psuedopupil. The lack of change in colour or general appearance around the pseudopupil in *A. tangeri* provides further evidence of lack of screening pigment migrations in this species. The four proximal pigment cells encircling each crystalline cone tip do not appear to make any contact with, or constrict the proximal part of the tract in any way, unlike the diaphragm pupil-type apertures of some arthropods [162, 167–169, 308, 309]. The tapered proximal tips of the crystalline cones intersect around the outside of the rhabdom, and so it is my belief that when the underlying rhabdom expands in width, the proximal crystalline cone tract simply widens with it, possibly assisted by some shortening of the cells to maintain constant volume [214]. This would explain the similar timescales of the crystalline cone and rhabdom changes.

5.4.1.1 Physiological changes are subdued during dark periods in daytime

During daytime, a very slight physiological dark-adaptation response appears to happen within the first 30-60 minutes of dark exposure. Both the rhabdom and deep pseudopupil undergo a very slight (but perhaps negligible) increase in width in this time. Compared to the dark-adaptation processes measured after sunset, these changes were minimal and not likely to result in large absolute sensitivity changes [241]. The pseudopupil only grew by 25% over the first hour of darkness and was much smaller than the night state after 3 hours in the dark (59% increase at night). The aperture dynamics appear to be strongly controlled by circadian clocks, which mostly prevent widening during periods of darkness in daylight hours. Very similar phenomena have been demonstrated by ophthalmoscopy in *Scylla* crabs [173] and the beetle *Tenebrio molitor* [289]. As suggested previously, this narrower daytime crystalline cone tip aperture may simply match the size of the rhabdom, to which it is connected.

The crab *L. variegatus* begins rhabdom synthesis and widening, involving a "disorganised" rhabdom stage after short periods (>20 mins) in daytime dark conditions [182]. However, in *A. tangeri*, there appeared to be only a very slight growth in the cross-sectional area of rhabdom during the first hour of dark-adaptation during daytime, by 1.5 times (compared to 6.5 times at night). The cytoplasm of photoreceptors were largely empty of organelles (relative to dusk and dawn) and rhabdoms appeared ordinary and orderly. The individual fixed after 3 hours in the dark, had a rhabdom of similar size to the fully light-adapted crab's rhabdoms fixed at the same time. The latter was used as a control for circadian effects, so this similar size suggests the slightly wider size may be typical for that period of day. Therefore, the rhabdom appears not to expand at all during daytime, remaining narrow during long periods in near-darkness.

To avoid capture, fiddler crabs must be able to distinguish fast-moving birds from other objects at a considerable distance away, meaning they may only occupy a very small portion of their visual field. Therefore, they require keen contrast sensitivity, motion detection and spatial resolution at all times on the mudflat surface during daylight hours [114, 115, 125]. The slight (to negligible) anatomical changes in the eye, even after 3 hours in near-darkness, further support the idea that the eye stays physiologically light-adapted in the burrow during daytime. Maintaining the visual system in a light-adapted state means the crab stays prepared for essential predator detection tasks on surfacing in a very bright scene.

5.4.2 Sensitivity increases in dim light

Despite minimal physiological response to dim light during daytime, behavioural responses to the looming stimulus indicated that there was an increase in absolute sensitivity that resulted in improved contrast sensitivity within a few minutes. This is likely to be partly, or completely due to temporal summations, which were shown in *G. dampieri* to occur during daytime to cope with dim light conditions (see previous chapter, Fig. 4.6). Temporal summations are a neural mechanism to increase the integration time over which photons are collected by photoreceptors to produce a signal, thus pooling light over time [34]. It appears that this strategy may take several minutes to take effect when placed in dim light, as no fiddler crab detected the looming stimulus before 6 minutes and the mean time of first detection of was ~9 minutes.

Spatial summation is an alternative method of increasing sensitivity. The lamina, made of cartridges (which each correspond to a single ommatidium) contains lamina monopolar cells that in some animals, send out long lateral dendrite extensions to integrate signals with their neighbours, at the expense of spatial resolution [30, 34, 191, 198, 199]. Fiddler crab eyes are elongated vertically and have specialised to include equatorial streak of high spatial acuity with which to view their visual horizon. This is an important aspect of their visual ecology during daytime, helping to detect predators at distance and interact with conspecifics [97, 113, 114, 117, 118]. In addition, given the energetic cost of their relatively high temporal acuity vision [192, 277], there is surely strong selection for fast vision too (>70 Hz in *G. dampieri*). At night, there are fewer bird predators present and fiddler crabs can focus on the safer interactions with conspecifics in close proximity, so perhaps their visual needs after dark are matched with a balanced spatiotemporal filter [34] and there may therefore be differences in strategy between species according to their nocturnal activities. It would be interesting to compare spatial resolving power in light- and dark-adapted fiddlers to look for evidence of spatial summations, although one must consider the confounding effect of increased acceptance angles through crystalline cone and rhabdom diameter widening that occur when dark-adapted at night [173, 214]. Further evidence can be obtained from examining whether there are lateral branching dendrites from the laminar monopolar cells. So far, there have been no reports of this to support spatial integration in a crab, but there may be alternative strategies in higher order interneurons for integration

across neighbouring ommatidia [30, 34].

As hypothesised, the ERG experiment showed that time of day had a significant effect on the rate and extent of dark-adaptation. This was particularly evident in the first 16 minutes. During daytime, there was an initial boost in sensitivity and then it largely levelled out, on average. At night, sensitivity was increased much beyond this and much larger response amplitudes were measured. In some ways, the results resemble the hypothesised outcome, however, the presence of the stimulus clearly had a large effect on the individual results over time. After the first 12-minute initial boost in sensitivity, many of the crabs experienced a sudden decrease in sensitivity, to a massive extent in some individuals. This was particularly evident after sunset and was then followed by another increase in response amplitude after some time.

When the crabs had no LED stimulation during dark-adaptation, their final responses at 60 minutes were much greater than when their adaptation was interrupted every 4 minutes. This implies that even though the LED was fairly dim, this light exposure to their newly sensitive eyes after 12 minutes was enough to reverse the dark-adaptation response and cause a decrease in sensitivity. After they had then effectively light-adapted again, the stimulus would begin to appear dim again to less sensitive eyes, evoking only a small response and allowing their sensitivity to increase again. If this experiment had been carried out for longer, perhaps this would happen over and over again. It demonstrates the strong disruptive effect that even dim intermittent light exposure can have on the process of dark-adaptation. The large effect it had on individual responses is something to consider when working with animals that are assumed to be dark-adapted, and utmost caution is important to prevent accidental light exposure.

5.4.3 Adapting to bright light

It is often faster for an animal visual system to light-adapt, than it is to dark-adapt. In humans for example, after exposure to bright light, the eye takes more than 30 minutes to become fully dark-adapted and maximally sensitive in dim light [310]. This is linked to the very slow regeneration times of light-activated rhodopsin in rod photoreceptors (required for dim light vision), compared to the fast and relatively insensitive cone cell rhodopsins used in bright light [311]. Moving from dim to bright light, a neural mechanism must switch the human eye back to fast cone-mediated vision and rapidly decrease retinal sensitivity to avoid damage to the light sensitive cells. This is effective in less than a minute, although it can take 10 minutes for the cones to achieve maximal spatial acuity and colour discrimination [310].

The visual system in arthropods is very different to ours, but many animals still require adaptations to cope with fluctuations in brightness, which can be extreme [34]. Arthropod rhodopsin has two inter-convertible states, ground state rhodopsin and (thermostable) metarhodopsin [24]. Conversion between the two requires a photon and although it varies between species, this relatively simple pathway can be very fast, facilitating high-speed vision in bright light [24, 312].

It means that bleaching of photoreceptors is a problem that many arthropods do not have to deal with [313].

In the dark-adapted crab, exposure to bright light evokes the degradation of the wide, sensitive rhabdom to a narrower tract via pinocytosis. In this process, microvilli are shortened from the base and the membrane material recycled via organelles in the photoreceptor soma (see [156, 164, 165, 181–183, 291, 292] for details on cell processes). In *L. variegatus* it has been previously suggested that while rhabdom synthesis (dark-adaptation) at dusk occurs rapidly (~30 mins), rhabdom shedding (light-adaptation) at dawn happens more slowly over several hours [201].

The partially widened rhabdoms of daytime dark-adapted *A. tangeri* eyes (measured in chapter 3) are likely to be a vestige of unfinished degradation of the night-state rhabdom at dawn. Some light exposure seems necessary to fully narrow the rhabdom to complete the light-adaptation process in the morning. A similar delayed and incomplete rhabdom shedding process was measured in laboratory-housed *L. variegatus* rhabdoms when they remained in darkness during the morning, instead of exposure to their usual light phase. However, eyes of this species fixed 30 minutes before the lights usually come on in their laboratory, still had very wide rhabdoms [314], exceeding even the night size reported in [182]. Only *after* laboratory "dawn" (06:00 am when lights usually switch on), did they begin to narrow to the daytime light-adapted size in crabs exposed to artificial lighting (and to a lesser extent in crabs maintained in darkness). In contrast, Arikawa *et al.* [165] found that *H. sanguineus* rhabdoms had already begun degradation 30 minutes before laboratory "dawn", being of a significantly smaller size than at night, with evidence of active pinocytosis. In both species of crab, the full rhabdom shedding mechanism took 2 hours or more to complete after lights on [165, 314]. Perhaps this timescale is more suited to the slower solar irradiance intensity increases of dawn in a natural habitat, than an abrupt switch-on of artificial aquarium lights.

In *A. tangeri*, light-adaptation processes appeared to have begun well before dawn with partial degradation of the wide nighttime rhabdom. At midnight it measured 18.4 ± 4.5 μm^2 in cross-section, but in a crab fixed ~2 hours before dawn (05:30 am) under a natural sky, the rhabdoms were already narrowed to 5.3 μm^2. Unfortunately, the weather that morning was overcast and perhaps as a consequence, there appeared to be little further narrowing over the next 4 hours. The individual fixed at 09:30 am had a 4.7 μm^2 mean rhabdom area, which is larger than the usual midday bright light-adapted rhabdom (3.3 ± 0.4 μm^2). The difference in weather and natural light conditions meant it cannot be known if the rhabdom had completed its light-adaptation by this time of day (2 hours after sunrise). It is possible that on darker days, the rhabdom stays slightly wider than on very bright days. Unfortunately, the bulk of the dawn rhabdom degradation process was missed, so we are no wiser on how long it takes. It appears to begin well before sunrise though, as in *H. sanguineus* [165]. To properly assess the rate of light-induced rhabdom shedding processes at dawn, this experiment should be repeated, ideally

collecting more samples from an earlier time (~03:00 am) until late morning, in case the rhabdom begins to widen many hours before dawn. Conducting the experiment under clear sky conditions would allow comparison with eyes fixed in other experiments of chapter 3. In addition, it would be interesting to measure changes in the rhabdom under controlled darkness to assess the circadian control element.

Suddenly exposing the dark-adapted eye to bright light at midday caused the rhabdom to narrow from an intermediate size to the typical narrow daytime diameter within 30 minutes. However, organelle presence in the TEMs suggest that the full process could take a while longer than this (Fig. 5.17). After 10 minutes, pinocytotic vesicles have filled the region directly surrounding the rhabdom, and can be seen within the cytoplasmic bridges of the palisade, through to the cell soma. Here, the vesicles are visibly incorporating into multivesicular bodies. The rhabdom has reached an advanced stage of degradation by 20 minutes and the microvilli look irregular in length and appearance, often very short. The rhabdom condition is not as poor as Arikawa *et al.* [165] described in *H. sanguineus*, when they were suddenly exposed to 15 minutes light exposure in the morning. The authors attributed the severe disorganisation and atypical degraded microvilli to the sudden shock of bright light. In fiddler crabs, sudden light exposure is something the eyes would experience daily, as the first burrow emergence of the day is often abrupt. Furthermore, their behaviours in the seconds that follow surfacing indicate that the visual system is immediately effective in bright light. This may explain why the microvilli in rhabdoms mostly maintain an ordinary appearance throughout the light-adaptation process.

By 30 minutes, the rhabdom appears to have regained a regular appearance, but pinocytotic vesicles can still be seen budding off from the microvillar bases and there is some fine granular material in some of the palisade bridges (and in place of one microvillus of the rhabdom, Fig. 5.17), suggesting an active transport process taking place. After 60 minutes, this is still visible to a lesser extent, along with a crowded cytoplasms full of organelles involved with cell recycling. The somas have started to clear by 120 minutes but pinocytotic vesicles at microvillar bases are still visible, which is surprising given the rhabdom had probably completed its diameter reduction ~90 minutes earlier.

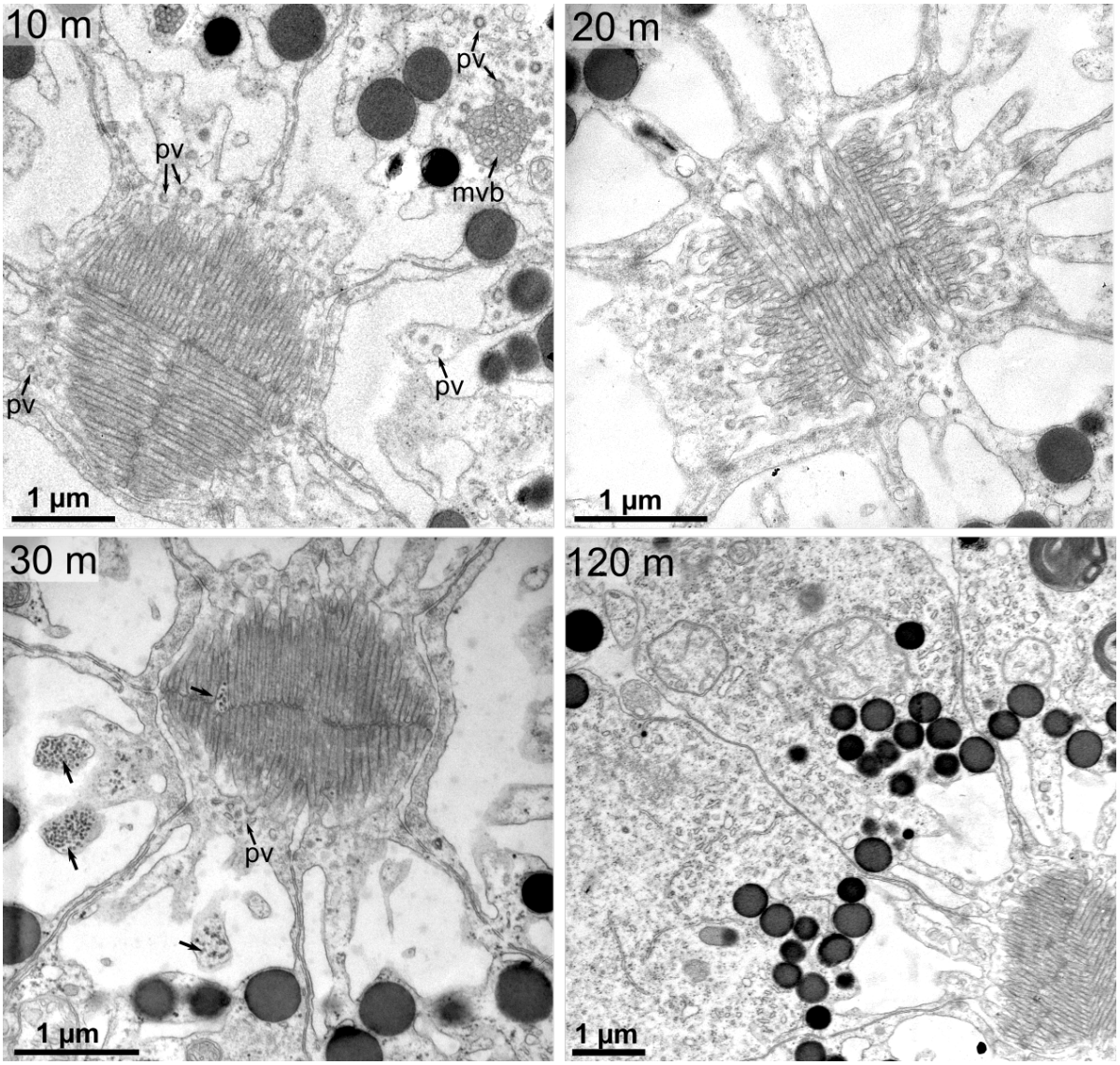

FIGURE 5.17. TEMs showing the rhabdoms of previously dark-adapted ommatidia after 10, 20, 30 & 120 minutes exposure to bright light at midday. After **10 minutes**, pinocytotic vesicles (pv) can be seen around the microvillar bases and in the palisade bridges, moving into the soma to be incorporated into multivesicular bodies (mvb). By **20 minutes**, this is at a very advanced stage and the microvilli are very short and irregular in places leaving large gaps between the palisade. After **30 minutes**, the rhabdom appears more regular, although evidence of active pinocytosis is visible and there are small granules in the palisade bridges (arrows) and even in the space where a missing microvillus projection should be, in the left side of the rhabdom. After **120 minutes**, the rhabdom appears typical of a fully light-adapted daytime state and cytoplasm has begun to empty of organelles.

To support the TEM evidence for lack of pigment migration in the eye in response to bright light, dark-adapted eyes were filmed with the ophthalmoscope while they were suddenly exposed to bright light. When this was replicated with *Drosophila melanogaster* (a fruit fly) using the same apparatus, the characteristic colour change that results from radial pigment migrations in the photoreceptors [166] could be easily observed within seconds (Fig. 5.18).

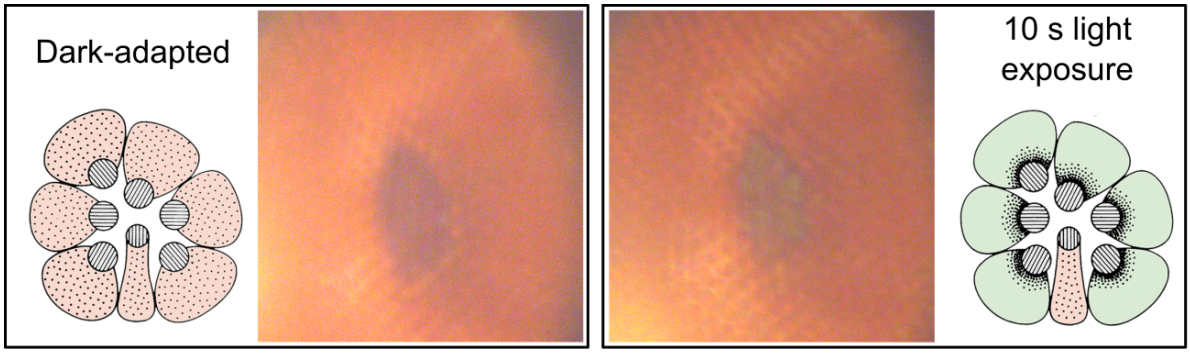

FIGURE 5.18. Ophthalmoscopic photographs of a *Drosophila* eye. In the left panel, immediately (~20 ms) after bright light exposure, the dark-adapted eye has a pseudopupil that appears dark red due to dispersed screening pigment granules in photoreceptors. In the right panel, the same eye is photographed again after 10 seconds of continuous bright light exposure. Green eye shine is visible in the pseudopupil due to migrations of pigment granules radially in towards the rhabdomeres. The same ophthalmoscope apparatus was used to collect these images, as for *A. tangeri*. Illustrations in each panel from ref: [166] show the corresponding pigment distributions (black dots) within the photoreceptors of an ommatidium in cross-section.

Exposing dark-adapted *A. tangeri* eyes to light for 10 seconds resulted in no change in deep pseudopupil diameter or appearance with ophthalmoscopy (there was no change even after 5 minutes). Some change within this timeframe would be expected if radial pigment migration had occurred, as in mantis shrimp where these take 2-5 seconds [236]. Therefore, this provides further evidence for lack of pigment migrations as a fast physiological response to bright light.

5.4.4 Contrast sensitivity on exiting the burrow

The results of the optokinetic response experiment do not closely resemble the null (H_0) or experimental (H_1) hypotheses (Fig. 5.4), but show features of both. Fiddler crabs that had been dark-adapted for 1-15 minutes produced a high number of optokinetic responses, almost equal to the fully light-adapted crabs, implying that a short period in the burrow does not impair contrast sensitivity on surfacing. Overall however, the results indicated that contrast sensitivity in bright light deteriorates gradually with time spent in the dark, particularly during periods of 15-60

minutes. This decline in contrast sensitivity is presumably due to dark-adaptation processes in the eye increasing sensitivity to dim light, which result in over-excitation or oxidative stress in the photoreceptors, or even temporary blindness when the crab later returns to bright light [153, 290]. After ~1 hour, adaptation processes seemed to have reached completion and there was only a minor reduction in responses with further time spent in darkness. It is worth noting that many of the dark-adapted crabs that produced very few OKR responses, tended to clean their eyes more when they were taken out of the dark and most only began to respond with OKRs towards the end of the 30 second period. This suggests that the visual system becomes overwhelmed and ineffective at first (perhaps eye cleaning is a reaction to poor visual ability), but very soon adjusts to enable vision in bright light.

There was a significant difference in responses of fully dark-adapted crabs (shown no light that day) compared to crabs adapted to dark for 2-3 hours. This difference is likely to be due to a partially widened rhabdom in the former group, left over from the night. TEM data suggests that the rhabdom stays narrow during daylight hours after it has fully light-adapted in the morning, even after 3 hours in near-darkness. The optokinetic response data were noisy and unlike the trial experiment conducted the previous year, some of the fully dark-adapted crabs (expected to produce very few responses) were able to follow the stimulus grating fairly well. I believe that this is because a drum of larger diameter was used in the trials, although the grating bars remained the same angular size (6 degrees) on the stimulus. This meant that in the present experiment, crabs were closer to the stimulus and small imperfections on the paper (e.g. creases or seams between sheets) may have become resolvable to the crabs, providing some higher-contrast texture cues. Ideally, presenting stimuli using a projector or monitor would prevent these problems. However, it is difficult to reproduce the high light intensities experienced under bright sunlight with that apparatus.

Anatomy data suggest that any optical sensitivity increase occurring after 15-60 minutes spent in dim light is unlikely to be due to physiological changes such as pigment migrations or increases in rhabdom volume or acceptance angles. Therefore, the change in visual performance in bright light over this period is likely to be on a neurological or biochemical level, not visible with histology preparations. In the previous chapter, it was demonstrated that the fiddler crab *G. dampieri* increases absolute sensitivity in dim light during daytime using temporal summations. Therefore, this strategy may also explain the "unseen" changes in absolute and contrast sensitivity that occurred over time in *A. tangeri*.

Although it was not investigated as part of my study, there is also the possibility of spatial integration occurring in the dark-adapted fiddler crab. This would reduce the ability of the crab to resolve fine spatial frequencies in dim light. Although it is unlikely that it would have affected ability to detect the relatively wide 6° bars of the stimulus grating used at my experimental rotation velocity, the increased light-gathering power that the spatial integration achieves may be responsible for over-saturating the visual system in those first few seconds of bright light

exposure. Motion detection and optomotor responses in the crab are thought to be controlled by lobula plate tangential cells [315, 316], in the same way as insects. These motion detection cells can be remarkably sensitive, responding to single photon detection in fly photoreceptors and allowing optokinesis in very dim light [30, 317–319]. This is thought to be at least partly due to spatial summations [30, 35, 199, 318]. Nalbach [303] describes a parallel system of three different velocity-tuned eye motion channels in the crab *Carcinus*. The channel tuned to very fast movements habituates very quickly, whereas slower stimulus velocities (within the range used in my experiment) maintain a optokinetic response "memory". Low light intensities reduces gain of the optokinetic response with greater delays but there is no change to the motion detection system. In *A. tangeri*, we cannot rule out spatial integration as an additional mechanism to cope with dark periods, which then result in a short initial over-saturation of the visual system when returning to bright light.

Results of the behavioural and ERG experiments discussed earlier indicate that dark adaptation processes gradually increase sensitivity over several minutes in daytime. Temporal summations occur when voltage-gated potassium channels (K_v channels) in the photoreceptor membrane become less active, which reduces the conductance of the membrane and filters out fast signals, whilst favouring and amplifying slow ones [191, 320, 321]. While the mechanisms have been studied in locusts, flies and horseshoe crabs [192, 282, 320, 322–325], there is little on the topic for crustaceans. At night, circadian clock-mediated serotonin release plays an important role in slowing temporal resolution to boost absolute sensitivity in locusts [282]. However, questions remain regarding how dynamically and rapidly the eye of fiddler crab (or any arthropod) can switch between fast to slow strategy vision, with extreme light and dark exposure during daylight hours. Results of experiments in this chapter suggest that the process of altering photoreceptor membrane conductance is gradual, taking many minutes. Researchers testing temporal properties of *Bombus* bee vision also noted that long periods of dark-adaptation (they suggested 30-60 minutes) are required for the visual system to produce the single quantum bumps usually measured in a *deeply* dark-adapted state [273]. Similar questions remain for any spatial integration mechanisms, as the presence of this mechanism is, so far, unknown in the fiddler crab.

5.4.5 Conclusions

The fiddler crab eye is likely to begin light-adaptation processes hours before dawn and the animal's first emergence into bright light from the burrow. The rhabdom, already partially narrowed, is able to reduce from its intermediate diameter to the fully narrow daytime tract in around 30 minutes on bright light exposure. After this, cell processes involved with membrane shedding and recycling appear to be ongoing for 2 hours or more in the soma, as in *H. sanguineus* and *L. variegatus* [165, 314].

Extensive microvillus membrane synthesis associated with dark-adaptation during sunset can fully widen the rhabdom within an hour, but only after onset of darkness. This is due to circadian

organelle processes in late afternoon preparing the photoreceptors to undertake this daily feat. During daytime, when the photoreceptor soma is relatively empty, even long periods of dark-adaptation have little or no effect at all on rhabdom volume. Comparing organelle presence and rhabdom appearance to other previously studied crabs, there appears to be a taxonomic difference in the cell processes involved with rhabdom widening. The fiddler crab *A. tangeri*, resembles *H. sanguineus* more closely than *L. variegatus* due to lack of total rhabdomere disassembly at dusk, although there was evidence of some similarities with both species [165, 314]. Acceptance angles also increase dramatically after sunset in the first hour of dark-adaptation, whereas they stay relatively narrow during daytime. The crystalline cone aperture size may be a direct reflection of the rhabdom diameter, to which the cone cell tips are connected.

The lack of physiological changes during dark-adaptation in daytime did not prevent increases in absolute or contrast sensitivity from occurring for optimising vision in dim light. This was demonstrated by behavioural tests with *A. tangeri* and an ERG test with *G. dampieri* (assumed to have similar eye physiology and adaptation strategies). This boost in sensitivity is likely to be due to temporal (and possibly spatial) summations, which appear to take several minutes (perhaps up to an hour) in dark conditions to take full effect. The process of switching cell membrane conductance from fast to slow is mediated via K_v channels, but little is currently known about how fast this happens.

Optokinetic responses under bright sunlight after various periods adapting to darkness (as if in the burrow), suggest that periods of up to 15 minutes spent in the burrow do not compromise contrast sensitivity, which remains optimised for bright light vision immediately after surfacing. However, it becomes poorer after the crab has spent 15 minutes or more inside. However, as many animals regained ability to follow the grating towards the end of the 30 second experiment time, it suggests that light-adaptation processes (such as switching back to fast temporal resolution) to enable bright light vision are rapid. This is in accordance with observations of their natural behaviour when exiting the burrow. They can confidently leave the safety of the burrow entrance after less than 1 minute on surfacing after long periods underground, whilst effectively monitoring the bright scene for predators.

CHAPTER 6

INFLUENCE OF BIOLOGICAL CLOCKS ON FIDDLER CRAB ACTIVITY

This chapter contains two sets of observational data collected during fieldwork trips alongside my main experiments. The first was devised after observations made during behavioural ball "treadmill" experiments (refer to apparatus in section 4.2.1, used in chapters 4 and 5). Those experiments required tethered fiddler crabs to walk across the top of a ball, that rotated below them. On perception of a simulated object looming towards them, the crabs responded reliably by freezing still for several seconds before resuming their walking. The majority of the time, this worked well and they walked for the duration of their tests without stopping much between stimulus presentations. Occasionally though, within a period of time on a given day, I found that many of the crabs would be very unwilling to walk, sitting still on top of the ball for the duration of the test. On a couple of days, the crabs were so inactive that I had to completely abandon my experiments for the day. Here, I explore some reasons for these frustrating and seemingly random collective changes in temperament by monitoring their spontaneous locomotor activity over tidal cycles in a laboratory setting. Secondly, I provide some evidence of foraging and courtship behaviours at night among the fiddler crab population on the El Rompido mudflats.

6.1 Introduction

6.1.1 Background

Using behaviour as a response variable, one must contemplate all the possible factors that may affect the likelihood of a response, outside of those that are easily controlled experimentally. Many animals possess biological clocks with which to predict solar (24 hr) and lunar (24.8 hr) cycles, that shape the rhythms of their own activity [326, 327]. These "clocks" are biochemical oscillators

that auto-regulate via feedback loops [328]. They help to coordinate automatic rhythmic changes in animal physiology or behaviour. Animals living on intertidal wetlands are exposed to a complex environment of cyclical changes in habitat desiccation, salinity, temperature (of water and sediment), pH, dissolved chemicals, oxygen availability and light etc. Some of these factors can vary by extremes over a few centimetres or minutes. Predictions of environmental changes could be imperative to survival.

Fiddler crabs, being ectothermic, are highly dependent on external temperature to allow the metabolic rate necessary for locomotor movements [217, 329]. Wolfrath [217] counted numbers of *A. tangeri* crabs twice weekly throughout 16 months in 1989 and 1990, on the Ria Formosa mudflats, Portugal (a site ~100 km west along the coast from El Rompido). She reported an absence of surface activity in December, January and February and stated that a surface temperature of >18°C is necessary for this species to leave the burrow to forage at low tide.

Another such consideration for an intertidal animal is an autonomous tidal rhythm of activity. Fiddler crabs spend at least half their time relatively motionless in a burrow while the tide is high and during cold nights. During diurnal low tides, they become very active, feeding and interacting with one another on the mudflat. There have been several accounts of nocturnal activity in *A. tangeri* by those who have studied them [111, 216, 217]. During visits to El Rompido during this project, I also observed the crabs actively foraging on the mudflat in the dark. This led to the hypothesis explored in previous chapters, that their visual systems adapt effectively to see in dim conditions at night. Alternatively, they may risk foraging without useful visual information, with fewer avian predators in pursuit.

Bennett *et al.* [209] were first to demonstrate that the fiddler crab *Gelasimus pugnax* (previously *Uca pugnax*) maintained rhythmic surges of increased activity under constant laboratory conditions. These coincided with the low tide times of the shores from which they were collected. Their semidiurnal peaks of high activity remained closely matched to the tides for around a week, after which time they became less pronounced and began to align themselves with lunar zenith and nadir. They also noted that activity was highest on average during the mornings of each day (06:00 – 12:00), suggesting a preference for diurnal activity. Since this study, there have been many others that demonstrate that fiddler crabs [205–208], among intertidal animals from nearly all major groups [326, 327, 330] possess tide-associated and circadian patterns of activity, which can persist for weeks or months in laboratories lacking natural cues. Myself and other researchers who have conducted experiments testing aspects of fiddler crab vision [55, 331], have remarked on their reduced behavioural motivations and locomotive activity during high tides. This could significantly influence the results of a behavioural experiment and deserves consideration.

6.1.2 Aims and hypotheses

The fiddler crab *A. tangeri* has been the study species of choice for many researching aspects of crustacean vision [37, 54, 68, 95, 103, 111, 216]. In my own experiments I took advantage of their distinctive freeze response to a looming visual stimulus. During trial experiments crabs showed differences from time to time in their responsiveness to handling, attempting escape from their holding containers, and most crucially, the extent to which they walked on the treadmill used in behavioural experiments. Lower activity seemed to coincide with the high tide times of the shoreline from which they had been caught a day or two previously. Therefore, this led to the present investigation testing the effect of tidal cycle, temperature and light/dark phase on locomotor activity levels in *A. tangeri*. The animals were monitored with time-lapse photography for a week, which is the maximum duration an individual subject is retained in the field laboratory before release. This meant that, although they were not exposed to tidal cues, solar illumination and temperature cues were present.

I also aimed to provide additional evidence to demonstrate that there is spontaneous foraging activity during dark nights among the population of *A. tangeri* fiddler crabs on the mudflats in El Rompido, used throughout the investigations of this project. Video footage was collected of the crabs active on the mudflat surface after sunset during summer months.

6.2 Materials and Methods

6.2.1 Activity monitoring in the laboratory

This study took place between from 10 - 17 May 2018 at a field laboratory a few hundred meters from the mudflat habitat of the fiddler crabs in El Rompido, Spain. Eight male *A. tangeri* crabs were collected on 10 May at ~18:30 during low tide. At 21:00 they were separated into transparent round plastic containers filled with 1-2 cm depth seawater and some paper towel that they could walk over or hide under as refuge. They were periodically given fish flake food and clean seawater when necessary, but only in the 2 hrs of non-recording periods between high and low tides. The rest of the time they were left undisturbed below a digital timelapse camera (GoPro Hero5, San Mateo, USA). The crabs were not completely isolated from one another as they were placed side-by-side in transparent containers, allowing transmission of visual and seismic cues.

The crabs were photographed from above every 2 minutes for just over seven days (22:56 on 10 May to 13:15 on 17 May) producing a time-lapse series; see Fig. 6.1a for an example image showing the apparatus. The crabs were housed indoors to minimise, but not eliminate temperature declines below 18°C. A digital thermometer recorded temperature constantly from an uninhabited plastic container with 1-2 cm seawater, placed next to the crabs (just out of view in photo). They received natural solar illumination from a large full-length window screened with light-diffusing film to disperse strong sunlight or shadows across the experimental area. The laboratory remained unlit by artificial lights throughout, however at night, a dim red lamp with sensor to detect low light levels switched on automatically to illuminate the crabs from above. The emission spectrum for this lamp peaked at 632 nm (Fig. 6.1b), which is at the extremity of their spectral sensitivity [37]. If detectable at all, it would appear as a very dim light to their visual system. This lamp, along with automatically adjusting exposure time on the camera, allowed successful imaging of the crabs throughout a 24-hour light cycle with minimal stimulation of their visual systems.

The data were analysed by comparing sequential time-lapse photographs using a binary scoring system, which identified whether the crab had moved (score 1) or not (score 0) within the 2-minute interval between photographs. Very slight movements (e.g. a slight change in claw position but no overall body/leg movement) were scored as 0 because the crabs were not always completely still during periods of inactivity. Temperature in each photograph was recorded via the thermometer in view and the stage in light cycle (day, night, sunrise, sunset) was noted.

Statistical analyses were performed with R software (version 3.5.1; http://www.R-project.org/) and the package “lme4” [257]. A generalised linear mixed-effects model (GLMER) for binary responses was fitted to the data. Using Chi-squared tests, the model was simplified to a minimal working model by analysing the statistical significance of each of the variable terms, including lighting conditions, water temperature and tidal cycle.

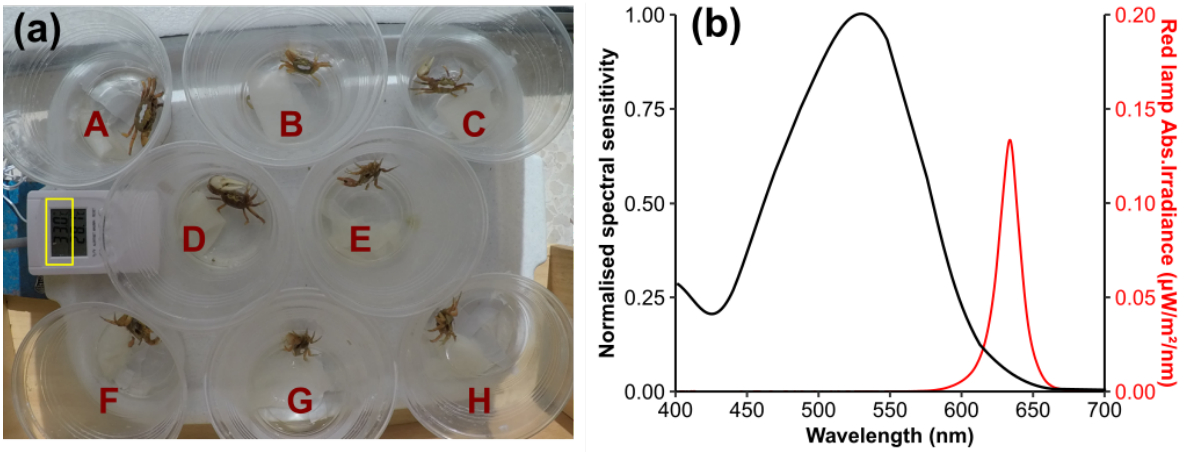

FIGURE 6.1. **(a)** Example image from the time-lapse data showing the experimental set-up in daylight hours with the eight crabs labelled A-H in their separate pots, alongside a thermometer displaying water temperature inside yellow box (from another pot just out of view). **(b)** Normalised spectral sensitivity curve for *A. tangeri* from ref: [37] (black) and the emission spectrum of the dim red lamp used to illuminate the experiment for the camera at night (red curve).

6.2.2 Nocturnal activity on the mudflat

On 9 August 2018 near the end of the annual breeding period, some video footage was obtained using a video camera (Sony HDR-SR11E) with inbuilt near-infrared (NIR) light, invisible to both humans and crabs (see Fig. 6.2 for emission spectrum). The camera was directed at fiddler crabs on the mudflats at El Rompido, to provide some observational evidence of visual signalling (waving) among the male crabs during and after sunset in dim light. Their behaviours were recorded until 22:00 local time, 33 minutes after sunset [332].

In late September 2019, further attempts were made to obtain some quantitative data on the number of crabs active on the mudflat as a function of time while light levels declined during evening low tides. The same NIR video camera was used as the previous year, but unfortunately, the video quality obtained was poor because the NIR lamp on the camera was not bright enough to sufficiently illuminate a large area of the mudflat. The lamp produced a small (<1 m^2) bright spot in the centre of the image but the edges were too dark to see the burrow entrances or crabs.

After several evenings of failed attempts marking out sample areas with quadrats, which disappeared from view as the sun went down, I settled for a few close-range sequences of small areas. The camera was mounted on a tripod and positioned over a 0.5 m^2 area of mudflat containing several burrows in view. This was set up as quickly as possible to minimise disturbance of the nearby crabs. The area was then vacated, leaving the the video to record the crabs to emerging from their burrows undisturbed.

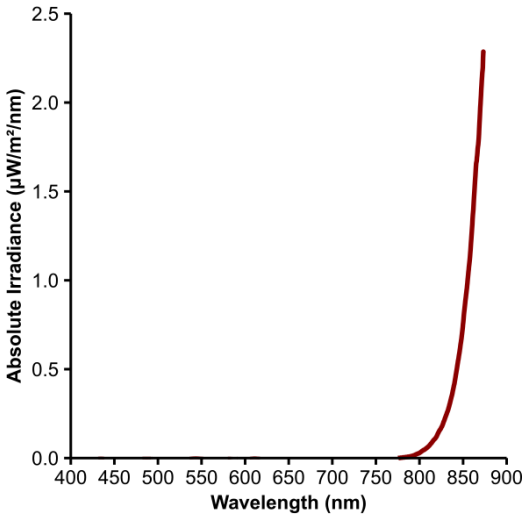

FIGURE 6.2. Emission spectrum of the near-infrared lamp on the video camera used to illuminate the mudflat and crabs during filming at night in the natural habitat.

The results presented (section 6.3.2) are from the sequence filmed latest after sunset, between 22:24 and 22:38 local time on 28 September 2019. Still images from the video (frame rate = 25/sec) were sampled every 300 frames (12 sec apart) producing an image stack. From these, all visible burrow entrances were marked out and a point was plotted on the position of visible crabs in each image, overlaid as a Scalable Vector Graphic, producing a position track (coloured differently) for each individual crab.

Decreases in light levels over the mudflat during the dusk period were measured over the four consecutive evenings prior (24 to 27 September 2019) via an optical fibre with 600 nm diameter, held up in a fixed position above any equipment or persons to sample sky irradiance. The light spectra were measured approximately every 10 minutes with a calibrated High Sensitivity spectrometer (USB2000, Ocean Insight, Largo, USA) and integration times were adjusted between measurements. The precise sunset times of the region used in the analysis were obtained from an astronomical database [332].

6.3 Results

6.3.1 Patterns of locomotor activity

Dawn arrived at ~07:20 am and it was dark by ~22:05 during the week of this experiment. Weather conditions were warm and sunny all week and due to the eastern aspect of the window in which they were kept, temperatures increased fairly rapidly from ~17°C at sunrise, up to 30-35°C at ~11:00am. After this they decreased fairly rapidly again to settle between 20-25°C for the remainder of the light period. During the evenings and nights, cooling was very gradual and a minimum temperature of 16-18°C occurred just before dawn (Fig. 6.3).

During inactive periods, the crabs would often remain motionless for several minutes, or occasionally hours. During active periods they moved almost constantly, trying to climb the sides of their containers. There were some considerable individual differences in overall activity. Within individuals, activity was noisy and could be sporadic. Crab C moulted during the afternoon high tide on the 15^{th} May and remained quite inactive during the low tide that followed, but after that resumed usual activity again. Patterns appeared when the data for each crab were pooled and visualised as % activity per 2-minute (Fig. 6.3) or 30-minute (Fig. 6.4) time interval.

Fiddler crabs were more active during low tides than high tides overall (Fig. 6.5a). In the heatmap-style actogram (Fig. 6.3), low water periods spanning dawn and dusk, contain large proportions of orange/pink areas, indicating high % activity levels, particularly in the evenings. On the first two mornings of the experiment, the crabs were highly active during the cool early mornings, but on the following four days, % activity was very reduced in early daylight hours (~07:30 - 09:30), coinciding with daily temperature minima. Subsequent increases in activity appeared to follow the ambient temperature and light escalations of the morning (Fig. 6.4). After the sun set just after 22:00, temperatures declined very gradually. Most nights, the crabs became slightly less active after sunset. The high tide periods, spanning afternoons and nights, contain a much higher proportion of purple/blue areas in Fig. 6.3, signalling lower activity levels than at low tide. There was a distinct preference for diurnal activity, with long periods of collective inactivity during nocturnal high tides, when it was cooler. In Fig. 6.4 a V-shaped curve of activity occurred within high water periods, with minimum troughs that coincided with the high water mark or shortly after.

A general linear mixed effects model (glmer) for binary responses was fitted to the data, predicting fiddler crab activity as a function of time, including crab identity as a random effect. Three additional fixed effects were included in the maximal model and all terms produced significant results when a model without them was compared to the original one with a Chi-squared test. Tidal phase had a significant effect on crab activity ($X^2_{(1)}$=597.7, p<0.001). Light phase, scored as **(1)** night, **(2)** sunrise/sunset, or **(3)** day ($X^2_{(1)}$=11.137, p<0.001) and ambient temperature ($X^2_{(1)}$=588.4, p<0.001) also had strong effects on the activity of the crabs.

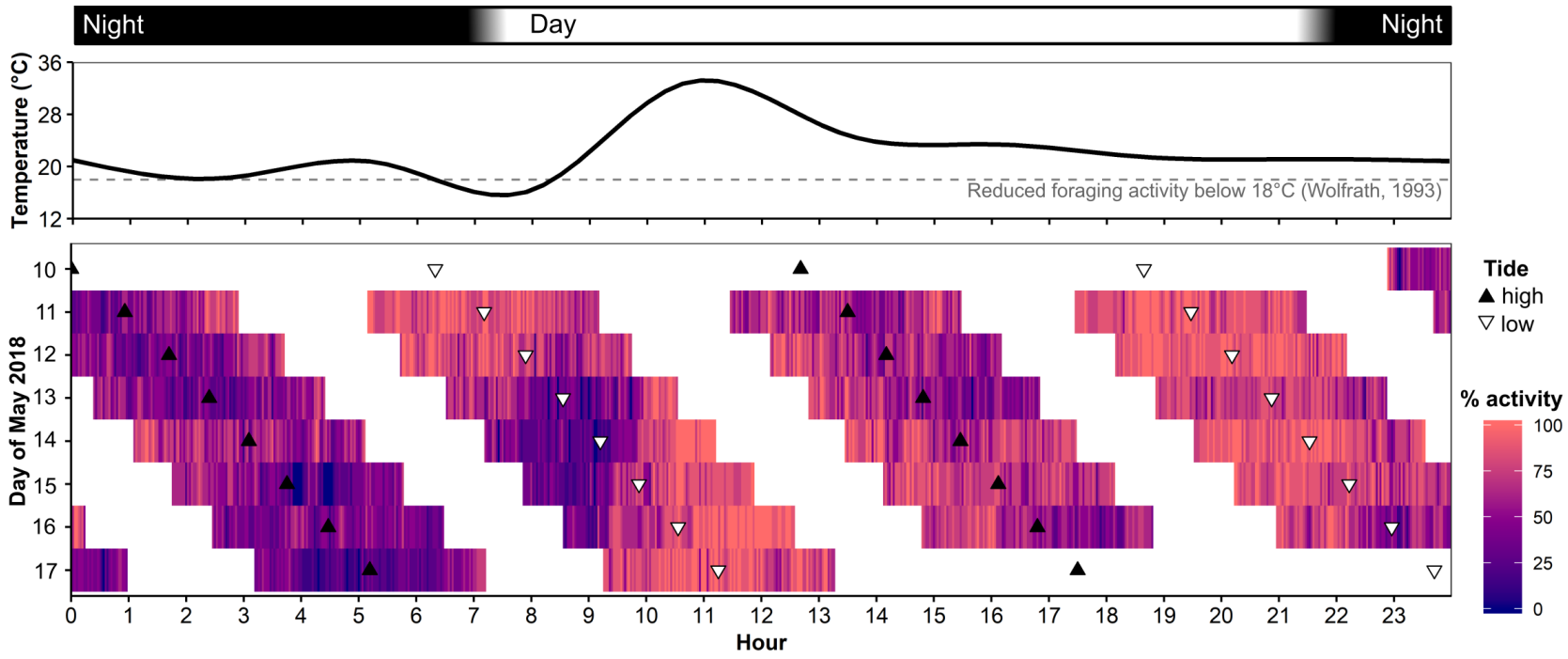

FIGURE 6.3. Actogram showing the percentage of *A. tangeri* crabs (n=8) that had been active within 2-minute periods as a heat map. These data span the seven days from 10-17th May 2018 and cover 2 hours either side of low and high water at the El Rompido mudflat from which they were collected (max and min water levels are marked by black and white triangles, respectively). Dark and light periods are indicated in the top panel and the mean water temperature over time within the experimental containers is shown below. A grey dashed line indicates the 18°C surface temperature threshold, below which activity is inhibited in this species [217].

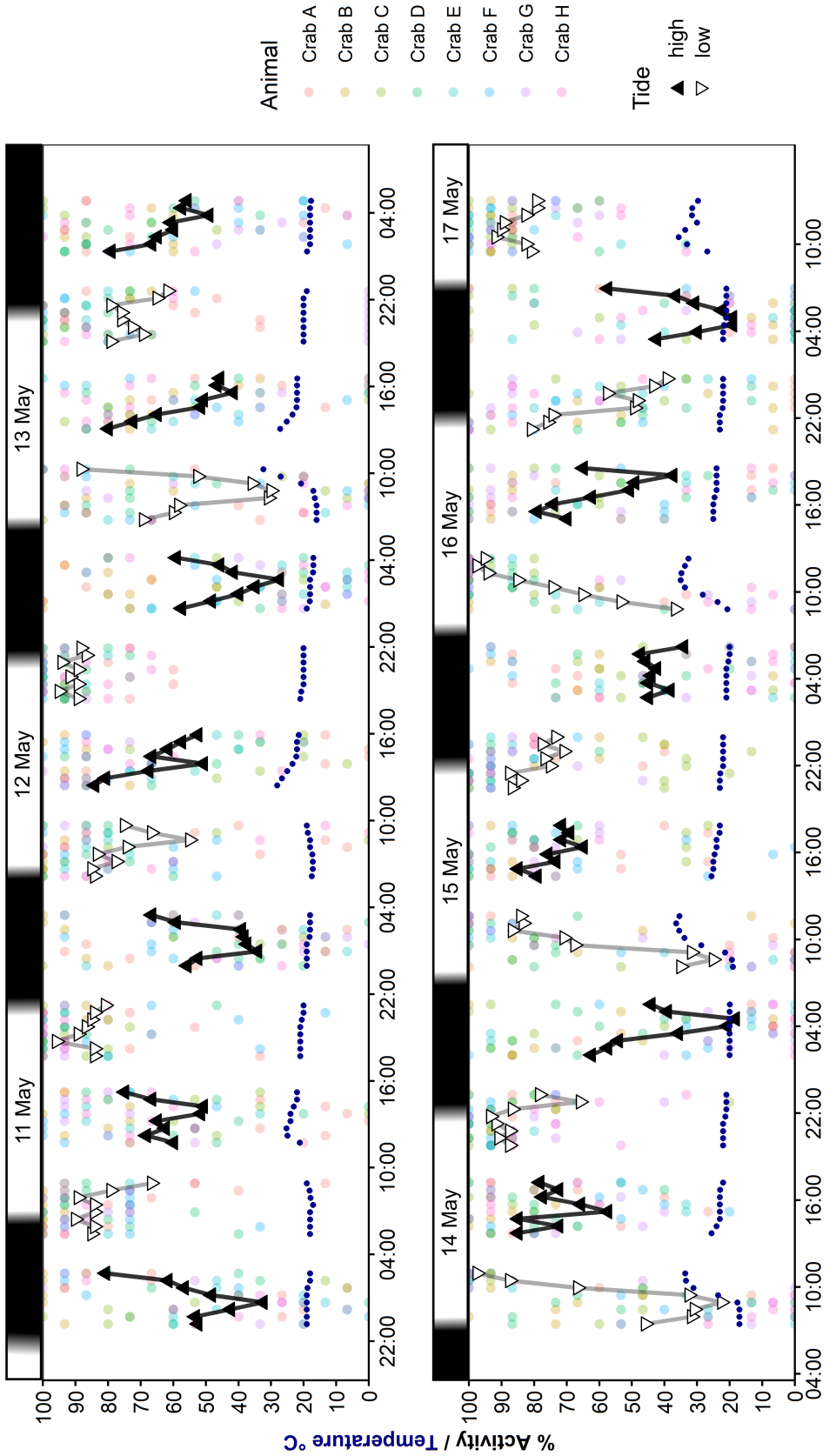
Animal
Crab A
Crab B
Crab C
Crab D
Crab E
Crab F
Crab G
Crab H
Tide
high
low
11 May
12 May
13 May
14 May
15 May
16 May
17 May
% Activity / Temperature °C

FIGURE 6.4.

⇐ FIGURE 6.4. Percentage activity pooled over a 30-minute period, with shaded circles colour-coded according to individual crabs. Mean percentage activity is represented by triangles spanning high tides (black), and low tides (white). Data span 2 hours both sides of low and high water at the El Rompido mudflat from which crabs were collected, over 7 days. Light/dark periods and date are shown above the plots. Mean water temperatures for each 30-min period are plotted as dark blue circles using the same 0-100 scale as the % activity data.

Summarising all the data (Fig. 6.5a), fiddler crabs were more active during low tides (mean 73.4 ± 19.2%) and daylight hours (71.0 ± 18.3%), than high tides (55.4 ± 16.4%) and nights (54.5 ± 18.3%). Temperature showed a weak positive correlation with % activity (R^2 = 0.18; Fig. 6.5b), but this was mostly due to a few high temperature points above 25°C from daytime low tides, so it is not possible to conclude that the high temperatures were solely responsible for the increased activity, as there is a strong direct interaction with time of day.

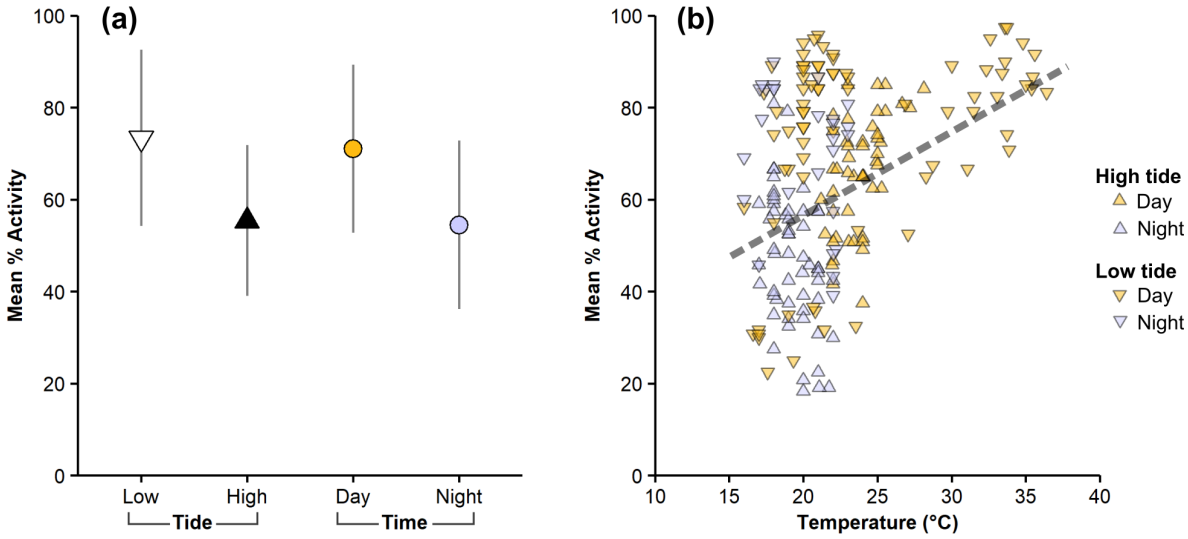

FIGURE 6.5. Summary of results. **(a)** Average % activity for all observations is shown by triangle symbols for high and low tides, while circle points show average values for day and night periods, with standard deviation bars. **(b)** Mean % activity of fiddler crabs, averaged by 30-min intervals, is plotted against ambient temperature. Symbols are shaped according to tide (high/low) and are coloured according to time (day/night). Grey dashed line shows a very weak positive correlation (y= 1.9x + 20.5; R^2 = 0.18), which appears to be influenced by a group of high temperature values that occurred during daytime low tides.

6.3.2 *Afruca* activity after dusk

Various photographs and frames of video sequences from 9 August 2018 depict high fiddler crab activity in dim light on the mudflat in El Rompido (Fig. 6.6). The observations demonstrate that my study population of *A. tangeri* are active at night, at least 30 minutes after sunset, if conditions are suitable. Many of the images show male crabs standing up on legs with the dominant cheliped in the air during a wave; a behaviour that continued along with tapping of the cheliped against the body, late into the evening. These white chelipeds appeared very conspicuous against the dark mud to the human eye and on camera.

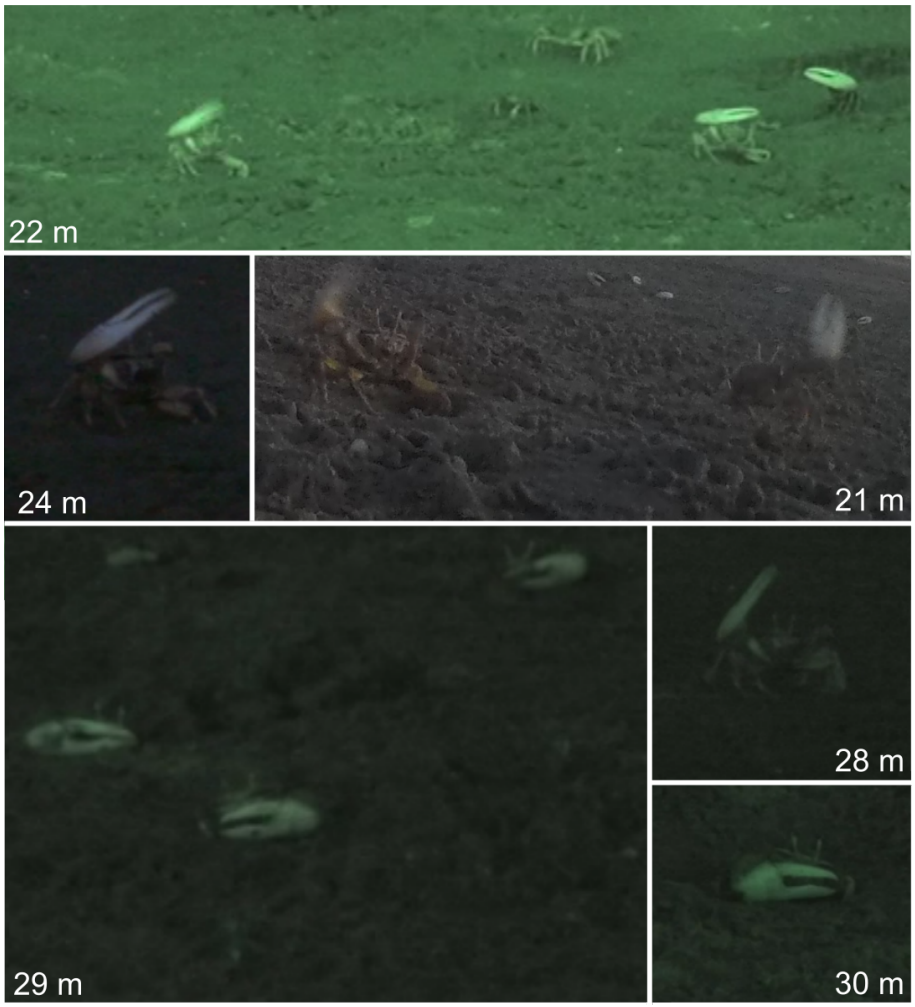

FIGURE 6.6. Frames extracted from video sequences of the El Rompido mudflat between 21:48 and 21:57 local time, on 9 August 2018. The images demonstrate the high activity levels of the crabs at various time-points after sunset, indicated in minutes (m), with examples of males performing waving displays. Near-infrared illumination from a video camera with which they were filmed was used on all video, except the photograph at 21 minutes, which was captured with a GoPro Hero5, blurred due to long exposure times.

Light level spectra measured during four consecutive evenings (24-27 September 2019) are plotted together in Fig. 6.7. Irradiance decreased by 7 orders of magnitude during the 2-hour period from 30 minutes before sunset, to 90 minutes after sunset. Measurements after this fell below the noise level of the spectrometer. The following evening, 28th September, fiddler crab activity was recorded on the mudflat. Courtship behaviours were no longer occurring at this time of year, but crabs remained active at night. On this particular evening there was a new super moon. Weather was clear and fine on all five evenings, with air temperatures >22°C.

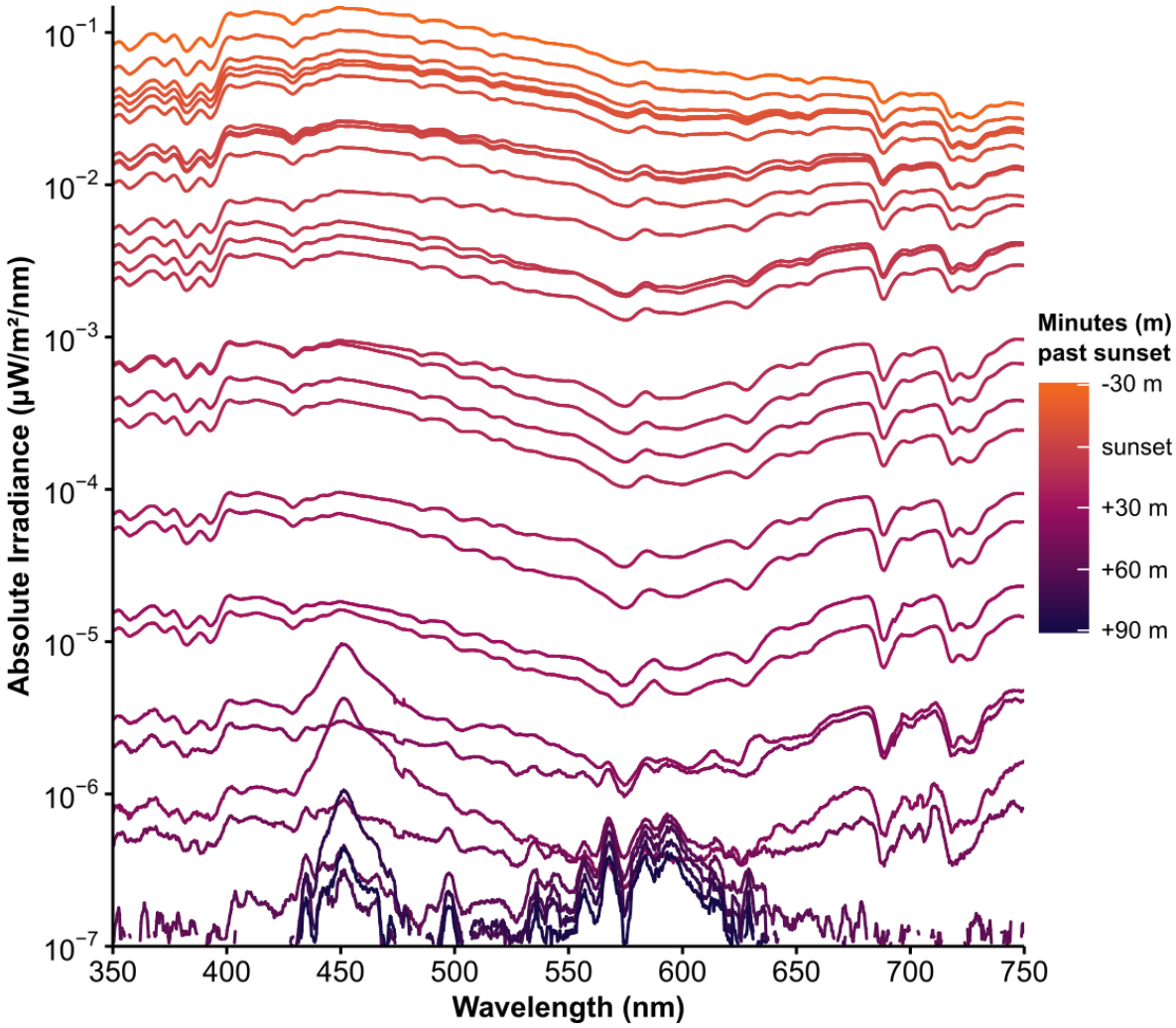

FIGURE 6.7. Spectra of light level declines on the El Rompido mudflat during dusk, measured from the sky over four evenings between 24 and 27 September 2019. Absolute irradiance on a $\log_{10}$ scale is shown for each wavelength in the visible spectrum. Line colour indicates the number of minutes that the measurement was taken before (-) or after (+) sunset.

From the nine burrow entrances inside the 0.5 m^2 sample area, six crabs appeared and their positions every 12 sec are marked by points of different colours (Fig. 6.8). The sun set at 20:17 and this 14-minute video sequence, started 2 hrs, 7 min after sunset at 22:24. The first crab emerged from burrow no.3 after just 26 sec from the video start, and the last to surface came up after 5 min, 6 sec. Four crabs (1,2,3,8) travelled some distance whilst feeding but stayed close (<30 cm) to their burrow. Two crabs (4,5) remained still in their burrow entrance and did not feed. Three crabs (6,7,9) did not emerge at all, but the absence of visible mud plugs sealing the burrows was noted. Therefore, in this small sample area and time-frame, two thirds of the burrow occupants were present on the mudflat surface after sunset when light levels were very low.

On an observational note, the fiddler crabs I encountered were uncharacteristically bold at night. When approached with torches, despite obvious visual and mechanosensory cues to my presence, they continued to feed until I was just inches away before running to safety.

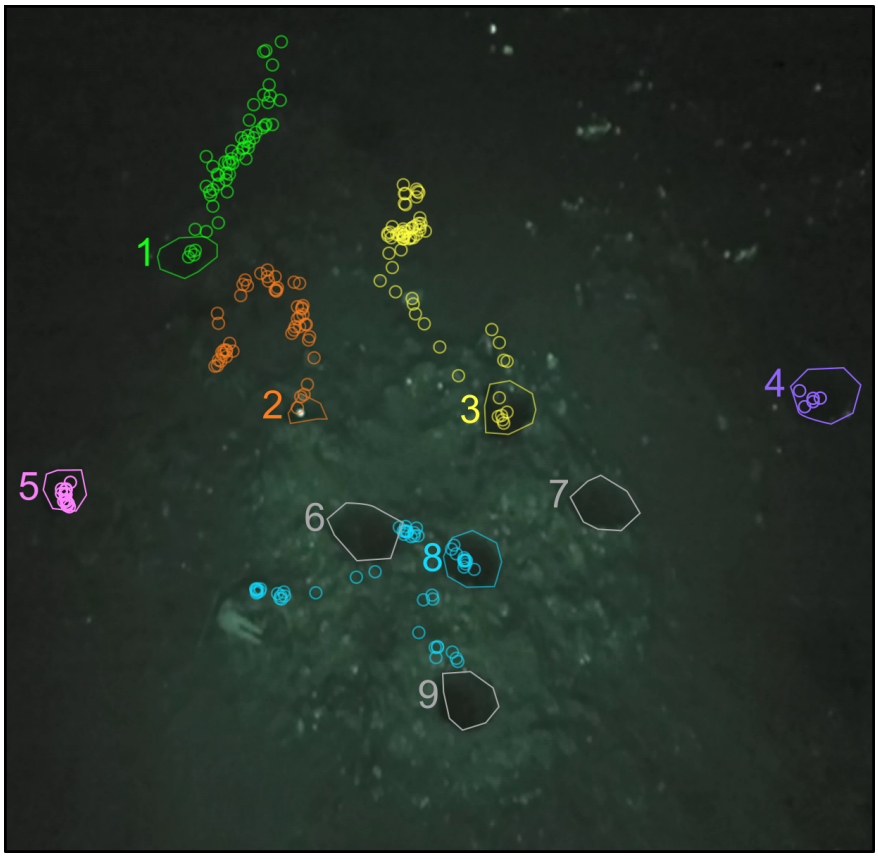

FIGURE 6.8. A frame from a video sequence of the mudflat is overlaid with outlines of nine *Afruca tangeri* burrow entrances. Points in different colours for each individual (numbered 1-9), mark the locations of fiddler crabs in video frames every 12 sec. The burrow entrances of three inactive crabs are indicated in grey. The video was recorded 2 hrs, 7 min after sunset, 22:24 - 22:38 local time.

6.4 Discussion

6.4.1 Tidal clocks in fiddler crabs

When pooled together, the patterns of laboratory activity observed in *A. tangeri* can be strongly linked to tidal cycles, as well as circadian light and temperature fluctuations. That they are so affected by tidal phase is not surprising, given that one of the most meticulously matched examples of tide-associated rhythms that exists was found in another fiddler crab species, *Minuca pugnax* [206, 209, 333]. This may explain the collective changes in general activity and responsiveness observed in the fiddler crabs during behavioural laboratory experiments.

Due to the complex nature of the oceans, their physical properties vary greatly with location and tidal cycles do not always follow a strict 12.4-hour period. Therefore, using positions of the moon and sun to predict tide amplitudes and timings is not straightforward [334]. In many places high tides do not coincide with the moon at zenith. Often the moon is not visible in the sky to an animal when it is below the horizon, or obscured by clouds, sunlight, water or substrate. Therefore, having an inbuilt clock to predict high and low water times is very advantageous to intertidal animals, allowing them to maximise feeding or mating opportunities effectively and to avoid predators, getting stranded or being washed out with tidal currents.

Researchers are beginning to understand the internal drivers for biological rhythms. For decades there has been a contentious debate about whether 12.4-hr tidal rhythms in crustaceans are a result of one or two biological clocks [335]. Some argued that the two peaks in activity per day are controlled by just one 12.4-hr circatidal clock [208, 327, 336, 337], and others gave evidence for the existence of two distinct circalunidian clocks with 24.8hr periods operating separately and in antiphase [330, 338, 339]. Both models fail to fully explain the experimental data and are based on pooled data from fiddler crabs under constant laboratory conditions [340]. Perhaps they vastly underestimate and oversimplify the task undertaken by individual crabs to survive in their complex and changeable habitats. This is a very interesting topic with individual researchers swapping sides over time from study to study, but in the interest of staying on topic it will not be explored further in this particular investigation.

Of all the cyclical changes experienced on intertidal mudflats, temperature may be the most limiting factor on fiddler crab activity, due to its strong impact on their metabolic rate [341]. In winter the crabs are exposed to minimum air temperatures of 5°C and in summer it might reach 33°C on the El Rompido mudflat [342]. In the present experiment, there were certainly increases in activity with warmer temperatures, but the crabs were not completely inactive during temperature minima of 16-18°C around dawn, as Wolfrath [217] suggested. The crabs likely experience cooler diurnal temperatures deep inside the burrow, than than on the surface [343]. So the temperature threshold for metabolic rate reduction causing inhibition of foraging behaviour, may be considerably lower than 18°C. At night, observational evidence shows that darkness does not appear to inhibit fiddler crab activity by itself. However, night is associated

with colder air temperatures, which may explain the relatively lower activity during the dark period.

6.4.2 Methodology critique

This experiment was designed to run for two weeks, but unfortunately due to camera malfunction a few days in, it had to be restarted (with new crabs). This meant that there was not enough time left to cover a full tidal cycle as planned. Unfortunately, this meant there is no data for activity while the tides were in antiphase with respect to the times in the first week. Ideally, new freshly-caught males would be used for week two, to control for the effect of habitation to the laboratory conditions and lack of tidal cues.

To more clearly identify the effect of tidal phase on activity levels, previous researchers controlled illumination and temperature during their experiments [206, 209, 333, 338, 339]. Using a dim red lamp or better still, a NIR-sensitive camera and lighting, activity could have been monitored in constant darkness and thermostat heating used to control temperature. However, for full representation of the conditions that crabs are kept for vision experiments, temperature and light were allowed to fluctuate naturally in the experimental arena, and had significant effects on activity. It is worth mentioning that in the week of this experiment, low tides spanned dusk and dawn coinciding with great changes in solar illumination; whereas light phase remained stable during high tides. Nevertheless, tidal phase was still shown to have a strong significant impact on activity in this experiment. For example, crabs were consistently more motionless during the warm afternoons at high tide, than they were for low tide periods before and after.

Fiddler crabs are highly social and forage in close proximity to one another at low tide, then spend high tides alone in the burrow. The crabs were not fully isolated, so their movements may have influenced each other. Separating them more effectively to eliminate visual or vibration cues from neighbours would make data from each individual more independent.

I considered automating analysis of the photo series using DeepLabCut [344], which uses machine learning to recognise the shapes of crabs in various positions and lighting scenarios. I found that their movements were often nuanced however (e.g. tucking in legs and claws or drifting in the water or sliding slowly down the side of the containers when stationary), which would prove too difficult to teach the software. Consequently, I opted for human analysis instead, randomising the order of sequences, to prevent knowledge of tidal phase creating researcher bias.

6.4.3 Nocturnal activity

The *A. tangeri* population on the El Rompido mudflats is indeed active at night. The footage demonstrates that the crabs continue to forage in the dark at least 2.5 hours after sunset when temperature remains above 22°C. A warm climate is an essential condition for nocturnal activity in fiddler crabs and is therefore restricted to the summer months [217, 340, 341, 343].

Wolfrath [217] and von Hagen [216] also described nighttime activity in *A. tangeri*, and Altevogt & von Hagen [111] related increased nocturnal activity in this species to new moon phases or moonless nights. Incidentally, there was a new super-moon at 20:26 on the evening of filming (28 September 2019), which may explain why they were active in high numbers that night. Two weeks later, when low water again coincided with sunset, but the moon was full, fewer fiddler crabs were foraging on the mudflats at night (personal observation), despite the similarly warm conditions. Fiddler crabs are known to synchronise reproductive events with new and full moons. These moon phases are associated with spring tides, which enhance tidal dispersion of their larvae [105]. However, the breeding season had already finished for the year, so a potential driver for high new moon activity could be increased foraging times due to extreme low tides, especially for animals living on the lower intertidal zone. Alternatively, moonless nights and new moons may provide protection from visual detection by predators under cover of darkness. On this note, the observation of more relaxed temperaments among the crabs in the dark had not gone unnoticed by the local people who prefer to capture them at night (personal communication). The males will occasionally lose a dominant claw to the local seafood restaurants. It would be very interesting to study the reasons for any nocturnal changes in decisions involved with predator avoidance and escape responses.

Courtship and mating in *A. tangeri* happens by night, as well as by day [216]. The footage on 9 August 2018 showed that male crabs continued their claw-waving behaviour for at least 30 minutes after sunset, perhaps suggesting effective vision in dim conditions. Waving only occurs during breeding months [217] and functions as a visual signal to attract females [50]. To the human eye at least, as the light fades, the brilliant white claws become highly conspicuous against the dark mud background [93]. Meanwhile, the rest of the body shows much temporal and spatial polymorphic variation within and between individuals, but relative to other fiddler crabs, is generally dull [54]. Perhaps signalling activity after dusk in this species has driven selection for a highly reflective cheliped with uniform white colouration, at a potential cost of increased visibility to predators.

Wolfrath [217] and von Hagen [216] described a switch in male courtship behaviours, from waving displays in daytime, to drumming the sediment surface with the dominant claw at night. I also observed this behaviour in increasing frequency as the light faded. Based on her observations of other fiddler crab species, Crane [50] suggested that drumming is likely to happen during all *A. tangeri* copulations, but is unseen inside the burrow during daytime. At night, with reduced visual capabilities, they shift to drumming outside to attract females toward their burrows via mechanosensory cues.

During daytime, about an hour before the sediment floods with an incoming tide, fiddler crabs are known to cease their foraging activities and remain motionless in their burrow entrance for several minutes; carapace to the sun [216, 217]. This behaviour was termed "posing" by von Hagen [216], the reason for it unknown. Before the rising water reaches them, the crabs plug

their burrows and remain inside for high tide. Less is known about this behaviour at night. Do they pose at the burrow entrance in the absence of warm sunshine in the dark? Two of the crabs did appear to pose throughout the video surveillance, remaining stationary in their burrow entrances. In addition, three of the burrows did not produce a crab on the surface, although they were not visibly plugged. Perhaps these crabs were still hiding after the disturbance caused whilst setting up the camera equipment. This disturbance and sudden appearance of the camera on its tripod, may also explain why these crabs took caution to remain very still within their burrow entrances throughout this short surveillance period.

Time constraints meant that returning to El Rompido to properly quantify nocturnal behaviours on the mudflats and explore the drivers behind them was not possible. Ideally though, this would be carried out with bright NIR flood lights to illuminate larger areas of the mudflat at low tide. Several NIR-sensitive cameras could record fiddler crab activity in 1 m^2 transects for the entire night from before dusk until sunrise, over several different nights. Analyses could be performed to relate these numbers to air temperatures, light levels, moon phase, time of year and weather conditions. During the breeding months, it would also be interesting to quantify the frequency of visual versus mechanosensory courtship signals by male fiddler crab chelipeds over time.

6.4.4 Conclusions

Afruca tangeri are active both diurnally and nocturnally at low tide on the mudflat. Foraging behaviour continues for at least 2.5 hours and visual signalling for at least 30 minutes on some nights, although further study is needed to learn how much longer this persists at night and what factors limit these activities (light levels, moon phase etc.). Temperature constraints are certain to limit nocturnal activity to summer nights.

In the laboratory, the data obtained in a week from eight *A. tangeri* individuals, plus many previous studies on this topic, provide a convincing argument that activity in this species is highly influenced by both temperature and tidal cycles. This persists even after several days or weeks of removal from natural habitats. Consequently, the possible effects of tidal phase must be considered in all experiments using locomotive behaviour as a response variable in fiddler crabs. For the treadmill behavioural experiments in chapters 4 and 5, this meant I included tidal phase as a fixed effect term in the statistical models used to analyse the results. In both cases, however, tidal phase was not found to have a significant effect on probability of responding to the experimental visual stimuli.

CHAPTER 7

LIGHT EXPOSURE AND POLARIZATION SENSITIVITY

This chapter contains an experiment designed to explore the effect of differing light exposures on the orthogonal microvillus bands in the rhabdoms of *A. tangeri* fiddler crabs. This side project began with an observation that rhabdom edges were always straight in dark-adapted eyes and often indented (with scallop-shaped or zig-zag edges) in light-adapted eyes. This chapter investigates the hypothesis that having shorter microvilli of a horizontal orientation is an adaptive response to strong reflective glare in their environment. The experiment had limited success, as some of the samples were not viable and there was little evidence of adaptive changes in response to polarized light. The results revealed, above all, some lessons on the nature of the rhabdom shape in three dimensions.

7.1 Introduction

7.1.1 Background

Polarization sensitivity is the ability to discriminate the electric field vector component of light [33]. Fiddler crabs, and many other crustaceans sensitive to polarized light, possess microvilli in the rhabdom of photoreceptors R1-7, that are arranged in highly ordered orthogonal rows, with horizontal or vertical orientation with respect to the visual horizon [19]. In fiddler crabs, the photoreceptors R1, R2, R5 and R6 contribute vertically-orientated microvilli, which can compare photon excitation levels with photoreceptors R3, R4 and R7, that contribute horizontally-orientated microvilli [89, 210]. This provides an opponent system with which to compare angle and degree of polarized light across their visual scene [19, 89]. Ability to detect polarization cues in the environment has been shown to be an important aspect of fiddler crab visual ecology [67–69, 111].

Fiddler crabs live in mudflat habitats that are rich in polarization contrasts [210]. The sky has a strong polarization pattern, which moves in relation to the azimuth of the sun [57–59]. Behavioural experiments have revealed that fiddler crabs use a polarised skylight compass to navigate [111, 345–347] and can also use the contrasts of relatively unpolarized objects against the polarized sky background to enhance detection of predators [67–69]. Sunlight reflecting off the waterlogged mudflats, with adjacent water bodies and streams, create strong reflections (Fig. 7.1) rich in horizontally polarized light [210]. Fiddler crabs themselves also reflect horizontally-polarized light from the shiny cuticle of their carapace, which may be involved with conspecific signalling [52].

FIGURE 7.1. Reflections of sunlight from the mudflats at El Rompido are rich in horizontally-polarized light creating a strong glare in the eyes of animals, such as fiddler crabs, living on its surface.

7.1.2 Biological polarizing filters

Anyone who has spent time near the sea on a sunny day will know how bright reflections from the water and tidal flats can be. Many people protect their eyes from this glare by wearing sunglasses with polarizing lenses to filter out the strong horizontal component. Some animals that live in environments rich in polarized light, have evolved optical strategies to filter and reduce strong horizontal reflections. A good example is the hemipteran *Gerris lacustris* (the common pondskater, or waterstrider), which spends its adult life as an active and fast-moving predator living on the flat surface of fresh water bodies, using its hydrophobic legs to walk over the water using the surface tension. This insect preys mostly on other stranded insects that fall onto the water surface, whilst monitoring for their own predators, that may appear from below the water. Strong sunlight reflecting off the water surface can affect the pondskater's ability to see through the

glare into the water below, potentially making it vulnerable to predators.

Gerris lacustris have ommatidia that are orientated dorsally (skywards), laterally and ventrally, down at the water (Fig. 7.2a) with an acute zone streak close to the eye equator [348], reminiscent of the fiddler crab. The open rhabdoms in the majority of the eye (dorsal and lateral), have eight rhabdomeres, four with vertically-orientated microvilli and four with horizontally-orientated microvilli (Fig. 7.2b), providing the typical opponent system to allow polarization vision. The ventral-most region of the eye, with view of the water surface below, shows some regional specialisation. The ommatidia have a different rhabdomere arrangement to the rest of the eye, whereby the proximal rhabdom lacks horizontally-orientated microvilli, meaning all are aligned the same way along the dorsoventral axis of the animal [211] (Fig. 7.2c). The ability to detect only vertically-polarized light in the ventral eye provides a useful filtering function for glare [211, 349]. The ommatidia with view of the water directly below have reduced ability to detect horizontally-polarized reflections from the surface, allowing a better view through the surface to facilitate detection of predators approaching from the depths [211, 350] (Fig. 7.2d). This "matched filter" may also enhance the contrast of stranded insects against the background water surface, rich in polarized reflections [211, 349, 350].

Alkaladi *et al.* [210] found a less extreme version of an inbuilt polarizing filter system in two Australian fiddler crabs, *Gelasimus vomeris* and *Tubuca signata* (previously in genus *Uca*). Instead of having ommatidia that lack structures sensitive to horizontally-polarized light, they found that the distal-most tips of rhabdoms in the equatorial eye have bands of horizontally-orientated microvilli that are thinner in terms of number of rows, than the vertical ones (Fig. 7.3a). After a short distance (~50 μm) these bands become equal in thickness for the rest of the rhabdom's length. The thickness of both bands increases gradually along its length from distal to proximal. They also noted that in the dorsal eye, the rhabdom is scalloped so that horizontal microvilli occupy around half the space as the vertical ones. Modelling photon absorption along the rhabdom, they proposed that these organisations across the eye tune the receptors to the degree and information content of polarized light in the visual scene.

As a side project, I decided to investigate whether *A. tangeri* employ similar strategies in their rhabdoms to reduce detection of high intensity horizontal reflections in their mudflat habitat. Preliminary investigations revealed that *A. tangeri* do not appear to have this distal region of shortened horizontally-polarized rhabdom bands. However, differences between light- and dark-adapted eyes were apparent in the shape of the rhabdom. The light-adapted eyes always have an indented edge to the rhabdom (refer to Fig. 3.13b in chapter 3). This is also prevalent in the dorsal eye of *T. signata* [210]), seemingly because of shorter microvilli in bands with horizontal sensitivity, although due to cutting angle in one plane only, this could not be confirmed. The eyes viewed in preliminary investigations were sectioned across the eye equator, the same as samples analysed by Alkaladi *et al.* [210]. Therefore, in the present experiment, the eye samples were sectioned at 90° to this, in a vertical (dorsoventral) plane to allow comparisons.

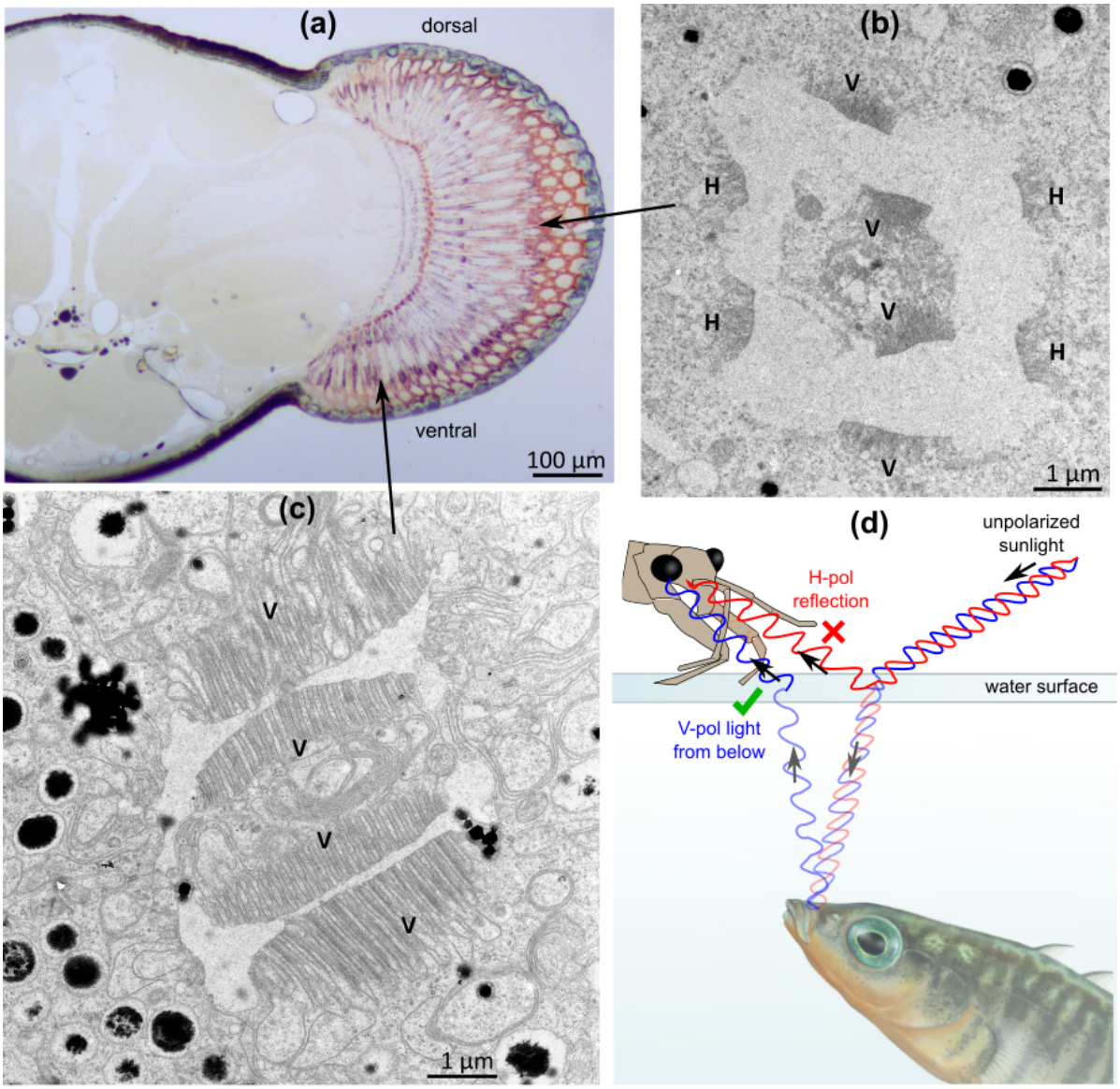

FIGURE 7.2. **(a)** Thick (1500 nm) unstained section through the head of *Gerris lacustris*, showing the beautifully pigmented ommatidia with dorsal, lateral and ventral view of the environment. **(b)** TEM of transverse section through an ommatidium in the lateral eye. The open rhabdom has microvilli with horizontal (H) and vertical (V) orientations, allowing polarization sensitivity. **(c)** The ventral eye has ommatidia comprised only of vertical rhabdomeres with microvilli in line with the dorsoventral axis of the head. **(d)** Illustration of *G. lacustris* on the water surface. Sunlight is strongly polarized in a horizontal plane when it reflects off the water surface, producing optical glare for this insect living on the surface. The photoreceptors in ommatidia of the ventral eye facing the water are not sensitive to horizontally-polarized light (as in **c**), and thus remove the glare component from their ventral visual system. This allows better sensitivity to vertically-polarized light passing through the water surface from below, allowing better predator detection.

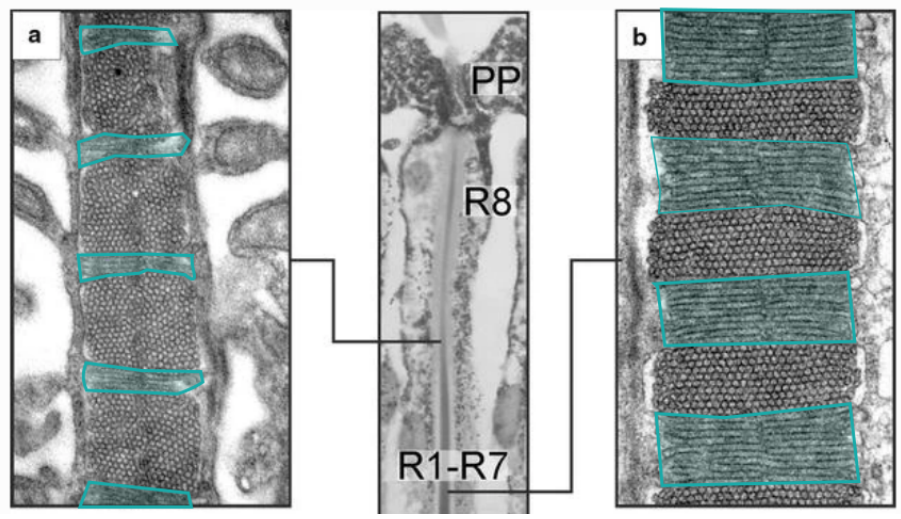

FIGURE 7.3. TEM showing distal R1-7 rhabdom organisation of the fiddler crab *Gelasimus vomeris*. **(a)** The initial section immediately following R8 has a smaller proportion of horizontally-oriented microvilli (blue areas) than vertical, due to fewer rows of microvilli per band. **(b)** A short distance proximally, the bands have become equal in thickness. A light micrograph of this region of an ommatidium is shown (centre) for location reference, with primary pigment cells (PP), R8 and R1-7 photoreceptors labelled. Figure adapted from ref: [210].

7.1.3 Aims and hypotheses

The difference in rhabdom shape between light- and dark-adapted eyes is likely due to pinocytotic processes. The bases of the microvilli bud off and shorten the projections in response to bright light [156, 164, 165, 181–183, 214, 291, 292]. The aim of this experiment was to test the hypothesis that *A. tangeri* disproportionately shorten microvilli in horizontally-sensitive photoreceptors when exposed to a strong degree of horizontally polarized light, as a filtering mechanism for glare, as proposed in *T. signata* [210]. This was achieved by exposing dark-adapted eyes to bright sunlight through horizontal-polarizing filter. A second group of crabs were adapted behind vertical-polarizing filter to test whether this would cause an increased shortening of the vertically-orientated microvilli, and smaller proportional area of these bands in the rhabdom. In addition to this, some crabs were exposed to bright unfiltered sunlight, or adapted behind neutral density filter with similar (but slightly lower) filtering power for overall intensity as the polarizing filter. This served as an approximate control. A fifth group of crabs remained dark-adapted.

While rhabdom band arrangements were examined and measured in dorsal and equatorial eye regions, the ventral part of the eye was not sampled as preliminary investigations revealed no indented rhabdoms or uneven banding patterns (also reported by Alkaladi *et al.* [210]).

7.2 Materials and Methods

7.2.1 Experimental design

Fiddler crabs (n=30) with carapace widths measuring 26-27 mm were collected from the mudflats at El Rompido on 6th October 2019. They were divided into five treatment groups, each containing six crabs (three male, three female), before being put into individual containers containing 1-2 cm seawater. They were placed in a darkroom at sunset (20:05) where they spent the night. The next dawn, without exposing their eyes to any light other than a dim red lamp (no wavelength emission below 600 nm), Groups 1-4 were prepared for their experimental treatment of 30 minutes light exposure.

Crabs to be exposed to horizontally or vertically polarized light were tethered below a horizontal bar using adhesive tape over the carapace. To maintain their constant alignment with respect to the horizontal or vertical incoming light, the eyestalks were also fixed with a dab of glue to a small wooden stick on their carapace, so that they remained in their natural upright position during light exposure. They also had their claws restrained with tape to prevent dislodgement and were positioned inside a light-proof box with an open front panel window (Fig. 7.4a). A polarizing filter was placed either in horizontal orientation **(Group 1: H-pol)** or vertical orientation **(Group 2: V-pol)** in the window so that sunlight passing through to enter ommatidia in the frontal eyes, had a high degree of polarization. The other two groups to be exposed to unpolarized light treatments were placed free-moving together in a bowl with 1-2 cm seawater with an open top allowing bright sunlight exposure **(Group 3: Bright)**, or with a neutral density (ND) filter above them **(Group 4: ND filter**). The ND filter was transmissive for 46% of light at each of the visible spectrum wavelengths (400-650 nm), which was slightly more transmissive than the polarizing filter, which transmitted 36% of total light in the visible spectrum when measured with a spectrometer (Fig. 7.4b). The final group of six crabs was maintained in a dark-adapted state **(Group 5: Dark)** and eyes from this group were dissected in the darkroom using dim red illumination only.

Starting mid-morning, the six crabs in Group 1 were taken from the darkroom and placed outside on the beach in their adaptation container for 30 minutes, to expose their eyes to bright light, initiating a light-adaptation response. The subsequent three groups leaving the darkroom were separated by 10 minutes to allow time for dissections (separate stopwatches were used to keep time). They were positioned south-east towards the sun to allow bright light to pass through the filters. After 30 minutes, they were transported back into the darkroom and their eyes were dissected into chilled fixative immediately using only dim red light to prevent further adaptation, before euthanizing. It was noted that some crabs in Groups 1 and 2 (H-pol and V-pol) appeared distressed having been out of water for 30 minutes. Once all eyes, including those of Group 5 (still dark-adapted), had been dissected and chilled in fixative for 2 hours in darkness, the eyes were further dissected away from the eyestalks using a dissection microscope.

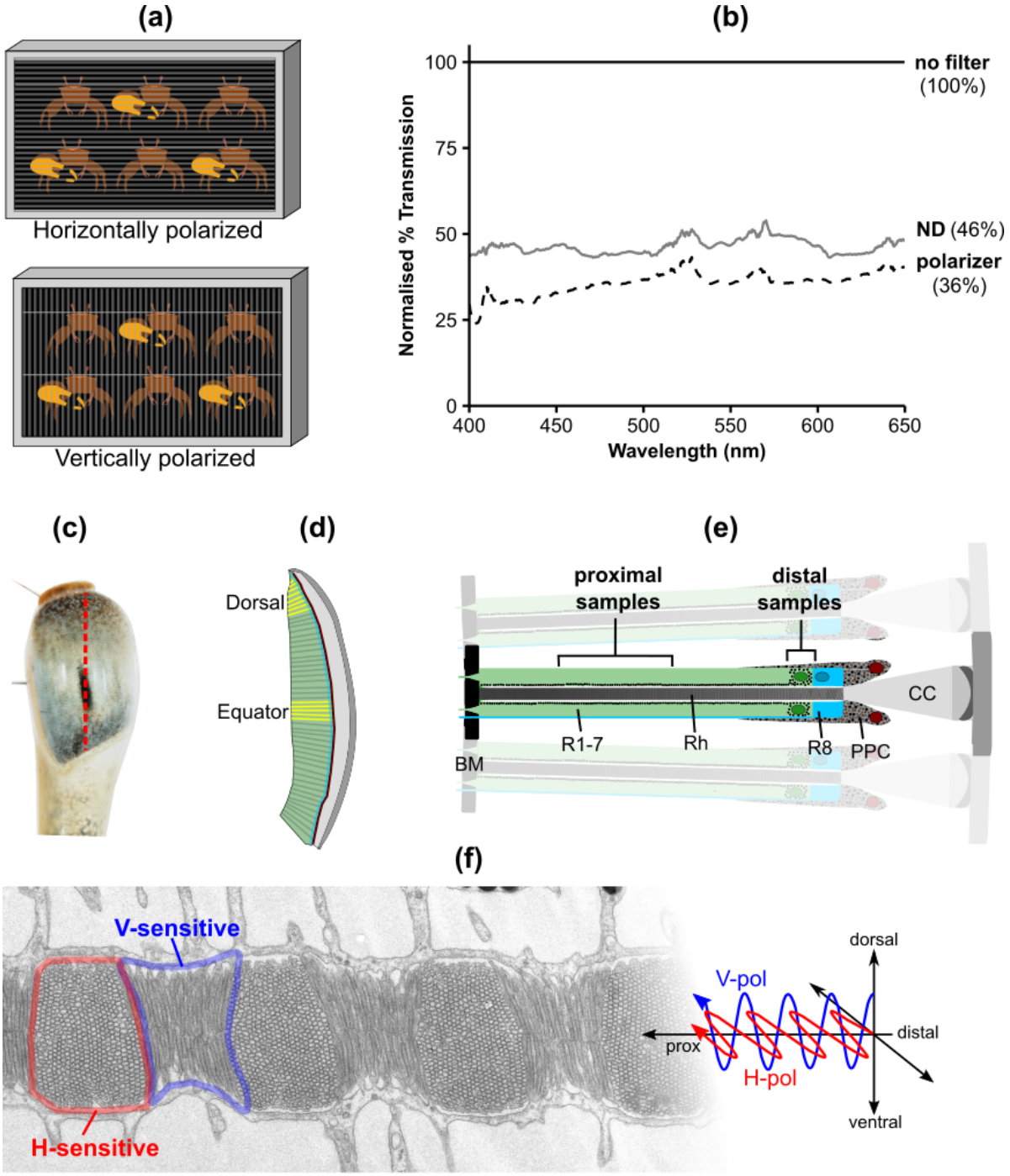

FIGURE 7.4. **(a)** Crabs in Groups 1 and 2 were tethered from the carapace with eyes fixed upright inside a box. The open front panel was screened with horizontal or vertical polarizing filter to maintain a constant angle and high degree of polarization exposure for the frontal eye. They were positioned outside on a beach facing southeast toward the sun for 30 minutes to adapt. **(b)** Transmission of light passing through the ND filter (grey solid line) and polarizing filters (dashed line) after normalising to a % of a measurement collected ..... (*continued on next page...*)

FIGURE 7.4. (*cont...*) from a controlled intensity light source with no filter (black solid line). Total % transmission across the visible spectrum normalised the no filter measurement is indicated in brackets. **(c)** Red dotted line shows the vertical (dorsoventral) axis along which the frontal eyes were sectioned. **(d)** Diagram of a typical eye section, with retina shaded green. Locations of sampled photoreceptors in dorsal and equatorial eye regions are highlighted yellow. **(e)** Diagram of an ommatidium showing approximate locations for sample TEMs along the rhabdom. Images were collected of the distal-most region of the R1-7 rhabdom (near cell nuclei) and a more proximal region of the R1-7 rhabdom, halfway along its length. **(f)** TEM of a rhabdom in longitudinal section showing the alternate bands of microvilli from photoreceptors R3, R4 & R7, sensitive to vertically-polarized light (blue), and the microvilli from photoreceptors R1, R2, R5 & R6, sensitive to horizontally-polarized light (red). A diagram shows the e-vector of vertically- (blue) and horizontally-polarized (red) light waves, with respect to the microvillus organisation as they propagate through the rhabdom.

Sample preparation for electron microscopy was carried out as described in chapter 2 section 2.3. Thin (70 nm) sections were cut vertically along the dorsoventral axis of the eye exposing ommatidia of the frontal eye, as this was the eye region directed toward the polarizing filter in Groups 1 and 2 (Fig. 7.4c). The sections were imaged with TEM, sampling 3-6 rhabdoms from four eye regions per eye using 2900x magnification. Ommatidia were sampled from both dorsal and equatorial eye regions (Fig. 7.4d). Rhabdoms were imaged in the distal-most region of the R1-7 photoreceptors by their nuclei, as well as proximally, around half way down its length (Fig. 7.4e).

7.2.2 Data analysis and statistics

Using in-built functions in Fiji-ImageJ software [213], the areas of at least 21 horizontal and vertical bands of microvilli on the images were measured (Fig. 7.4f) from at least three ommatidia per sample location. From these data, mean areas of horizontal and vertical microvilli were calculated per eye region, as well as proportion of the rhabdom consisting of horizontal microvilli (H-pol / H-pol + V-pol). Rhabdom diameter was measured across its widest horizontal band in each image. Statistical tests were performed using R software (version 3.5.1; http://www.R-project.org/). Rhabdom diameters and proportional area of horizontal microvilli in the rhabdom were compared across treatments using ANOVAs and pairwise TukeyHSD test comparisons.

A single equatorial ommatidium from a dark-adapted crab (in daytime) was imaged along its whole length with TEM, providing a continuous image of its entire rhabdom from distal tip at the crystalline cone interface, to basement membrane. Using Fiji ImageJ software, number of rows of microvilli were counted from horizontally- and vertically-sensitive bands at 22 different locations from the first (distal) row to the last. The data were compared directly to equivalent results from *T. signata* in ref: [210].

7.3 Results

7.3.1 Sample quality

Unfortunately, some of the samples could not be analysed and were excluded from the data set, including all Group 1 eyes exposed to horizontally-polarized light and three individuals from Group 2 (vertically-polarized). These crabs had probably spent too long out of water during the experiment and as a result of gill desiccation and stress, their eyes were not well preserved with very disordered rhabdoms with lysed membranes (showing signs of apoptosis, see Appendix Fig. A.4 for example). All other individuals produced good quality eye tissue although some had rhabdoms with loose microvilli, perhaps due to sudden exposure and adaptation to bright light, causing extensive membrane reorganisation [165].

7.3.2 Rhabdom diameter

Rhabdom diameters are significantly greater in the dark-adapted Group 5 than in all other light-exposed eyes (ANOVA, $F_{(3,80)} = 49.2$, $p<0.001$; Fig. 7.5) and are in accordance with cross-sectional area measurements in chapter 3 for midday dark-adapted eyes. Rhabdoms exposed to light for 30 minutes are significantly narrower in Groups 2-4 (direct, ND-filtered and polarized sunlight), however there were no significant differences between these three treatments (TukeyHSD, p=0.868 to 0.998).

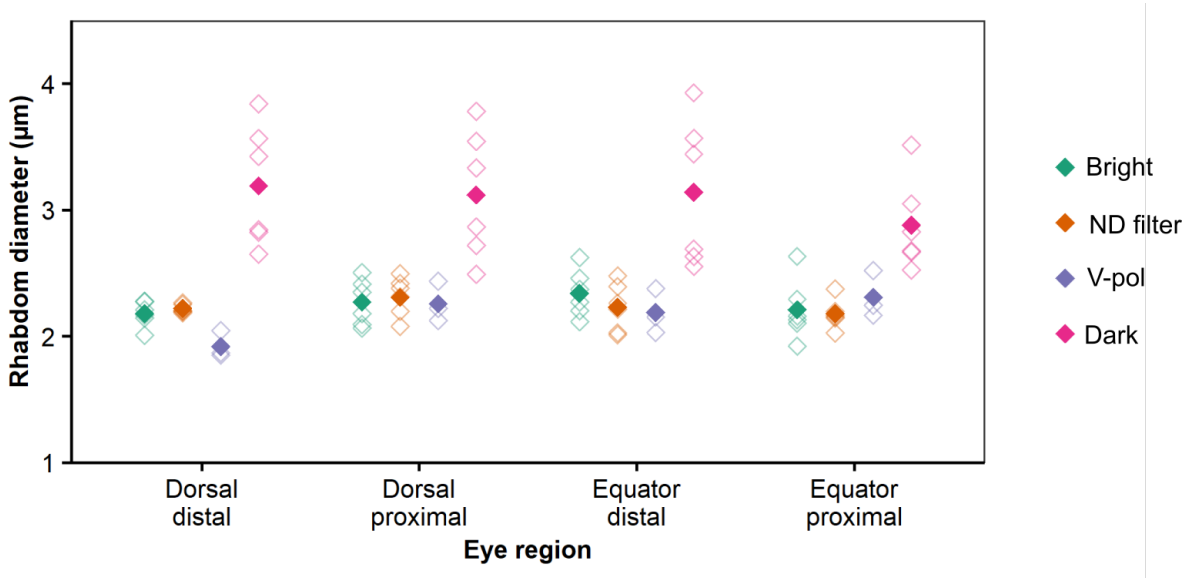

FIGURE 7.5. Diameter across distal and proximal rhabdom tracts are plotted for dorsal and equatorial regions of eyes exposed to different light treatments. Mean values for individuals are marked by open diamonds and group means per treatment are indicated with shaded diamonds, colours correspond to light treatment.

7.3.3 Microvillar arrangements

In *G. vomeris* and *T. signata*, the R1-7 rhabdom has shorter horizontally-sensitive rows in the distal-most 50 μm of its length [210] (Fig. 7.6a). However, in the dark-adapted *A. tangeri* eye examined, the number of rows of microvilli per horizontally- and vertically-sensitive band remain proportionally equal throughout the length of the rhabdom (Fig. 7.6b). No instances of uneven rhabdom bands (differing number of rows of microvilli) were found in any of the treatments, including TEMs of the distal R1-7 rhabdom of equatorial eye regions. Aside from this, there are some similarities in the *A. tangeri* and *T. signata* curves (Fig. 7.6a,b), such as the general increase in number of rows per band from distal to proximal. There is also the same short section (spike) of unusually high numbers of rows, around 20 - 35 μm along its length (from distal tip). This is present in the vertical curve for *T. signata* and in both bands in *A. tangeri*.

Horizontally-sensitive microvilli occupy a larger proportion of the rhabdom area than the vertically-sensitive bands in nearly all rhabdoms examined (Fig. 7.6c). The bands are closest to equal (0.50) in the dark-adapted eyes, where rhabdoms are always straight. Eyes exposed to bright light have the highest proportion horizontal microvilli in the rhabdom.

Dorsal eye: In the distal rhabdoms, there is a significant difference between treatments (ANOVA, $F_{(3,17)}$=3.47, p=0.039), whereby the bright light-exposed group has a significantly larger proportion of horizontal microvilli than the dark-adapted group (TukeyHSD, p=0.038). All other pairwise Tukey tests revealed no significant differences (p=0.192 - 0.987). In proximal rhabdoms, the proportion of horizontal microvilli is similar across all treatments (ANOVA, $F_{(3,17)}$=2.60, p=0.086). Rhabdoms in dorsal eye regions do not appear heavily indented (Fig. 7.7), but distal rhabdoms exposed to bright light had the most indentation, followed by ND filter. The wider rhabdoms of the dark-adapted eyes have straight edges.

Eye equator: Differences between treatments are more pronounced here than in the dorsal eye, especially in distal rhabdoms (ANOVA, $F_{(3,17)}$=23.96, p<0.001). Here, proportion of horizontal microvilli in bright light-exposed eyes is largest (0.65), significantly greater than in the other three treatments (TukeyHSD, p<0.001). Eyes adapted behind ND-filter have a lower proportion of horizontal microvilli than bright, but still significantly higher than dark-adapted crabs (p=0.023). Eyes exposed to vertically-polarized light have a similar proportion to dark-adapted eyes (p=0.308). Proximal rhabdoms show the same trend of differences as distal rhabdoms (ANOVA, $F_{(3,17)}$=24.72, p<0.001), but to a slightly reduced extent. Bright light exposure produced rhabdoms with significantly larger areas of horizontal microvilli than all other treatments (p<0.004) and crabs shaded by ND-filter have significantly more horizontal microvilli than dark-adapted crabs (p=0.002). There are notable differences in the shape of the rhabdom tract between treatments (Fig. 7.8). Dark-adapted eyes always have very straight edges, while distal equatorial rhabdoms in all light-exposed treatments tend to have a scalloped edge, as a result of a smaller area of microvilli in vertically-sensitive bands. This is most pronounced in the bright light group. This indentation is subtle or absent in the proximal rhabdoms of the same eyes.

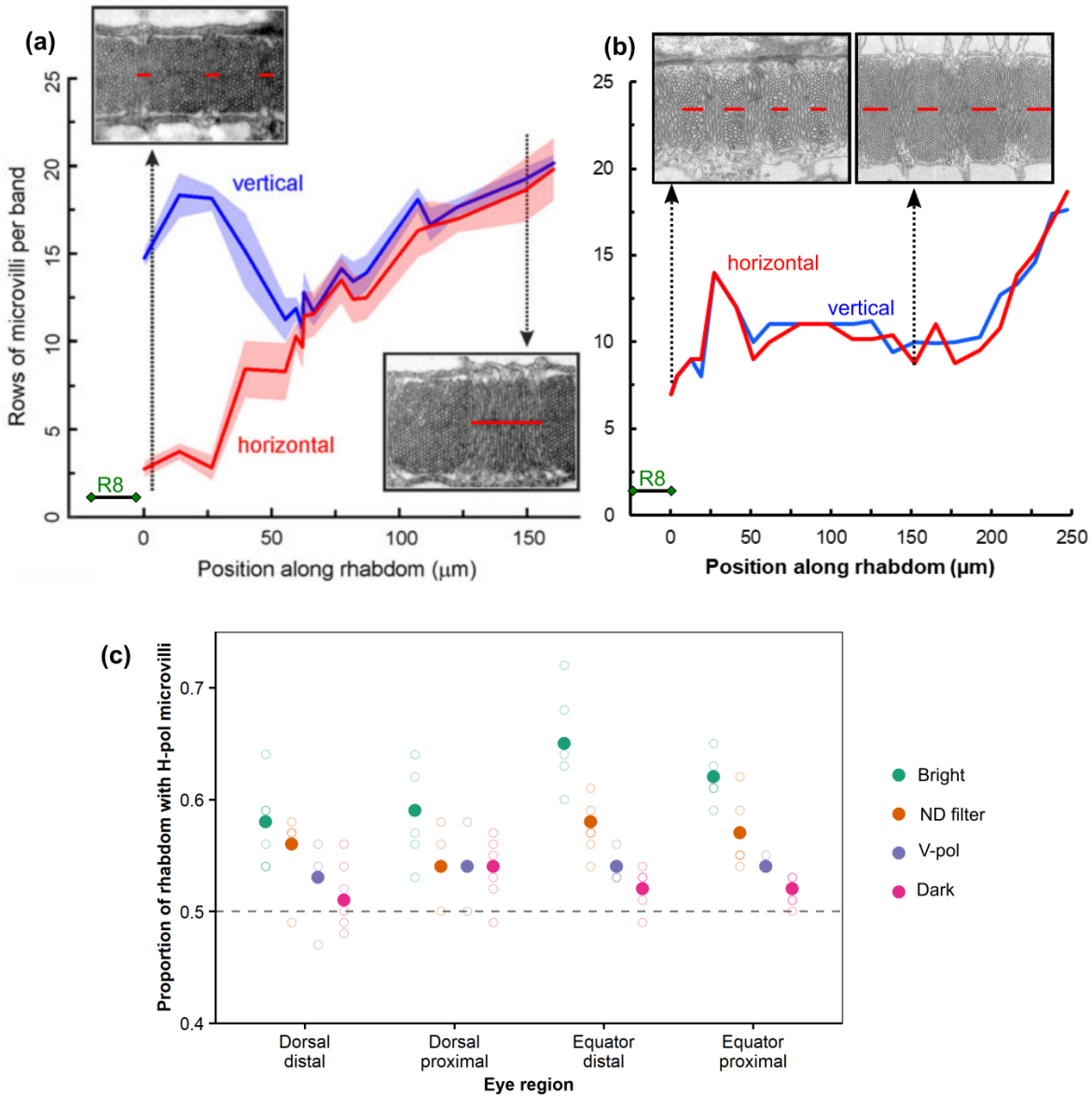

FIGURE 7.6. The number of rows of microvilli per horizontal/vertical band length along the length of a single equatorial rhabdom (distance from distal to proximal). **(a)** Figure from ref: [210] showing data for *T. signata*, next to **(b)** equivalent data collected from a dark-adapted *A. tangeri*. Inset TEM images illustrate the banding pattern at distal (left) and proximal (right) locations in the rhabdom as indicated by vertical dotted arrows. Length of horizontally-sensitive bands are indicated with red lines. **(c)** The proportion of cross-sectional area occupied by horizontally-oriented microvilli are shown for distal and proximal rhabdoms in dorsal and equatorial eye regions (measured from TEMs). Eyes were exposed to differing light treatments for 30 minutes before. Mean values for individuals are marked by open circles and group means per treatment are represented by filled circles. Dashed line marks equal proportion of horizontal and vertical microvilli (0.5).

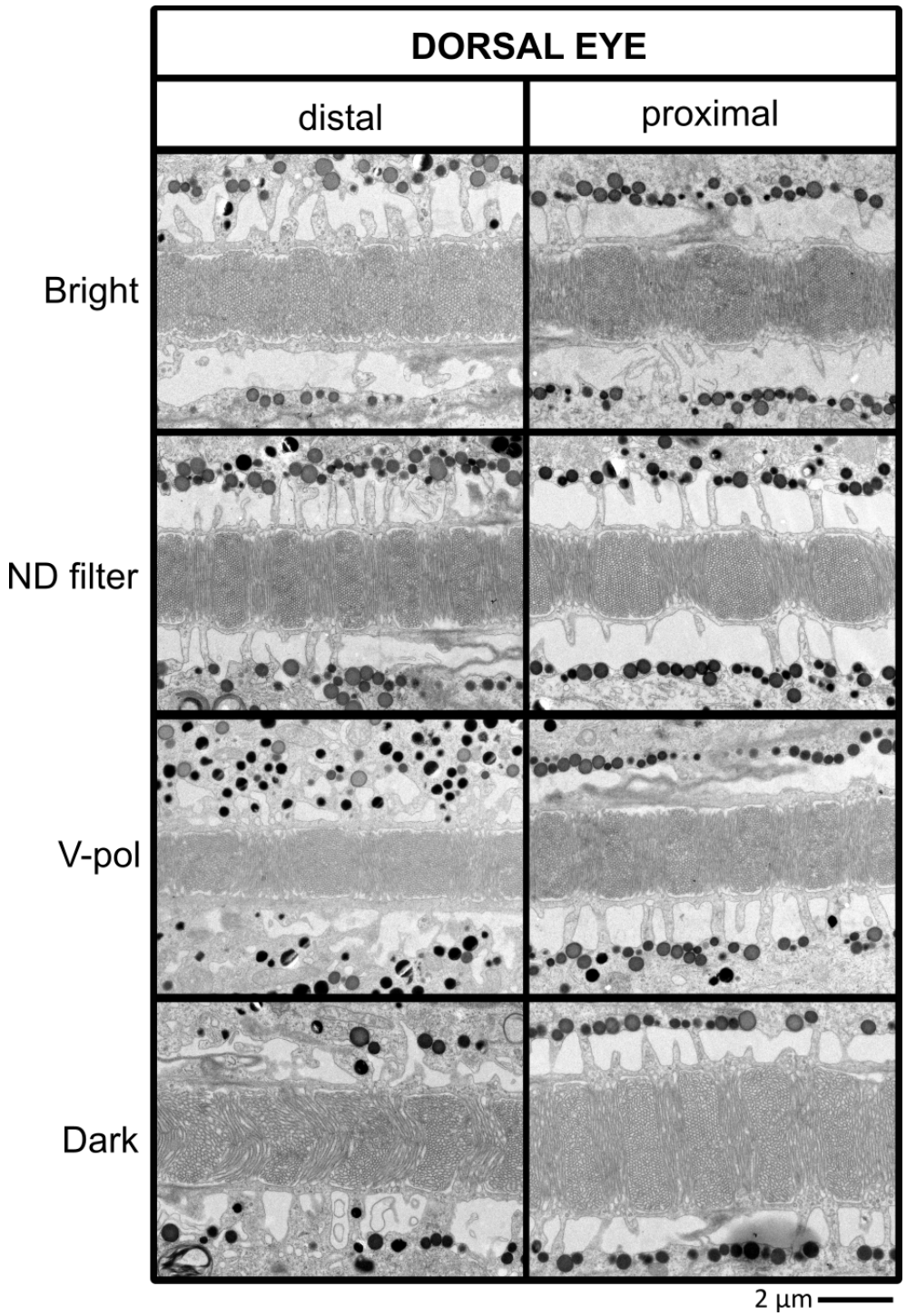

FIGURE 7.7. Example TEMs of the distal and proximal rhabdom tracts, longitudinal view, in the dorsal eye for each of the four treatments. The shape of the rhabdom is slightly indented in eyes exposed to bright or ND-filtered light, but mostly straight in V-pol exposed and dark-adapted eyes.

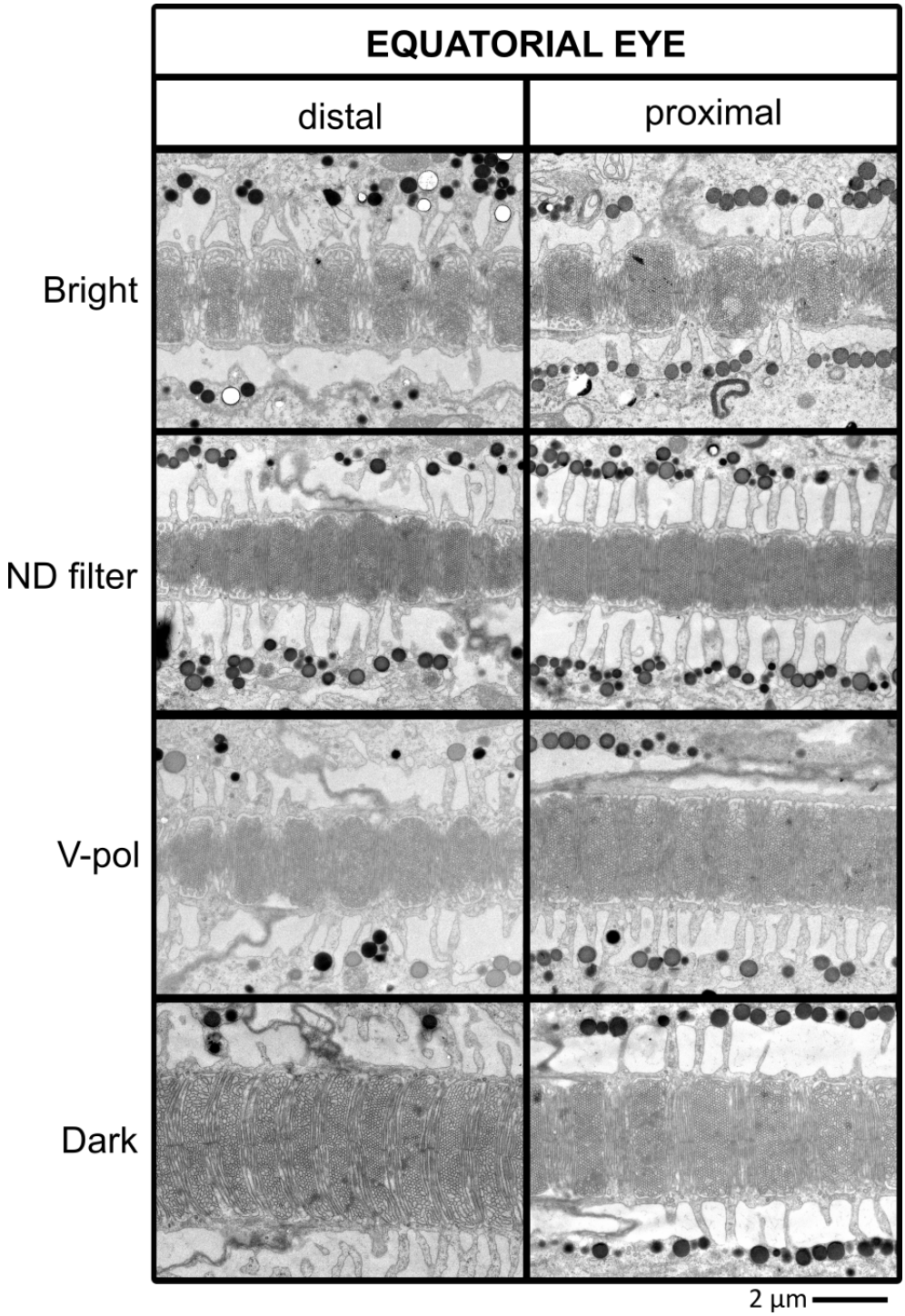

FIGURE 7.8. Example TEMs of the distal and proximal rhabdom tracts, longitudinal view, in the equatorial eye for each of the four treatments. The distal equatorial rhabdom tends to have a indented (zig-zag) edge in light-exposed eyes, which is less pronounced in the proximal rhabdom. Note the wide and very straight-edged rhabdoms of dark-adapted crabs.

7.4 Discussion

It was hypothesised that the indentation creating scalloped edges to light-adapted rhabdoms is a result of shorter horizontally-orientated microvilli, which may function to produce preferential polarization sensitivity to vertical light waves, in order to effectively screen out some of the horizontally-polarized glare from bright tidal flats. This was based on preliminary data of sections cut in a horizontal plane, in addition to similar findings in the rhabdoms of two other fiddler crab species [210]. After producing sections of the eye in a vertical (dorsoventral) plane, microvillar organisations were contradictory to the hypothesis, whereby horizontal bands occupied larger areas of rhabdom, rather than vertical.

Unless there are differences in the thickness of the bands due to fewer microvillus rows of one orientation (not prevalent in *A. tangeri*), it appears that the difference in area is mostly due to the plane in which the rhabdom is cut (Fig. 7.9a,b). Vertical (dorsoventral) sections give the impression of larger horizontal bands as these will be sliced perpendicular to the microvilli (Fig. 7.9c), while horizontal sections cut through the microvilli of the vertical bands give the impression that these bands are larger (Fig. 7.9d). Therefore, whether the sections are made in horizontal or vertical planes across the eye, the set of microvillus bands that are being cut through transversely (resulting in the microvilli appearing as small circles on the TEM), will occupy a larger portion of area in the 2D image of the rhabdom.

In a dark-adapted state, the eyes always have a very straight rhabdom, whereby both sets of microvilli occupy an equal area. This implies that the rhabdom is very cylindrical along its length in this condition. During adaptation to light, extensive pinocytosis shortens each microvillus from its base, creating a rhabdom shape that is not perfectly round. In any given cross-section, the rhabdom becomes a slightly oval or rectangular in shape, regardless of the orientation of the microvilli (Fig. 7.9e,f). Therefore, as it narrows in response to bright light, the 3D shape of the rhabdom becomes indented in two planes, rather than one, forming a stack of orthogonal ovals / rectangles (refer to the simplified 3D model of the rhabdom shape in Fig. 7.9g).

Alkaladi *et al.* [210] also noted heavy indentation of dorsal rhabdoms in *T. signata*. Like my own hypothesis, they interpreted the uneven cross-sectional area of orthogonal bands to mean that photoreceptors (R3, R4 and R7) contributed shorter microvilli than the other photoreceptors and therefore proposed that this was an additional mechanism to filter out horizontally-polarized light from the sky. The eyes would need to be sectioned again vertically (dorsoventral) to see whether, like *A. tangeri*, the indentation happens in both planes when light-adapted.

In the present experiment, eyes had been exposed to bright light for just 30 minutes, assumed to be a sufficient duration for pinocytotic process and rhabdom adjustments to reach completion. This was based on results from the previous chapter (section 5.3.1) as in 30 minutes, the rhabdom diameter had reached the typical daytime size. However, as discussed (section 5.4.3), further examination of the organelles showed that pinocytotic processes are in progress for much longer than 30 minutes. This may explain the loose appearance of microvilli in some of the eye samples.

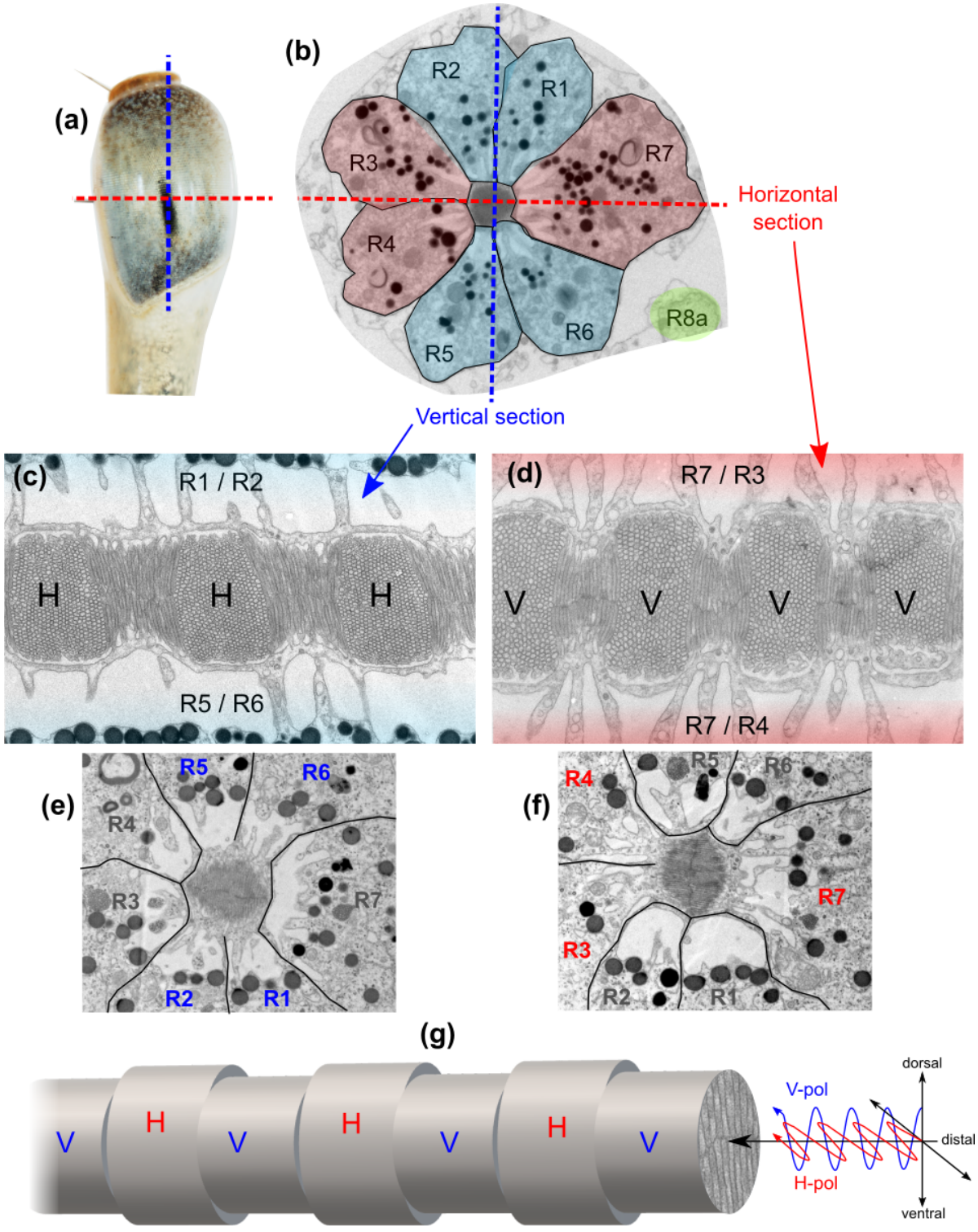

FIGURE 7.9. Dashed lines show horizontal (red) and vertical (blue) planes of sectioning on **(a)** a photo of a whole eye and, **(b)** a TEM of an ommatidium (transverse view), just ventral to eye equator. The cell arrangements .....*(continued on next page....)*

FIGURE 7.9. *cont.* ... are shown with blue shade for photoreceptors that produce vertically-orientated microvilli and red shade for horizontally-orientated microvilli. TEMs from light-adapted eyes sectioned along these planes with rhabdoms in view along their long axis, both look similar, whether they are **(c)** vertically sectioned as the eyes in this experiment were, or **(d)** horizontally sectioned (as in [210]). Note that in both, it is the microvilli cut across their short axis that take up the largest area in the image. **(e,f)** Rhabdoms in transverse section from adjacent ommatidia in the same eye that has been adapting to bright light for 30 minutes. Both have an oval-shaped rhabdom, but note the differing (perpendicular) orientation of its short axis between the two images. In **(e)**, the rhabdom was cut through a band consisting of vertically-oriented microvilli from R1, R2, R5 and R6, and is elongated horizontally. In **(f)**, the rhabdom was cut through a band of horizontally-oriented microvilli from R3, R4 and R7, so is elongated vertically. **(g)** The 3D shape of the rhabdom when light-adapted. Both vertical (V) and horizontal (H) bands of microvilli have an oval shape across the rhabdom, and are longest where microvilli from opposite photoreceptors meet in the middle, producing a ridged shape to the rhabdom in both axes.

There were no regions of rhabdom with fewer rows of horizontal microvilli than vertical, so *A. tangeri* do not appear to have the uneven banding pattern that is prevalent in the distal rhabdoms of the equatorial eye regions in *G. vomeris* and *T. signata* [210]. This is the only major difference in eye anatomy that has been identified between *A. tangeri* and other documented fiddler crab species [89, 210, 214]. The fiddler crabs species come from different subfamilies and ocean realms, so this region of relatively shorter horizontal bands in equatorial distal rhabdoms of the Australian Gelasiminae species may have evolved since their last common ancestor with *A. tangeri*.

The rhabdoms of the blue crab *Callinectes sapidus* become particularly oval-shaped / rectangular when light-adapted [202], presumably creating a rhabdom with very bumpy edges. This characteristic indented, or scalloped rhabdom shape has also been noted in other crabs species including the shore crab *Hemigrapsus penicillatus* [203] and purple rock crab *Leptograpsus variegatus* [183]. The edges of rhabdoms of this shape (lacking smooth sides) may interfere and scatter light, as it propagates down the rhabdom. The results of this experiment, suggest that bright light causes a change in rhabdom shape, becoming narrower and indented due to pinocytosis of the microvilli, but there is not likely to be a change in proportional disparity of volume of horizontally- and vertically-sensitive microvilli. This means that horizontal glare filtering (by reducing its detection) is unlikely to be a strategy used in this species.

The disparity in area of horizontally- and vertically-oriented microvilli reflected the degree to which the rhabdom edge was indented in shape, which also corresponded to the overall intensity of light that the eyes were exposed to. The effect was strongest in individuals exposed to bright light with no filter, due to high rates of pinocytosis as the eyes react to sudden bright light

exposure. Crab eyes shaded by a layer of ND filter (46% transmissive) or polarized filter (36% transmissive) appear to have had slightly lower rates of pinocytosis, leading to a less pronounced change in rhabdom shape, although the diameter of these rhabdoms were wider than those that were exposed to bight light. The ND filter was slightly more light-transmissive to the polarizing filter, which may explain the small difference between them in terms of proportion of horizontal microvilli. The distal rhabdom of the eye equator was the eye region that appeared to be the most modified by pinocytosis in all light-exposed eyes. This may be because the ommatidia here view the sediment-sky horizon, where multiple scattering in the atmosphere causes a a streak of very bright (white) skylight, 5°-10° above the horizon [114]. The horizon is also very important in their visual ecology for detecting conspecifics and predators, requiring high contrast sensitivity and spatial acuity (facilitated by one or two acute visual streaks [117]).

A high degree of vertically-polarized light does not seem to cause excessive pinocytosis of the vertical microvilli of R1, R2, R4 and R5 rhabdomeres, when compared to unpolarized light exposure (ND filter). This is perhaps not surprising, given the unlikelihood and rarity of a natural scene reflecting a high degree of vertically-polarized light. It is worth noting that the natural scene viewed by the crabs during adaptation (the beach) is likely to have had high degree of horizontally polarized light, so the V-pol treatment may have experienced lower light intensities than the H-pol group, especially in eye regions viewing the strong ground / water surface reflections which are rich in horizontal polarizations. The crabs were facing towards the rising sun so the sky would have been relatively unpolarised for the mid-upper region of the eye [59]. Ideally, the experiment should have been carried out in controlled light conditions using artificial light (with some UV wavelengths).

It is unfortunate that none of the eye samples exposed to horizontally-polarized light were viable, as it would have been interesting to see whether there was any difference between them due to orientation of the polarizer. Having said this, they would not have been exposed to any more horizontally-polarized light than the bright light exposed crabs (as the polarizer only removes light from other planes). Ideally though, this experiment should be repeated in order to successfully test the effect that a high degree of horizontally-polarized light exposure has on rhabdoms. As this is a common feature of their habitats, there is more chance that they would have evolved a mechanism to cope with horizontal glare. There may still be a subtle but measurable difference in volume of each band, and further investigations should ideally measure rhabdoms twice, after sectioning in both planes to compensate for the oval rhabdom shapes, or better still in 3D using Serial block-face scanning electron microscopy. From observations of light-adapted rhabdoms cut in these two orthogonal planes, it appears that, although both have a scallop shape, it is more pronounced in rhabdoms cut horizontally (e.g. compare panels c and d in Fig. 7.9), which would mean horizontal microvilli are, in fact, slightly shorter than vertical. It is also very important to design a method ensuring gill hydration, as even 30 minutes out out of water was too long for some of the Group 1 and 2 crabs in this test. Given the underwhelming

differences in other treatments and the time involved with producing the TEM data, a repeat of this experiment was decided against.

7.4.1 Conclusions

This experiment did not go exactly as planned and the results are rather inconclusive. The results do not eliminate the possibility that strong horizontal glare produces shorter horizontal microvilli than vertical, however there is little evidence for it either. The data suggest that *A. tangeri* do not adjust the length of their microvilli, or the proportion to which horizontal vs. vertical bands are expressed along rhabdoms in the dorsal or equatorial eye in response to differing light conditions. They appear to lack a strategy to reduce horizontally-polarized glare or boost sensitivity to a particular polarity, albeit I was not able to measure the effect that a high degree of horizontally-polarized light had on the rhabdom. The indentations and oval-shaped rhabdoms created from pinocytotic shortening of the microvilli, apply to both horizontal and vertically-orientated microvilli bands. This creates an undulating 3D shape formed by a stacks of orthogonal oval disks. Further study is needed to fully investigate differences in volume of rhabdomeres with opposing polarization sensitivity. The optimal method to investigate this would be to image rhabdoms in three dimensions using serial block-face scanning electron microscopy, segment the horizontal and vertical bands (perhaps focussing on the distal equatorial rhabdoms) and then compare their volumes.

CHAPTER 8

CONCLUSIONS AND FUTURE RESEARCH

This PhD project aimed to address important questions on how the fiddler crab eye reacts to extreme changes in brightness. *Afruca tangeri* and *Gelasimus dampieri* are species involved with current advances in crustacean vision research and therefore, they were selected as study animals in this project. They represent very similar animals with analogous biology and ecology, but are separated in distance by ocean realms [132] and phylogeny [91, 92]. Despite their similar characteristics, they are now classified in different fiddler crab subfamilies. In this chapter, I summarise the key findings of this work and discuss some ongoing ideas for future research to better understand the visual systems of these animals.

8.1 Key findings

- Fiddler crabs are largely associated with bright tropical mudflat habitats and *A. tangeri* also continues to forage after sunset, with male crabs observed using conspecific visual signals during breeding periods on moonless nights in dim light.
- There is no evidence of screening pigment migrations as an optical strategy to moderate light flux to the rhabdom. This is true of granules within primary pigment cells, which surround the crystalline cone tips above photoreceptors, as well as within photoreceptor cells, where the granules form a sheath lining the palisade vacuole surrounding the rhabdom.
- During daytime, ommatidia in *A. tangeri* have narrow rhabdoms and crystalline cone tracts. Behavioural tests reveal that the eye has relatively poor contrast sensitivity in this condition. ERG responses show that *G. dampieri* eyes are also least sensitive when light-adapted during daylight hours.

- To increase sensitivity at dusk, the crystalline cone tip aperture widens to allow more light to reach the rhabdom. This takes over an hour to complete.
- The cross-sectional area of the rhabdom increases rapidly each evening by an average factor of 5.6, via elongations of the microvilli. This increases the volume of visual pigment-bearing membrane in each ommatidium and thus, boosts photon capture and overall sensitivity of the eye when dark-adapted. This takes up to an hour to complete and is a strategy shared by many other crabs, although there may be taxonomic differences in the precise mechanisms.
- Behavioural experiments confirmed that contrast sensitivity in *A. tangeri* is highest when dark-adapted after sunset. Similarly, ERGs showed that *G. dampieri* is also most sensitive in this condition.
- The crystalline cone tract and rhabdom require darkness to widen to their full extent and the processes are largely inhibited by bright light, which provokes pinocytosis (narrowing) of the rhabdom.
- If light-adaptation is prolonged with bright LEDs after sunset, behavioural tests and ERGs showed that fiddler crab eyes still become more sensitive relative to daytime, despite the rhabdom remaining narrow and only a slight increase in crystalline cone tract diameter.
- There are also endogenous circadian clock controls on dark-adaptation. Crystalline cone widening and rhabdomere expansion only occurs in the dark after sunset when the photoreceptor cells have prepared organelles ready for the extensive microvillus membrane assembly process.
- During periods of darkness within daylight hours (as if in the burrow), the rhabdoms do not widen and crystalline cone tracts remain narrow. This, combined with lack of pigment migrations, mean that the *A. tangeri* eye remains physiologically light-adapted, even after 3 hours in near-darkness.
- Before dawn and first light exposure on exiting the burrow, rhabdoms and crystalline cones begin to narrow, reaching a partially light-adapted state. Bright light exposure is required for the eye to complete its pinocytosis of microvilli, causing full narrowing of the rhabdom. Similarly, the cone tract only narrows completely on light-exposure.
- Although the rhabdom reaches its narrow daytime size within 30 minutes of light exposure, full membrane recycling processes take several hours to complete, as indicated by organelle presence in the photoreceptor soma.
- Incomplete reduction of cone tract and rhabdom diameters in *A. tangeri* crabs that have not yet been light-exposed that day, result in greater contrast sensitivity than fully light-

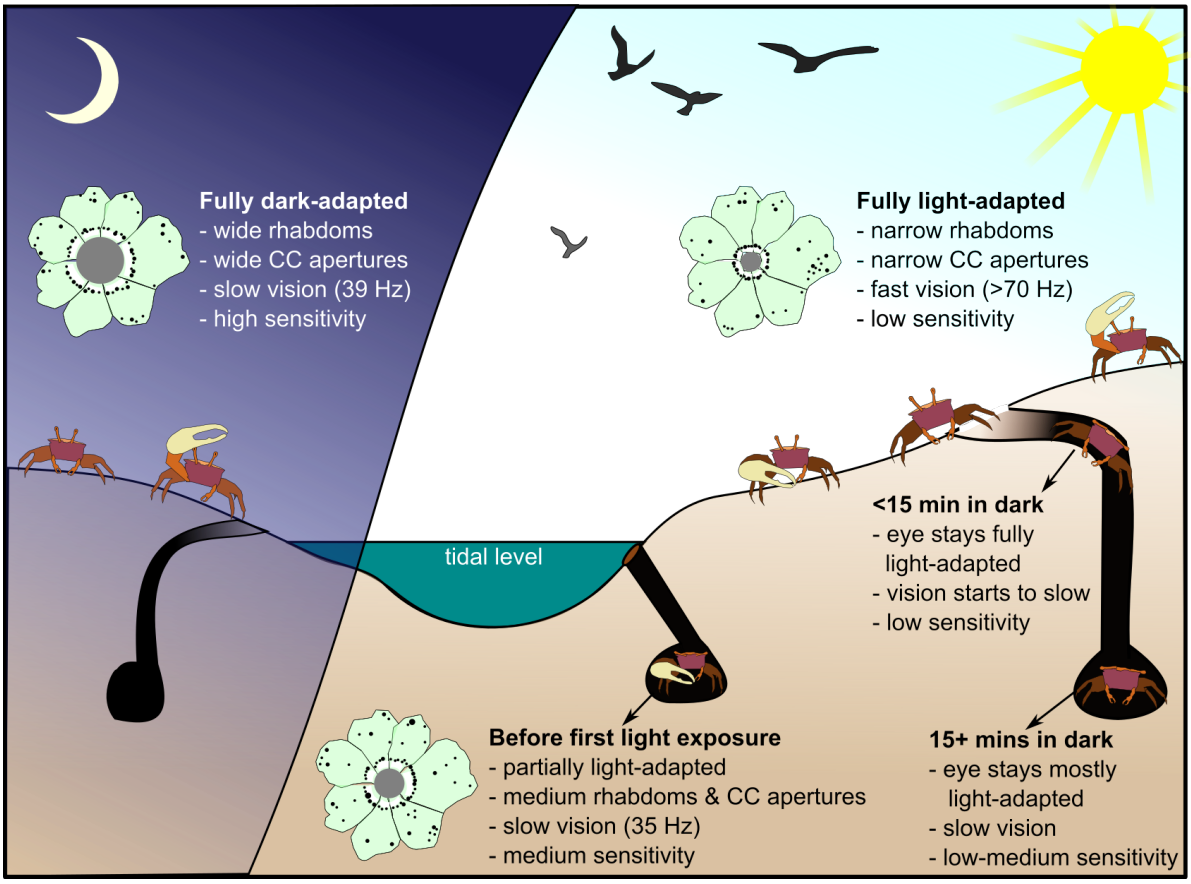

FIGURE 8.1. Major characteristics of fiddler crab vision from night (left) to day (right) as they adapt and cope with extreme changes in brightness, in and out of their burrows. Diagrammatic ommatidia in cross-section show the relative sizes of rhabdoms (grey) and unchanging pigment granule distributions (black dots) in the cytoplasm of photoreceptors (pale green).

adapted crabs. The same is true of *G. dampieri*, who produced significantly higher ERG responses when dark-adapted. Neither dark-adapted species were as sensitive during daytime than they are after sunset.

- The results of *A. tangeri* behavioural assays and ERG responses obtained from *G. dampieri* compliment well the anatomical findings from *A. tangeri* and confirm that light- and dark-adaptation processes to alter sensitivity are subject to light intensity *and* circadian control in both species.

- There is some sensitivity change during periods of daytime dark-adaptation that cannot be explained by anatomical changes. Temporal summations are an additional dark-adaptation strategy used in *G. dampieri* to improve sensitivity in dim light during daytime and night.

This was demonstrated via ERGs by the ability of the light-adapted eye to resolve faster flicker (cFFF>70 Hz) than when dark-adapted (cFFF<40 Hz) in daytime.

- Temporal summations are equally effective in daytime as after sunset, as no significant difference was found in the cFFF of dark-adapted *G. dampieri* between these times.
- Behavioural tests showed gradual increases in contrast sensitivity in *A. tangeri* during adaptation to dim light in daytime. This suggests that *A. tangeri* also use temporal summations, because no visible anatomical changes seem to occur during this time.
- Further research is needed to investigate how long it takes for membrane potentials to change to enable temporal summations after first exposure to darkness; it appears to be a gradual process taking many minutes.
- ERGs revealed that absolute sensitivity of the *G. dampieri* eye gradually increases when placed in darkness. During daytime, temporal summations are likely to be responsible for this initial boost in sensitivity, but it does not increase to the full extent, relative to night. This is probably due to lack of physiological dark-adaptation responses (as in *A. tangeri*), which begin only after sunset.
- Light exposure, even when dim and intermittent, disrupts dark-adaptation processes and reverses them. This may be a combination of light-induced photoreceptor cell membrane potential changes, pinocytosis of the rhabdom and changes to crystalline cone aperture diameter.
- During daytime, periods of less than 15 minutes in the dark (burrow) do not compromise *A. tangeri* contrast sensitivity in the first 30 seconds on returning to bright sunlight.
- A longer period of dark-adaptation (15-120 minutes) begins to gradually reduce contrast sensitivity in bright light, however, not to the extent of "fully dark-adapted" crabs that have yet to be exposed to light that day. After light-adapting in the morning, fiddler crabs stay functionally optimised for visual predator detection in bright light despite frequently sheltering in the burrow for short periods.
- The effect of the visual system being "blinded" or overwhelmed by bright light after long periods in the burrow is unlikely to last long. Most crabs who were initially unable to detect a pale contrast grating in bright light began to follow it with optokinetic nystagmus responses after less than a minute.
- Fiddler crabs exposed to artificial light pollution on the beach at El Rompido did not have significantly narrower rhabdoms than crabs adapted to low levels of light pollution, or near-complete darkness. Therefore, light pollution levels encountered at the study location were not sufficient to cause significant pinocytosis of the rhabdom.

- Tidal cycle has a strong effect on crab locomotive activity and behavioural motives. However it did not significantly affect the results of vision experiments in this thesis.
- *Afruca* do not possess relatively shorter bands of horizontal microvilli (than vertical) in their distal rhabdoms of the equatorial eye, as is found in two Australian fiddler crab species [210].
- Pinocytosis of microvilli during light-adaptation creates rhabdoms with oval cross-sections. To facilitate polarization vision, the microvilli are arranged in alternating orthogonal bands of vertical and horizontal orientation. This creates a stack of oval shapes, so the rhabdom tract is undulating with scalloped edges when the eye is cut in both horizontal and vertical planes. Strong vertically polarized light does not cause preferential pinocytosis of vertically oriented microvilli.
- The green shore crab *Carcinus maenas* has very wide rhabdoms at night to facilitate sensitive vision for a primarily nocturnal lifestyle. These narrow during daytime bright light-exposure, like many other crabs. They also use pigment migrations in primary pigment cells (and possibly photoreceptors) to moderate light flux in different adaptation states.

8.2 Future research directions

8.2.1 *Gelasimus dampieri*

It remains to be determined whether *G. dampieri* is active after sunset, so some observational study in its natural habitat is required to confirm this. A strictly diurnal ant *Cataglyphis bicolor* does not exhibit circadian changes in sensitivity (ERG responses). This ant, as well as another strictly diurnal species, *Myrmecia croslandi*, do not undergo any changes in ommatidial dimensions, unlike other *Myrmecia* and *Camponotus* ants, which are active after sunset and exhibit rhabdom and cone tract changes akin to fiddler crabs [162, 167, 168]. In *G. dampieri*, the larger rhabdom area and sensitivity increase at night (shown by ERG) suggests that this species does undergo the necessary adaptation to enhance vision for some degree of nocturnal activity.

Due to lack of available animals at the time, flight restrictions, and lessons learnt in how to transport fixed tissue samples for TEM, further anatomical study is required to properly investigate adaptive changes in *G. dampieri* eyes and provide quantitative data. My observations from histology suggest that rhabdom changes do occur, as in *A. tangeri*, but there could also be some change in the primary pigment cells (PPCs), which may potentially allow this crab an additional adaptation strategy to cope with changes in light intensity.

8.2.2 Cells and anatomical features yet to study

In this project, I identified the major anatomical changes (or lack thereof) associated with light- and dark-adaptation in the eyes of *A. tangeri* using TEM, light microscopy and some synchrotron X-ray tomography. However, there are some cells or features of the eye that were not studied quantitatively. These include pigment distributions within the secondary pigment cells (SPCs). The main cell bodies of SPCs are located just distal to the primary pigment cells (PPCs) and form strips extending up and down in a dorsal-ventral direction across the eye (Fig. 8.2a,b). A very thin cytoplasmic process extends distally from each SPC cell body between crystalline cones (Fig. 8.2b,c; see also Fig. 3.6a,d,e), ultimately attaching to the cornea. In the dorsal eye, SPCs contain a variety of pigment granules, which vary in their reflective and transmissive properties (Fig. 8.2c, top panel; see also Fig. 8.3a). However, in the rest of the eye, the distal processes appear empty. This makes them difficult to locate on sections and they are too fine and low contrast to resolve with synchrotron radiation in the 3D data sets. Serial blockface scanning electron microscopy (SEM) would be an effective method of examining these cells properly and looking for differences between adaptation states. Figure 8.2 contains example images in which these cells are particularly conspicuous and orderly. In the majority of equivalent micrographs, these cells do not show up at all or appear irregular and difficult to distinguish from other nearby cells. They may be particularly liable to damage during dissections, I have observed that sometimes the pigment granules of SPCs "swim" out of the eye when the edges are cut from the eye stalk.

An alternative method of assessing changes in the SPCs is to examine intact eyes in living crabs using a light microscope or macro photography. Fingerman [171] described distal pigment movements in *Leptuca pugilator* at night and proximal retractions during day. These, he measured in the width of the translucent (crystalline cone) part of a backlit eye under a microscope (see *A. tangeri* example in Fig. 8.3a). The translucent area decreased in width (proportionally to the total eye width) at night and he attributed this to distal migrations of screening pigments up between crystalline cones, although cell type was not specified. It would be interesting to repeat his experiment with *A. tangeri*, perhaps improving the technique (his study was conducted using equipment available in the late 1960s). There may be taxonomic differences among Ocypodid crabs in the use of this strategy.

The SPC pigments give the eye its outward colour and there is great variation between *A. tangeri* individuals (Fig. 8.3b). In at least one case, heterochromacy is possible between eyes of the same individual (Fig. 8.3c). There is a brown SPC pigment between crystalline cones of the dorsal eye, where ommatidia are exposed to very bright light from a panoramic view of the sky. Often, one or two will have a direct view of the sun and this extra pigment in the dorsal SPC processes (Fig. 8.3a, arrow) provides additional screening of excess damaging solar radiation [47, 89]. It also prevents light leaking between crystalline cones, maintaining high resolution vision in the dorsal eye which must monitor for avian predators in the sky as they fly across visual fields sampled by single ommatidia. The SPCs may also provide camouflage for the eye,

which would otherwise appear very dark [47, 89].

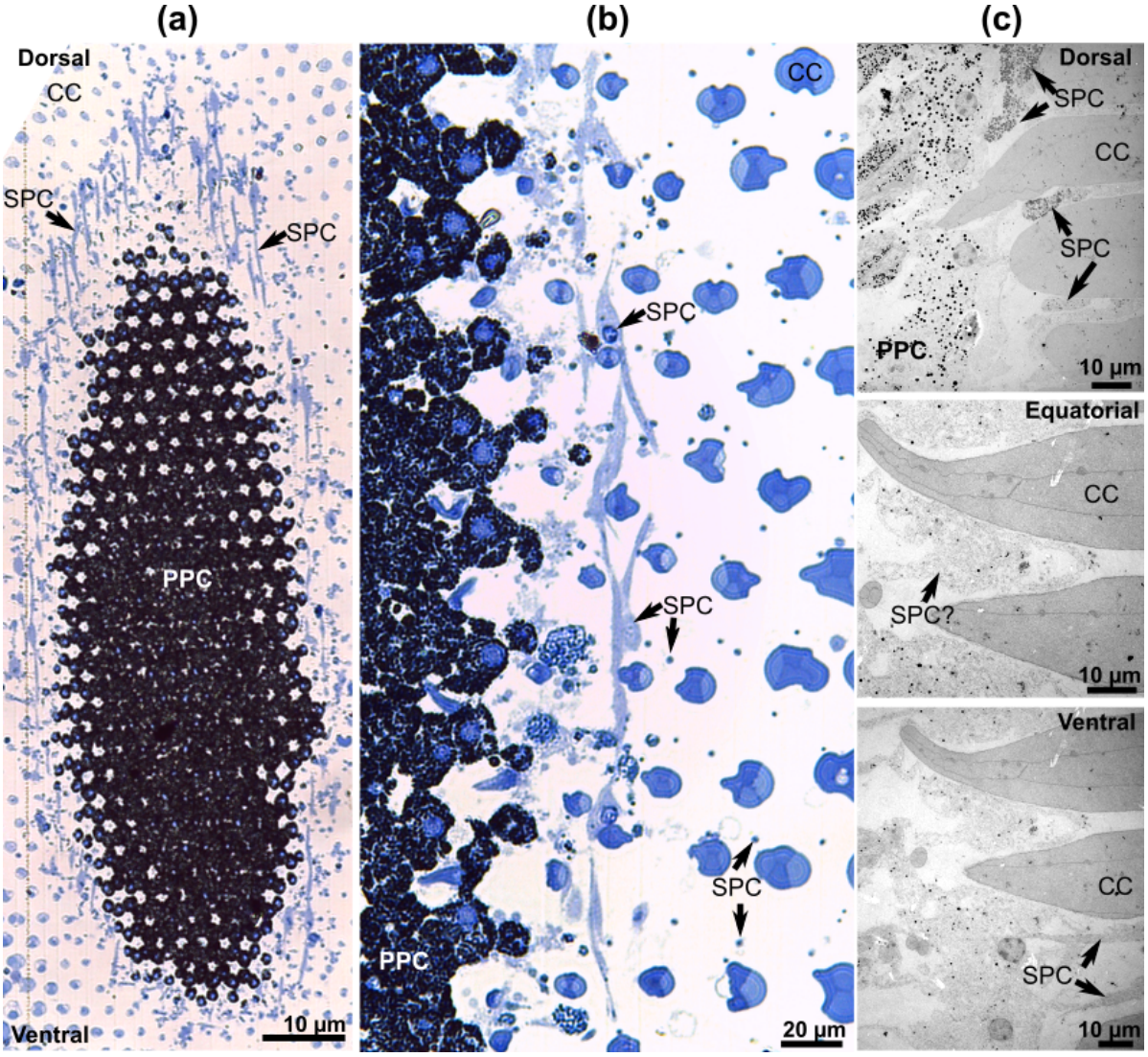

FIGURE 8.2. **(a)** Light micrograph of an *A. tangeri* eye with cell bodies of secondary pigment cells (SPCs) appearing as strips which extend up and down the eye in a dorsoventral direction. They appear pale relative to the dark PPC layer, just proximal to them. **(b)** In an oblique section of the equatorial eye, the proximal SPC cell bodies contain the nucleus (see top arrow). Very thin cytoplasmic processes of the SPCs extend distally (right) appearing as small dots around crystalline cones (CC) in cross-section, ultimately anchoring to the cornea. **(c)** TEMs of longitudinal sections of the eye show SPCs in different eye regions. Dorsally, the cells contain a mix of pigment granules, but in equatorial and ventral regions, they look empty and are difficult to distinguish from other cells. Condition of fixed eyes: **a,b** = light-adapted after sunset; **c** = dark-adapted during day.

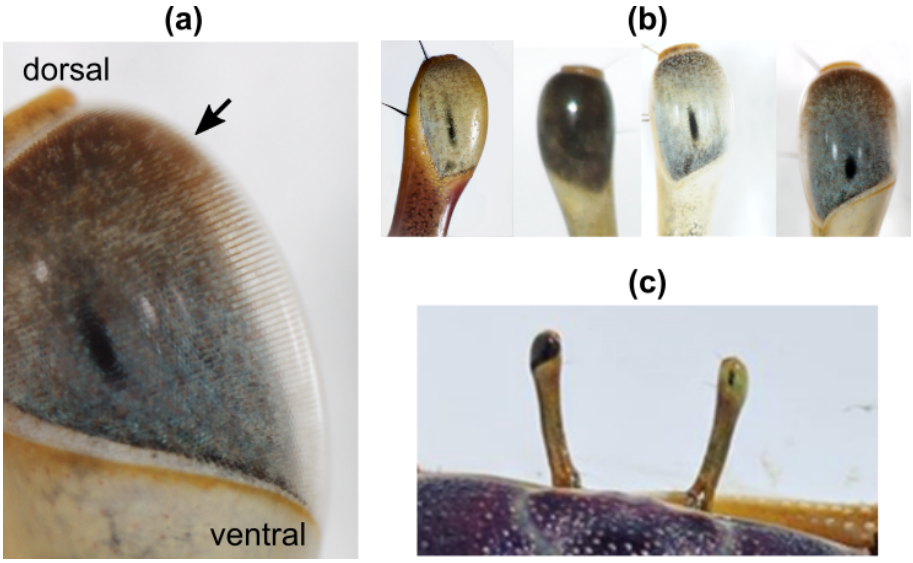

FIGURE 8.3. **(a)** Light passing through the crystalline cone region of an intact *A. tangeri* eye, is absorbed by brown screening pigment within SPC distal processes in the dorsal region of the eye (arrow). In the equatorial and ventral regions, the distal SPC processes are mostly empty, making this cone region translucent. **(b)** Natural variation in eye colours given by SPC pigments exists within the population of *A. tangeri* in El Rompido. To the human eye, these colours include white, blue, green, pale grey, brown, yellow and black. **(c)** A male fiddler crab (posterior view) with unusual heterochromatic eyes. His left eye is almost black, while is right eye is yellow/green.

Crystalline cones require further measurement in three dimensions (e.g. using synchrotron X-ray tomography) to determine whether they change in volume from day to night, and to confirm whether their length decreases at night, as suggested by light microscopy data. Histology methods can cause deformation of the proximal cone cell tract as the cells are very soft. Therefore, measuring them in 3D from intact eyes, perhaps sampling equivalent eye regions in several size-matched eyes per treatment, would provide a reliable method to measure changes and understand how the proximal tips widen at night. The R8 cells do not appear to change in shape and contain no pigment granules, but the microvilli of the rhabdom also extend to widen this section of the rhabdom, like the R1-7, however, no measurements were made as part of my study.

There are additional cell types within the inter-ommatidial space, which were not examined, including spherical cells containing large dark pigment granules (Fig. 8.4a), which appear to be randomly and sparsely distributed in the eye. Other low contrast cells which may contain organelles (e.g. Fig. 8.4b,c), or appear empty are often attached to the outside of photoreceptor columns, possibly assisting in membrane recycling or structural functions, or perhaps having a light-reflecting purpose to optically isolate the ommatidia. These cells are not regularly distributed, so were not examined in this project.

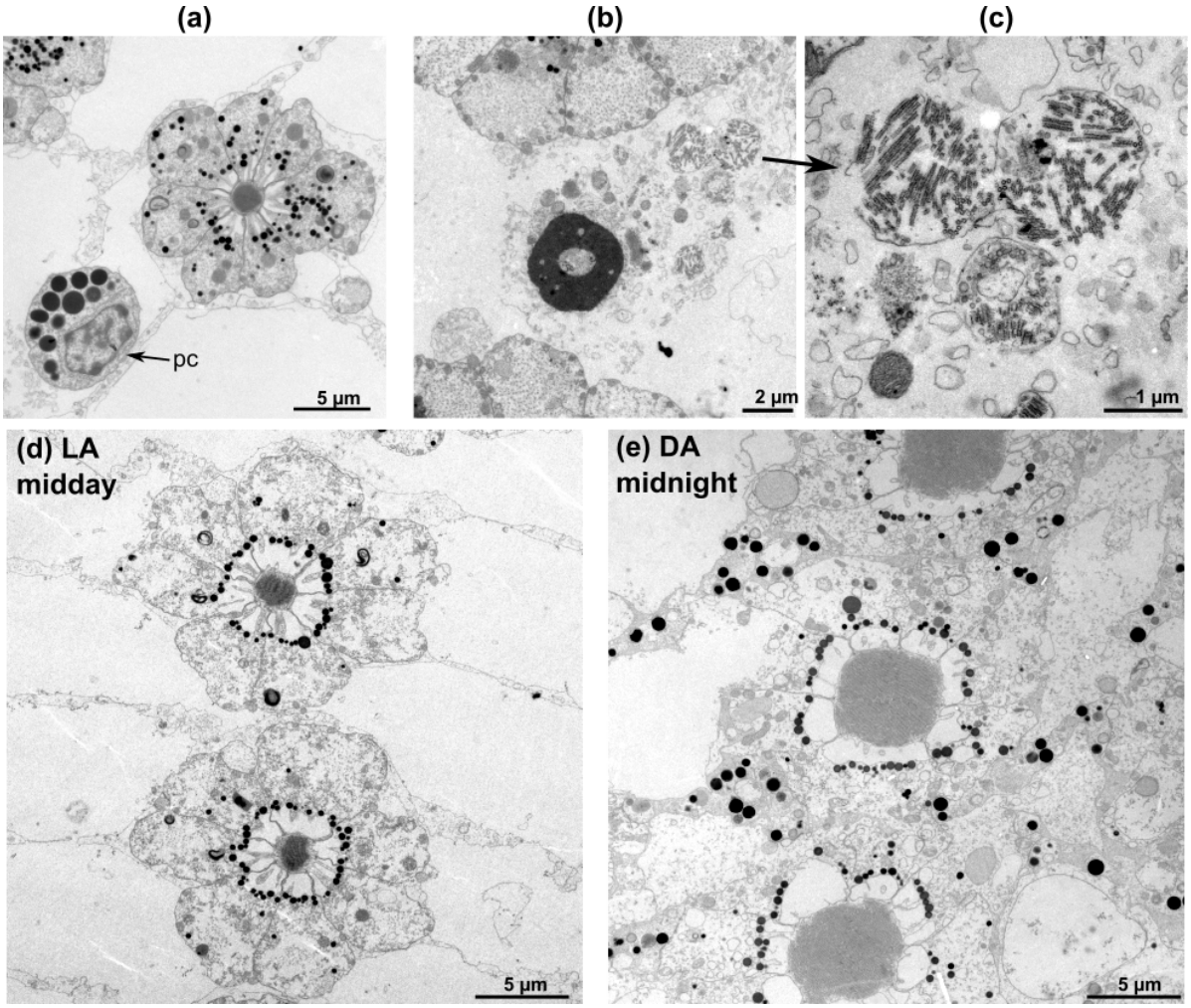

FIGURE 8.4. **(a)** A spherical accessory pigment cell (pc) in the inter-ommatidial space of a light-adapted eye (midday). **(b)** A cell of unknown function containing unusual organelles, seen only once in the inter-ommatidial space of a dark-adapted eye (midday). **(c)** Same as **b**, higher magnification to show organelles. **(d)** In light-adapted (LA) eyes, ommatidia are separated by extracellular space. **(e)** In an eye fixed at midnight after dark-adapting for 3 hours (DA), the ommatidia are tightly packed and photoreceptor cells are in contact with neighbours within a row.

In a few eye samples, difference in compactness of the ommatidia was noted between adaptation states. In most eyes there is intercellular space separating neighbouring ommatidia, at least always during daytime and in light-adapted eyes (Fig. 8.4d). However, although it is rare, ommatidia in a dark-adapted eye at night will occasionally appear closely packed with photoreceptors from neighbouring columns in contact (Fig. 8.4e), especially around the widest nuclear region. The opposite was noticed by Arikawa *et al.* [165] in the crab *Hemigrapsus*, and the authors suggest that compactness in daytime is due to distal elongations of reflecting pigment cells which

stretch between the ommatidia and push them close together. *Afruca* do not appear to possess equivalent reflecting cells, however there is some unknown material/cells in the inter-ommatidial spaces in the eye with compact arrangement (Fig. 8.4e), which is absent in eyes with separated ommatidia. This would be interesting to examine further.

8.2.3 Regional adaptation in compound eyes

An arthropod compound eye is formed of hundreds to thousands of ommatidia [7]. Visual information is passed from the photoreceptor axons through a series of optic neuropils: the lamina, medulla, lobula, lobula plate, lateral protocerebrum and protocerebral tract (optic nerve) [261]. There are one set of these neuropils per eye and in the crab, they are contained within the eye stalk [20]. Here, optical processing takes place before visual information is sent to the central supraesophageal ganglion [261]. It is therefore possible that the eyes can operate independently. Stowe [182] blinded one eye of *Leptograpsus* crabs with black paint to maintain it in darkness, while the other eye was exposed to light. On fixing the eyes and examining the rhabdoms, she found that the two eyes had reacted independently to the light, the painted eye becoming dark-adapted with larger rhabdoms, while the other remained fully light-adapted.

In the locust, masking a region of the eye from light with black tape a few hours before dusk will cause rhabdoms in those ommatidia to widen early to a dark-adapted state, while the light-exposed ommatidia of the same eye remain narrow [351] (Fig. 8.5). This shows that in the insect at least, individual ommatidia can respond independently to differing light intensities.

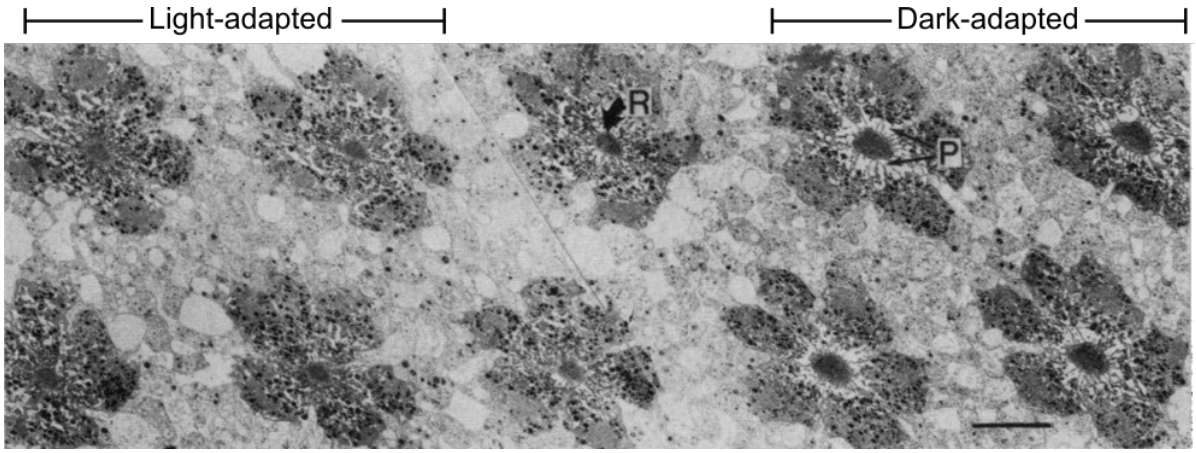

FIGURE 8.5. TEMs of 10 locust ommatidia in cross-section, 1 hour before dusk. Those on the left were exposed to light and have narrow rhabdoms (R). On the right, the ommatidia were masked with tape 4 hours previously and have the wide rhabdoms and prominant palisade (P) associated with dark-adapted eyes. Scale bar, 10 μm. Figure from ref: [351].

Fiddler crabs have a panoramic visual scene that varies greatly in its intensity, polarization and spectral properties. While one region of the eye is facing the sun and exposed to strong specular reflections from the substrate or water bodies, the other side of the same eye facing 180° away will have a much darker and more uniform view [114]. The sky also varies in brightness and its characteristics change with azimuth of the sun [352]. To what extent can individual ommatidia in the fiddler crab operate independently to cope with a panoramic scene that varies extremely in brightness? Masking part of an eye from light at dawn or dusk may extend, or prompt early dark-adaptation in that region of ommatidia. As the eye does not respond to dim light with physiological change during daylight hours, masking part of the eye around midday is unlikely to result in measurable change (as seen in locusts [351]) at this time. This may be useful for fiddler crabs, given that the eye must cope with panoramic scenes of varying brightness, which move across the compound eye as the animal walks. Temporal summations do take effect during daytime however (refer to chapter 4), and differences in photoreceptor membrane potentials may arise between eye regions exposed for several minutes to a scene with bright and dim regions. This could potentially be tested with electrophysiology using intracellular recordings from photoreceptors between opposite sides of the eye, with one side exposed to bright direct light, while the other side faces away from it.

8.2.4 Vision in orbital grooves

Fiddler crabs regularly lower their eyes into deep orbital grooves for cleaning and protection [113] (Fig. 8.6a). The eyes are lowered when entering the burrow and often in very dim conditions in the laboratory when the crab is inactive. If a crab is in a vulnerable situation and cannot escape a perceived predator, it will sometimes lower one or both eyes to protect them from harm. The lowered eyes sit horizontally at almost 90° to the normal upright position and the frontal portion of the eye is visible in the groove, presumably with a sideways view of the world. The view is blocked for the lateral eye, which is most sensitive to movement [302]. During foraging, fiddler crabs tend to maintain their body position so that they are sideways-on between their burrow and a potential predator, to enable the fastest possible threat-detection and escape [353]. It would be interesting to test if functional vision across the whole eye somehow switches off in an eye when lowered, potentially by a mechanism in the mobile eye stalk joint, which suppresses the neural signals coming from the optic lobes toward the supraesophageal ganglion when the eye folds down. This is perhaps a far-fetched idea, but maintaining eye position with respect to the horizon is clearly important to fiddler crabs [118], especially for polarization vision. Therefore it may be beneficial to suppress vision of lowered eyes to prevent a sideways, potentially disorientating view of surroundings when eyes are down.

Irrespective of body position, fiddler crabs tilt their eyes to orientate them vertically with respect the horizon [118] (Fig. 8.6b), attempting to maintain a stationary eye position in relation to their visual scene. Optokinetic eye movements associated with motion vision and motor control

in crabs are known to be synchronous between the two eyes in certain conditions [303, 305]. Visual cues (over statocystic and leg-proprioceptive information) are especially important to semiterrestrial flat-world crabs for compensatory eye position adjustments when moving through a habitat [304]. The strong eye coupling of yaw optokinetic movements (stimulated by a rotating visual stimulus) may be part of the same mechanism that controls vertical preference for eye orientation in the fiddler crab, using gaze-fixation on features of the horizon during locomotion to stabilise their own body position within their visual scene.

During experiments using the treadmill, I took one or two opportunities to test whether the eyes might lose visual function when fully lowered, when occasionally, a crab would sit motionless on top of the ball with both eyes lowered down into the orbital grooves. Presenting a high contrast loom to a crab at this time did appear to elicit a subtle sudden movement like a slight retraction of legs and claws. This would suggest that the frontal eye in its groove facing the direction of the looming stimulus was operational. However, this is based only on a couple of observations, no data were collected, so a proper controlled experiment might be designed to confirm this (using behavioural responses to high contrast and easily-detectable looming stimuli).

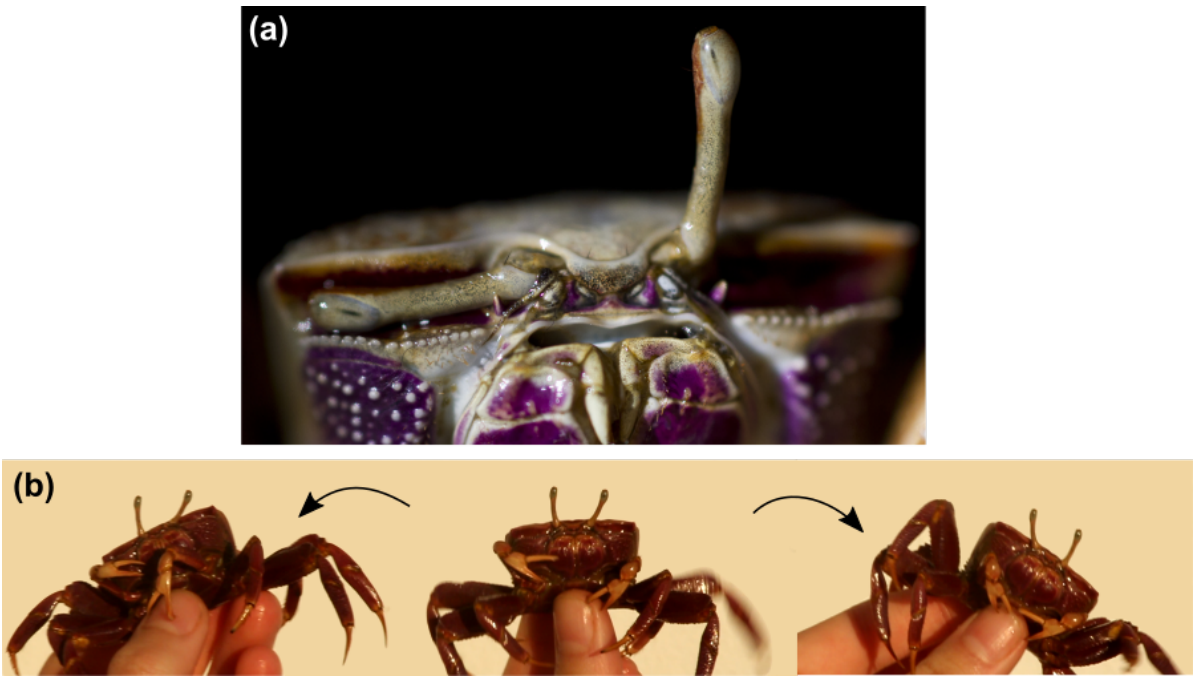

FIGURE 8.6. **(a)** Male fiddler crab (*A. tangeri*) with his right eye lowered into its orbital groove for cleaning. The frontal region of the eye faces out from within the groove. Photo by Kate Feller (2016), retrieved with permission. **(b)** A fiddler crab tries to keep her eyes orientated vertically with respect to the horizon as her body is titled side-to-side.

8.2.5 Changes in spatial and temporal resolution

Whether fiddler crabs use spatial summation as a dark-adaptation strategy was not investigated as part of my PhD work, so this question remains. A mechanism for this might exist in the first optic neuropil, int the form of laterally branching dendrites of the monopolar cells, as in hawkmoths, cockroaches and sweat bees [30, 34, 191, 198, 199]. Alternatively it may occur further downstream in tangential cells of the third optic neuropil, the lobula plate. This neuropil is thought to be conserved and analogous between crustaceans and insects [315, 316], and in the latter, it has been well studied and known to be heavily involved with motion detection and optomotor responses [354, 355]. In the fly at least, the lobula plate tangential cells integrate stimulation signals from neighbouring ommatidia in order to operate successfully in very dim light, which sacrifices spatial resolving power [317–319]. It would be interesting to test via optokinetic stimulation and electrophysiology (and perhaps anatomical examinations), whether a similar mechanism occurs in the fiddler crab. Potential effects of optical processes which increase acceptance angles of individual ommatidia [173, 214] may have to be unpicked when analysing the results however.

Slower temporal resolution in dim light improves absolute sensitivity of an eye by amplifying slow signals and removing fast ones. During phototransduction, the amplification given to each temporal frequency in a signal is determined by the membrane impedance of the photoreceptor cell membrane, which acts as a bandpass frequency filter [191]. Membrane impedance is a product of the capacitance and resistance properties of the cell membrane and can be dynamically altered by opening or closing K_v channels (trans-membrane voltage-activated potassium channels) [282, 321, 324, 325]. As well as controlling the bandwidth of the signal, the K_v channels open to repolarize the photoreceptor cell after a light-induced current [192, 320]. K_v channels have been studied in various flies, locust and *Limulus* photoreceptors [192, 282, 320, 322–325], however currently, we can only assume crabs have analogous mechanisms for switching between fast and slow vision. In the locust, the neurotransmitter serotonin operates with a circadian rhythm to moderate changes in K_v channels and membrane resistance [282]. From day to night, the membrane conductance changes from sustained to transient (inactivating), which shifts the photoreceptor activation speeds from fast to slow. In the fiddler crab *G. dampieri*, temporal summations can also come into effect during daytime as a dark-adaptation strategy (refer to chapter 4).

The majority of experiments on arthropod temporal resolution have compared between species that operate in different light environments, e.g. [192, 195, 250, 278], or have investigated differences between animals of the same species that had been pre-adapted to light or dark for long periods and/or compared between day and night, e.g. [199, 275, 356]. There are no studies (currently known to me) that have monitored responses over time as the compound eye of an animal adapts between bright and dark environments. Therefore, little is known about how long the shift in membrane potential (and thus temporal resolution strategy) takes to occur

and whether it is a sudden or gradual process. From the progressive increases in *G. dampieri* ERG responses over several minutes during dark-adaptation, in addition to gradual increase in behavioural response probability to low contrast looms in *A. tangeri* (chapter 5), a gradual change in membrane potential to improve sensitivity in dim light seems more likely. It makes sense for changes in membrane conductance to be gradual or delayed so that contrast sensitivity remains maximised for distinguishing differences in intensity within a visual scene. It would be very interesting to test the timescale of the membrane conductance changes using electrophysiology in the fiddler crab, although careful experimental design is necessary to ensure that stimulus light exposure does not compromise the desired adaptation state. If spatial integration is also used as a dark-adaptation strategy, the timescale of these changes also deserves investigation.

8.2.6 Polarization vision

The question remains whether strong horizontally-polarized reflections from the mudflat surface result in increased pinocytosis of horizontally-sensitive microvilli, relative to vertical. The oval shape of the rhabdoms in both bands mean any difference is likely to be slight. Serial blockface SEM would be the ideal examination technique, should new samples be successfully acquired. In addition, *in vivo* methods of testing disparity in sensitivity of polarization channels could be performed with ERG electrophysiology.

8.2.7 Colour vision

One of the most glaring areas of fiddler crab vision left to explore, is function of the R8 cell and capability for true colour vision. The small size and interweaving design of the R8 cell has made isolated study of it particularly difficult [18, 37], so its function is poorly understood in crabs. Analogous R8 cells commonly contribute a short region of the distal-most rhabdom across Malacostracan crustaceans [19]. Its rhabdom is not ordered to facilitate polarization sensitivity and it varies in length across the eye, being longest in equatorial regions, perhaps maintaining the same proportional length (personal observation from *A. tangeri*). Short wavelength (UV-blue) detection, UV filtering and polarization filtering functions have been proposed for R8 in other species [19].

It is likely that fiddler crabs do possess colour vision abilities (see Introduction, section 1.1.5 for full explanation). They appear to possess two or three classes of photoreceptor in each ommatidium perhaps depending on species, which contain opsins with different spectral sensitivity [37, 42, 44–47, 97]. It is typical that animals with multiple receptors have colour vision, however it is widely accepted that true colour vision must be demonstrated with animal behaviour [49]. Fiddler crabs are not ideal candidates for behavioural training or choice experiments, but a couple of studies trying to exploit phototaxis [55] and mating behaviours [39, 56] in species from the Gelasiminae subfamily have provided some evidence to suggest they can discriminate wavelengths and prefer certain colours. Convincing colour vision experiments can be notoriously

difficult to execute and intensity-matching requires excellent knowledge of the spectral sensitivity of receptors [49, 357]. This is especially challenging if their behavioural repertoire makes training to colours or choice tests unfeasible. Future experiments exploiting fiddler crabs' strong scare responses to a moving, especially looming stimulus may be the best approach. A looming stimulus in which the background and loom consist of different regions of dichromatic colour space could be adjusted until the two become totally isoluminant to the animal, testing whether the observer can separate its spectral composition from its overall intensity. To a monochromat, the two regions in the stimulus would become unresolvable at this contrast and they would not respond to it. Alternatively, the conspicuous optokinetic eye movements or full body optomotor responses to moving stripe gratings could be used, however, motion detection is often independent of colour vision [358–360], so this type of experiment may not be suitable.

Spectral sensitivity may shift during a 24-hour period due to screening pigments or optical properties of the light path. It would be interesting to investigate whether during daytime, the very narrow diameter (sometimes <800 nm) of the crystalline cone tip functions as a short-pass filter. Differential interference of red light, with wavelengths approaching the size of the narrow aperture, could result in blue-shifted spectral sensitivity when light-adapted. At night, acceptance angles widen to allow more light and longer wavelengths to reach the rhabdom with little interference. Perhaps this could cause a spectral sensitivity shift to longer (red) wavelengths. In *G. dampieri*, Jessop *et al.* [45] produced ERG data to support a 25 nm spectral shift, showing that longer wavelengths are detected more reliably by this crab in the evening, although their models (which included screening pigment migrations and opsin expression but no other optical changes) could not definitively explain why.

8.3 Final conclusions and research impacts

This PhD project made detailed examinations of the *A. tangeri* eye to identify the previously unknown anatomical mechanisms for light- and dark-adaptation in fiddler crabs, describing the circadian rhythms of rhabdom and crystalline cone changes between day and night. Details of these findings have been published in a peer-reviewed journal [214], providing scientists with some insight into how their visual systems respond to changes in light intensity and time of day. Previously, animals were often pre-adapted to light or dark for varying times before experiments without fully understanding the effects. This research has shown, for example, that temporarily exposing a dark-adapted fiddler crab to light during daytime, even for just 30 minutes, causes anatomical light-adaptation changes to occur in the eye that cannot be reversed during daylight hours, even after several hours in darkness. Thus, this crab with its narrow rhabdoms would have eyes that are significantly less sensitive than a crab that has not been exposed to any light that day, regardless of how long one dark-adapts them for prior to an experiment. This would likely result in significant differences in the spatial resolution,

ability to detect contrasts and ERG response amplitudes (etc.) of these animals. The insights gathered in this research means that it is possible to knowledgeably factor in this information and carefully control adaptation state, when conducting future experiments to test aspects of their vision. Complimentary behavioural experiments, in addition to ERGs (using *G. dampieri*), demonstrate the effect that the physiological adaptation states have on absolute and contrast sensitivity in fiddler crabs. They undergo great circadian changes in sensitivity from day to night. An ERG experiment also revealed use of temporal summations, resulting in slower vision at night and when dark-adapted, which accounts for some of the sensitivity increases that could not be explained by changes in physiology of the ommatidia. There are still plenty of research questions left to explore in order to advance this field of research and gain a better insight into how these animals see the world.

APPENDIX

ADDITIONAL DATA

Table A.1: Mean measurements of the lower crystalline cone tract area in cross-section for each crab. The diameter of the pupillary opening between primary pigment cells (surrounding an aperture), is also shown as measurements of shortest distance between pigment granules from opposite pigment cells, data also shown in chapter 3.

Crab ID	Treatment	Mean aperture area of CC (μm²)	Shortest distance between pigment granules (μm)
217	Day Light-adapted	1.18	6.19
223	Day Light-adapted	4.29	5.66
435	Day Light-adapted	3.64	5.21
436	Day Light-adapted	2.68	5.32
437	Day Light-adapted	3.37	6.58
438	Day Light-adapted	2.08	5.58
307	Midnight Light-adapted	6.23	6.32
308	Midnight Light-adapted	3.98	5.61
431	Midnight Light-adapted	5.84	5.21
432	Midnight Light-adapted	9.10	6.03
433	Midnight Light-adapted	6.55	6.38
434	Midnight Light-adapted	6.17	6.71
211	Day Dark-adapted	4.26	5.08
425	Day Dark-adapted	3.34	6.15
426	Day Dark-adapted	5.49	6.15
427	Day Dark-adapted	3.93	6.23
428	Day Dark-adapted	6.30	6.54
429	Day Dark-adapted	8.18	6.77
305	Midnight Dark-adapted	26.01	8.15
306	Midnight Dark-adapted	20.28	4.74
319	Midnight Dark-adapted	12.14	6.70
320	Midnight Dark-adapted	28.58	8.28
321	Midnight Dark-adapted	22.85	7.47
324	Midnight Dark-adapted	15.55	6.52

Table A.2: Mean cross-sectional area of rhabdoms in *A. tangeri* individuals under four adaptation states. Data also shown in chapter 3.

Crab ID	Treatment	Mean rhabdom area (μm²)
116	Day Light-adapted	3.18
118	Day Light-adapted	2.98
119	Day Light-adapted	2.84
108	Day Light-adapted	3.64
109	Day Light-adapted	2.74
110	Day Light-adapted	3.20
217	Day Light-adapted	4.04
435	Day Light-adapted	3.49
105	Midnight Light-adapted	4.18
106	Midnight Light-adapted	4.19
107	Midnight Light-adapted	3.68
307	Midnight Light-adapted	3.82
308	Midnight Light-adapted	3.89
309	Midnight Light-adapted	4.10
431	Midnight Light-adapted	4.53
432	Midnight Light-adapted	5.66
114	Day Dark-adapted	8.00
211	Day Dark-adapted	5.79
310	Day Dark-adapted	6.16
115	Day Dark-adapted	6.97
023	Day Dark-adapted	7.86
028	Day Dark-adapted	8.12
031	Day Dark-adapted	6.01
425	Day Dark-adapted	7.54
104	Midnight Dark-adapted	20.88
111	Midnight Dark-adapted	12.47
112	Midnight Dark-adapted	16.25
113	Midnight Dark-adapted	13.46
306	Midnight Dark-adapted	18.05
319	Midnight Dark-adapted	25.24
320	Midnight Dark-adapted	17.64
321	Midnight Dark-adapted	23.33

Table A.3: Measurements of the frontal-posterior and medial-lateral diameters of two eyes from X-ray synchrotron tomographs at seven angles of elevation. The eyes were of very similar overall dimensions. Data from chapter 3.

Degree of elevation (°)	**Measurement**	**Light-adapted Midday (µm)**	**Dark-adapted Midnight (µm)**
	Vertical length	2839	3079
67	Fro-Pos	1516	1539
	Med-Lat	1612	1548
51	Fro-Pos	1772	1775
	Med-Lat	1849	1860
30	Fro-Pos	1877	1905
	Med-Lat	1928	1985
0	Fro-Pos	1917	1940
	Med-Lat	1920	1980
-30	Fro-Pos	1883	1903
	Med-Lat	1811	1900
-47	Fro-Pos	1805	1804
	Med-Lat	1676	1768
-63	Fro-Pos	1693	1606
	Med-Lat	1514	1685
	Mean diameter	**1770**	**1800**
	SD	**145**	**153**

FIGURE A.1. The image depicts Stimulus E with Weber contrast -0.311 used in the behavioural looming stimulus experiments of chapters 4 and 5. While the black circle in the centre was initially not visible to 60% of light-adapted crabs during daytime, it could be quite easily be detected by the human eye when displayed on the experimental LCD monitor, even when light-adapted in a bright room. If viewed on a computer monitor rather than print (depending on your screen settings), you may be able to detect the black disk in the centre. This suggests that the fiddler crab eye is very insensitive to dim light (relative to the human eye) when light-adapted during daylight hours.

Table A.4: Summarised results of the optokinetic response experiment of chapter 5. Data for mean number of optokinetic responses ± standard deviation are shown for crabs pooled into groups according to number of minutes they were dark-adapted prior to their turn in the experiment. Number of individuals (n) are indicated for each group. These data are illustrated in Fig. 5.14b.

Minutes dark-adapted	***n***	**No. optokinetic responses**
0, light-adapted	32	20.2 ± 3.9
1 to 15	11	19.2 ± 3.9
16 to 30	14	15.4 ± 6.2
31 to 45	14	14.6 ± 5.2
46 to 60	16	11.7 ± 5.9
61 to 75	14	11.3 ± 4.3
76 to 90	17	12.8 ± 3.9
91 to 105	13	8.8 ± 5.4
106 to 120	11	10.2 ± 4.5
121 to 135	13	9.3 ± 3.8
136 to 150	16	10.6 ± 4.0
151 to 165	14	8.7 ± 4.0
166 to 180	13	9.7 ± 5.3
Fully dark-adapted	30	5.3 ± 3.8

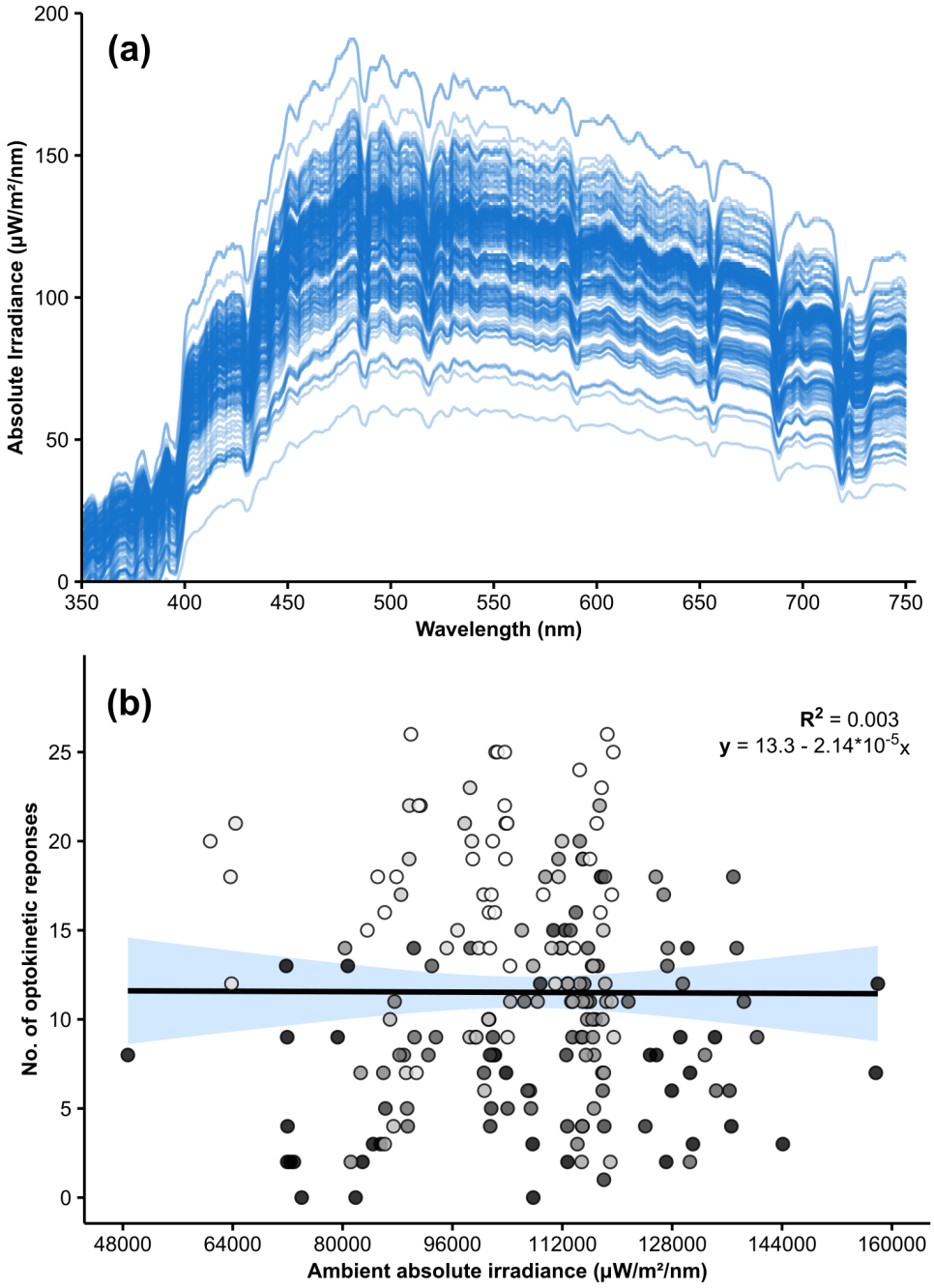

FIGURE A.2. **(a)** Absolute irradiance spectra for ambient light measurements (under bright skies) taken during each fiddler crab's optokinetic response test, see chapter 5. **(b)** Number of optokinetic responses plotted against the total irradiance measured during each individual crab's experiment. Regression line (with blue shade for standard error) and a R^2 value of 0.003, show that there was no correlation between the two variables. Points are shaded from white (light-adapted) to dark according to how long they were dark-adapted prior to experiments.

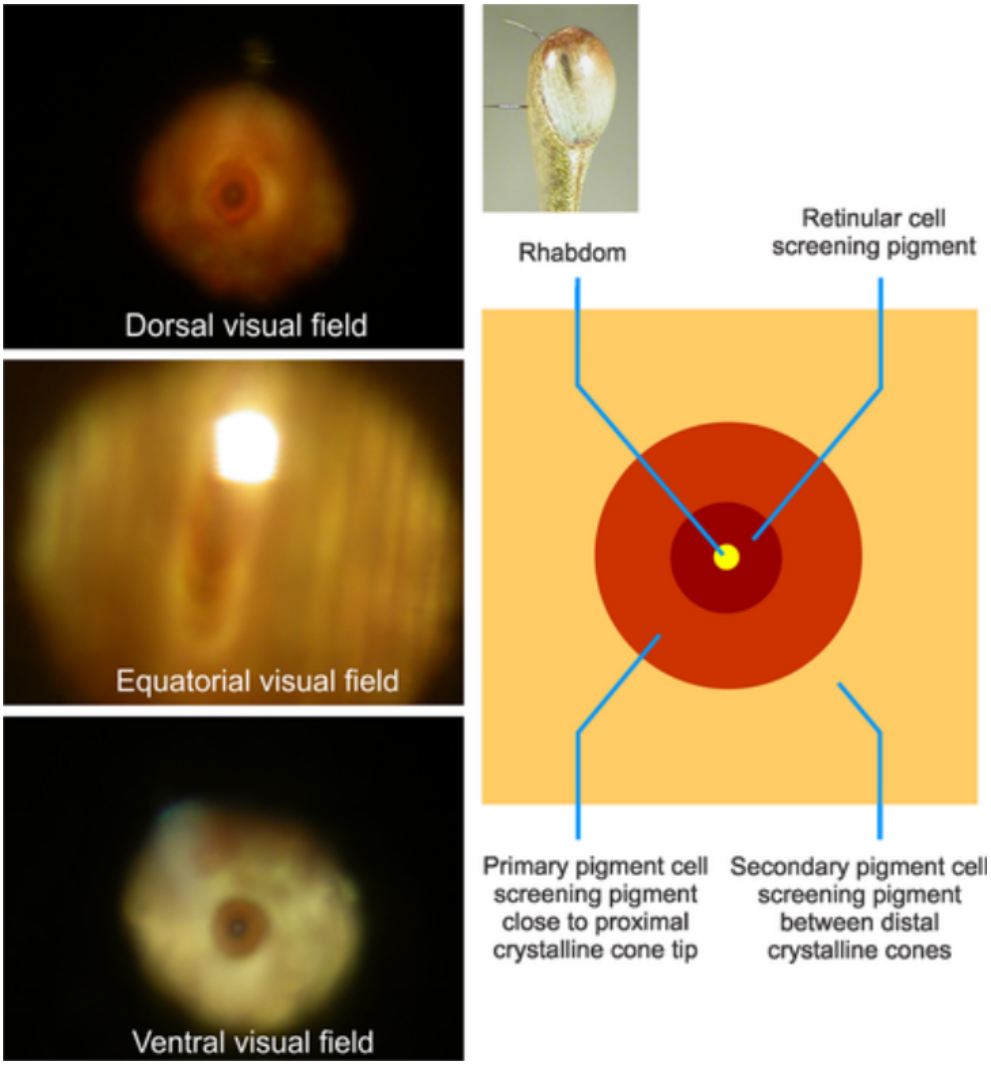

FIGURE A.3. The deep pseudopupil of dorsal, ventral and equatorial eye regions in *G. vomeris*, imaged with ophthalmoscopy by Alkaladi & Zeil in their Fig. 14, ref: [89]. Note the chromatic differences in screening pigments and the strong clarity and definition of the cell regions in the dorsal and ventral eye, compared to the more blurred-looking elongated pseudopupil at the eye equator.

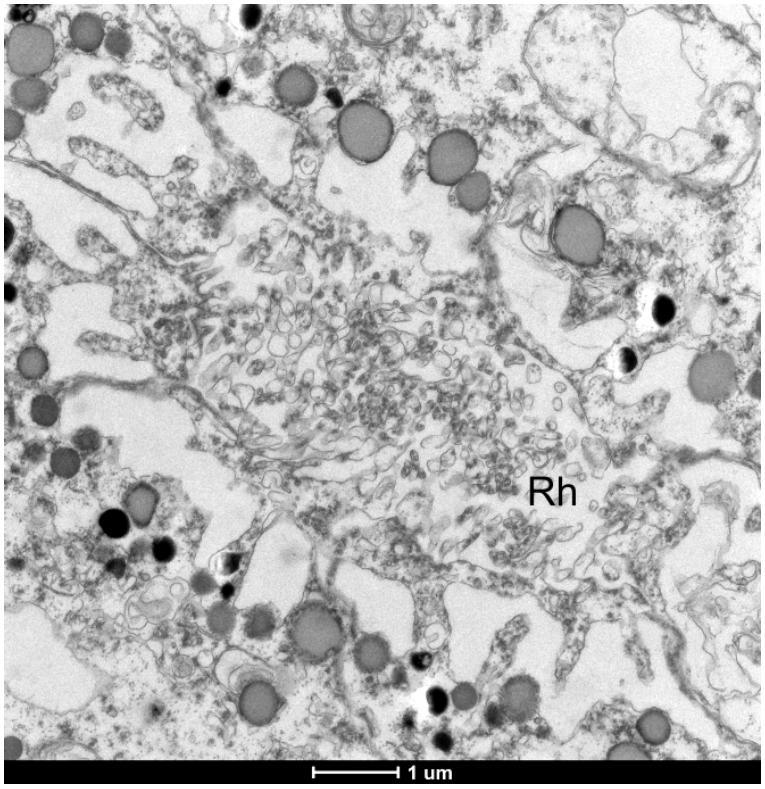

FIGURE A.4. Example TEM of a rhabdom (Rh) of a crab exposed to horizontally-polarized light (Group 1) in the chapter 7 experiment. Gill desiccation during the experiment in crabs adapted behind polarizing filter meant that the cells in the eye tissues were not healthy at the time of fixation, showing signs of apoptosis. As a result, the nine affected samples had to be excluded from the data set.

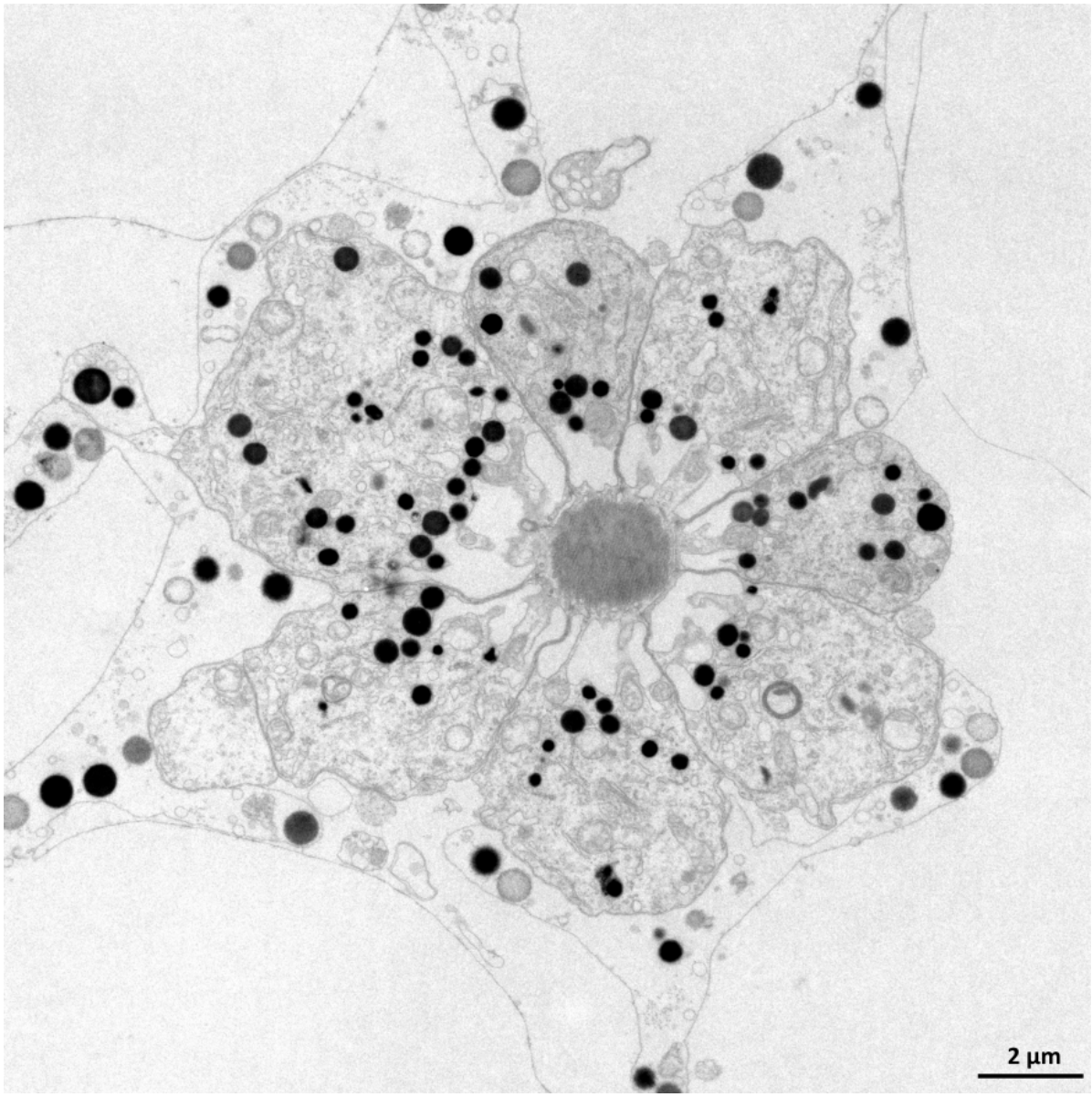

FIGURE A.5. One of my nicest TEM images showing an ommatidium in transverse section from a dark-adapted *A. tangeri* crab (midday).

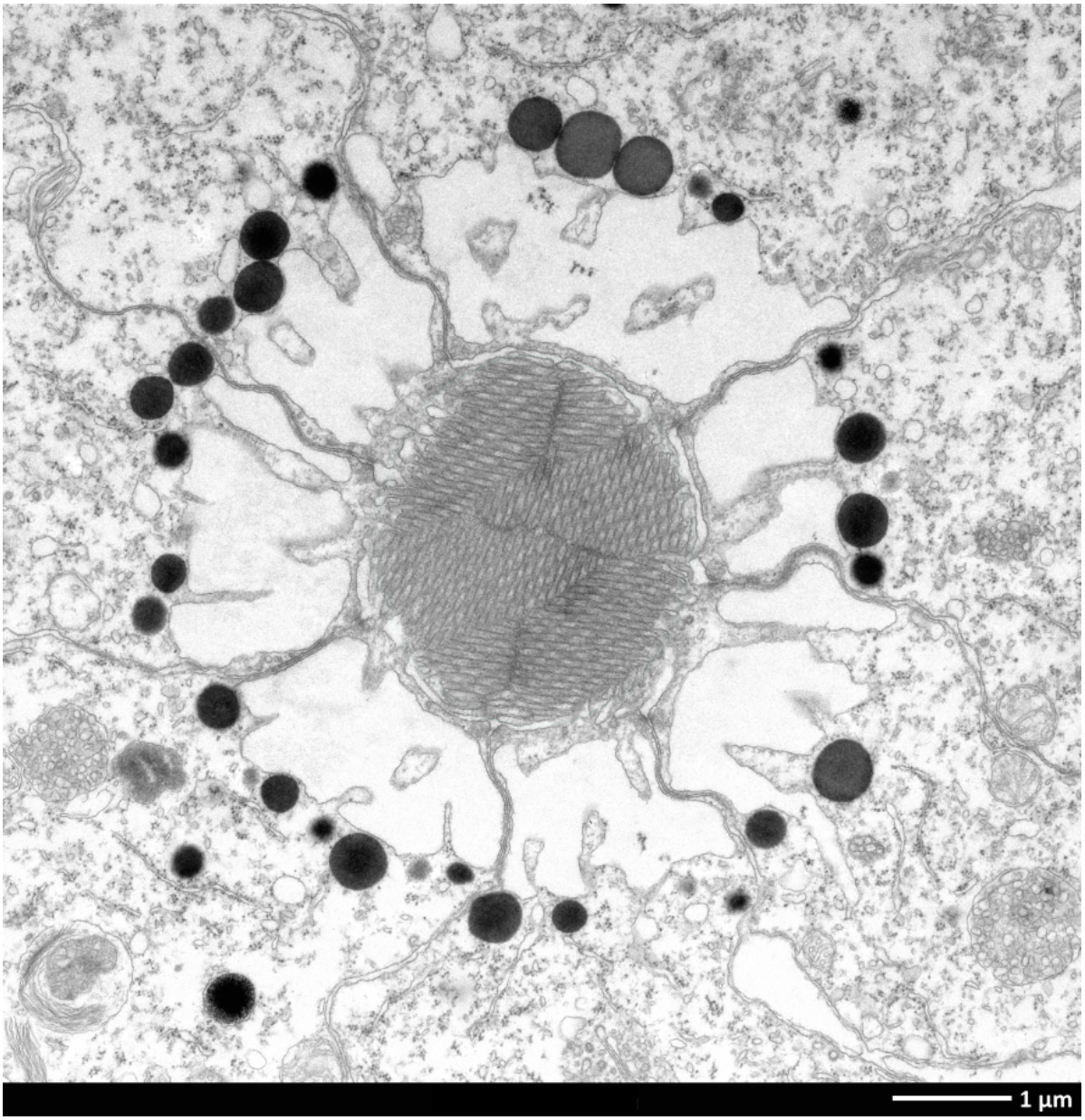

FIGURE A.6. Another one of my favourite TEM images showing a rhabdom surrounded by palisade vacuole and pigment granules in transverse section from a dark-adapted *A. tangeri* crab (midday).

References

[1] Schoenemann, B., Pärnaste, H. and Clarksond, E. N. [2017], Structure and function of a compound eye, more than half a billion years old, *Proceedings of the National Academy of Sciences of the United States of America* **114**(51), 13489–13494.

[2] Stansbury, M. S. and Moczek, A. P. [2013], The evolvability of arthropods, *in* Arthropod Biology and Evolution: Molecules, Development, Morphology, Springer-Verlag Berlin Heidelberg, pp. 479–493.

[3] Sliney, D. H. [2016], What is light? The visible spectrum and beyond, *Eye* **30**(2), 222–229.

[4] Cronin, T. W. and Bok, M. J. [2016], Photoreception and vision in the ultraviolet, *Journal of Experimental Biology* **219**(18), 2790–2801.

[5] Dimitrova, T. L. and Weis, A. [2008], The wave-particle duality of light: A demonstration experiment, *American Journal of Physics* **76**(2), 137–142.

[6] Johnsen, S. [2012], *The Optics of Life: A Biologist's Guide to Light in Nature*, Princeton University Press, Princeton.

[7] Land, M. F. and Nilsson, D.-E. [2012], *Animal Eyes*, Oxford University Press, Oxford, UK.

[8] Nilsson, D. E. [1988], A new type of imaging optics in compound eyes, *Nature* **332**(6159), 76–78.

[9] Warrant, E. and Dacke, M. [2011], Vision and visual navigation in nocturnal insects, *Annual Review of Entomology* **56**(1), 239–254.

[10] Horridge, A. [2005], The spatial resolutions of the apposition compound eye and its neurosensory feature detectors: observation versus theory, *Journal of Insect Physiology* **51**, 243–266.

[11] Barlow, H. B. [1952], The size of ommatidia in apposition eyes, *Journal of Experimental Biology* **29**(4), 667–674.

[12] Yau, K. W. and Hardie, R. C. [2009], Phototransduction motifs and variations, *Cell* **139**(2), 246–264.

[13] Ranganathan, R., Harris, W. A. and Zuker, C. S. [1991], The molecular genetics of invertebrate phototransduction, *Trends in Neurosciences* **14**(11), 486–493.

[14] Terakita, A. [2005], The opsins, *Genome Biology* **6**(3), 213.

[15] Shichida, Y. and Matsuyama, T. [2009], Evolution of opsins and phototransduction, *Philosophical Transactions of the Royal Society B: Biological Sciences* **364**(1531), 2881–2895.

[16] Tsukamoto, H. and Terakita, A. [2010], Diversity and functional properties of bistable pigments, *Photochemical and Photobiological Sciences* **9**(11), 1435–1443.

[17] Briscoe, A. D. and Chittka, L. [2001], The evolution of color vision in insects, *Annual Review of Entomology* **46**(1), 471–510.

[18] Cronin, T. W. and Forward, R. B. [1988], The visual pigments of crabs - I. Spectral characteristics, *Journal of Comparative Physiology A* **162**(4), 463–478.

[19] Marshall, J. and Cronin, T. W. [2014], Polarization vision in crustaceans, *in* G. Horváth, ed., Polarized Light and Polarization Vision in Animal Sciences, Second Edition, Springer-Verlag Berlin Heidelberg, pp. 1–649.

[20] Sztarker, J., Strausfeld, N., Andrew, D. and Tomsic, D. [2009], Neural organization of first optic neuropils in the littoral crab *Hemigrapsus oregonensis* and the semiterrestrial species *Chasmagnathus granulatus*, *Journal of Comparative Neurology* **513**(2), 129–150.

[21] Chase, R. [1975], The electrophysiology of transduction, retinal interaction and axonal conduction in invertebrate photoreceptors, *Comparative Biochemistry and Physiology Part A: Physiology* **52**(4), 571–576.

[22] Laughlin, S. B. and Lillywhite, P. G. [1982], Intrinsic noise in locust photoreceptors, *The Journal of Physiology* **332**(1), 25–45.

[23] Belusic, G. [2011], ERG in Drosophila, *in* Electroretinograms, InTechOpen. Accessed on 06/08/2020, from: https://www.intechopen.com/books/electroretinograms/erg-in-drosophila.

[24] Stavenga, D. G. and Hardie, R. C. [2011], Metarhodopsin control by arrestin, light-filtering screening pigments, and visual pigment turnover in invertebrate microvillar photoreceptors, *Journal of Comparative Physiology A: Neuroethology, Sensory, Neural, and Behavioral Physiology* **197**(3), 227–241.

[25] Snyder, A. W., Stavenga, D. G. and Laughlin, S. B. [1977], Spatial information capacity of compound eyes, *Journal of Comparative Physiology A* **116**(2), 183–207.

[26] Parag, K. V. and Vinnicombe, G. [2017], Point process analysis of noise in early invertebrate vision, *PLoS Computational Biology* **13**(10), e1005687.

[27] Field, G. D., Sampath, A. P. and Rieke, F. [2005], Retinal processing near absolute threshold: From behavior to mechanism, *Annual Review of Physiology* **67**(1), 491–514.

[28] Pelli, D. G. and Bex, P. [2013], Measuring contrast sensitivity, *Vision Research* **90**, 10–14.

[29] O'Carroll, D. C. and Wiederman, S. D. [2014], Contrast sensitivity and the detection of moving patterns and features, *Philosophical Transactions of the Royal Society B: Biological Sciences* **369**(1636).

[30] Warrant, E. J. [2017], The remarkable visual capacities of nocturnal insects: Vision at the limits with small eyes and tiny brains, *Philosophical Transactions of the Royal Society B: Biological Sciences* **372**(1717).

[31] Eisen-Enosh, A., Farah, N., Burgansky-Eliash, Z., Polat, U. and Mandel, Y. [2017], Evaluation of critical flicker-fusion frequency measurement methods for the investigation of visual temporal resolution, *Scientific Reports* **7**(1), 1–9.

[32] Roberts, N. W., Porter, M. L. and Cronin, T. W. [2011], The molecular basis of mechanisms underlying polarization vision, *Philosophical Transactions of the Royal Society B: Biological Sciences* **366**(1565), 627–637.

[33] Foster, J. J., Temple, S. E., How, M. J., Daly, I. M., Sharkey, C. R., Wilby, D. and Roberts, N. W. [2018], Polarisation vision: overcoming challenges of working with a property of light we barely see, *Science of Nature* **105**(3-4).

[34] Warrant, E. J. [1999], Seeing better at night: Life style, eye design and the optimum strategy of spatial and temporal summation, *Vision Research* **39**(9), 1611–1630.

[35] Stöckl, A., Smolka, J., O'carroll, D. and Warrant, E. [2017], Resolving the trade-off between visual sensitivity and spatial acuity- Lessons from hawkmoths, *Integrative and Comparative Biology* **57**(5), 1093–1103.

[36] Gonzalez-Bellido, P. T., Wardill, T. J. and Juusola, M. [2011], Compound eyes and retinal information processing in miniature dipteran species match their specific ecological demands, *Proceedings of the National Academy of Sciences of the United States of America* **108**(10), 4224–4229.

[37] Jordao, J. M., Cronin, T. W. and Oliveira, R. F. [2007], Spectral sensitivity of four species of fiddler crabs (*Uca pugnax, Uca pugilator, Uca vomeris* and *Uca tangeri*) measured by *in situ* microspectrophotometry, *Journal of Experimental Biology* **210**(3), 447–453.

[38] Stavenga, D., Smits, R. and Hoenders, B. [1993], Simple exponential functions describing the absorbance bands of visual pigment spectra, *Vision Research* **33**(8), 1011–1017.

[39] Detto, T. [2007], The fiddler crab *Uca mjoebergi* uses colour vision in mate choice, *Proceedings of the Royal Society B: Biological Sciences* **274**(1627), 2785–2790.

[40] Johnson, M. L., Gaten, E. and Shelton, P. M. [2002], Spectral sensitivities of five marine decapod crustaceans and a review of spectral sensitivity variation in relation to habitat, *Journal of the Marine Biological Association of the United Kingdom* **82**(5), 835–842.

[41] Martin, F. G. and Mote, M. I. [1982], Color receptors in marine crustaceans: A second spectral class of retinular cell in the compound eyes of *Callinectes* and *Carcinus*, *Journal of Comparative Physiology A* **145**(4), 549–554.

[42] Falkowski, M. [2017], The spectral and temporal properties of fiddler crab photoreceptors in the context of predator avoidance, PhD thesis, The University of Western Australia.

[43] Smolka, J. [2009], Sampling visual space: topography, colour vision and visually guided predator avoidance in fiddler crabs (*Uca vomeris*), PhD thesis, The Australian National University.

[44] Horch, K., Salmon, M. and Forward, R. [2002], Evidence for a two pigment visual system in the fiddler crab, *Uca thayeri*, *Journal of Comparative Physiology A: Neuroethology, Sensory, Neural, and Behavioral Physiology* **188**(6), 493–499.

[45] Jessop, A.-L., Ogawa, Y., Bagheri, Z. M., Partridge, J. C. and Hemmi, J. M. [2020], Photoreceptors and diurnal variation in spectral sensitivity in the fiddler crab *Gelasimus dampieri*, *The Journal of Experimental Biology* p. jeb.230979.

[46] Rajkumar, P., Rollmann, S. M., Cook, T. A. and Layne, J. E. [2010], Molecular evidence for color discrimination in the Atlantic sand fiddler crab, *Uca pugilator*, *The Journal of Experimental Biology* **213**(Pt 24), 4240–8.

[47] Alkaladi, A. S. [2008], The functional anatomy of the fiddler crab compound eye, PhD thesis, Australian National University.

[48] Cronin, T. W., Johnsen, S. N., Marshall, J. and Warrant, E. J. [2014], *Visual Ecology*, Princeton University Press.

[49] Kelber, A., Vorobyev, M. and Osorio, D. [2003], Animal colour vision - Behavioural tests and physiological concepts, *Biological Reviews of the Cambridge Philosophical Society* **78**(1), 81–118.

[50] Crane, J. [1975], *Fiddler Crabs of the World : Ocypodidae : Genus Uca*, Princeton University Press, New Jersey.

[51] Hemmi, J. M., Marshall, J., Pix, W., Vorobyev, M. and Zeil, J. [2006], The variable colours of the fiddler crab *Uca vomeris* and their relation to background and predation, *Journal of Experimental Biology* **209**(20), 4140–4153.

[52] Zeil, J. and Hofmann, M. [2001], Signals from 'crabworld': cuticular reflections in a fiddler crab colony, *Journal of Experimental Biology* **204**(14).

[53] Detto, T., Hemmi, J. M. and Backwell, P. R. Y. [2008], Colouration and colour changes of the fiddler crab, *Uca capricornis*: A descriptive study, *PLoS ONE* **3**(2), e1629.

[54] Cummings, M. E., Jordão, J. M., Cronin, T. W. and Oliveira, R. F. [2008], Visual ecology of the fiddler crab, *Uca tangeri:* effects of sex, viewer and background on conspicuousness, *Animal Behaviour* **75**(1), 175–188.

[55] Hyatt, G. W. [1974], Behavioural evidence for light intensity discrimination by the fiddler crab, *Uca pugilator* (Brachyura, Ocypodidae), *Animal Behaviour* **22**(4), 796–801.

[56] Dyson, M. L., Perez, D. M., Curran, T., McCullough, E. L. and Backwell, P. R. [2020], The role of claw color in species recognition and mate choice in a fiddler crab, *Behavioral Ecology and Sociobiology* **74**(10), 1–11.

[57] Strutt, J. [1871], On the light from the sky, its polarization and colour, *The London, Edinburgh, and Dublin Philosophical Magazine and Journal of Science* **41**(271), 107–120.

[58] Horváth, G., Barta, A. and Hegedüs, R. [2014], Polarization of the sky, *in* Polarized Light and Polarization Vision in Animal Sciences, Second Edition, Springer Berlin Heidelberg, pp. 367–406.

[59] Pfeiffer, K., Negrello, M. and Homberg, U. [2011], Conditional perception under stimulus ambiguity: Polarization- and azimuth-sensitive neurons in the locust brain are inhibited by low degrees of polarization, *Journal of Neurophysiology* **105**(1), 28–35.

[60] Temple, S. E., McGregor, J. E., Miles, C., Graham, L., Miller, J., Buck, J., Scott-Samuel, N. E. and Roberts, N. W. [2015], Perceiving polarization with the naked eye: Characterization of human polarization sensitivity, *Proceedings of the Royal Society B: Biological Sciences* **282**(1811), 1–9.

[61] Hawryshyn, C. W. [2010], Ultraviolet polarization vision and visually guided behavior in fishes, *Brain, Behavior and Evolution* **75**(3), 186–194.

[62] Novales Flamarique, I. [2019], Swimming behaviour tunes fish polarization vision to double prey sighting distance, *Scientific Reports* **9**(1), 1–8.

[63] Dacke, M., Doan, T. A. and O'Carroll, D. C. [2001], Polarized light detection in spiders, *Journal of Experimental Biology* **204**(14), 2481–2490.

[64] Shashar, N. [2014], Polarization vision in cephalopods, *in* Polarized Light and Polarization Vision in Animal Sciences, Second Edition, Springer Berlin Heidelberg, pp. 217–224.

[65] Muheim, R. [2011], Behavioural and physiological mechanisms of polarized light sensitivity in birds, *Philosophical Transactions of the Royal Society B: Biological Sciences* **366**(1565), 763–771.

[66] Horváth, G. [2014], *Polarized Light and Polarization Vision in Animal Sciences, Second edition*, Springer Berlin Heidelberg.

[67] How, M. J., Christy, J. H., Temple, S. E., Hemmi, J. M., Justin Marshall, N. and Roberts, N. W. [2015], Target detection is enhanced by polarization vision in a fiddler crab, *Current Biology* **25**(23), 3069–3073.

[68] Smithers, S. P., Roberts, N. W. and How, M. J. [2019], Parallel processing of polarization and intensity information in fiddler crab vision, *Science Advances* **5**(8).

[69] How, M. J., Pignatelli, V., Temple, S. E., Marshall, N. J. and Hemmi, J. M. [2012], High e-vector acuity in the polarisation vision system of the fiddler crab *Uca vomeris*, *Journal of Experimental Biology* **215**(12), 2128–2134.

[70] Schwind, R. [1989], A variety of insects are attracted to water by reflected polarized light, *Naturwissenschaften* **76**(8), 377–378.

[71] Kriska, G., Bernáth, B., Farkas, R. and Horváth, G. [2009], Degrees of polarization of reflected light eliciting polarotaxis in dragonflies (*Odonata*), mayflies (*Ephemeroptera*) and tabanid flies (*Tabanidae*), *Journal of Insect Physiology* **55**(12), 1167–1173.

[72] Sharkey, C. R., Partridge, J. C. and Roberts, N. W. [2015], Polarization sensitivity as a visual contrast enhancer in the Emperor dragonfly larva, *Anax imperator*, *Journal of Experimental Biology* **218**(21), 3399–3405.

[73] Johnsen, S., Marshall, N. J. and Widder, E. A. [2011], Polarization sensitivity as a contrast enhancer in pelagic predators: Lessons from *in situ* polarization imaging of transparent zooplankton, *Philosophical Transactions of the Royal Society B: Biological Sciences* **366**(1565), 655–670.

[74] Dacke, M. [2014], Polarized light orientation in ball-rolling dung beetles, *in* Polarized Light and Polarization Vision in Animal Sciences, Second Edition, Springer Berlin Heidelberg, pp. 27–39.

[75] Wehner, R. and Müller, M. [2006], The significance of direct sunlight and polarized skylight in the ant's celestial system of navigation, *Proceedings of the National Academy of Sciences of the United States of America* **103**(33), 12575–12579.

[76] Homberg, U., Heinze, S., Pfeiffer, K., Kinoshita, M. and El Jundi, B. [2011], Central neural coding of sky polarization in insects, *Philosophical Transactions of the Royal Society B: Biological Sciences* **366**(1565), 680–687.

[77] Kraft, P., Evangelista, C., Dacke, M., Labhart, T. and Srinivasan, M. V. [2011], Honeybee navigation: Following routes using polarized-light cues, *Philosophical Transactions of the Royal Society B: Biological Sciences* **366**(1565), 703–708.

[78] Cronin, T. W. [2018], A different view: sensory drive in the polarized-light realm, *Current Zoology* **64**(4), 513–523.

[79] Chiou, T. H., Mäthger, L. M., Hanlon, R. T. and Cronin, T. W. [2007], Spectral and spatial properties of polarized light reflections from the arms of squid (*Loligo pealeii*) and cuttlefish (*Sepia officinalis* L.), *Journal of Experimental Biology* **210**(20), 3624–3635.

[80] Izumi, M., Sweeney, A. M., DeMartini, D., Weaver, J. C., Powers, M. L., Tao, A., Silvas, T. V., Kramer, R. M., Crookes-Goodson, W. J., Mäthger, L. M., Naik, R. R., Hanlon, R. T. and Morse, D. E. [2010], Changes in reflectin protein phosphorylation are associated with dynamic iridescence in squid, *Journal of The Royal Society Interface* **7**(44), 549–560.

[81] Messenger, J. B. [1977], Evidence that *Octopus* is colour blind, *Journal of Experimental Biology* **70**(1), 49–55.

[82] Mäthger, L. M., Barbosa, A., Miner, S. and Hanlon, R. T. [2006], Color blindness and contrast perception in cuttlefish (*Sepia officinalis*) determined by a visual sensorimotor assay, *Vision Research* **46**(11), 1746–1753.

[83] Templin, R. M., How, M. J., Roberts, N. W., Chiou, T. H. and Marshall, J. [2017], Circularly polarized light detection in stomatopod crustaceans: A comparison of photoreceptors and possible function in six species, *Journal of Experimental Biology* **220**(18), 3222–3230.

[84] Gagnon, Y. L., Templin, R. M., How, M. J. and Justin Marshall, N. [2015], Circularly polarized light as a communication signal in mantis shrimps, *Current Biology* **25**(23), 3074–3078.

[85] Chiou, T.-H., Cronin, T. W., Caldwell, R. L. and Marshall, J. [2005], Biological polarized light reflectors in stomatopod crustaceans, *in* J. A. Shaw and J. S. Tyo, eds, Polarization Science and Remote Sensing II, SPIE.

[86] Sweeney, A., Jiggins, C. and Johnsen, S. [2003], Polarized light as a butterfly mating signal, *Nature* **423**(6935), 31–32.

[87] Chiou, T. H., Kleinlogel, S., Cronin, T., Caldwell, R., Loeffler, B., Siddiqi, A., Goldizen, A. and Marshall, J. [2008], Circular polarization vision in a stomatopod crustacean, *Current Biology* **18**(6), 429–434.

[88] Labhart, T. [2016], Can invertebrates see the e-vector of polarization as a separate modality of light?, *Journal of Experimental Biology* **219**(24), 3844–3856.

[89] Alkaladi, A. and Zeil, J. [2014], Functional anatomy of the fiddler crab compound eye (*Uca vomeris*: Ocypodidae, Brachyura, Decapoda), *Journal of Comparative Neurology* **522**(6), 1264–1283.

[90] Glantz, R. M. and Schroeter, J. P. [2006], Polarization contrast and motion detection, *Journal of Comparative Physiology A: Neuroethology, Sensory, Neural, and Behavioral Physiology* **192**(9), 905–914.

[91] Shih, H. T., Ng, P. K., Davie, P. J., Schubart, C. D., Türkay, M., Naderloo, R. and Jones, D. [2016], Systematics of the family Ocypodidae Rafinesque, 1815 (Crustacea: Brachyura), based on phylogenetic relationships, with a reorganization of subfamily rankings and a review of the taxonomic status of *Uca* Leach, 1814, *sensu lato* and its subgenera, *Raffles Bulletin of Zoology* **64**, 139–175.

[92] Rosenberg, M. S. [2019], A fresh look at the biodiversity lexicon for fiddler crabs (Decapoda: Brachyura: Ocypodidae). Part 1: Taxonomy, *Journal of Crustacean Biology* **39**(6), 729–738.

[93] Jordão, J. M. and Oliveira, R. F. [2001], Sex differences in predator evasion in the fiddler crab *Uca tangeri* (Decapoda: Ocypodidae), *Journal of Crustacean Biology* **21**(4), 948–953.

[94] Backwell, P. R., Matsumasa, M., Double, M., Roberts, A., Murai, M., Keogh, J. S. and Jennions, M. D. [2007], What are the consequences of being left-clawed in a predominantly right-clawed fiddler crab?, *Proceedings of the Royal Society B: Biological Sciences* **274**(1626), 2723–2729.

[95] Oliveira, R. and Custódio, M. [1998], Claw size, waving display and female choice in the European fiddler crab, *Uca tangeri*, *Ethology Ecology & Evolution* **10**(3), 241–251.

[96] Dennenmoser, S. and Christy, J. H. [2013], The design of a beautiful weapon: Compensation for opposing sexual selection on a trait with two functions, *Evolution* **67**(4), 1181–1188.

[97] Smolka, J. and Hemmi, J. M. [2009], Topography of vision and behaviour, *Journal of Experimental Biology* **212**(21), 3522–3532.

[98] Wolfrath, B. [1992], Field experiments on feeding of European fiddler crab *Uca tangeri*, *Marine Ecology Progress Series* **90**(1), 39–43.

[99] Ens, B., Klaassen, M. and Zwarts, L. [1993], Flocking and feeding in the fiddler crab (*Uca tangeri*): Prey availability as risk-taking behaviour, *Netherlands Journal of Sea Research* **31**(4), 477–494.

[100] DeRivera, C. E. and Vehrencamp, S. L. [2001], Male versus female mate searching in fiddler crabs: A comparative analysis, *Behavioral Ecology* **12**(2), 182–191.

[101] Christy, J. H. [2007], Predation and the reproductive behavior of fiddler crabs (Genus *Uca*), *in* Evolutionary Ecology of Social and Sexual Systems: Crustaceans as Model Organisms, Oxford University Press.

[102] Oliveira, R. F., McGregor, P. K., Burford, F. R., Custódio, M. R. and Latruffe, C. [1998], Functions of mudballing behaviour in the European fiddler crab *Uca tangeri*, *Animal Behaviour* **55**(5), 1299–1309.

[103] Latruffe, C., McGregor, P. K. and Oliveira, R. F. [1999], Visual signalling and sexual selection in male fiddler crabs *Uca tangeri*, *Marine Ecology Progress Series* **189**, 233–240.

[104] Nakasone, Y. and Murai, M. [1998], Mating behavior of *Uca lactea perplexa* (Decapoda: Ocypodidae), *Journal of Crustacean Biology* **18**(1), 70–77.

[105] Greenspan, B. N. [1982], Semi-monthly reproductive cycles in male and female fiddler crabs, *Uca pugnax*, *Animal Behaviour* **30**(4), 1084–1092.

[106] Forward, R. B., Tankersley, R. A. and Rittschof, D. [2001], Cues for metamorphosis of Brachyuran crabs: An overview, *American Zoologist* **41**(5), 1108–1122.

[107] Yamaguchi, T. [2002], Survival rate and age estimation of the fiddler crab, *Uca lactea* (De Haan, 1835) (Decapoda, Brachyura, Ocypodidae), *Crustaceana* **75**(8), 993–1014.

[108] Pardo, J. C., Stefanelli-Silva, G., Christy, J. H. and Costa, T. M. [2020], Fiddler crabs and their above-ground sedimentary structures: a review, *Journal of Ethology* **38**(2), 137–154.

[109] Natálio, L. F., Pardo, J. C., Machado, G. B., Fortuna, M. D., Gallo, D. G. and Costa, T. M. [2017], Potential effect of fiddler crabs on organic matter distribution: A combined laboratory and field experimental approach, *Estuarine, Coastal and Shelf Science* **184**, 158–165.

[110] Clark, H. L. and Backwell, P. R. [2017], Territorial battles between fiddler crab species, *Royal Society Open Science* **4**(1).

[111] Altevogt, R. and von Hagen, H.-O. [1964], Über die orientierung von *Uca tangeri* Eydoux im Freiland, *Zeitschrift für Morphol und Ökologie der Tiere* **53**(6), 636–656.

[112] Hemmi, J. M. [2003], Burrow surveillance in fiddler crabs II. The sensory cues, *Journal of Experimental Biology* **206**(22), 3951–3961.

[113] Zeil, J., Nalbach, G. and Nalbach, H. O. [1986], Eyes, eye stalks and the visual world of semi-terrestrial crabs, *Journal of Comparative Physiology A* **159**(6), 801–811.

[114] Zeil, J. and Hemmi, J. M. [2006], The visual ecology of fiddler crabs, *Journal of Comparative Physiology A* **192**(1), 1–25.

[115] Zeil, J. M. and Al-Mutairi, T. W. [1996], The variation of resolution and of ommatidial dimensions in the compound eyes of the fiddler crab *Uca lactea annulipes* (Ocypodidae, Brachyura, Decapoda), *The Journal of experimental biology* **199**(7), 1569–77.

[116] Land, M. and Layne, J. [1995], The visual control of behaviour in fiddler crabs. I. Resolution, thresholds and the role of the horizon, *Journal of Comparative Physiology A* **177**(1), 81–90.

[117] Bagheri, Z. M., Jessop, A.-L., Kato, S., Partridge, J. C., Shaw, J., Ogawa, Y. and Hemmi, J. M. [2020], A new method for mapping spatial resolution in compound eyes suggests two visual streaks in fiddler crabs, *The Journal of Experimental Biology* **223**(1), jeb210195.

[118] Layne, J., Land, M. and Zeil, J. [1997], Fiddler crabs use the visual horizon to distinguish predators from conspecifics: A review of the evidence, *Journal of the Marine Biological Association of the United Kingdom* **77**(1), 43–54.

[119] Milner, R. N., Detto, T., Jennions, M. D. and Backwell, P. R. [2010], Hunting and predation in a fiddler crab, *Journal of Ethology* **28**(1), 171–173.

[120] Backwell, R. P. Y. [2019], Synchronous waving in fiddler crabs: a review, *Current Zoology* **65**(1), 83–88.

[121] Land, M. F. [1999], The roles of head movements in the search and capture strategy of a tern (Aves, Laridae), *Journal of Comparative Physiology A: Sensory, Neural, and Behavioral Physiology* **184**(3), 265–272.

[122] Smolka, J., Zeil, J. and Hemmi, J. M. [2011], Natural visual cues eliciting predator avoidance in fiddler crabs., *Proceedings. Biological sciences* **278**(1724), 3584–92.

[123] Hemmi, J. M. [2005*a*], Predator avoidance in fiddler crabs: 1. Escape decisions in relation to the risk of predation, *Animal Behaviour* **69**(3), 603–614.

[124] Hemmi, J. M. [2005*b*], Predator avoidance in fiddler crabs: 2. The visual cues, *Animal Behaviour* **69**(3), 615–625.

[125] Smolka, J., Raderschall, C. A. and Hemmi, J. M. [2013], Flicker is part of a multi-cue response criterion in fiddler crab predator avoidance, *Journal of Experimental Biology* **216**(7), 1219–1224.

[126] Hemmi, J. M. and Pfeil, A. [2010], A multi-stage anti-predator response increases information on predation risk, *Journal of Experimental Biology* **213**(9), 1484–1489.

[127] Hemmi, J. M. and Zeil, J. [2005], Animals as prey: perceptual limitations and behavioural options, *Marine Ecology Progress Series* **287**, 274–278.

[128] Bagheri, Z. M., Donohue, C. G. and Hemmi, J. M. [2020], Evidence of predictive selective attention in fiddler crabs during escape in the natural environment, *The Journal of Experimental Biology* **223**.

[129] Oliva, D., Medan, V. and Tomsic, D. [2007], Escape behavior and neuronal responses to looming stimuli in the crab *Chasmagnathus granulatus* (Decapoda: Grapsidae), *Journal of Experimental Biology* **210**(5).

[130] Peer, N., Miranda, N. A. and Perissinotto, R. [2015], A review of fiddler crabs (genus *Uca* Leach, 1814) in South Africa, *African Zoology* **50**(3), 187–204.

[131] Barnatan, Y., Sztarker, J. and Tomsic, D. [2019], Unidirectional optomotor responses and eye dominance in two species of crabs, *Frontiers in Physiology* **1**, 586.

[132] Rosenberg, M. S. [2020], A fresh look at the biodiversity lexicon for fiddler crabs (Decapoda: Brachyura: Ocypodidae). Part 2: Biogeography, *Journal of Crustacean Biology* pp. 1–20.

[133] Howard, B. R., Barrios-O'Neill, D., Alexander, M. E., Dick, J. T., Therriault, T. W., Robinson, T. B. and Côté, I. M. [2018], Functional responses of a cosmopolitan invader demonstrate intraspecific variability in consumer-resource dynamics, *PeerJ* **1**(9), e5634.

[134] George, R. W. and Jones, D. S. [1982], *A Revision of the Fiddler Crabs of Australia (Ocypodinae:Uca)*, 14 edn, Record of the Western Australian Museum Supplement.

[135] Grosholz, E. D. and Ruiz, G. M. [1996], Predicting the impact of introduced marine species: Lessons from the multiple invasions of the European green crab *Carcinus maenas*, *Biological Conservation* **78**(1-2), 59–66.

[136] Hogarth, P. J. [1975], Pattern polymorphism and predation in the shore crab, *Carcinus maenas* (L.), *Crustaceana* **28**(1), 316–319.

[137] Todd, P. A., Oh, J., Loke, L. H. and Ladle, R. J. [2012], Multi-scale phenotype-substrate matching: Evidence from shore crabs (*Carcinus maenas* L.), *Ecological Complexity* **12**, 58–62.

[138] Wolf, F. [1998], Red and green colour forms in the common shore crab *Carcinus maenas* (L.) (Crustacea: Brachyura: Portunidae): Theoretical predictions and empirical data, *Journal of Natural History* **32**(10-11), 1807–1812.

[139] Rewitz, K., Styrishave, B., Depledge, M. H. and Andersen, O. [2004], Spatial and temporal distribution of shore crabs *Carcinus maenas* in a small tidal estuary (Looe Estuary, Cornwall, England), *Journal of Crustacean Biology* **24**(1), 178–187.

[140] Crothers J. H. [1968], The biology of the shore crab *Carcinus maenas* (L.) 2. The life of the adult crab, *Field Studies* **2**(5), 579–614.

[141] Compton, T. J., Leathwick, J. R. and Inglis, G. J. [2010], Thermogeography predicts the potential global range of the invasive European green crab (*Carcinus maenas*), *Diversity and Distributions* **16**(2), 243–255.

[142] Carlton, J. T. and Cohen, A. N. [2003], Episodic global dispersal in shallow water marine organisms: the case history of the European shore crabs *Carcinus maenas* and *C. aestuarii*, *Journal of Biogeography* **30**(12), 1809–1820.

[143] Ropes, J. W. [1968], The feeding habits of the green crab, *Carcinus maenas* (L.), *Fishery Bulletin* **67**(2), 183–203.

[144] Baeta, A., Cabral, H. N., Marques, J. C. and Pardal, M. A. [2006], Feeding ecology of the green crab, *Carcinus maenas* (L., 1758) in a temperate estuary, Portugal, *Crustaceana* **79**(10), 1181–1193.

[145] Parker, A. R. [1998], Colour in Burgess Shale animals and the effect of light on evolution in the Cambrian, *Proceedings of the Royal Society B: Biological Sciences* **265**(1400), 967–972.

[146] Trestman, M. [2013], The Cambrian Explosion and the origins of embodied cognition, *Biological Theory* **8**(1), 80–92.

[147] Meyer-Rochow, V. B. [2001], The crustacean eye: Dark/ light adaptation, polarization sensitivity, flicker fusion frequency, and photoreceptor damage, *Zoological Science* **18**(9), 1175–1197.

[148] Exner, S. [1891], *Die Physiologie der Facettierten Augen von Krebsen und Insecten*, Franz Deuticke Verlag, Leipzig.

[149] Hallberg, E. and Elofsson, R. [1989], Construction of the pigment shield of the crustacean compound eye: A review, *Journal of Crustacean Biology* **9**(3), 359.

[150] King, C. A. and Cronin, T. W. [1993], Cytoskeleton of retinular cells from the stomatopod, *Gonodactylus oerstedii*: possible roles in pigment granule migration, *Cell & Tissue Research* **274**(2), 315–328.

[151] Reisenman, C. E., Insausti, T. C. and Lazzari, C. R. [2002], Light-induced and circadian changes in the compound eye of the haematophagous bug *Triatoma infestans* (Hemiptera: Reduviidae), *Journal of Experimental Biology* **205**(2).

[152] Brown, F. [1961], Physiological rhythms, *in* T. H. Waterman, ed., The Physiology of Crustacea, Academic press, New York, pp. 401–430.

[153] Insausti, T. C., Le Gall, M. and Lazzari, C. R. [2013], Oxidative stress, photodamage and the role of screening pigments in insect eyes, *Journal of Experimental Biology* **216**(17), 3200–3207.

[154] Cronin, T. W., Bok, M. J., Marshall, N. J. and Caldwell, R. L. [2014], Filtering and polychromatic vision in mantis shrimps: Themes in visible and ultraviolet vision, *Philosophical Transactions of the Royal Society B: Biological Sciences* **369**(1636).

[155] Stavenga, D. G. [2002], Colour in the eyes of insects, *Journal of Comparative Physiology A: Neuroethology, Sensory, Neural, and Behavioral Physiology* **188**(5), 337–348.

[156] Stowe, S. [1980], Spectral sensitivity and retinal pigment movement in the crab *Leptograpsus variegatus* (*fabricius*), *Journal of Experimental Biology* **87**, 73–98.

[157] King, C. A. and Cronin, T. W. [1994], Investigations of pigment granule transport systems in *Gonodactylus oerstedii* (Crustacea: Hoplocarida: Stomatopoda) II, *Journal of Comparative Physiology A* **175**(3), 331–342.

[158] Stavenga, D. G. [2004], Angular and spectral sensitivity of fly photoreceptors. III. Dependence on the pupil mechanism in the blowfly *Calliphora*, *Journal of Comparative Physiology A: Neuroethology, Sensory, Neural, and Behavioral Physiology* **190**(2), 115–129.

[159] Land, M. F. and Osorio, D. C. [1990], Waveguide modes and pupil action in the eyes of butterflies, *Proceedings of the Royal Society B: Biological Sciences* **241**(1301), 93–100.

[160] Snyder, A. W. and Horridge, G. A. [1972], The optical function of changes in the medium surrounding the cockroach rhabdom, *Journal of Comparative Physiology* **81**(1), 1–8.

[161] Shaw, S. R. and Stowe, S. [1982], Photoreception, *in* H. E. Atwood and D. C. Sandeman, eds, The biology of Crustacea: Volume 3: Neurobiology, structure and function, Academic Press, New York.

[162] Narendra, A., Greiner, B., Ribi, W. A. and Zeil, J. [2016], Light and dark adaptation mechanisms in the compound eyes of *Myrmecia* ants that occupy discrete temporal niches, *Journal of Experimental Biology* **219**(16).

[163] Greiner, B. [2006], Adaptations for nocturnal vision in insect apposition eyes, *International Review of Cytology* **250**, 1–46.

[164] Eguchi, E. and Waterman, T. H. [1967], Changes in retinal fine structure induced in the crab *Libinia* by light and dark adaptation, *Zeitschrift für Zellforschung und Mikroskopische Anatomie* **79**(2), 209–229.

[165] Arikawa, K., Kawamata, K., Suzuki, T. and Eguchi, E. [1987], Daily changes of structure, function and rhodopsin content in the compound eye of the crab *Hemigrapsus sanguineus*, *Journal of Comparative Physiology A* **161**(2), 161–174.

[166] Katz, B. and Minke, B. [2009], *Drosophila* photoreceptors and signaling mechanisms, *Frontiers in Cellular Neuroscience* **3**, 2.

[167] Menzi, U. [1987], Visual adaptation in nocturnal and diurnal ants, *Journal of Comparative Physiology A* **160**(1), 11–21.

[168] Narendra, A., Alkaladi, A., Raderschall, C. A., Robson, S. K. A. and Ribi, W. A. [2013], Compound eye adaptations for diurnal and nocturnal lifestyle in the intertidal ant, *Polyrhachis sokolova*, *PLoS ONE* **8**(10), e76015.

[169] Williams, D. S. [1980], Organisation of the compound eye of a tipulid fly during the day and night, *Zoomorphologie* **95**(2), 85–104.

[170] Nilsson, D. E. and Ro, A. I. [1994], Did neural pooling for night vision lead to the evolution of neural superposition eyes?, *Journal of Comparative Physiology A* **175**(3), 289–302.

[171] Fingerman, M. [1970], Circadian rhythm of distal retinal pigment migration in the fiddler crab, *Uca Pugilator*, maintained in constant darkness and its endocrine control, *Journal of Interdisciplinary Cycle Research* **1**(2), 115–121.

[172] Ludolph, C., Pagnanelli, D. and Mote, M. I. [1973], Neural control of migration of proximal screening pigment by retinular cells of the swimming crab *Callinectes sapidus*, *Biological Bulletin* **145**(1), 159–170.

[173] Leggett, L. M. and Stavenga, D. G. [1981], Diurnal changes in angular sensitivity of crab photoreceptors, *Journal of Comparative Physiology A* **144**(1), 99–109.

[174] Vargas, M. A., Geish, M. A., Maciel, F. E., Cruz, B. P., de Moraes Vaz Batista Filgueira, D., de Jesus Ferreira, G., Nery, L. E. M. and Allodi, S. [2010], Influence of the dark/light rhythm on the effects of UV radiation in the eyestalk of the crab *Neohelice granulata*, *Comparative Biochemistry and Physiology - C Toxicology and Pharmacology* **151**(3), 343–350.

[175] De Moraes Vaz Batista Filgueira, D., Guterres, L. P., De Souza Votto, A. P., Vargas, M. A., Boyle, R. T., Trindade, G. S. and Nery, L. E. M. [2010], Nitric oxide-dependent pigment migration induced by ultraviolet radiation in retinal pigment cells of the crab *Neohelice granulata*, *Photochemistry and Photobiology* **86**(6), 1278–1284.

[176] Snyder, A. W. [1979], Physics of Vision in Compound Eyes, *in* H. Autrum, ed., Handbook of Sensory Physiology, v11/6a edn, Springer, Berlin, Heidelberg, pp. 225–313.

[177] Nilsson, D. E. and Odselius, R. [1981], A new mechanism for light-dark adaptation in the *Artemia* compound eye (Anostraca, Crustacea), *Journal of Comparative Physiology A* **143**(3), 389–399.

[178] Schönenberger, N. [1977], The fine structure of the compound eye of *Squilla* mantis (Crustacea, Stomatopoda), *Cell and Tissue Research* **176**(2), 205–233.

[179] Hardie, R. C. [2012], Phototransduction mechanisms in *Drosophila* microvillar photoreceptors, *Wiley Interdisciplinary Reviews: Membrane Transport and Signaling* **1**(2), 162–187.

[180] Nässel, D. R. and Waterman, T. H. [1979], Massive diurnally modulated photoreceptor membrane turnover in crab light and dark adaptation, *Journal of Comparative Physiology A* **131**(3), 205–216.

[181] Blest, A. D., Stowe, S. and Price, D. G. [1980], The sources of acid hydrolases for photoreceptor membrane degradation in a grapsid crab, *Cell and Tissue Research* **205**(2), 229–244.

[182] Stowe, S. [1981], Effects of illumination changes on rhabdom synthesis in a crab, *Journal of Comparative Physiology A* **142**(1), 19–25.

[183] Stowe, S. [1983], Phagocytosis of rhabdomeral membrane by crab photoreceptors (*Leptograpsus variegatus*), *Cell and Tissue Research* **234**(2), 463–467.

[184] Stowe, S. [1980], Rapid synthesis of photoreceptor membrane and assembly of new microvilli in a crab at dusk, *Cell and Tissue Research* **211**(3), 419–440.

[185] Williams, D. S. [1982], Ommatidial structure in relation to turnover of photoreceptor membrane in the locust, *Cell and Tissue Research* **225**(3), 595–617.

[186] Sakura, M., Takasuga, K., Watanabe, M. and Eguchi, E. [2003], Diurnal and circadian rhythm in compound eye of cricket (*Gryllus bimaculatus*): Changes in structure and photon capture efficiency, *Zoological Science* **20**(7), 833–840.

[187] Horridge, G., Duniec, J., Marcelja, L. and Director, I. [1981], A 24-hour cycle in single locust and mantid photoreceptors, *Journal of Experimental Biology* **91**(1).

[188] Piekos, W. B. [1989], Temporal separation of rhabdom shrinkage and mvb formation in the light-adapting crayfish retina, *Journal of Experimental Zoology* **250**(1), 17–21.

[189] Blest, A. D. and Day, W. A. [1978], The rhabdomere organization of some nocturnal *Pisaurid* spiders in light and darkness, *Philosophical Transactions of the Royal Society of London. B, Biological Sciences* **283**(993), 1–23.

[190] Frederiksen, R. and Warrant, E. J. [2008], Visual sensitivity in the crepuscular owl butterfly *Caligo memnon* and the diurnal blue morpho *Morpho peleides*: A clue to explain the evolution of nocturnal apposition eyes?, *Journal of Experimental Biology* **211**(6), 844–851.

[191] Honkanen, A., Immonen, E. V., Salmela, I., Heimonen, K. and Weckström, M. [2017], Insect photoreceptor adaptations to night vision, *Philosophical Transactions of the Royal Society B: Biological Sciences* **372**(1717).

[192] Laughlin, S. B. and Weckström, M. [1993], Fast and slow photoreceptors - a comparative study of the functional diversity of coding and conductances in the Diptera, *Journal of Comparative Physiology A* **172**(5), 593–609.

[193] Hoffman, D. M., Karasev, V. I. and Banks, M. S. [2011], Temporal presentation protocols in stereoscopic displays: Flicker visibility, perceived motion, and perceived depth, *Journal of the Society for Information Display* **19**(3), 271.

[194] Miall, R. C. [1978], The flicker fusion frequencies of six laboratory insects, and the response of the compound eye to mains fluorescent 'ripple', *Physiological Entomology* **3**(2), 99–106.

[195] Frank, T. M. [2000], Temporal resolution in mesopelagic crustaceans, *Philosophical Transactions of the Royal Society of London. Series B: Biological Sciences* **355**(1401), 1195–1198.

[196] Theobald, J. C., Coates, M. M., Wcislo, W. T. and Warrant, E. J. [2007], Flight performance in night-flying sweat bees suffers at low light levels, *Journal of Experimental Biology* **210**(22), 4034–4042.

[197] Reber, T., Vähäkainu, A., Baird, E., Weckström, M., Warrant, E. and Dacke, M. [2015], Effect of light intensity on flight control and temporal properties of photoreceptors in bumblebees, *Journal of Experimental Biology* **218**(9), 1339–1346.

[198] Ribi, W. A. [1977], Fine structure of the first optic ganglion (lamina) of the cockroach, *Periplaneta americana*, *Tissue and Cell* **9**(1), 57–72.

[199] Stöckl, A. L., O'Carroll, D. C. and Warrant, E. J. [2016], Neural summation in the hawkmoth visual system extends the limits of vision in dim light, *Current Biology* **26**(6), 821–826.

[200] Rosenberg, M. S. [2001], The systematics and taxonomy of fiddler crabs: A phylogeny of the genus *Uca*, *Journal of Crustacean Biology* **21**(3), 839–869.

[201] Stowe, S., Fukudome, H. and Tanaka, K. [1986], Membrane turnover in crab photoreceptors studied by high-resolution scanning electron microscopy and by a new technique of thick-section transmission electron microscopy, *Cell and Tissue Research* **245**(1), 51–60.

[202] Toh, Y. and Waterman, T. H. [1982], Diurnal changes in compound eye fine structure in the blue crab *Callinectes*. 1. Differences between noon and midnight retinas on an LD 11: 13 cycle, *Journal of Ultrasructure Research* **78**(1), 40–59.

[203] Toh, Y. [1987], Diurnal changes of rhabdom structures in the compound eye of the grapsid crab, *Hemigrapsus penicillatus*, *Journal of Electron Microscopy* **36**(4), 213–223.

[204] Toh, Y. [1990], Diurnal changes in the cytoplasmic organelles of the retinular cell in the compound eye of the grapsid crab, *Hemigrapsus penicillatus*, *Journal of Electron Microscopy* **39**(6), 492–500.

[205] Barnwell, F. H. [1966], Daily and tidal patterns of activity in individual fiddler crab (genus *Uca*) from the Woods Hole region, *The Biological Bulletin* **130**(1), 1–17.

[206] Palmer, J. D. [1988], Comparative studies of tidal rhythms. VI. Several clocks govern the activity of two species of fiddler crabs, *Marine Behaviour and Physiology* **13**(2), 201–219.

[207] Palmer, J. D. [1989], Comparative studies of tidal rhythms. VIII. A translocation experiment involving circalunidian rhythms, *Marine Behaviour and Physiology* **14**(4), 231–243.

[208] Zhang, L., Hastings, M. H., Green, E. W., Tauber, E., Sladek, M., Webster, S. G., Kyriacou, C. P. and Wilcockson, D. C. [2013], Dissociation of circadian and circatidal timekeeping in the marine crustacean *Eurydice pulchra*, *Current Biology* **23**(19), 1863–1873.

[209] Bennett, M. F., Shriner, J. and Brown, R. A. [1957], Persistent tidal cycles of spontaneous motor activity in the fiddler crab, *Uca pugnax*, *The Biological Bulletin* **112**(3), 267–275.

[210] Alkaladi, A., How, M. J. and Zeil, J. [2013], Systematic variations in microvilli banding patterns along fiddler crab rhabdoms, *Journal of Comparative Physiology A* **199**(2), 99–113.

[211] Schneider, L. and Langer, H. [1969], The structure of the rhabdome in the bifunctional compound eye of the pond skater, *Gerris lacustris*, *Zeitschrift für Zellforschung und Mikroskopische Anatomie* **99**(4), 538–559.

[212] Stockman, A. and Sharpe, L. T. [2000], The spectral sensitivities of the middle- and long-wavelength-sensitive cones derived from measurements in observers of known genotype, *Vision Research* **40**(13), 1711–1737.

[213] Schindelin, J., Arganda-Carreras, I., Frise, E., Kaynig, V., Longair, M., Pietzsch, T., Preibisch, S., Rueden, C., Saalfeld, S., Schmid, B., Tinevez, J.-Y., White, D. J., Hartenstein, V., Eliceiri, K., Tomancak, P. and Cardona, A. [2012], Fiji: an open-source platform for biological-image analysis, *Nature Methods* **9**(7), 676–682.

[214] Brodrick, E. A., Roberts, N. W., Sumner-Rooney, L., Schlepütz, C. M. and How, M. J. [2020], Light adaptation mechanisms in the eye of the fiddler crab *Afruca tangeri*, *Journal of Comparative Neurology* p. cne.24973.

[215] Knopf, G. N. [1966], Observations on behavioral ecology of the fiddler crab, *Uca Pugilator* (Bosc), *Crustaceana* **11**(3), 302–306.

[216] von Hagen, H.-O. [1962], Freilandstudien zur sexual und Fortpflanzungs-biologie von *Uca tangeri* in Andalusien, *Zeitschrift für Morphologie und Ökologie der Tiere* **51**(6), 611–725.

[217] Wolfrath, B. [1993], Observations on the behaviour of the European fiddler crab *Uca tangeri*, *Marine Ecology Progress Series* **100**, 111–118.

[218] Korte, R. [1965], Durch polarisiertes licht hervorgerufene optomotorik bei *Uca tangeri*, *Experientia* **21**(2), 98.

[219] Kyba, C. C., Kuester, T., De Miguel, A. S., Baugh, K., Jechow, A., Hölker, F., Bennie, J., Elvidge, C. D., Gaston, K. J. and Guanter, L. [2017], Artificially lit surface of Earth at night increasing in radiance and extent, *Science Advances* **3**(11), e1701528.

[220] Underwood, C. N., Davies, T. W. and Queirós, A. M. [2017], Artificial light at night alters trophic interactions of intertidal invertebrates, *Journal of Animal Ecology* **86**(4), 781–789.

[221] Kronfeld-Schor, N., Dominoni, D., de la Iglesia, H., Levy, O., Herzog, E. D., Dayan, T. and Helfrich-Forster, C. [2013], Chronobiology by moonlight, *Proceedings of the Royal Society B: Biological Sciences* **280**(1765).

[222] Skov, M. W., Hartnoll, R. G., Ruwa, R. K., Shunula, J. P., Vannini, M. and Cannicci, S. [2005], Marching to a different drummer: Crabs synchronize reproduction to a 14-month lunar-tidal cycle, *Ecology* **86**(5), 1164–1171.

[223] Kyba, C. C., Ruhtz, T., Fischer, J. and Hölker, F. [2011], Lunar skylight polarization signal polluted by urban lighting, *Journal of Geophysical Research Atmospheres* **116**(24).

[224] Gaston, K. J., Bennie, J., Davies, T. W. and Hopkins, J. [2013], The ecological impacts of nighttime light pollution: a mechanistic appraisal, *Biological Reviews* **88**(4), 912–927.

[225] Davies, T. W., Coleman, M., Griffith, K. M. and Jenkins, S. R. [2015], Night-time lighting alters the composition of marine epifaunal communities, *Biology Letters* **11**(4), 20150080.

[226] Bolton, D., Mayer-Pinto, M., Clark, G. F., Dafforn, K. A., Brassil, W. A., Becker, A. and Johnston, E. L. [2017], Coastal urban lighting has ecological consequences for multiple trophic levels under the sea, *Science of the Total Environment* **576**, 1–9.

[227] Legland, D. I. A.-C. and Andrey, P. [2016], MorphoLibJ: integrated library and plugins for mathematical morphology with ImageJ, *Bioinformatics* **32**(2), 3532—-3534.

[228] Stampanoni, M., Groso, A., Isenegger, A., Mikuljan, G., Chen, Q., Bertrand, A., Henein, S., Betemps, R., Frommherz, U., Böhler, P., Meister, D., Lange, M. and Abela, R. [2006], Trends in synchrotron-based tomographic imaging: the SLS experience, *in* U. Bonse, ed., Developments in X-Ray Tomography V, Vol. 6318, SPIE, p. 63180M.

[229] Paganin, D., Mayo, S. C., Gureyev, T. E., Miller, P. R. and Wilkins, S. W. [2002], Simultaneous phase and amplitude extraction from a single defocused image of a homogeneous object, *Journal of Microscopy* **206**(1), 33–40.

[230] Marone, F. and Stampanoni, M. [2012], Regridding reconstruction algorithm for real-time tomographic imaging, *Journal of Synchrotron Radiation* **19**(6), 1029–1037.

[231] Dag, O., Dolgun, A. and Konar, N. M. [2018], onewaytests: An R package for one-way tests in independent groups designs, *The R Journal* **10**(1), 175–199.

[232] Marshall, N. J., Cronin, T. W. and Frank, T. M. [2008], Visual adaptations in crustaceans: Chromatic, developmental, and temporal aspects, *in* Sensory Processing in Aquatic Environments, Springer-Verlag, pp. 343–372.

[233] Matsushita, A., Arikawa, K. and Eguchi, E. [1999], Appearance of opsin-containing vesicles as rhabdomeric precursors and their incorporation into the rhabdom around dusk in the compound eye of the crab, *Hemigrapsus sanguineus*, *Zoological Science* **16**(1), 25–34.

[234] Arikawa, K., Morikawa, Y., Suzuki, T. and Eguchi, E. [1988], Intrinsic control of rhabdom size and rhodopsin content in the crab compound eye by a circadian biological clock, *Experientia* **44**(3), 219–220.

[235] Stowe, S. [1982], Rhabdom synthesis in isolated eyestalks and retinae of the crab *Leptograpsus variegatus*, *Journal of Comparative Physiology A* **148**, 313–321.

[236] King, C. A. and Cronin, T. W. [1994], Investigations of pigment granule transport systems in *Gonodactylus oerstedii* (Crustacea: Hoplocarida: Stomatopoda) I, *Journal of Comparative Physiology A* **175**(3), 323–329.

[237] Miller, W. H. and Cawthon, D. F. [1974], Pigment granule movement in *Limulus* photoreceptors, *Investigative Ophthalmology* **13**(5), 401–405.

[238] Ramos, A. P., Gustafsson, O., Labert, N., Salecker, I., Nilsson, D.-E. and Averof, M. [2019], Analysis of the genetically tractable crustacean *Parhyale hawaiensis* reveals the organisation of a sensory system for low-resolution vision, *BMC Biology* **17**(1), 67.

[239] Knowles, F. G. [1950], The control of retinal pigment migration in *Leander serratus*, *The Biological bulletin* **98**(1), 66–80.

[240] Warrant, E. J. and McIntyre, P. D. [1996], The visual ecology of pupillary action in superposition eyes, *Journal of Comparative Physiology A* **178**(1), 75–90.

[241] Warrant, E. J. and Nilsson, D. E. [1998], Absorption of white light in photoreceptors, *Vision Research* **38**(2), 195–207.

[242] Salmon, M. and Atsaides, S. P. [1968], Visual and acoustical signalling during courtship by fiddler crabs (genus *Uca*), *American Zoologist* **8**, 623–639.

[243] Land, M. F. [1981], Optics and vision in invertebrates, *in* H. Autrum, ed., Handbook of Sensory Physiology, vii/6b edn, Springer Berlin, pp. 472–592.

[244] Peek, M. Y. and Card, G. M. [2016], Comparative approaches to escape, *Current Opinion in Neurobiology* **41**, 167–173.

[245] How, M. J., Christy, J., Roberts, N. W. and Marshall, N. J. [2014], Null point of discrimination in crustacean polarisation vision, *Journal of Experimental Biology* **217**(14), 2462–2467.

[246] Tomsic, D., Sztarker, J., Berón de Astrada, M., Oliva, D. and Lanza, E. [2017], The predator and prey behaviors of crabs: from ecology to neural adaptations., *The Journal of Experimental Biology* **220**(13), 2318–2327.

[247] Kohn, E. and Minke, B. [2011], Methods for studying *Drosophila* TRP channels, *in* M. X. Zhu, ed., TRP Channels, CRC Press/Taylor & Francis, pp. 423–446.

[248] Tomsic, D., Pedreira, M. E., Romano, A., Hermitte, G. and Maldonado, H. [1998], Context-US association as a determinant of long-term habituation in the crab *Chasmagnathus*, *Animal Learning & Behavior* **26**(2), 196–209.

[249] Warrington, R. E., Hart, N. S., Potter, I. C., Collin, S. P. and Hemmi, J. M. [2017], Retinal temporal resolution and contrast sensitivity in the parasitic lamprey *Mordacia mordax* and its non-parasitic derivative *Mordacia praecox*, *Journal of Experimental Biology* **220**(7), 1245–1255.

[250] de Souza, J. M. and Ventura, D. F. [1989], Comparative study of temporal summation and response form in hymenopteran photoreceptors, *Journal of Comparative Physiology A* **165**(2), 237–245.

[251] Boström, J. E., Dimitrova, M., Canton, C., Håstad, O., Qvarnström, A. and Ödeen, A. [2016], Ultra-rapid vision in birds, *PLoS ONE* **11**(3), e0151099.

[252] Potier, S., Lieuvin, M., Pfaff, M. and Kelber, A. [2020], How fast can raptors see?, *Journal of Experimental Biology* **223**(1).

[253] Fenk, L. M. and Schmid, A. [2011], Flicker-induced eye movements and the behavioural temporal cut-off frequency in a nocturnal spider, *Journal of Experimental Biology* **214**(21), 3658–3663.

[254] Aho, A. C., Donner, K., Helenius, S., Larsen, L. O. and Reuter, T. [1993], Visual performance of the toad (*Bufo bufo*) at low light levels: retinal ganglion cell responses and prey-catching accuracy, *Journal of Comparative Physiology A* **172**(6), 671–682.

[255] Porciatti, V. [2007], The mouse pattern electroretinogram, *Documenta Ophthalmologica* **115**(3), 145–153.

[256] Ogawa, Y., Ryan, L. A., Palavalli-Nettimi, R., Seeger, O., Hart, N. S. and Narendra, A. [2019], Spatial Resolving Power and Contrast Sensitivity Are Adapted for Ambient Light Conditions in Australian *Myrmecia* Ants, *Frontiers in Ecology and Evolution* **7**(FEB), 18.

[257] Bates, D., Mächler, M., Bolker, B. M. and Walker, S. C. [2015], Fitting linear mixed-effects models using lme4, *Journal of Statistical Software* **67**(1), 1–48.

[258] Lee, O. E. and Braun, T. M. [2012], Permutation tests for random effects in linear mixed models, *Biometrics* **68**(2), 486–493.

[259] Hothorn, T., Bretz, F. and Westfall, P. [2008], Simultaneous inference in general parametric models, *Biometrical Journal* **50**(3), 346–363.

[260] Doujak, F. E. [1985], Can a shore crab see a star?, *Journal of Experimental Biology* **116**(1), 385–393.

[261] Sztarker, J., Strausfeld, N. J. and Tomsic, D. [2005], Organization of optic lobes that support motion detection in a semiterrestrial crab, *Journal of Comparative Neurology* **493**(3), 396–411.

[262] Hemmi, J. M. and Tomsic, D. [2012], The neuroethology of escape in crabs: from sensory ecology to neurons and back, *Current Opinion in Neurobiology* **22**(2), 194–200.

[263] Bernays, E. A. and Wcislo, W. T. [1994], Sensory capabilities, information processing, and resource specialization, *The Quarterly Review of Biology* **69**(2), 187–204.

[264] Atick, J. J. [2011], Could information theory provide an ecological theory of sensory processing?, *Network: Computation in Neural Systems* **22**(1-4), 4–44.

[265] Zagorski, E. R. and Merry, J. W. [2014], How do eye size and facet lens size vary by age and sex in *Acheta domesticus*? , *BIOS* **85**(3), 151–159.

[266] Rutowski, R. L. [2000], Variation of eye size in butterflies: inter- and intraspecific patterns, *Journal of Zoology* **252**(2), 187–195.

[267] Spaethe, J. and Chittka, L. [2003], Interindividual variation of eye optics and single object resolution in bumblebees, *Journal of Experimental Biology* **206**(19), 3447–3453.

[268] Hamilton, R., Bach, M., Heinrich, S. P., Hoffmann, M. B., Odom, J. V., McCulloch, D. L. and Thompson, D. A. [2020], VEP estimation of visual acuity: a systematic review, *Documenta Ophthalmologica* pp. 1–50.

[269] Tatler, B., O'Carroll, D. C. and Laughlin, S. B. [2000], Temperature and the temporal resolving power of fly photoreceptors, *Journal of Comparative Physiology A: Sensory, Neural, and Behavioral Physiology* **186**(4), 399–407.

[270] Currea, J. P., Smith, J. L. and Theobald, J. C. [2018], Small fruit flies sacrifice temporal acuity to maintain contrast sensitivity, *Vision Research* **149**, 1–8.

[271] Chen, D. M., Christianson, J. S., Sapp, R. J. and Stark, W. S. [1992], Visual receptor cycle in normal and period mutant *Drosophila*: Microspectrophotometry, electrophysiology, and ultrastructural morphometry, *Visual Neuroscience* **9**(2), 125–135.

[272] Roebroek, J. G., van Tjonger, M. and Stavenga, D. G. [1990], Temperature dependence of receptor potential and noise in fly (*Calliphora erythrocephala*) photoreceptor cells, *Journal of Insect Physiology* **36**(7), 499–505.

[273] Skorupski, P. and Chittka, L. [2011], Photoreceptor processing speed and input resistance changes during light adaptation correlate with spectral class in the bumblebee, *Bombus impatiens*, *PLoS ONE* **6**(10).

[274] Pirhofer-Walzl, K., Warrant, E. and Barth, F. G. [2007], Adaptations for vision in dim light: Impulse responses and bumps in nocturnal spider photoreceptor cells (*Cupiennius salei* Keys), *Journal of Comparative Physiology A: Neuroethology, Sensory, Neural, and Behavioral Physiology* **193**(10), 1081–1087.

[275] Caves, E. M., Frank, T. M. and Johnsen, S. [2016], Spectral sensitivity, spatial resolution and temporal resolution and their implications for conspecific signalling in cleaner shrimp, *Journal of Experimental Biology* **219**(4), 597–608.

[276] Warrant, E. [2008], Nocturnal Vision, *in* R. Masland and T. Albright, eds, The Senses: A Comprehensive Reference Vol 2: Vision II, Elsevier, San Diego, pp. 53–86.

[277] Laughlin, S. B., De Ruyter Van Steveninck, R. R. and Anderson, J. C. [1998], The metabolic cost of neural information, *Nature Neuroscience* **1**(1), 36–41.

[278] Frank, T. M. [1999], Comparative study of temporal resolution in the visual systems of mesopelagic crustaceans, *Biological Bulletin* **196**(2), 137–144.

[279] Cohen, J. H. and Frank, T. M. [2006], Visual physiology of the antarctic amphipod *Abyssorchomene plebs*, *Biological Bulletin* **211**(2), 140–148.

[280] McFarland, W. N. and Loew, E. R. [1983], Wave produced changes in underwater light and their relations to vision, *Environmental Biology of Fishes* **8**(3-4), 173–184.

[281] Martinez, M. M. [2001], Running in the surf: hydrodynamics of the shore crab *Grapsus tenuicrustatus*, *Journal of Experimental Biology* **204**(17).

[282] Cuttle, M. F., Hevers, W., Laughlin, S. B. and Hardie, R. C. [1995], Diurnal modulation of photoreceptor potassium conductance in the locust, *Journal of Comparative Physiology A* **176**(3), 307–316.

[283] Barlow, R. B. and Kaplan, E. [1977], Properties of visual cells in the lateral eye of *Limulus in situ*: Intracellular recordings, *Journal of General Physiology* **69**(2), 203–220.

[284] Barlow, R. B., Kaplan, E., Renninger, G. H. and Saito, T. [1987], Circadian rhythms in *Limulus* photoreceptors: I. Intracellular studies, *Journal of General Physiology* **89**(3), 353–378.

[285] Kaplan, E., Barlow, R. B., Renninger, G. and Purpura, K. [1990], Circadian rhythms in *Limulus* photoreceptors: II. Quantum Bumps, *Journal of General Physiology* **96**(3), 665–685.

[286] Barlow, R. B. [1983], Circadian rhythms in the *Limulus* visual system, *Journal of Neuroscience* **3**(4), 856–870.

[287] Stowasser, A., Owens, M. and Buschbeck, E. K. [2017], Giving invertebrates an eye exam: an ophthalmoscope that utilizes the autofluorescence of photoreceptors., *The Journal of experimental biology* **220**(Pt 22), 4095–4100.

[288] Franceschini, N. [1972], Pupil and pseudopupil in the compound eye of *Drosophila*, *in* Information Processing in the Visual Systems of Anthropods, Springer Berlin Heidelberg, pp. 75–82.

[289] Ro, A. I. and Nilsson, D. [1993], The circadian pupil rhythm in *Tenebrio molitor*, studied noninvasively, *Naturwissenschaften* **80**(4), 186–189.

[290] Meyer-Rochow, V. B. [1994], Light-induced damage to photoreceptors of spiny lobsters and other crustaceans, *Crustaceana* **67**(1), 95–109.

[291] Sacunas, R. B., Papuga, M. O., Malone, M. A., Pearson, A. C., Marjanovic, M., Stroope, D. G., Weiner, W. W., Chamberlain, S. C. and Battelle, B.-A. [2002], Multiple mechanisms of rhabdom shedding in the lateral eye of *Limulus polyphemus*, *The Journal of Comparative Neurology* **449**(1), 26–42.

[292] Matsushita, A. and Arikawa, K. [1996], Disruption of actin filament organization by cytochalasin D inhibits rhabdom synthesis in the compound eye of the crab *Hemigrapsus sanguineus*, *Cell and Tissue Research* **286**(1), 167–174.

[293] Barnes, W. J. [1990], Sensory basis and functional role of eye movements elicited during locomotion in the land crab *Cardisoma Guanhumi*, *Journal of Experimental Biology* **154**, 99–119.

[294] Land, M. F., Marshall, J. N., Brownless, D. and Cronin, T. W. [1990], The eye-movements of the mantis shrimp *Odontodactylus scyllarus* (Crustacea: Stomatopoda), *Journal of Comparative Physiology A* **167**(2), 155–166.

[295] Land, M. F. [2014], Eye movements of vertebrates and their relation to eye form and function, *Journal of Comparative Physiology A: Neuroethology, Sensory, Neural, and Behavioral Physiology* **201**(2), 195–214.

[296] Cronin, T. W., Marshall, N. J. and Land, M. F. [1991], Optokinesis in gonodactyloid mantis shrimps (Crustacea; Stomatopoda; Gonodactylidae), *Journal of Comparative Physiology A* **168**(2), 233–240.

[297] Thomas, B. B., Seiler, M. J., Sadda, S. V. R., Coffey, P. J. and Aramant, R. B. [2004], Optokinetic test to evaluate visual acuity of each eye independently, *Journal of Neuroscience Methods* **138**(1-2), 7–13.

[298] Cameron, D. J., Rassamdana, F., Tam, P., Dang, K., Yanez, C., Ghaemmaghami, S. and Dehkordi, M. I. [2013], The optokinetic response as a quantitative measure of visual acuity in zebrafish, *Journal of Visualized Experiments* **80**, 50832.

[299] Sandeman, D. C., Erber, J. and Kien, J. [1975], Optokinetic eye movements in the crab, *Carcinus maenas* - I. Eye torque, *Journal of Comparative Physiology A* **101**(3), 243–258.

[300] Horridge, G. A. and Sandeman, D. C. [1964], Nervous control of optokinetic responses in the crab *Carcinus*, *Proceedings of the Royal Society of London. Series B. Biological Sciences* **161**, 216–246.

[301] Nalbach, H.-O., Thier, P. and Varju, D. [1985], Light-dependent eye coupling during the optokinetic response of the crab *Carcinus maenas* (L.), *Journal of Experimental Biology* **119**, 103–114.

[302] Nalbach, H.-O. and Nalbach, G. [1987], Distribution of optokinetic sensitivity over the eye of crabs: its relation to habitat and possible role in flow-field analysis, *Journal of Comparative Physiology A* **160**(1), 127–135.
URL: *https://link.springer.com/article/10.1007/BF00613448*

[303] Nalbach, H.-O. [1989], Three temporal frequency channels constitute the dynamics of the optokinetic system of the crab, *Carcinus maenas* (L.), *Biological Cybernetics* **61**(1), 59–70.

[304] Nalbach, H.-O., Zeil, J. and Forzin, L. [1989], Multisensory control of eye-stalk orientation in space: crabs from different habitats rely on different senses, *Journal of Comparative Physiology A* **165**(5), 643–649.

[305] Nalbach, H.-O. [1990], Multisensory control of eyestalk orientation in decapod crustaceans: An ecological approach, *Journal of Crustacean Biology* **10**(3), 382–399.

[306] Nalbach, H.-O., Thier, P. and Varjú, D. [1993], Binocular interaction in the optokinetic system of the crab *Carcinus maenas* (l.): Optokinetic gain modified by bilateral image flow, *Visual Neuroscience* **10**(5), 873–885.

[307] Matsushita, A. and Arikawa, K. [1997], Actin-based vesicular transport in the first 20 min after dusk is crucial for daily rhabdom synthesis in the compound eye of the grapsid crab *Hemigrapsus sanguineus*, *Journal of Experimental Biology* **200**(18).

[308] Walcott, B. [1971], Cell movement on light adaptation in the retina of *Lethocerus* (Belostomatidae, Hemiptera), *Zeitschrift für Vergleichende Physiologie* **74**(1), 1–16.

[309] Home, E. M. [1976], The fine structure of some carabid beetle eyes, with particular reference to ciliary structures in the retinula cells, *Tissue and Cell* **8**(2), 311–333.

[310] Miller, P. E. [2008], Structure and Function of the Eye, *in* Slatter's Fundamentals of Veterinary Ophthalmology, Elsevier Inc., pp. 1–19.

[311] Lamb, T. D. and Pugh, E. N. [2006], Phototransduction, dark adaption, and rhodopsin regeneration: The proctor lecture, *in* Investigative Ophthalmology and Visual Science, Vol. 47, The Association for Research in Vision and Ophthalmology, pp. 5138–5152.

[312] Schwemer, J. [1984], Renewal of visual pigment in photoreceptors of the blowfly, *Journal of Comparative Physiology A* **154**(4), 535–547.

[313] Bernard, G. D. [1983], Bleaching of rhabdoms in eyes of intact butterflies, *Science* **219**(4580), 69–71.

[314] Stowe, S. [1983], Light-induced and spontaneous breakdown of the rhabdoms in a crab at dawn; depolarisation versus calcium levels, *Journal of Comparative Physiology A* **153**, 365–375.

[315] Bengochea, M., Berón de Astrada, M., Tomsic, D. and Sztarker, J. [2018], A crustacean lobula plate: Morphology, connections, and retinotopic organization, *Journal of Comparative Neurology* **526**(1), 109–119.

[316] Sinakevitch, I., Douglass, J. K., Scholtz, G., Loesel, R. and Strausfeld, N. J. [2003], Conserved and convergent organization in the optic lobes of insects and isopods, with reference to other crustacean taxa, *Journal of Comparative Neurology* **467**(2), 150–172.

[317] Lillywhite, P. G. and Dvorak, D. R. [1981], Responses to single photons in a fly optomotor neurone, *Vision Research* **21**(2), 279–290.

[318] Dubs, A., Laughlin, S. B. and Srinivasan, M. V. [1981], Single photon signals in fly photoreceptors and first order interneurones at behavioral threshold., *The Journal of Physiology* **317**(1), 317–334.

[319] Reichardt, W. E. [1965], Quantum sensitivity of light receptors in the compound eye of the fly *Musca*, *Cold Spring Harbor symposia on quantitative biology* **30**, 505–515.

[320] Frolov, R., Immonen, E. V. and Weckström, M. [2016], Visual ecology and potassium conductances of insect photoreceptors, *Journal of Neurophysiology* **115**(4), 2147–2157.

[321] Niven, J. E., Vähasöyrinkl, M., Kauranen, M., Hardie, R. C., Juusola, M. and Weckström, M. [2003], The contribution of Shaker K+ channels to the information capacity of *Drosophila* photoreceptors, *Nature* **421**(6923), 630–634.

[322] Weckström, M. and Laughlin, S. B. [1995], Visual ecology and voltage-gated ion channels in insect photoreceptors, *Trends in Neurosciences* **18**(1), 17–21.

[323] Pepose, J. S. and Lisman, J. E. [1978], Voltage-sensitive potassium channels in *Limulus* ventral photoreceptors, *Journal of General Physiology* **71**(1), 101–120.

[324] Weckström, M., Hardie, R. C. and Laughlin, S. B. [1991], Voltage-activated potassium channels in blowfly photoreceptors and their role in light adaptation, *The Journal of Physiology* **440**(1), 635–657.

[325] Juusola, M. and Weckström, M. [1993], Band-pass filtering by voltage-dependent membrane in an insect photoreceptor, *Neuroscience Letters* **154**(1-2), 84–88.

[326] Palmer, J. [1995], *The Biological Rhythms and Clocks of Intertidal Animals*, Oxford University Press.

[327] Palmer, J. D. [2000], The clocks controlling the tide-associated rhythms of intertidal animals, *BioEssays* **22**(1), 32–37.

[328] Takahashi, J. S. [2017], Transcriptional architecture of the mammalian circadian clock, *Nature Reviews Genetics* **18**(3), 164–179.

[329] Mat, A. M., Dunster, G. P., Sbragaglia, V., Aguzzi, J. and De La Iglesia, H. O. [2017], Influence of temperature on daily locomotor activity in the crab *Uca pugilator*, *PLoS ONE* **12**(4).

[330] Chabot, C. C., Ramberg-Pihl, N. C. and Watson, W. H. [2016], Circalunidian clocks control tidal rhythms of locomotion in the American horseshoe crab, *Limulus polyphemus*, *Marine and Freshwater Behaviour and Physiology* **49**(2), 75–91.

[331] Langdon, J. W. [1971], Shape discrimination and learning in the fiddler crab *Uca pugilator*, PhD thesis, Florida State University.

[332] *Sunrise and sunset times in Playa El Rompido, September 2019 [Online]* [2019]. **URL:** *https://www.timeanddate.com/sun/@10342248?month=9&year=2019*

[333] Webb, H. M. and Brown, F. A. [1965], Interactions of diurnal and tidal rhythms in the fiddler crab, *Uca pugnax.*, *The Biological Bulletin* **129**(3), 582–91.

[334] Butikov, E. I. [2002], A dynamical picture of the oceanic tides, *Citation: American Journal of Physics* **70**, 663.

[335] Dugaw, C. J., Honeyfield, R., Taylor, C. M. and Verzi, D. W. [2009], Modeling activity rhythms in fiddler crabs, *Chronobiology International* **26**(7), 1355–1368.

[336] Naylor, E. [1996], Crab clockwork: The case for interactive circatidal and circadian oscillators controlling rhythmic locomotor activity of *Carcinus maenas*, *Chronobiology International* **13**(3), 153–161.

[337] Akiyama, T. [2014], Circatidal and circadian rhythms in crustacean swimming behavior, *in* Annual, Lunar, and Tidal Clocks, Springer Japan, pp. 65–80.

[338] Palmer, J. D. and Williams, B. G. [1986], Comparative studies of tidal rhythms. II. The dual clock control of the locomotor rhythms of two decapod crustaceans, *Marine Behaviour and Physiology* **12**(4), 269–278.

[339] Reid, D. G. and Naylor, E. [1990], Entrainment of bimodal circatidal rhythms in the shore crab *Carcinus maenas*, *Journal of biological rhythms* **5**(4), 333–47.

[340] Al-Musawi, L. I. and Wagner, E. [2012], Seasonal and lunar variation in the emergence time of a population of *Uca lactea annulipes* (Milne-Edwards, 1837) at a shore in Kuwait, *Chronobiology International* **29**(4), 408.

[341] Jimenez, A. G. and Bennett, W. A. [2007], Metabolic responses of sand fiddler crabs, *Uca pugilator*, in northwest Florida to seasonal temperature change, *Journal of Thermal Biology* **32**(6), 308–313.

[342] *Average Weather in El Rompido, Spain [Online]. Data from NASA's MERRA-2 Modern-Era Retrospective Analysis, 1990-2016* [2020].
URL: *https://weatherspark.com/y/32793/Average-Weather-in-El-Rompido-Spain-Year-Round*

[343] Powers, L. W. and Cole, J. F. [1976], Temperature variation in fiddler crab microhabitats, *Journal of Experimental Marine Biology and Ecology* **21**(2), 141–157.

[344] Nath, T., Mathis, A., Chen, A. C., Patel, A., Bethge, M. and Mathis, M. W. [2019], Using DeepLabCut for 3D markerless pose estimation across species and behaviors, *Nature Protocols* **14**(7), 2152–2176.

[345] Herrnkind, W. F. [1966], The ability of young and adult sand fiddler crabs, *Uca pugilator* (Bosc), to orient to polarized light, *American Zoologist* **6**, 298–299.

[346] Herrnkind, W. F. [1968], Adaptive visually-directed orientation in *Uca pugilator*, *Integrative and Comparative Biology* **8**(3), 585–598.

[347] Chiussi, R. and Díaz, H. [2001], Multiple reference usage in the zonal recovery behavior by the fiddler crab *Uca cumulanta*, *Journal of Crustacean Biology* **21**(2), 407–413.

[348] Dahmen, H. [2004], Eye specialisation in waterstriders: an adaptation to life in a flat world, *Journal of Comparative Physiology A* **169**, 623–632.

[349] Heinloth, T., Uhlhorn, J. and Wernet, M. F. [2018], Insect responses to linearly polarized reflections: Orphan behaviors without neural circuits, *Frontiers in Cellular Neuroscience* **12**, 50.

[350] Wehner, R. [1987], 'Matched filters' - neural models of the external world, *Journal of Comparative Physiology A* **161**(4), 511–531.

[351] Williams, D. S. [1982], Photoreceptor membrane shedding and assembly can be initiated locally within an insect retina, *Science* **218**(4575), 898–900.

[352] David K. Lynch, W. C. L. [2001], *Color and Light in Nature, Second edition*, Cambridge University Press.

[353] Land, M. and Layne, J. [1995], The visual control of behaviour in fiddler crabs II. Tracking control systems in courtship and defence, *Journal of Comparative Physiology A* **177**(1), 91–103.

[354] Douglass, J. K. and Strausfeld, N. J. [2003*a*], Retinotopic pathways providing motion-selective information to the lobula from peripheral elementary motion-detecting circuits, *The Journal of Comparative Neurology* **457**(4), 326–344.

[355] Douglass, J. K. and Strausfeld, N. J. [2003*b*], Anatomical organization of retinotopic motion-sensitive pathways in the optic lobes of flies, **62**(2), 132–150.

[356] Batra, R. J. and Barlow, R. B. [1990], Efferent control of temporal response properties of the *Limulus* lateral eye, *Journal of General Physiology* **95**(2), 229–244.

[357] Kelber, A. and Osorio, D. [2010], From spectral information to animal colour vision: Experiments and concepts, *Proceedings of the Royal Society B: Biological Sciences* **277**(1688), 1617–1625.

[358] Schaerer, S. and Neumeyer, C. [1996], Motion detection in goldfish investigated with the optomotor response is 'color blind', *Vision Research* **36**(24), 4025–4034.

[359] Orlando, E. and Schmid, A. [2011], Colour blindness of the movement-detecting system of the spider *Cupiennius salei*, *Journal of Experimental Biology* **214**(4), 546–550.

[360] Yamaguchi, S., Wolf, R., Desplan, C. and Heisenberg, M. [2008], Motion vision is independent of color in *Drosophila*, *Proceedings of the National Academy of Sciences of the United States of America* **105**(12), 4910–4915.